

Final Design Report for Reracking  
the Indian Point Unit No. 2  
Spent Fuel Pool

Consolidated Edison Company of New York, Inc.  
Indian Point Unit No. 2  
Docket No. 50-247  
May, 1980

**REGULATORY DOCKET FILE COPY**

TABLE OF CONTENTS

	<u>PAGE</u>
1. Introduction	1
2. History & Need for Increased Storage Capacity	1
3. Construction Costs	1
4. Alternatives to Increasing the Storage Capacity	3
4.1 Reprocessing of Spent Fuel	3
4.2 Independent Spent Fuel Storage Installations (ISFSI)	3
4.3 Storage at Another Reactor Site	3
4.4 Shutdown of Facility	3
5. Attachments	
Attachment A - Licensing Submittal Report for the Indian Point Unit No. 2 Spent Fuel Storage Racks	
Attachment B - Nuclear Analysis Report for the Indian Point Unit No. 2 Spent Fuel Storage Racks	
Attachment C - Radiological Analysis Report for the Indian Point Unit No. 2 Spent Fuel Storage Racks	
Attachment D - Thermal-Hydraulic Analysis Report for the Indian Point Unit No. 2 Spent Fuel Storage Racks	
Attachment E - Non-Linear Time History Seismic Sliding Analysis Report for the Indian Point Unit No. 2 Spent Fuel Storage Racks	
Attachment F - Structural Analysis Report for the Indian Point Unit No. 2 Spent Fuel Storage Racks	

## 1. Introduction

By letters dated February 27, 1979 and September 7, 1979 Consolidated Edison submitted to the NRC the documents entitled "Proposed Design Criteria for Reracking Indian Point Unit No. 2 Spent Fuel Pool" and "Preliminary Design Report for Reracking the Indian Point Unit No. 2 Spent Fuel Pool", respectively. The information contained herein supersedes the aforementioned documents and provides Consolidated Edison's final reracking submittal. In addition, the September 7, 1979 submittal provided proposed changes to the Indian Point Unit No. 2 Technical Specifications.

The high density spent fuel storage racks will provide storage locations for up to 980 fuel assemblies and will be designed to maintain the stored spent fuel, having an equivalent uranium enrichment of 3.5 weight percent U-235 in uranium, in a safe, coolable, and subcritical configuration during normal and abnormal conditions.

## 2. History & Need for Increased Storage Capacity

By letter dated March 4, 1975 and supplements dated May 9, 1975, July 23, 1975, August 19, 1975, September 11, 1975, October 1, 1975 and October 10, 1975 Consolidated Edison requested, from the NRC, authorization to increase the storage capacity of the Indian Point Unit No. 2 spent fuel pool from 264 to 482 storage locations. On December 16, 1975 the NRC issued Amendment No. 14 to Facility Operating License No. DPR-26 for Indian Point Unit No. 2, authorizing such modification.

Presently there are 200 spent fuel assemblies stored in the spent fuel pool. The projected refueling schedules and expected number of fuel assemblies to be discharged in the spent fuel pool, while maintaining full core reserve (FCR), are given in Table 1-1.

It is anticipated that the existing storage capacity would be reached in 1981, with FCR maintained.

## 3. Construction Costs

The total cost to rerack the Indian Point Unit No. 2 spent fuel pool has been estimated to be \$7,500,000. This estimate includes the following:

- o design, materials, fabrication
- o removal and disposal of old racks
- o transportation and installation of new racks
- o project management, licensing, quality assurance
- o contingency allowance
- o allowances for funds used during construction

Table 1-1

Projected Spent Fuel Discharges

<u>Calendar Year</u>	<u>Estimated Discharges- No. of Assemblies</u>
current inventory	200
1980	---
1981	72
1982	72
1983	---
1984	72
1985	72
1986	---
1987	72
1988	72
1989	---
1990	72
1991	72

#### 4. Alternatives to Increasing the Storage Capacity

##### 4.1 Reprocessing of Spent Fuel

None of the three commercial reprocessing facilities in the U.S., the General Electric Company's Midwest Fuel Recovery Plant (MFRP), the Nuclear Fuel Service (NFS) plant, and the Allied General Nuclear Services (AGNS) plant, are currently operating.

On April 7, 1977 the President of the United States issued a statement outlining a change in the national policy to defer indefinitely commercial reprocessing. Consequently the NRC issued an order dated December 30, 1977 terminating proceedings to license reprocessing facilities.

Due to this change in national policy Consolidated Edison cannot reprocess the Indian Point Unit No. 2 spent fuel.

##### 4.2 Independent Spent Fuel Storage Installations (ISFSI)

There are no independent spent fuel storage facilities available at this time. In addition Consolidated Edison does not foresee this alternative to be available within the next 5 years or to be economic even if it were.

While the storage pools at NFS and MFRP are currently functioning as ISFSI, Consolidated Edison does not have any contracts to store spent fuel at these facilities.

For the reasons stated above, storage of spent fuel at an ISFSI is not a realistic alternative.

##### 4.3 Storage at Another Reactor Site

Consolidated Edison owns only one other nuclear power plant, Indian Point Unit No. 1 which was shut down on October 31, 1974 and is presently in the defueled condition. The Indian Point Unit No. 1 spent fuel pools have Indian Point Unit No. 1 spent fuel and other core components stored in them. In addition to the cost of reracking an Indian Point Unit No. 1 spent fuel pool and other associated costs, there would be the added cost of periodically transferring the spent fuel from the Indian Point Unit No. 2 to the Indian Point Unit No. 1 spent fuel pool.

Storage of the spent fuel at another nuclear power plant owned by another utility does not appear to be a realistic alternative. With the present situation in spent fuel storage capacity Consolidated Edison cannot rely on another utility for spent fuel storage space.

##### 4.4 Shutdown of Facility

If Indian Point Unit No. 2 were forced to shutdown for lack of spent fuel storage space there would be a significant loss of economic benefit to our customers.

The present estimated additional fuel cost to replace the output of Indian Point Unit No. 2 on a day of full-power operation, utilizing existing oil-fired generating units, is approximately \$1,000,000. not including applicable taxes. The above figure, which is in 1980 dollars, would increase in subsequent years due to the anticipated escalation in the price of oil.

Due to the fact that presently Consolidated Edison, excluding Indian Point Unit No. 2, primarily utilizes oil fired generating units (gas turbines are used for peak load needs) and our national energy policy is to decrease the use of imported oil, the alternative to shut down the reactor is not realistic.

ATTACHMENT A

Licensing Submittal Report

for the

Indian Point Unit No. 2 Spent

Fuel Storage Racks

Consolidated Edison Company of New York, Inc.  
Indian Point Unit No. 2  
Docket No. 50-247  
May, 1980



**LICENSING SUBMITTAL REPORT  
FOR THE  
INDIAN POINT UNIT NO. 2  
SPENT FUEL STORAGE RACKS**

**Prepared for  
Consolidated Edison Company of New York, Inc.**



## TABLE OF CONTENTS

1.	DESIGN BASES	5
2.	STORAGE RACK DESCRIPTION	5
3.	STORAGE RACK EVALUATION	9
3.1	STRUCTURAL AND SEISMIC ANALYSIS	9
3.1.1	Applicable Codes, Standards and Specifications	9
3.1.2	Loads and Load Combinations	9
3.1.2.1	Load Cases	9
3.1.2.2	Load Combinations	13
3.1.3	Structural Acceptance Criteria	13
3.1.4	Method of Analysis	14
3.1.4.1	Rack Structural Analysis	14
3.1.4.2	Water Sloshing Effects	15
3.1.4.3	Fuel Assembly Impact Loads	15
3.1.4.4	Accidental Spent Fuel Assembly Drop Analysis	16
3.1.4.5	Spent Fuel Rack Stability Analysis	16
3.1.5	Results of Analysis	16
3.2	SLIDING ANALYSIS	17
3.2.1	Method of Analysis	17
3.2.2	Results of the Analysis	20
3.3	NUCLEAR ANALYSIS	21
3.3.1	Design Criterion and Assumptions	21
3.3.2	Criticality Configurations	22
3.3.2.1	Normal Configurations	22
3.3.2.2	Abnormal Configurations	24
3.3.3	Calculational Methods	27
3.3.3.1	Code Description	27
3.3.3.2	Uncertainties and Benchmark Calculations	27



3.3.4	Results of Analysis	28
3.3.4.1	Normal Configurations	28
3.3.4.2	Abnormal Configurations	29
3.4	THERMAL-HYDRAULIC ANALYSIS	29
3.4.1	Method of Analysis and Assumptions	29
3.4.2	Results of Analysis	31
3.5	RADIOLOGICAL ANALYSIS	32
3.5.1	Method of Analysis and Assumptions	32
3.5.2	Results of Analysis	33
3.6	SPENT FUEL RACK INSTALLATION	34
4.	REFERENCES	36

#### LIST OF FIGURES

2.1	Fuel Storage Rack Arrangement Plan	6
2.2	Indian Point 2 Borated SST Fuel Storage Rack (10x10)	8
3.1	15% of Gravity Response Spectra Horizontal	11
3.2	10% of Gravity Response Spectra Vertical	12
3.3	Pool Floor Absolute Acceleration Time History	18



**LICENSING SUBMITTAL REPORT  
FOR THE  
INDIAN POINT GENERATING STATION UNIT 2  
FUEL STORAGE RACKS**

**1. DESIGN BASES**

The high density spent fuel storage racks will provide storage locations for up to 980 fuel assemblies and will be designed to maintain the stored fuel, having an equivalent uranium enrichment of 3.5 weight percent U-235 in uranium in a safe, coolable, and subcritical configuration during normal and abnormal conditions.

**2. STORAGE RACK DESCRIPTION**

The spent fuel storage racks will be designed to provide a maximum storage capacity of 980 locations in the spent fuel pool. The fuel storage rack arrangement will contain several types of storage racks with arrays ranging from 8x8 to 10x10 configurations, as shown in Figure 2-1.

Each rack consists of an assembly of 2x2 modules (the 9x8 and 9x10 racks also include 2x3 modules). Each 2x2 or 2x3 modular cell unit consists of four (4) or six (6) cells spaced nominally 10-15/16 inches on centers. Each storage cell is a Type 304 stainless steel box with a nominal wall thickness of 0.0825 inches and a 9 inch inside dimension. The top opening of the storage cell is flared to facilitate insertion of the fuel assembly; the bottom member of the storage cell provides the level support surface required for the fuel assembly and contains the cooling flow orifice.

Four (4) borated stainless steel plates with a nominal 1.1 w/o boron concentration (each 7 inches wide by 145 inches long by 0.100 inch thick) will be attached by means of welded brackets to each storage cell within the four-cell module at an elevation corresponding to the active fuel region of an assembly placed within the cell.

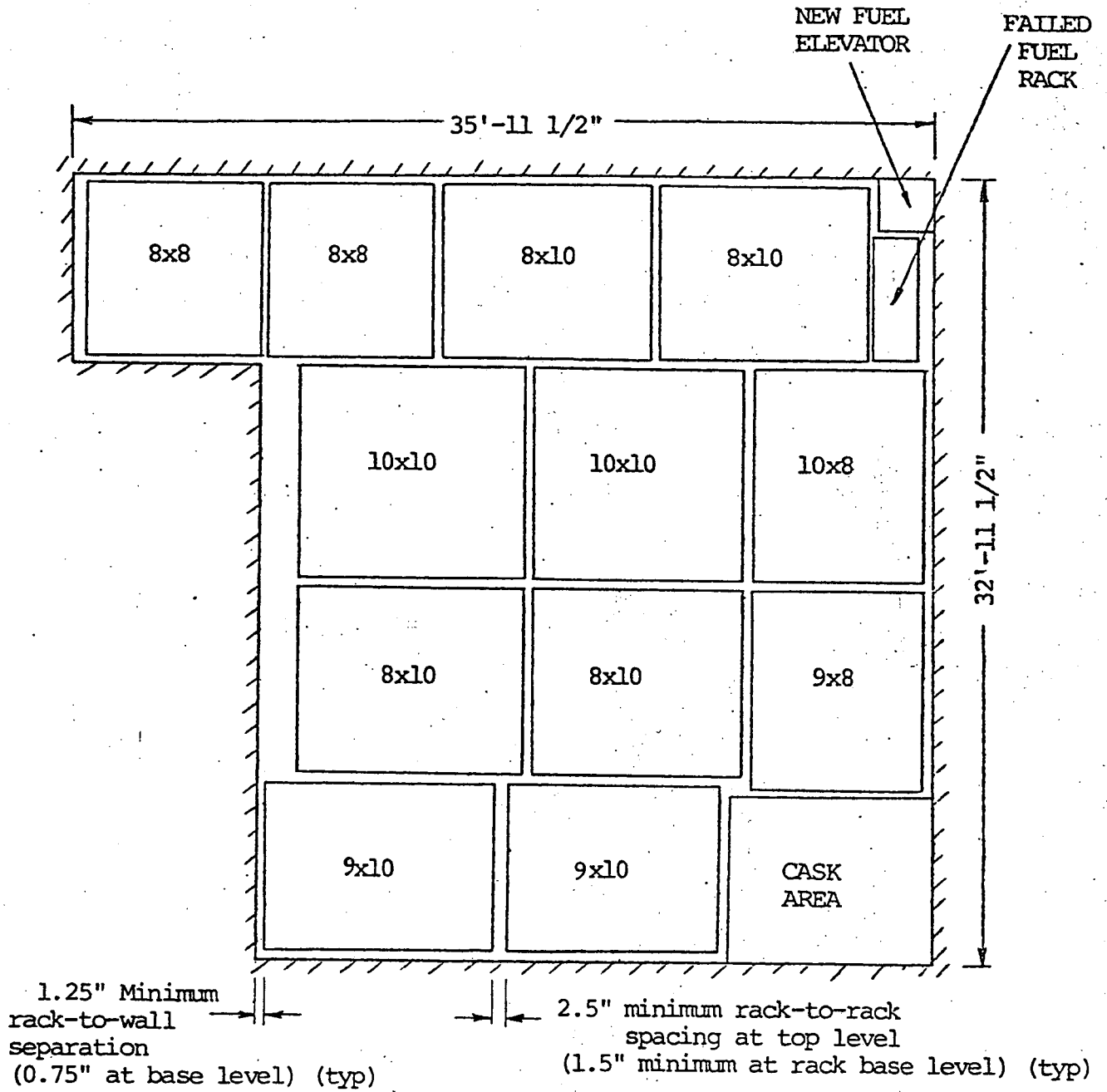


Figure 2.1 Fuel Storage Rack Arrangement Plan



Each modular cell unit (either 2x2 or 2x3) is supported by and welded to the rack base grid structure constructed from Type 304 stainless steel wide flange and box beam members. A schematic drawing of a representative 10x10 rack structure and an individual 2x2 modular cell unit is shown in Figure 2.2. Continuous spacer bars are provided at the top of the storage cells to ensure that the required pitch is maintained between storage cells in both directions (north/south and east/west) under lateral load conditions. The spacer bars which are supported on the storage cells also maintain the vertical alignment of the cells. Support pads attached to the bottom of the rack base raise the rack above the pool floor to the height required to clear existing anchor pins on the pool floor area and to provide an adequately sized cooling water supply plenum for natural circulation. Each support pad contains a remotely adjustable jack screw to permit the rack to be leveled following wet installation. The rack support pads will rest directly on the pool floor wherever possible. In case of interference with the existing floor shims, the pads will rest on local plates designed to bridge over the shims.

The storage racks are free-standing structures that are free to slide horizontally on the pool floor. The storage racks are positioned on the pool floor so that adequate clearances are provided between racks and between the racks and pool structures to avoid impacting of the sliding racks during seismic events. The horizontal seismic loads transmitted from the rack structure to the pool floor are only those associated with friction between the rack structure and the pool liner. The vertical deadweight and seismic loads are transmitted directly to the pool floor by the support feet.

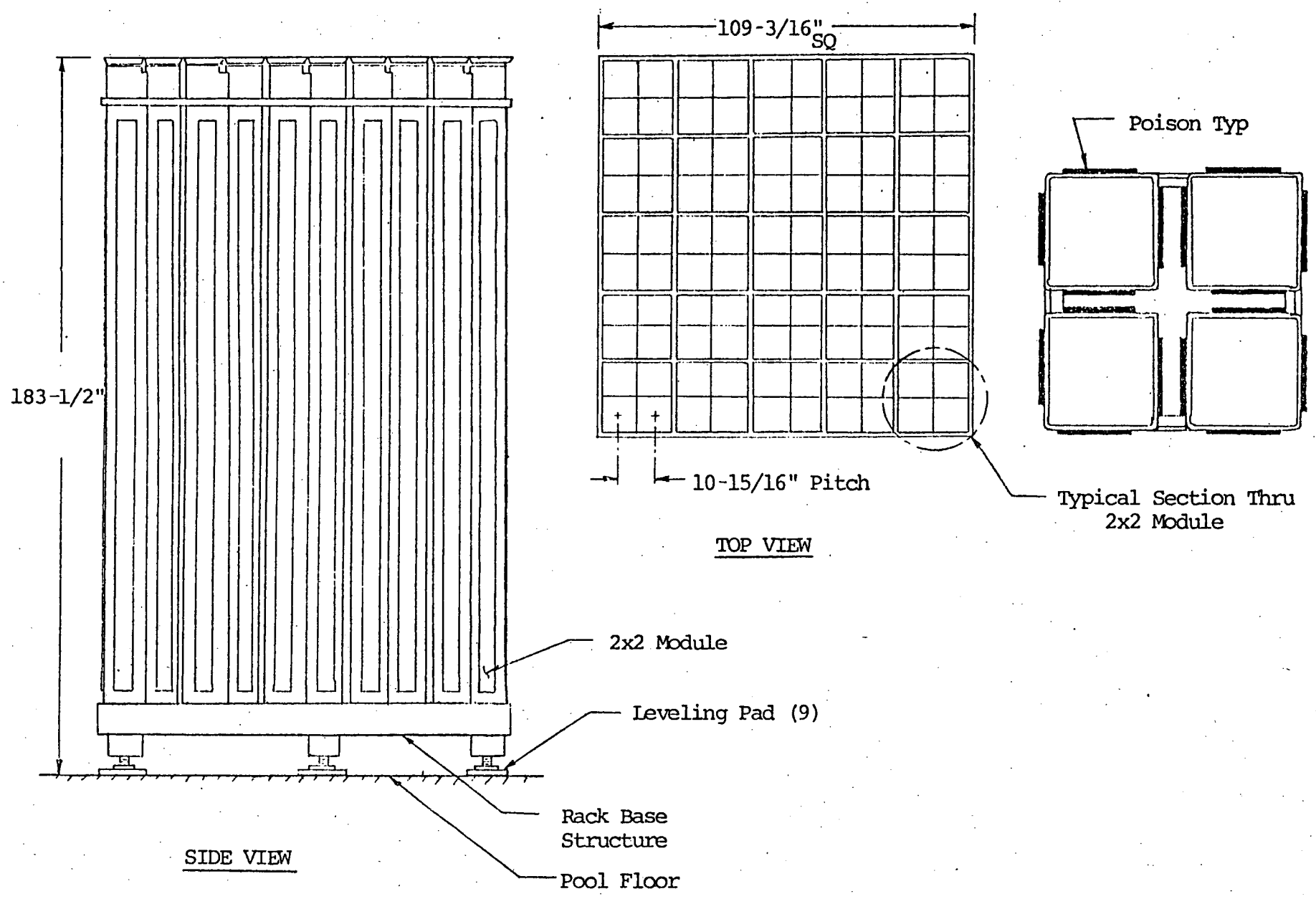


Figure 2.2 Indian Point 2  
Borated SST Fuel Storage Rack (10x10)



### 3. STORAGE RACK EVALUATION

#### 3.1 STRUCTURAL AND SEISMIC ANALYSIS

The Indian Point Generating Station Unit 2 (Indian Point 2) high density spent fuel storage racks have been designed to meet the requirements for Seismic Category I structures. Detailed structural and seismic analyses of the high density storage racks have been performed to verify the adequacy of the design to withstand the loadings encountered during installation, normal operation, the severe and extreme environmental conditions of the Operating Basis and Design Basis Earthquakes and the abnormal loading conditions of an accidental fuel assembly drop event.

##### 3.1.1 Applicable Codes, Standards and Specifications

The design codes and regulatory guides listed in References 1 through 5 have been used in the structural design/analysis of spent fuel storage racks.

##### 3.1.2 Loads and Load Combinations

The following load cases and load combinations have been considered in the analysis in accordance with the requirements of USNRC Standard Review Plan, Section 3.8.4 (Reference 3) and the USNRC Position Paper (Reference 4).

###### 3.1.2.1 Load Cases

###### Load Case 1 - Deadweight of Rack, D + L (Normal Load)

Under normal operating conditions, the rack is subjected to the deadweight loading of the rack structure itself plus the loads resulting from the storage cells and a full complement of fuel assemblies stored in the cells.

###### Load Case 2 - Deadweight Of Rack Plus 1g Vertical Installation Load, D + I.L. (Normal Load)

During installation the rack is subjected to the loading resulting from its own structural weight, weight of empty storage cells, plus a 1g vertical load resulting from a suddenly applied crane load.



Load Case 3 - Deadweight of Rack Plus Uplifting Load, (D + U.L.) (Abnormal Load)

The possibility of the fuel handling bridge fuel hoist grapple getting hooked on a fuel storage cell was considered. The axial upward force considered for this load case was 3,000 pounds, applied at two critical locations.

Load Case 4 - Operating Basis Earthquake, E (Severe Environmental Load)

The rack, fuel assemblies, and virtual water mass are subject to the simultaneous loading of the horizontal and vertical components of the seismic response acceleration spectra specified for the Operating Basis Earthquake (2/3 DBE) in the Indian Point 2 Fuel Storage Rack Specifications (Reference 6) and presented in Figure 3.1 and 3.2. The effects of fuel assembly impact during a seismic event are taken into account.

Load Case 5 - Design Basis Earthquake, E' (Extreme Environmental Load)

Same as Load Case 4 except that the seismic response acceleration spectra corresponding to the Design Basis Earthquake (DBE) was used in the analysis (Figure 3.1 and 3.2).

Load Case 6 - Assembly Drop Impact Load, D.L. (Abnormal Load)

The possibility of dropping a spent fuel assembly on the rack from the highest possible elevation during spent fuel handling was considered. A 1650 pound weight (spent fuel assembly) was postulated to drop on the rack from a conservatively selected height of 48 inches above the top of the rack. Three cases were considered: (1) a direct drop on the top of a 2x2 module; (2) a subsequent tipping of the assembly onto the surrounding storage cans; (3) a straight drop through the storage cell and impact onto the rack base grid structure. During fuel handling operations, the fuel assembly will actually be lifted less than 48 inches above the top of the storage cells.

Thermal Loading, T (Normal Load)

The stresses and reaction loads due to thermal loadings are insignificant since clearances are provided to allow unrestrained growth of the racks for the maximum pool temperature of 150°F.

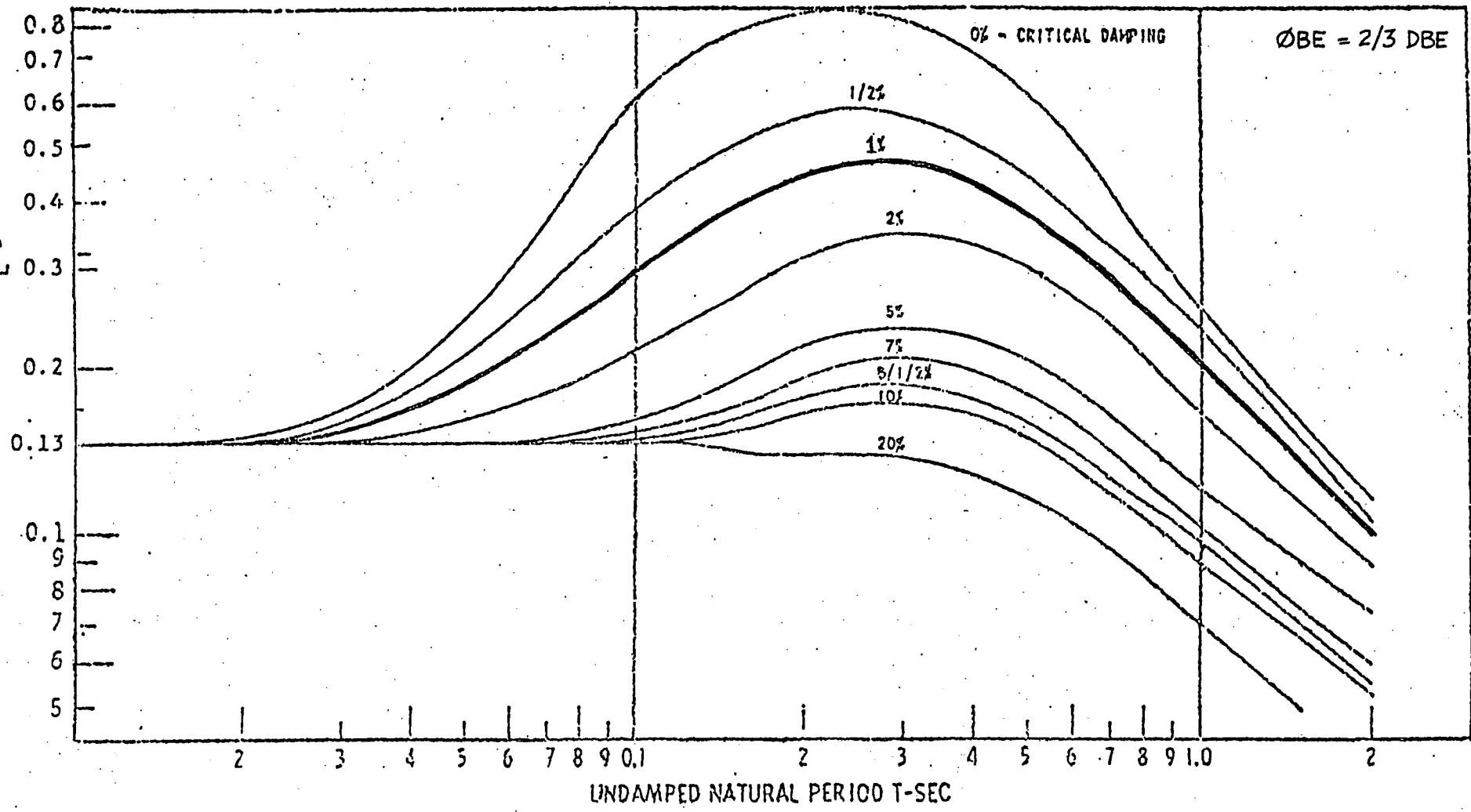


FIGURE 3-1 15% OF GRAVITY RESPONSE SPECTRA (DBE) HORIZONTAL

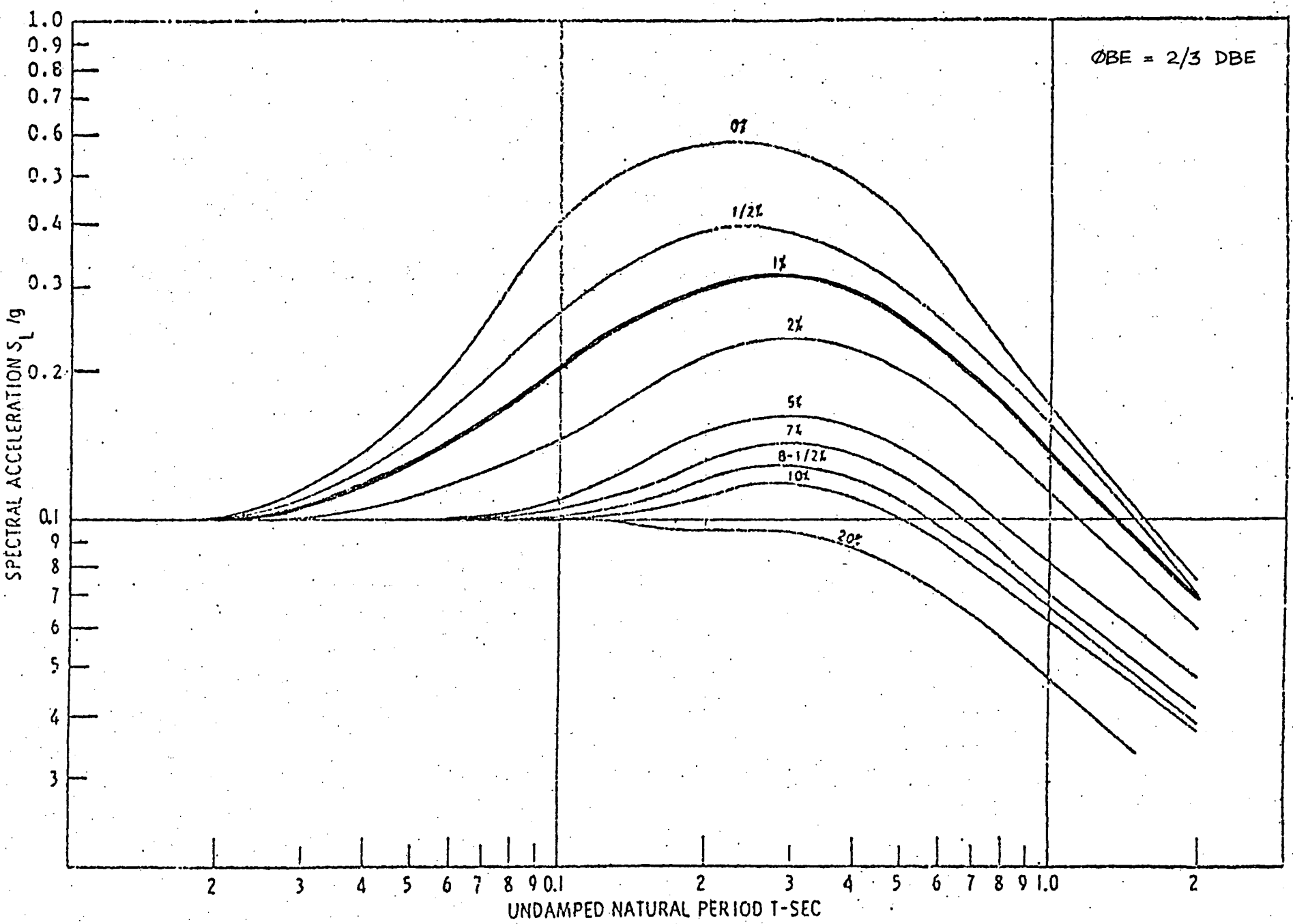


FIGURE 3-2. 10% OF GRAVITY RESPONSE SPECTRA (DBE) VERTICAL



3.1.2.2 Load Combinations

A. For service load conditions, the following load combinations are considered:

- (1) D + L
- (2) D + L + T
- (3) D + I.L.
- (4) D + L + E
- (5) D + L + E + T

B. For factored load conditions, the following load combinations are considered:

- (6) D + L + T + E'
- (7) D + T + U.L.
- (8) D + L + T + D.L.

3.1.3 Structural Acceptance Criteria

The following allowable stress limits constitute the structural acceptance criteria used for each of the loading combinations presented in Section 3.1.2.2.

<u>Load Combinations</u>	<u>Limit*</u>
1, 3, 4	S
2, 5	1.5S
6, 7	1.6S or F <sub>y</sub> (whichever is less)
8	**

Where S is the required section strength based on the elastic design methods and the allowable stresses defined in Part 1 of the AISC "Specification for the Design, Fabrication and Erection of Structural Steel for Buildings," February 12, 1969. The yield stress value (F<sub>y</sub>) for Type 304 stainless steel is taken as 30.0 ksi from the American Society for Testing and Materials, Specification ASTM-A240.

\* The acceptance criteria are based on the applicable sections of the NRC Position Paper on Fuel Storage Racks, SRP 3.8.4, and AISC Specification for the Design, Fabrication and Erection of Structural Steel for Building, The Uniform Building Code.

\*\* The acceptance criteria for Load Combination 8, the accidental spent fuel assembly drop on the rack, is that the resulting impact will not adversely affect the overall structural integrity of the rack, the leak-tightness integrity of the fuel pool floor and liner plate and that the deformation of the impacted storage cells will not adversely affect the value of K<sub>eff</sub> or ability to cool adjacent fuel elements.



### 3.1.4 Method of Analysis

#### 3.1.4.1 Rack Structural Analysis

A 10x10 rack has been analyzed in detail. This rack conservatively represents the controlling structural case since it has the longer beam span and will be loaded by greater seismic loads than the smaller racks. The dynamic (frequency) characteristic of the rack is essentially controlled by the dynamic characteristics of its component 2x2 or 2x3 modular cell units. Although the fundamental frequency of the 2x3 modular cell unit is higher than that of the 2x2 modular cell units, the design seismic spectra are such that the lateral seismic G loading for the 2x2 and 2x3 modular cell units will be essentially similar.

In order to perform static, dynamic and stress analyses of the fuel storage rack structure, the rack has been mathematically modeled as a finite element structure consisting of discrete three-dimensional elastic beam and plate elements interconnected at a finite number of nodal points. Stiffness characteristics of the structural members are related to the plate thickness, cross sectional area, effective shear area and moment of the inertia of the element section.

Appropriate support connections are provided at the support feet for both static and dynamic analysis. The feet locations have been selected to represent a conservative support configuration that will result in maximum stresses in the rack base structure. Six degrees of freedom (three translations and three rotations) are permitted at each nodal point.

For the static deadweight and live load analysis, the distributed masses of the structural elements, storage cells and fuel elements are lumped at the 2x2 module system nodal points. Similarly, for Load Case 2, rack installation and removal analysis, the distributed masses of the structural elements and the cells are lumped at the 2x2 module system nodal points. The effect of suddenly applied crane load is considered by applying a 1g vertical load in addition to the deadweight loading. For Load Case 3, a net vertical uplift load of 3,000 pounds is applied at the worst location of the storage rack.



For the horizontal and vertical seismic analyses, a mathematical model was developed to represent the 10x10 rack. This model consists of twenty-five (25) lumped mass cantilever beams (representing twenty-five 2x2 modules) rigidly attached to the rack base structure and attached to each other at the top by spacer bars. Each lumped mass cantilever beam has three masses and has the same dynamic (frequency) characteristics as a 2x2 module. This model is used in calculating the maximum stresses in the rack base structure and the reaction loads and stresses in the rack support feet. The distributed masses corresponding to the fuel assembly storage cells, poison elements and contained plus hydrodynamic mass are lumped at appropriate nodal points. The hydrodynamic mass calculations are based on recommendations given in References 7 and 8. The horizontal and vertical weights are distributed such that the resulting lumped mass multi-degree-of-freedom model best represents the dynamic characteristics of the fuel storage rack. The seismic analysis are performed for the fully loaded racks only since this loading condition results in lower frequency, higher seismic accelerations, higher stresses and reaction loads.

The static, seismic and stress analyses for the fuel storage racks were performed utilizing the STARDYNE computer code (Ref. 9). Details of the mathematical model, input and calculated data are presented in Reference 10.

#### 3.1.4.2 Water Sloshing Effects

The sloshing effects of water on the fuel racks have been evaluated using the analytical methods given in USAEC's TID7024 "Nuclear Reactors and Earthquakes," Reference 11.

#### 3.1.4.3 Fuel Assembly Impact Loads

Clearances are provided between fuel assemblies and the storage cells to avoid interferences during fuel storage and removal operations. The storage cell/fuel assembly clearance or gap results in the impacting of the fuel assembly and storage cell during a seismic event. The Indian Point 2 fuel storage racks have been analyzed



using the linear response spectrum modal superposition methods of dynamic analysis. In these seismic analyses, the effect of impacting masses has been conservatively accounted for by imposing the following assumptions:

- (1) All storage cells contain the fuel assembly.
- (2) All fuel assemblies simultaneously impact the storage cells.
- (3) The effect of fuel assembly impact is a two-fold increase in the seismic inertia loadings produced by the impacting fuel assemblies mass\*.
- (4) The impact and seismic inertia loads of the impacting masses are added to the seismic inertia loads of the non-impacting masses.

#### 3.1.4.4 Accidental Spent Fuel Assembly Drop Analysis

Linear and non-linear analysis techniques using energy balance methods are used to evaluate the structural damage resulting from a spent fuel assembly drop onto the rack.

#### 3.1.4.5 Spent Fuel Rack Stability Analysis

The stability of the free-standing fuel storage rack has been evaluated using energy balance methods.

#### 3.1.5 Results of Analysis

The results of the seismic and structural analysis indicate that the stresses in the rack structure resulting from the loadings associated with the normal and abnormal conditions are within allowable stress limits for Seismic Category I structures.

The fundamental frequency of vibration of the fuel storage rack is 3.390 cps. For Operating Basis Earthquake, the maximum calculated bending stresses in the storage cell are 7.97/14.85 ksi (18.0/18.0 ksi allowable), and in the storage rack base structure is 15.46 ksi (20.0 ksi allowable). For Design Basis Earthquake (DBE), the maximum calculated bending stresses in the storage cell are 18.94/13.74 ksi (28.8/28.8 ksi allowable) and in the storage rack base structure is 21.0 ksi (30.0 ksi allowable). The maximum combined stress ratio of 0.812 (1.0 allowable) for the storage cell results from the maximum DBE seismic loading.

\* The use of an impact factor of 2.0 is conservative as verified by comparing the base shear and overturning moment response results of the linear response spectrum modal superposition analysis (NES 81A0610, Ref. 10) and the non-linear time history analysis (NES 81A0615, Ref. 12).



Sloshing of pool water in a seismic event will have insignificant effects on the fuel storage racks.

The analysis of the accidental fuel assembly drop condition indicates acceptable local structural damage to the storage cells with no buckling or collapse, and no puncturing of the stainless steel liner. Therefore, no significant changes in the value of  $k_{eff}$  will occur and the leak-tightness of the fuel pool will be maintained.

It is concluded that the designs of the Indian Point 2 high density fuel storage racks are adequate to withstand the loadings of normal and abnormal conditions.

### 3.2 SLIDING ANALYSIS

#### 3.2.1 Method of Analysis

The Indian Point 2 High Density Spent Fuel Storage Racks have been designed to meet the requirements for Seismic Category 1 structures. A detailed non-linear time history seismic analysis has been performed to evaluate the maximum sliding of the storage racks and to determine the maximum frictional resistance load transmitted by the storage racks to the pool floor liner plate during the Design Basis Earthquake (DBE).

The Indian Point Unit 2 spent fuel pool floor absolute acceleration time history shown in Figure 3.3 (Ref. 6) was used to evaluate the sliding response of the storage rack structure. This 10-second duration acceleration time history represents the 1% damping spectra for the Design Basis Earthquake.

A 10x10 storage rack and the stored fuel assemblies have been represented by a two dimensional lumped mass finite element model. The model consists basically of two coincident finite element cantilever beams; one representing the 100 storage cells and the other 100 stored fuel assemblies attached to a "floor" mass by means of a non-linear sliding element.

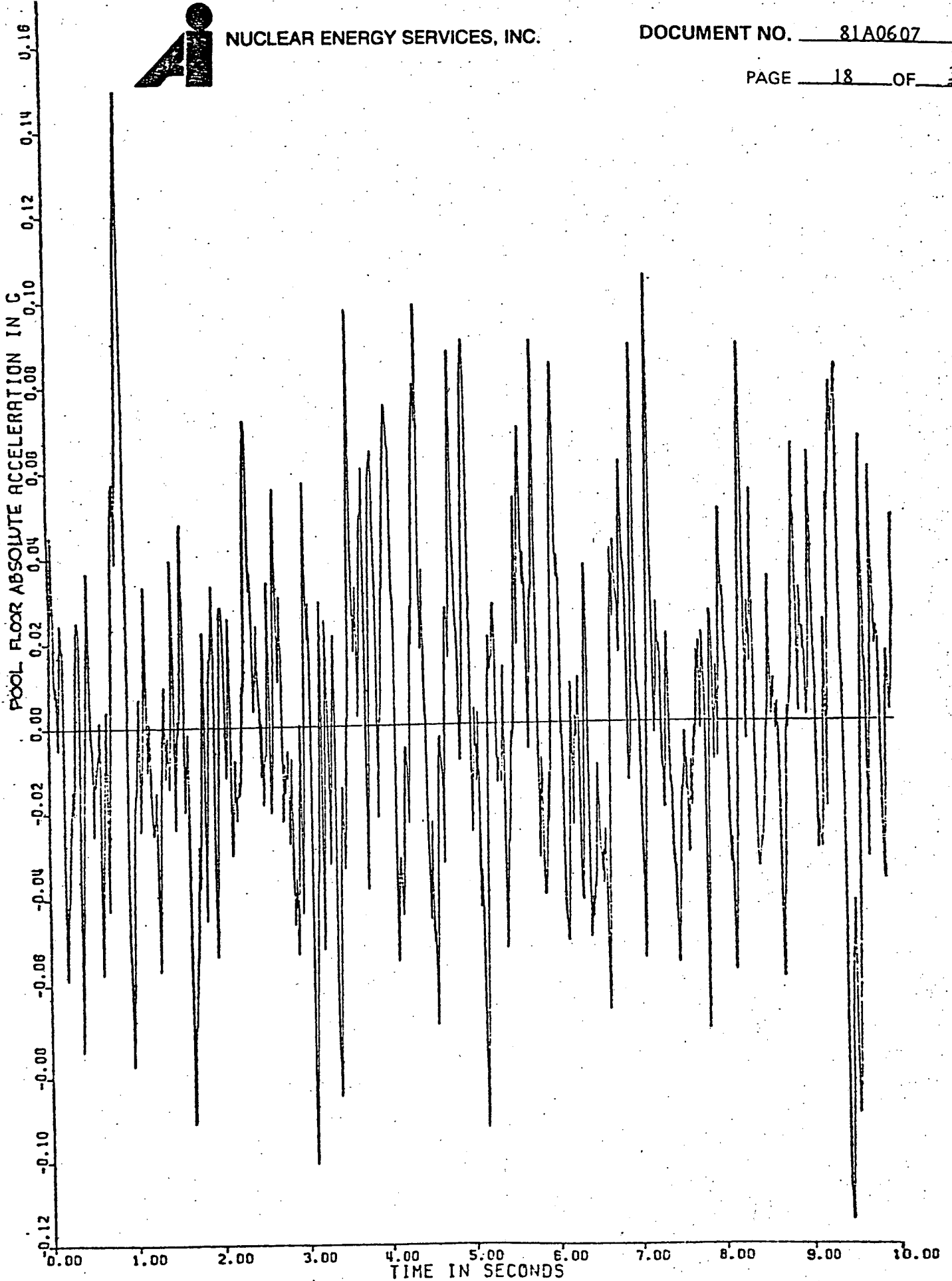


FIGURE 3-3 POOL FLOOR ABSOLUTE ACCELERATION TIME HISTORY



The fuel element cantilever beam consists of masses lumped at the model nodal points interconnected by discrete beam elements. Each lumped mass represents the tributary weight of the fuel element mass. The stiffness characteristics of the beam elements are related to the effective flexural rigidity of the fuel assemblies.

The storage rack cantilever beam similarly consists of lumped masses interconnected by discrete elastic beam elements. Each lumped mass represents the tributary weight of the storage cells, water trapped inside the cells and the virtual water mass to account for the hydrodynamic effects. The stiffness characteristics of the storage rack beam elements are related to the dynamic characteristics (fundamental frequency of vibration) of the storage rack as determined by the Lanczos Modal Extraction method of analysis.

In order to account for fuel assembly impact, adjacent masses of the fuel assembly beam and the storage rack beam are laterally coupled by means of non-linear spring/gap elements. The non-linear spring/gap elements permit the adjacent masses to impact each other whenever the gap closes during a seismic event. The stiffness of the non-linear spring is taken as the stiffness value for each spacer grid. An initial gap of 0.287 inch, reflecting the lateral gap between the fuel assembly and the storage cell wall, is provided. The non-linear spring/gap elements are effective for fuel assembly impact on either side of the storage cell.

The two cantilever beams representing the storage cells and fuel assemblies are attached to the pool floor mass by means of the non-linear sliding element to best represent the rack standing freely on the pool floor. The sliding of the rack is initiated when the lateral force in the sliding element exceeds the frictional resistance force which is equal to the coefficient of friction times the vertical weight of the rack. The effective vertical weight is taken as the vertical bouyant weight of the storage rack less the uplift loads due to the vertical component of the Design Basis Earthquake.

The non-linear time history seismic analysis calculations are performed by means of step-by-step integration technique (Houbolt Method, Ref. 13) using the ANSYS computer program (Ref. 14).



### 3.2.2 Results of the Analysis

The results of the non-linear time history seismic analysis of the Indian Point 2 free-standing high density fuel storage rack performed with the ANSYS computer code are contained in Reference 12.

The maximum accumulated sliding displacement of an individual storage rack relative to its initial floor location has been calculated to be 0.125 inches, conservatively assuming a low coefficient of friction value of 0.20. This maximum displacement value represents the accumulated storage rack sliding response during the 10 seconds of the applied time history.

The maximum rack top deflection was calculated to be 0.697 inches for a conservatively high coefficient of friction of 1.5, which precludes any sliding between the rack and the pool floor. The maximum cell horizontal displacement due to rack tilting was calculated to be 0.662 inches. The maximum rack cell displacement (rack sliding plus cell top flexural deflection) is therefore 0.822 inches at the flared opening level. (The flexural deflection and horizontal displacement due to tilting cannot both occur at their maximum values simultaneously since both mechanisms are caused by the same available external energy.)

It has therefore been concluded that the gaps provided at the top elevation between storage racks (2.5 inch minimum) and between pool walls and adjacent storage racks (1.25 inch minimum) are sufficient to preclude any collision of adjacent structures during a Design Basis Earthquake event. It should be noted, that the assumption used in this evaluation of two adjacent storage racks sliding towards one another during the seismic event with simultaneously opposite deflections of the rack tops is unlikely and hence very conservative.

For the higher coefficient of friction of 1.5, the time history response results in a maximum combined frictional resistance load of 170,933 pounds between the storage rack and the pool floor liner plate. The maximum frictional resistance load for an individual rack support foot is 28,500 pounds.



### 3.3 NUCLEAR ANALYSIS

A detailed nuclear analysis has been performed for the NES designed fuel storage racks for Indian Point 2 to demonstrate that, for all anticipated normal and abnormal configurations of fuel assemblies within the fuel storage racks, the  $k_{\text{eff}}$  of the system is less than the criticality criterion of 0.95 for 3.5 w/o, 15x15 Westinghouse fuel assemblies. Certain conservative assumptions about the fuel assemblies and racks have been used in the calculations.

The principal method of calculation used to determine the  $k_{\text{eff}}$  of the Indian Point 2 spent fuel storage racks was the Monte Carlo code KENO IV with a cross section set using 123 energy groups. Cross section input for the 123 energy group set was generated from the XSDRN library using the AMPX module NITAWL.

Parametric studies to determine the effects on  $k_{\text{eff}}$  of changes in fuel rack dimensions, temperature, and fuel assembly enrichment were performed with diffusion theory. Fuel, water and structural cross sections were determined using the HAMMER code, while blackness theory was used to determine the cross sections for the borated steel sheets.  $k_{\text{eff}}$  values were calculated using EXTERMINATOR, a multigroup, two-dimensional diffusion theory code.

#### 3.3.1 Design Criterion and Assumptions

The criticality design criterion established for the Indian Point 2 high density fuel storage racks is that the multiplication constant ( $k_{\text{eff}}$ ) shall be less than 0.95 for all normal and abnormal configurations as determined by Monte Carlo calculation.

The following conservative assumptions have been used in the criticality calculations performed to verify the adequacy of the rack design:

- (1) The fuel is fresh and of a specified enrichment (3.5 w/o) greater than or equal to that of any fuel available.



- (2) The reference configuration contains an infinite square array of storage locations spaced 10-15/16 inches on centers. This is conservative because the array is not infinite, but finite.
- (3) The absorption of the fuel assembly spacers is ignored.
- (4) Any burnable poisons in the fuel assemblies are ignored.
- (5) Any soluble poison in the pool water is ignored.

### 3.3.2 Criticality Configurations

The potential configurations of fuel within the racks can be classified as either normal or abnormal configurations. Normal configurations result from variation in the placement of fuel within the storage cell, variation in fuel assembly dimensions and/or fuel loading because of the manufacturing process, and the variation in fuel storage rack dimensions permitted in fabrication. Abnormal configurations are typically the result of accidents or malfunctions such as the seismic event, a malfunction of the fuel pool cooling system (excessive changes in pool water temperature), a dropped fuel assembly, etc.

#### 3.3.2.1 Normal Configurations

##### (1) Reference Configuration

The reference configuration consists of an infinite array of storage cells having nominal dimensions: 10-15/16 inch pitch, 0.0825 inch cell wall thickness, poison sheets 0.100 inch thick with 1.1 nominal w/o boron concentration, 9 inch cell inside dimension. Each storage cell contains a centrally located fresh 15x15 Westinghouse fuel assembly with a maximum enrichment of 3.5 w/o. The water temperature within the rack is 68°F.



(2) Eccentric Configuration

It is possible for a fuel assembly not to be positioned centrally within a storage cell because of the clearance allowed between the assembly and the cell wall. This clearance is nominally 0.2775 inches on each side of the fuel assembly. Calculations have been performed to determine the effects of eccentrically located fuel. In these calculations it was assumed that four fuel assemblies were diagonally displaced within their storage cells as far as possible towards each other.

(3) Fuel Assembly Tolerance

The important fuel assembly parameter determining  $k_{\text{eff}}$  is the ratio of the amount of  $U^{235}$  to that of water. The amount of  $U^{235}$  per assembly is controlled to within a few tenths of a percent by weighing pellet stacks as the fuel is built and by using a known enrichment. The fuel assembly parameters which determine the volume of water in an assembly are the clad O.D. and the fuel rod pitch. These parameters are closely controlled to typically within  $\pm 0.4\%$ . The effects of these fuel assembly tolerances on  $k_{\text{eff}}$  have been determined to be negligible on the basis of simple  $k_{\text{oo}}$  cell calculations. Consequently, fuel assembly tolerances were not considered further in this analysis.

(4) Fuel Design Variation

Calculations were performed to determine the sensitivity of  $k_{\text{eff}}$  to variations of fuel enrichment from the maximum reference enrichment of 3.5 w/o.

(5) Cell Pitch Variation

Calculations were performed to determine the sensitivity of  $k_{\text{eff}}$  to changes in pitch, the center-to-center spacing between storage cells. The pitch was varied from 10-7/8 to 11.0 inches. The criticality configuration was similar to that of the reference configuration except for the obvious change in center-to-center spacing.



(6) Cell Wall Thickness Variation

The reference case wall thickness was 0.0825 inch for the stainless steel sheet forming the cell walls. This thickness was varied from 0.090 to 0.080 inch to determine the effect on  $k_{eff}$ .

(7) Poison Concentration Variation

The borated stainless steel sheets contain a nominal 1.1 w/o boron in steel. This concentration was reduced to 1.0 w/o to determine the sensitivity of  $k_{eff}$  to variations in this parameter.

(8) Poison Sheet Thickness Variation

The borated stainless steel sheets are nominally 0.100 inch thick. This dimension was reduced by 1/16 inch to determine the sensitivity of  $k_{eff}$  to variation to this parameter.

(9) Cell Inside Diameter Variation

The storage cell inside dimension is a nominal 9.0 inches. This dimension was reduced to 8-15/16 inches to establish the sensitivity of  $k_{eff}$  to variations in this parameter.

(10) "Worst Case" Normal Configuration

The "worst case" configuration considers the effect of eccentric fuel assembly positioning, the fuel enrichment, the minimum average pitch (center-to-center spacing) permitted by fabrication, the minimum wall thickness, the minimum poison concentration, the maximum poison sheet thickness, and the cell I.D.

3.3.2.2 Abnormal Configurations

(1) Single Storage Cell Displacement

Displacement of a single storage cell within the array is precluded by the welded construction and the presence of structure between cells. Therefore, the effect of such a displacement is taken to be zero.



(2) Fuel Handling Incident

Accidental placement of fuel between the fuel racks or the racks and pool wall will be prevented by structural material. It is, however, conceivable that an assembly could be laid across the top of a fuel rack. In this case, the distance between the tops of the stored fuel and the bottom of the misplaced fuel will be greater than 17 inches, a distance which according to calculations effectively "decouples" the two groups of fuel. No increase in  $k_{\text{eff}}$  will result from this incident.

(3) Pool Temperature Variation

Calculations were performed to determine the sensitivity of  $k_{\text{eff}}$  for the reference configuration to variations in the spent fuel pool temperature. The pool temperature was varied from 68°F (minimum pool water temperature at Indian Point 2), where water density is maximum, to 250°F, the approximate boiling point of water near the bottom of the fuel rack.

(4) Fuel Drop Incident

The maximum height through which a fuel assembly can be dropped onto the fuel storage racks is limited. The dropped fuel assembly will most likely impact the tops of the fuel storage rack cells. Because of the fuel rack design, damage will be limited to the upper 1 inch (5 inches for new fuel drop) of the storage cells. Since the active fuel region is about 11 inches (7 inches for new fuel drop) below this area, no significant change in fuel/cell geometry will occur. However, it is possible for a dropped fuel assembly to enter a cell cleanly and impact directly on the fuel stored in the cell. The effect of this type of fuel drop incident was evaluated from a criticality viewpoint by assuming that the stored assembly would be compressed axially.

A calculation based on an axial compression of 2 feet yielded a 0.06 decrease in  $k_{\text{oo}}$  of the fuel cell. It has been concluded, therefore, that this incident would reduce  $k_{\text{eff}}$  and need not be considered further in this analysis.



(5) Heavy Object Drop

In the unlikely event that a heavy object is dropped on the storage rack with sufficient impact to cause structural deformation, it has been concluded that  $k_{eff}$  will decrease. The basis for this conclusion is that the principal effect of dropping a heavy object will be to squeeze water from the rack. Both in the case of compacted fuel and voided pool water, depletion of water leads to a decrease in  $k_{eff}$ .

It would not be possible for a dropped heavy object to eject the poison material from the rack; the crushing effect of the heavy object could only act to compress the fuel and poison together.

(6) Seismic Incident

Seismic analyses have determined that during a DBE the pitch between two adjacent fuel assemblies could narrow locally, due to oscillations about nodal points determined by structural members locating the cells within the racks. However, at the same time, the local pitch at other locations is greater by the same amount. Thus, the net effect, although the pitch may vary locally, is that the average pitch is unaffected. In the event that the entire rack is displaced by a seismic event, the average pitch will also be unaffected.

It is concluded, therefore, that if the fuel assemblies deflect independently in random directions or move together in a single direction, the average pitch between assemblies and, consequently, the  $k_{eff}$  are unaffected.

(7) "Worst Case" Abnormal Configuration

The "worst case" abnormal configuration considers the effect of the most adverse abnormal condition in combination with the "worst case" normal configuration.



### 3.3.3 Calculational Methods

For the reference configuration discussed in Section 3.3.2.1(1), the  $k_{\text{eff}}$  was determined from a three-dimensional Monte Carlo calculation using KENO IV with a 123 group cross section set. Check calculations of the reference configuration as well as the parametric studies were performed with two-dimensional diffusion theory using HAMMER and EXTERMINATOR. Details on the calculational methods, codes and input/output data are presented in Reference 15.

#### 3.3.3.1 Code Description

(1) KENO IV

KENO IV is a 3-D multigroup Monte Carlo code used to determine  $k_{\text{eff}}$  (Ref. 16).

(2) HAMMER

HAMMER (Ref. 17) is a multigroup integral transport theory code which is used to calculate lattice cell cross sections for diffusion theory codes. This code has been extensively benchmarked against  $D_2O$  and light water moderated lattices with good results.

(3) EXTERMINATOR

EXTERMINATOR (Ref. 18) is a 2-D multigroup diffusion theory code used with input from HAMMER to calculate  $k_{\text{eff}}$  values.

#### 3.3.3.2 Uncertainties and Benchmark Calculations

The errors in Monte Carlo criticality calculations can be divided into two classes.

- (1) Uncertainty due to the statistical nature of the Monte Carlo methods.
- (2) Errors due to bias in the calculational technique.

The first class of errors can be reduced by simply increasing the number of neutrons tracked. For rack criticality calculations, the number of neutrons tracked is selected to reduce this error to less than 1%.



The second class of error is accounted for by benchmarking the calculational method against experimental results. In the benchmarking process, the calculational method is used to determine the criticality value for a critical experiment configuration. The difference between the calculated criticality value and the experimental value is identified as the calculational bias. Once determined, this bias can be applied to other calculational results obtained for similar configurations to improve the degree of calculational accuracy.

NES has performed benchmark calculations with KENO IV for several appropriate critical experiments performed by Babcock and Wilcox (Ref. 19), Battelle Northwest Laboratories (Ref. 20), and Allis Chalmers (Ref. 21). The results of the KENO IV calculation indicate that the calculated  $k_{\text{eff}}$  values are greater than the experimental values.

### 3.3.4 Results of Analysis

#### 3.3.4.1 Normal Configuration

The  $k_{\text{eff}}$  determined by KENO IV using the 123 group cross section set was 0.933 with an uncertainty of  $\pm 0.006$  at the 95% confidence level. Results for normal configuration can be summarized as follows:

	<u><math>k_{\text{eff}}</math></u>	<u><math>\Delta k_{\text{eff}}</math></u>
1. Reference Configuration	0.933	-
2. Eccentric Positioning		0.004
3. Enrichment Variation		0.000(Max used)
4. Minimum Cell Pitch ( $\pm 1/64$ in)		0.0013
5. Cell Wall Thickness ( $\pm 0.0025$ in)		0.0003
6. Minimum Poison Concentration ( $\pm 0.1w/o$ )		0.004
7. Poison Sheet Thickness ( $\pm 0.004$ in)		0.0013
8. Cell ID ( $\pm 1/16$ in)		0.006
9. Statistical Uncertainty in KENO		0.006



The effects of the above normal variations are combined statistically as follows:

$$\Delta k_{\text{eff}} = (0.004^2 + 0.0013^2 + 0.0003^2 + 0.004^2 + 0.0013^2 + 0.006^2 + 0.006^2)^{1/2} = 0.0104$$

The result for the "worst case" normal configuration is  $0.933 \pm 0.010$ .

#### 3.3.4.2 Abnormal Configurations

The  $k_{\text{eff}}$  of the rack was studied for temperatures ranging from 68°F to 250°F. Results show that the rack has a negative temperature coefficient with the highest  $k_{\text{eff}}$  occurring at the Indian Point 2 minimum pool water temperature of 68°F. Therefore, the  $\Delta k_{\text{eff}}$  associated with the spent fuel pool water temperature variation is zero in this analysis.

As discussed in Section 3.3.2.2, the  $\Delta k_{\text{eff}}$ 's caused by single storage cell displacement, fuel handling accident, fuel drop accident, heavy object drop and seismic incident are negligible, and no allowance on  $k_{\text{eff}}$  is made for any of these abnormal configurations.

The "worst case" abnormal configuration combines the change in  $k_{\text{eff}}$  due to the occurrence of the most adverse abnormal condition with the  $k_{\text{eff}}$  value associated with the "worst case" normal configuration. However, since none of the abnormal conditions gives a positive  $\Delta k$ , the "worst case" abnormal condition is simply equal to the "worst case" normal condition:  $0.943 \pm 0.000 = 0.943$ .

The  $k_{\text{eff}}$  value of 0.943 meets the criticality design criterion and substantially below 1.0. Therefore, it has been concluded that the spent fuel racks for Indian Point 2 are safe from a criticality standpoint when loaded with the specified fuel.

### 3.4 THERMAL-HYDRAULIC ANALYSIS

#### 3.4.1 Method of Analysis and Assumptions

Fuel storage racks have been designed to increase the present fuel storage capacity of the Indian Point 2 spent fuel storage pool to a total of 980 assemblies.



The maximum heat loads resulting from the expanded spent fuel storage capacity, have been calculated for two cases: the normal batch discharge and the abnormal full core discharge.

- (1) The normal case assumes conservatively discharging a maximum of 90 fuel assemblies every 18 months with 90 hours of cooling time after shutdown. A plant capacity factor of 85% was assumed. The maximum heat load is scheduled to occur after the discharge of nine batches with adequate storage kept in reserve for a full core discharge.
- (2) The assumed abnormal case is the discharge of a full core (193 assemblies) at any time during the cycle. The maximum heat load has been determined to occur soon after the startup following the scheduled refueling outage. Cooling time to discharge is 400 hours after shutdown.

Decay heat generation is calculated according to Branch Technical Position APC SB 9-2, (Ref. 22). Rated reactor power is assumed to be 3216 Mwt.

The increase of the pool water bulk temperature as a function of time has been determined assuming a failed heat removal system for normal and abnormal cases. Maximum pool water bulk temperature was assumed to be 150°F. The heatup rates and times to reach boiling temperature of 212°F were based on complete mixing of the pool water.

The adequacy of natural circulation flow throughout the fuel racks to cool the fuel assemblies was verified. The natural circulation flow was calculated by establishing a thermal-hydraulic balance for the worst row of assemblies (from a recent batch discharge with a 90-hour cooling period). The flow was maintained by the thermal driving head produced by the decay heat generation of each assembly. The pool was modeled as a large volume with a bulk temperature unaffected by local disturbances. The pressure losses considered in the analysis included:



- (1) Friction losses in the downcomer region, in the rack inlet plenum and in the fuel assembly.
- (2) Losses in turns.
- (3) Form losses in the fuel assemblies at the inlet, outlet, and grid locations.

Flow to the worst row of cells was assumed to be available from the narrowest downcomer only. Coolant from the cask handling area and rack-to-rack gaps was conservatively neglected. All fuel assemblies were assumed to have been freshly discharged (90-hour cooling time) with radial peaking factors of 1.2. A maximum bulk pool temperature of 150°F was assumed. Details of calculational methods, assumptions and conclusions are presented in Reference 23.

#### 3.4.2 Results of Analysis

The maximum normal heat load has been calculated to result in a decay heat generation of  $27.2 \times 10^6$  Btu/hr, assuming a 90-hour cooling period after shutdown.

The maximum abnormal heat load resulting from the emergency discharge of a full core (193 assemblies) into the pool two months after a scheduled shutdown and one month after the startup. Results in a decay heat generation rate of  $31.6 \times 10^6$  Btu/hr, assuming a 400-hour cooling period.

The Indian Point 2 spent fuel pool heat removal system is rated to remove  $30.8 \times 10^6$  Btu/hr from the system with a pool water temperature of 135°F. If the water temperature is allowed to increase to 150°F,  $40.7 \times 10^6$  Btu/hr can be extracted from the spent fuel water. Consequently, the cooling capacity is adequate for both the reload design and abnormal discharge cases.

In case of a complete failure of the Indian Point 2 spent fuel heat removal system, the maximum heat-up rates calculated for the maximum normal and abnormal heat loads anticipated are 13.0 and 15.1°F/hr, respectively. The total times available to perform repairs for the maximum normal and abnormal heat loads are 4.8 and 4.1 hours, respectively before makeup is required for pool boil-off. The makeup required is approximately 57 and 66 gpm of water for normal and abnormal heat loads.



The adequacy of the natural circulation flow to cool the worst row in the rack configuration was verified by establishing a thermal-hydraulic balance. The chief concern is the possibility of local boiling due to flow starvation in some cells of the rack matrix as a result of excessive pressure losses in the natural circulation loops established in the spent fuel pool.

The analysis shows that even under the most conservative assumption, the natural circulation in the pool is adequate to preclude boiling by a substantial margin, assuming a bulk pool temperature of 150°F. The maximum temperature increase in the assembly with minimum flow is 76.8°F, resulting in an outlet temperature of 226.8°F. This is below the saturation temperature of 239°F, corresponding to the static head at the top of the fuel assembly.

It should be noted that the maximum assembly outlet temperature of 226.8°F reported above is unlikely to occur in the pool, as it is the result of excessively conservative assumptions postulated to establish a calculational boundary. In the analysis, the major portion of the total pressure drop in the natural circulation loop is caused by the selection of the narrowest gap in the pool as the sole flow path to the bottom plenum from the water above the racks. The expected mode of natural circulation is for the coolant to reach the plenum via least-resistant flow paths, such as the cask area, the north wall downcomer gap of 11-9/10", the failed fuel elevator area, and between the 2-1/2" gap between racks, all of which have been neglected in the analysis.

### 3.5 RADIOLOGICAL ANALYSIS

#### 3.5.1 Method of Analysis and Assumptions

A radiological analysis has been performed on the spent fuel storage pool at Indian Point 2 for an expanded storage capacity of 980 assemblies. This analysis included conservative estimates of exposure rates due to radionuclides in the spent fuel storage pool and spent fuel assembly movement in the pool. Accident analyses were also performed on spent fuel assembly drop and cask drop accidents in accordance with the methods outlined by Regulatory Guide 1.25 (Ref. 24). Assumption and methodology used in these evaluations are presented in Reference 25.



The radiological analysis has been performed using the following assumptions:

- (1) The radionuclide concentrations in the primary coolant are based upon 0.12% failed fuel.
- (2) Fuel pool nuclide concentrations for all isotopes were computed considering normal cleanup prior to refueling.
- (3) There is a uniform mix of reactor coolant and refueling water.
- (4) Refueling operations begin no earlier than 90 hours after shutdown (Ref. 6).
- (5) The pool water is considered as a self-attenuating slab source with a constant source distribution,  $S(x) = S$ . The fuel element is modeled as a line source.
- (6) A peaking factor of 1.65 has been included in the fuel handling accident analysis to account for the radial peaking per Regulatory Guide 1.25. For the cask drop evaluation with damage to an entire core of 193 assemblies, a peaking factor of 1.0 was used.
- (7) There is assumed to be a minimum of 9ft-4in of water covering the fuel pins.
- (8) An accident (X/Q) value of  $6.6 \times 10^{-4} \text{ sec/m}^3$  has been used in the calculations (Ref. 6).

### 3.5.2 Results of Analysis

Using the source terms corresponding to 0.12% failed fuel in the reactor core, an exposure rate of  $\chi = 1.10 \text{ mR/hr}$  has been calculated at the surface of the pool from nuclides distributed in the pool water.

The dose rate to an operator on the bridge hoist in the fuel storage building or on the manipulator crane in the containment building during fuel movement has been estimated to be less than 3.0 mR/hr 90 hours after shutdown. This dosage would be incurred only during actual movement of spent fuel.



The calculation of the absorbed doses to the total body and thyroid due to fission product releases from a fuel element as a result of a spent fuel assembly handling accident 90 hours following operation at a power level of 3216 MWt, using the methodology of Regulatory Guide 1.25 yields:

$$D_{\text{total body}} = 3.11 \text{ Rem}$$

$$D_{\text{thyroid}} = 26.6 \text{ Rem}$$

The absorbed doses to the total body and thyroid in a cask drop accident occurring 90 days after shutdown are:

$$D_{\text{total body}} = 12.7 \text{ Rem}$$

$$D_{\text{thyroid}} = 1.79 \text{ Rem}$$

These absorbed doses are less than a small fraction of the limits specified by 10 CFR Part 100.

### 3.6 SPENT FUEL RACK INSTALLATION

The spent fuel racks will be free standing, and free to slide horizontally on the pool floor, as there will be no lateral bracing between racks or between racks and pool walls. Adequate clearances are provided so that there will be no collisions between racks or the pool walls during the worst event (the design basis earthquake). All loads imparted to the racks are transmitted to the pool floor through support feet attached to the bottom of the racks. The rack support feet will be designed to avoid colliding with existing shims and pins on the pool floor during the DBE. In most cases, the feet can be positioned on the pool floor to avoid existing shims when installing the racks. In a few instances, stainless steel plates will be designed to bridge over shims and carry the support feet, allowing the feet to slide on the plates and transmitting loads to the pool floor without contacting shims.



The racks and bridging plates will be installed in a wet pool. Provisions will be made to install enough new high density racks before existing racks are removed so that existing fuel will always remain in the pool.

The racks will be designed so that the amount of work in the pool and the removal of fixed items in the pool (i.e., brackets, etc. that would require cutting to remove) are kept to a practical minimum. No floor shims or pins, all of which are welded to the pool floor, will have to be removed.

It is anticipated that remote tooling will be used to remove a half dozen welded brackets and to place two dozen bridging plates over existing shims on the pool floor. The plates will not be attached to the floor. Actual leveling will also be done remotely, by tools used to screw support feet up or down. If required, divers will be used to assist in any of the above operations.

Existing racks will be removed from the pool and decontaminated. Decontamination results will determine whether the racks will be disposed as clean waste or whether they will have to be cut up and packed for disposal as radioactive waste.



#### 4. REFERENCES

1. USNRC Regulatory Guide 1.29, "Seismic Design Classification," Rev. 3, Sept. 1978.
2. USNRC Regulatory Guide 1.92: "Combination of Modes and Spatial Components in Seismic Response Analysis," Rev. 1, February 1976.
3. USNRC Standard Review Plan, Section 3.8.4.
4. USNRC: "Position Paper for Review and Acceptance of Spent Fuel Storage and Handling Applications," April 14, 1978 and Supplement January 18, 1979.
5. American Institute of Steel Construction: "Manual of Steel Construction," Seventh Edition, 1970.
6. Consolidated Edison Company, "Design, Fabricate, Deliver and Installation of Spent Fuel Storage Racks," Specification No. MP79-001, Rev. 2, March 1979.
7. Dong, R. G. "Effective Mass and Damping of Submerged Structures," Lawrence Livermore Laboratory, UCRL-52342, April 1978.
8. Fritz, R. J. "The Effects of Liquids on the Dynamic Motions of Immersed Solids," Journal of Engineering for Industry, Trans. ASME, February 1972.
9. MRI/STARDYNE 3 - Static and Dynamic Structural Analysis Systems for Scope 3.4 Operating System User's Information Manual, Revision A, Control Data Corporation, August 1976.
10. Nuclear Energy Services Inc., "Structural Analysis Report for Indian Point Generating Station Unit 2 Fuel Storage Racks," NES-81A0610, November 1979.
11. "Nuclear Reactors and Earthquakes" prepared by Lockheed Aircraft Corporation and Holmes and Narver, Inc., TID 7024; Atomic Energy Commission, Washington D.C.



12. Nuclear Energy Services, Inc., "Non-linear Time History Seismic Sliding Analysis Report for Indian Point Generating Station Unit 2," Document NES 81A0615, Nov. 1979.
13. Houbolt, J.C., "The Recurrence Matrix Solution for the Dynamic Response for Elastic Aircraft Structures," Journal of Aeronautical Science, Volume 17, 1950.
14. Swanson Analysis Inc., "ANSYS - Engineering Analysis System," Revision 3, Update 37J, Boeing Computer Services 6600, January 1977.
15. Nuclear Energy services, Inc., "Nuclear Analysis Report for the Indian Point Generating Station Unit 2 Spent Fuel Storage Racks," NES-81A0608, December 1979.
16. ORNL-4938, "KENO IV - An Improved Monte Carlo Criticality Program," L.M. Petrie, N.F. Cross, November 1975.
17. DP-1064, the HAMMER System, J.E. Sutch and H.C. Honeck, January 1967.
18. ORNL-4078, EXTERMINATOR-2, T.B. Fowler et al, April 1967.
19. Bromley, W.D., Olszewski, L.S. Safety Calculations and Benchmarking of Babcock & Wilcox Designed Close Spaced Fuel Storage Racks, Nuclear Technology, Vol. 41, Mid-December 1978, p. 346.
20. Bierman, S.R., Durst, B.M., Critical Separation Between Clusters of 4.29 wt%  $^{235}\text{U}$  Enriched  $\text{UO}_2$  Rods in Water with Fixed Neutron Poisons, May 1978, NUREG/GR-0073-RC.
21. NES 81A0260 "Criticality Analysis of the Atcor, Vandenberg Cask" R.J. Weader, February, 1975.



22. USNRC Branch Technical Position APCS 9-2, "Residual Decay Energy for Light Water Reactors for Long-term Cooling," December 24, 1975.
23. Nuclear Energy Services, Inc., "Thermal-Hydraulic Analysis Report for the Indian Point Generating Station Unit 2 Fuel Storage Racks, NES-81A0609, November 1979.
24. USNRC Regulatory Guide 1.25.
25. Nuclear Energy Services, Inc., "Radiological Analysis Report Indian Point Generating Station Unit 2 Fuel Storage Racks," NES-81A0614, November 1979.

ATTACHMENT B

Nuclear Analysis Report  
for the  
Indian Point Unit No. 2 Spent  
Fuel Storage Racks

Consolidated Edison Company of New York, Inc.  
Indian Point Unit No. 2  
Docket No. 50-247  
May, 1980



**NUCLEAR ANALYSIS REPORT  
FOR THE  
INDIAN POINT UNIT NO. 2  
SPENT FUEL STORAGE RACKS**

**Prepared for  
Consolidated Edison Company of New York, Inc.**



## TABLE OF CONTENTS

	<u>PAGE</u>
1. SUMMARY	6
2. INTRODUCTION	8
3. DESCRIPTION OF SPENT FUEL STORAGE RACKS	9
4. CRITICALITY DESIGN CRITERION AND CALCULATIONAL ASSUMPTIONS	
4.1 Criticality Design Criterion	12
4.2 Calculational Assumptions	12
5. CRITICALITY CONFIGURATIONS	14
5.1 Normal Configurations	14
5.1.1 Reference Configuration	14
5.1.2 Eccentric Configuration	14
5.1.3 Fuel Assembly Tolerance	16
5.1.4 Fuel Design Variation	16
5.1.5 Fuel Rack Variation	16
5.1.6 Cell Wall Thickness Variation	16
5.1.7 Poison Concentration Variation	17
5.1.8 Borated Steel Sheet Thickness Variation	17
5.1.9 Cell Inside Diameter Variation	17
5.1.10 "Worst Case" Normal Configuration	17
5.2 Abnormal Configurations	18
5.2.1 Single Storage Cell Displacement	18
5.2.2 Fuel Handling Incident	18
5.2.3 Pool Temperature Variation	18
5.2.4 Fuel Drop Incident	18
5.2.5 Heavy Object Drop	19
5.2.6 Seismic Incident	19
5.2.7 "Worst Case" Abnormal Configuration	20
6. CRITICALITY CALCULATIONAL METHODS	21
6.1 Method of Analysis	21
6.2 Reference Configuration	21
6.3 Uncertainties and Benchmark Calculations	23
6.4 Code Description	24
6.4.1 KENO IV	24
6.4.2 HAMMER	24
6.4.3 EXTERMINATOR	24



## TABLE OF CONTENTS (CONT'D)

	<u>PAGE</u>
7. RESULTS OF CRITICALITY CALCULATIONS	25
7.1 Reference Configuration	25
7.2 $K_{eff}$ Values for Normal Configurations	25
7.2.1 Eccentric Configuration	25
7.2.2 Fuel Design Variation	25
7.2.3 Fuel Rack Pitch Variation	26
7.2.4 Fuel Rack Cell Wall Thickness Variation	26
7.2.5 Poison Content Variation	26
7.2.6 Poison Sheet Thickness Variation	26
7.2.7 Cell Inside Dimension Variation	26
7.2.8 "Worst Case" Normal Configuration	27
7.3 $K_{eff}$ Values for Abnormal Configurations	27
7.3.1 Spent Fuel Pool Temperature Variation	27
7.3.2 Other Abnormal Configurations	28
7.3.3 "Worst Case" Abnormal Configuration	28
8. REFERENCES	39



## LIST OF FIGURES

	<u>PAGE</u>
3.1 Fuel Storage Rack Arrangement Plan	10
3.2 Borated SST Fuel Storage Rack (10x10)	11
5.1 Reference and Eccentric Fuel Configuration	15
6.1 Reference Configuration	22
7.1 $\Delta k_{\text{eff}}$ vs. Enrichment	29
7.2 $\Delta k_{\text{eff}}$ vs. Pitch	30
7.3 $\Delta k_{\text{eff}}$ vs. Wall Thickness	31
7.4 $\Delta k_{\text{eff}}$ vs. Boron Concentration	32
7.5 $\Delta k_{\text{eff}}$ vs. Borated Steel Sheet Thickness	33
7.6 $\Delta k_{\text{eff}}$ vs. Cell ID	34
7.7 $\Delta k_{\text{eff}}$ vs. Pool Water Temperature	35
7.8 $\Delta k_{\text{eff}}$ vs. Pool Water Density	36

## LIST OF TABLES

7.1 Fuel Parameters	37
7.2 Parameters and Results of Variation Calculations	38



## 1. SUMMARY

A detailed nuclear analysis has been performed for the NES (Nuclear Energy Services, Inc.) designed fuel storage racks for the Indian Point Generating Station Unit 2 (Indian Point 2). This analysis demonstrates that, for all anticipated normal and abnormal configurations of fuel assemblies within the fuel storage racks, the  $k_{eff}$  of the system is less than the criticality criterion of 0.95 for 3.5 w/o, 15x15 Westinghouse fuel assemblies. Certain conservative assumptions about the fuel assemblies and racks have been used in the calculations.

Both normal and abnormal configurations were considered in the analysis. The reference configuration consists of a square array, infinite in lateral extent, of storage cells spaced 10-15/16 inches on centers. Each storage location contains one centrally located 15x15 Westinghouse fuel assembly. Storage cells consist of a square stainless steel box with inner dimension of 9.0 inches and wall thickness of 0.0825 inch. Criticality control is provided by 0.100-inch thick borated stainless steel sheets, 7 inches wide, 145 inches long, affixed to each outside wall of the steel boxes. This reference configuration provides a base of comparison relative to which effects of normal and abnormal variations have been measured. Normal configurations include: eccentrically positioned fuel, fuel enrichment variation, dimensional and material variations permitted by fabrication tolerances, and variation in the density of the boron in the borated stainless steel sheets.

Abnormal configurations include: pitch variation due to seismic events, spent fuel pool temperature variations and fuel handling accidents such as misplaced fuel assemblies.

The principal method of calculation used to determine the  $k_{eff}$  of the Indian Point 2 spent fuel storage racks was the Monte Carlo code KENO IV with a cross section set of 123 energy groups. Cross section input for the 123 energy group set was generated from the XSDRN library using the AMPX module NITAWL.

Parametric studies to determine the effects on  $k_{\text{eff}}$  of changes in fuel rack dimensions, temperature, and fuel assembly enrichment were performed with diffusion theory. Fuel, water and structural cross sections were determined using the HAMMER code, while blackness theory was used to determine the cross sections for the borated steel sheets.  $k_{\text{eff}}$  values were calculated using EXTERMINATOR, a multigroup, two-dimensional diffusion theory code.

The  $k_{\text{eff}}$  value calculated by KENO for the reference configuration is 0.933. Variations in  $k_{\text{eff}}$  due to normal configuration changes and calculational uncertainty were determined to be 0.010. The  $\Delta k_{\text{eff}}$  due to the "worst case" abnormal configuration is 0.000. Combining these two  $\Delta k_{\text{eff}}$  values with the  $k_{\text{eff}}$  for the reference configuration of 0.933 results in a final  $k_{\text{eff}}$  value equal to 0.943. This value meets the criticality design criterion and is substantially below 1.0. Therefore, it has been concluded that the high density storage racks for Indian Point 2 when loaded with the specified fuel are safe from a criticality standpoint.



## 2. INTRODUCTION

The NES design for Indian Point 2 high density spent fuel storage racks achieves high storage density through the use of borated stainless steel sheets placed on the walls of the storage cells. Details of the rack materials and structure are given in Section 3.

A detailed nuclear analysis has been performed to demonstrate that, for all anticipated normal and abnormal configurations of fuel assemblies within the fuel storage racks, the  $k_{\text{eff}}$  of the system is substantially below 1.0. Certain conservative assumptions about the fuel assemblies and racks have been used in the calculations. These are described in Section 4 along with the criticality design criterion for the fuel assemblies and racks.

The reference configuration which forms the basis of the criticality calculations represents the storage racks in nominal dimensions at 68°F with all fuel assemblies centrally located within their storage cells. Variations from this reference configuration were studied, and included effects of wall thickness and pitch variations, fuel enrichment and poison content variations, cell inside dimension variations, water temperature variations and eccentric fuel positioning. Fuel handling accidents were studied and their effects determined. The configurations studied are described in detail in Section 5. A description of the calculational methods, benchmarking results, and computer codes is given in Section 6. The results of the criticality analysis are presented in Section 7.



### 3. DESCRIPTION OF SPENT FUEL STORAGE RACKS

Five sizes of fuel storage racks, with 8x8, 8x9, 8x10, 9x10, and 10x10 storage cell arrays, will be used in the Indian Point 2 spent fuel storage pool (see Figure 3.1). The total number of fuel storage locations within the pool will be 980.

The wall of each storage cell is made up of a nominal 0.0825 inch ( $0.080^{+0.005}_{-0.000}$ ) thick sheet of Type 304 stainless steel, formed into a square with an inner dimension of 9.0 inches. On the outside of each of the four sides of this wall, a borated stainless steel sheet containing 1.1 nominal w/o of boron is placed for criticality control. This sheet is 0.100 inch thick, 7 inches wide and 145 inches long, and is centrally located on the outer wall of the storage cell.

Storage cells are maintained at a center-to-center spacing of 10-15/16 inches by welded spacers. See Figure 3.2 for a schematic drawing of a representative 10x10 rack.

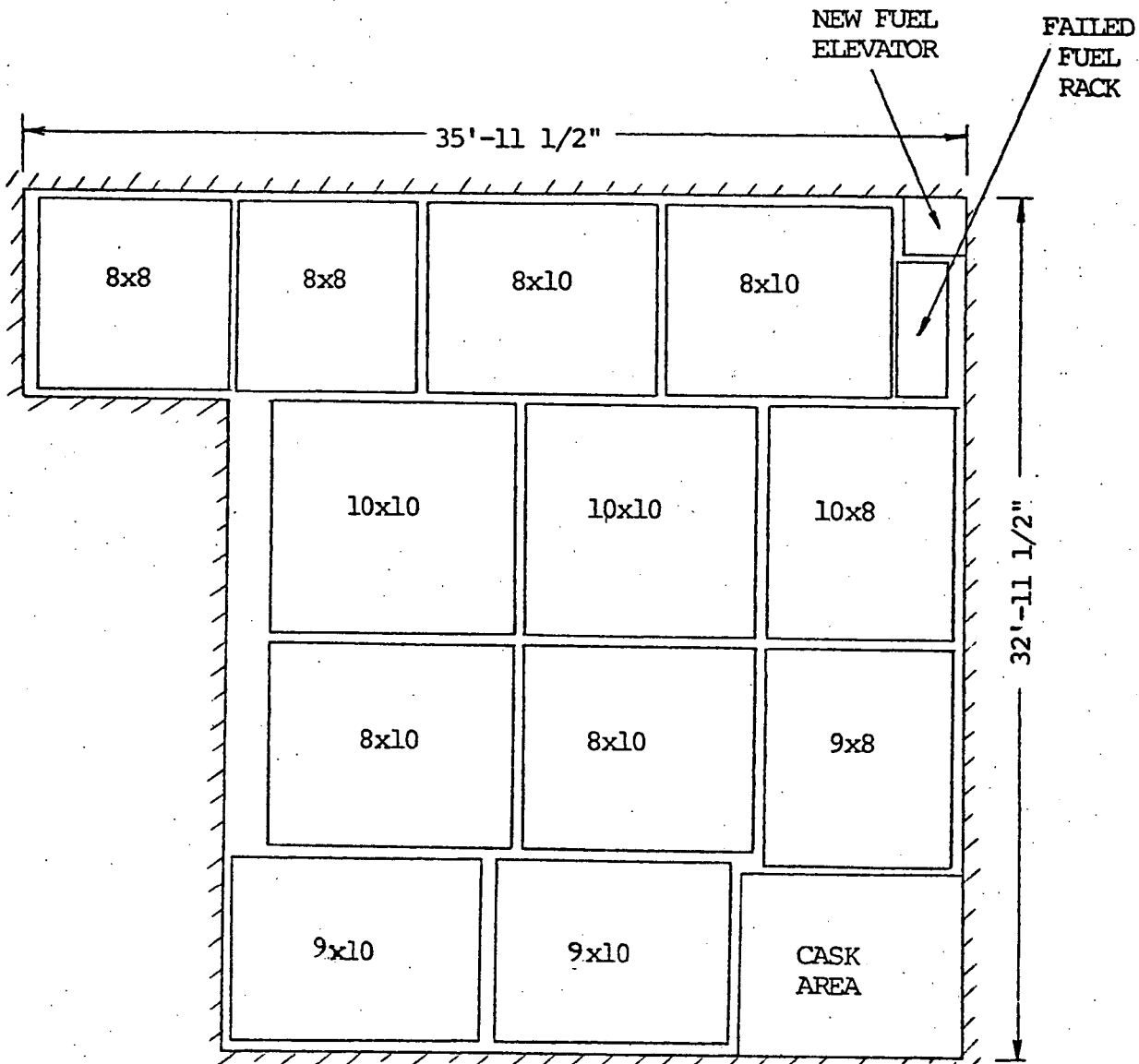


Figure 3.1 Fuel Storage Rack Arrangement Plan

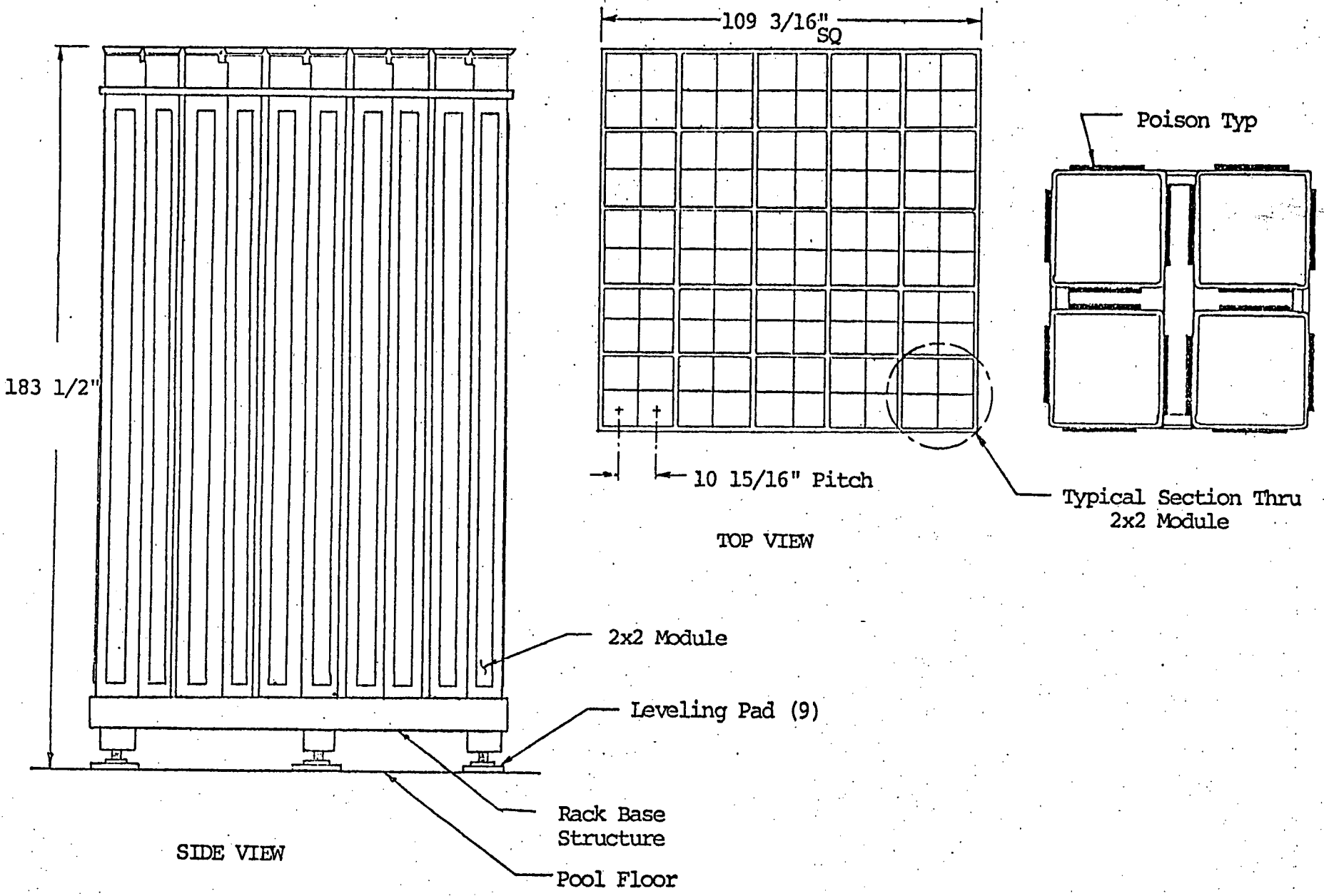


Figure 3.2 Indian Point 2  
Borated SST Fuel Storage Rack (10x10)



#### 4. CRITICALITY DESIGN CRITERION AND CALCULATIONAL ASSUMPTIONS

##### 4.1 CRITICALITY DESIGN CRITERION

A satisfactory value of  $k_{\text{eff}}$  for a spent fuel pool involves considerations of safety, licensability and storage capacity requirements. These factors demand a  $k_{\text{eff}}$  substantially below 1.0 for safety and licensability but high enough to achieve the required storage capacity.

The published position of the NRC on fuel storage criticality, stated in a communique to all reactor licensees (Ref. 1) is as follows:

"The neutron multiplication factor in spent fuel pools shall be less than or equal to 0.95, including all uncertainties, under all conditions".

Furthermore, NRC, in evaluating the design, will "check the degree of subcriticality provided, along with the analysis and the assumptions".

On the basis of this information, the following criticality design criterion has been established for the Indian Point 2 high density fuel storage racks: "The neutron multiplication factor ( $k_{\text{eff}}$ ) shall be less than 0.95 for all normal and abnormal configurations as determined by Monte Carlo calculation".

##### 4.2 CALCULATIONAL ASSUMPTIONS

The following conservative assumptions have been used in the criticality calculations performed to verify the adequacy of the rack design:

1. The fuel is fresh and of a specified enrichment (3.5 w/o) greater than or equal to that of any fuel available.



2. The reference configuration contains an infinite square array of storage locations spaced  $10\text{-}15/16$  inches on centers. This is conservative because the array is not infinite, but finite.
3. The absorption of the fuel assembly spacers is ignored.
4. Any burnable poisons in the fuel assemblies are ignored.
5. Any soluble poison in the pool water is ignored.



## 5. CRITICALITY CONFIGURATIONS

In order to verify the design adequacy of the Indian Point 2 high density storage rack, it is necessary to establish the multiplication constants for the various arrangements or configurations of fuel assemblies and storage cells that are possible within the racks. These arrangements or configurations can be classified as either normal or abnormal configurations. Normal configurations result from variation in the placement of fuel within the storage cell, variation in fuel assembly dimensions and/or fuel loading because of the manufacturing process, and the variation in fuel storage rack dimensions permitted in fabrication. Abnormal configurations are typically the result of accidents or malfunctions such as the seismic event, a failure in the fuel pool cooling system (excessive changes in pool water temperature), a dropped fuel assembly, etc. The following sections present the normal and abnormal configurations which have been considered in this analysis.

### 5.1 NORMAL CONFIGURATIONS

#### 5.1.1 Reference Configuration

The reference configuration consists of an infinite array of storage cells having nominal dimensions (see Section 3) each containing a fresh 15x15 Westinghouse fuel assembly centrally located within the storage cell. The water temperature within the rack is 68°F.

#### 5.1.2 Eccentric Configuration

It is possible for a fuel assembly not to be positioned centrally within a storage cell because of the clearance allowed between the assembly and the cell wall. This clearance is nominally 0.2775 inches on each side of the fuel assembly.

Calculations have been performed to determine the effects of eccentrically located fuel. In these calculations it was assumed that four fuel assemblies were diagonally displaced within their storage cells as far as possible towards each other (see Figure 5.1).

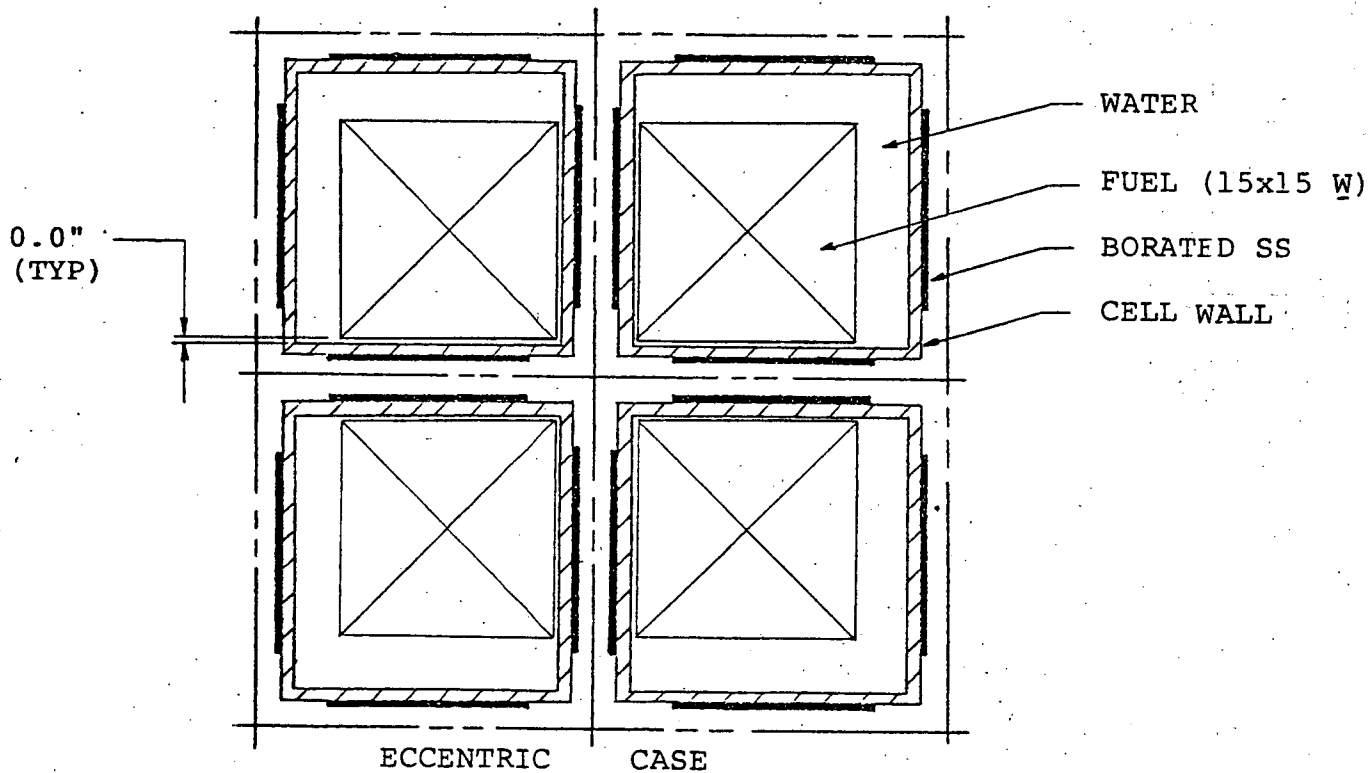
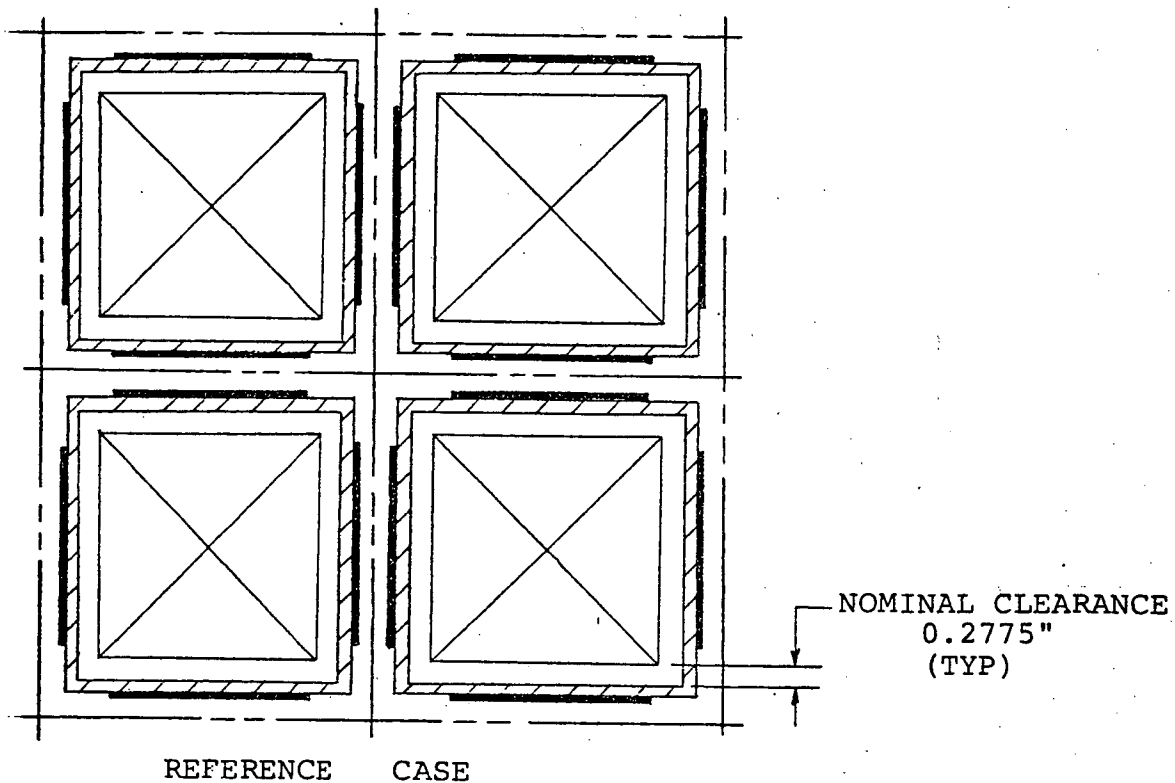


FIG. 5.1 REFERENCE AND ECCENTRIC FUEL CONFIGURATIONS



### 5.1.3 Fuel Assembly Tolerance

The important fuel assembly parameter determining  $k_{eff}$  is the ratio of the amount of  $U^{235}$  to that of water. The amount of  $U^{235}$  per assembly is controlled to within a few tenths of a percent by weighing pellet stacks as the fuel is built and by using a known enrichment. The fuel assembly parameters which determine the volume of water in an assembly are the clad O.D. and the fuel rod pitch. These parameters are closely controlled to typically within  $\pm 0.4\%$ . The effects of these fuel assembly tolerances on  $k_{eff}$  have been determined to be negligible on the basis of simple  $k_{oo}$  cell calculations. Consequently, fuel assembly tolerances were not considered further in this analysis.

### 5.1.4 Fuel Design Variation

Calculations were performed to determine the sensitivity of  $k_{eff}$  to variations of fuel enrichment from the base enrichment of 3.5 w/o. The criticality configuration used for these calculations was that of the reference configuration with the exception of fuel enrichment which was reduced to 3.3 w/o.

### 5.1.5 Fuel Rack Pitch Variation

Calculations were performed to determine the sensitivity of  $k_{eff}$  to changes in pitch, the center-to-center spacing between storage cells. The pitch was varied from 10-7/8 to 11.0 inches. The criticality configuration was similar to that of the reference configuration except for the obvious change in center-to-center spacing.

### 5.1.6 Cell Wall Thickness Variation

The base case wall thickness was 0.0825 inch for the stainless steel sheet forming the cell walls. This thickness was varied from 0.090 to 0.080 inch to determine the effect on  $k_{eff}$ .



#### 5.1.7 Poison Concentration Variation

The borated stainless steel sheets contain a nominal 1.1 w/o boron in steel. This concentration was reduced to 1.0 w/o to determine the sensitivity of  $k_{\text{eff}}$  to variations in this parameter.

#### 5.1.8 Borated Steel Sheet Thickness Variation

The borated stainless steel sheets are nominally 0.100 inches thick. This dimension was reduced by 1/16 inch to determine the sensitivity of  $k_{\text{eff}}$  to variation in this parameter.

#### 5.1.9 Cell Inside Diameter Variation

The storage cell inside dimension is a nominal 9.0 inches. This dimension was reduced to 8-15/16 inches to establish the sensitivity of  $k_{\text{eff}}$  to variations in this parameter.

#### 5.1.10 "Worst Case" Normal Configuration

The "worst case" configuration considers the effect of eccentric fuel assembly positioning, the fuel enrichment, the minimum average pitch (center-to-center spacing) permitted by fabrication, the minimum cell wall thickness, the minimum poison concentration, the minimum borated stainless steel sheet thickness, and the cell I.D.



## 5.2 ABNORMAL CONFIGURATIONS

### 5.2.1 Single Storage Cell Displacement

Displacement of a single storage cell within the array is precluded by the welded construction and the presence of structure between cells. Therefore, the effect of such a displacement is taken to be zero.

### 5.2.2 Fuel Handling Incident

Accidental placement of fuel between the fuel racks or the racks and pool wall will be prevented by structural material. It is, however, conceivable that an assembly could be laid across the top of a fuel rack. In this case, the distance between the tops of the stored fuel and the bottom of the misplaced fuel will be greater than 17 inches, a distance which according to calculations effectively "decouples" the two groups of fuel. No increase in  $k_{\text{eff}}$  will result from this incident.

### 5.2.3 Pool Temperature Variation

Calculations were performed to determine the sensitivity of  $k_{\text{eff}}$  for the reference configuration to variations in the spent fuel pool temperature. The pool temperature was varied from 68°F (minimum pool water temperature at Indian Point 2), where water density is maximum, to 250°F, the approximate boiling point of water near the bottom of the fuel rack.

### 5.2.4 Fuel Drop Incident

The maximum height through which a fuel assembly can be dropped onto the fuel storage racks is limited. The dropped fuel assembly will most likely impact the tops of the fuel storage rack cells. Because of the fuel rack design, damage will be limited to the upper 1 inch (5 inches for new fuel drop) of the storage cells. Since the active fuel



region is about 11 inches (7 inches for new fuel drop) below this area, no significant change in fuel/cell geometry will occur. However, it is possible for a dropped fuel assembly to enter a cell cleanly and impact directly on the fuel stored in the cell. The effect of this type of fuel drop incident was evaluated from a criticality viewpoint by assuming that the stored assembly would be compressed axially.

A calculation based on an axial compression of 2 feet yielded a 0.06 decrease in  $k_{oo}$  of the fuel cell. It has been concluded, therefore, that this incident would reduce  $k_{eff}$  and need not be considered further in this analysis.

#### 5.2.5 Heavy Object Drop

In the unlikely event that a heavy object is dropped onto the storage rack with sufficient impact to cause structural deformation, it has been concluded that  $k_{eff}$  will decrease. The basis for this conclusion is that the principal effect of dropping a heavy object will be to squeeze water from the rack. Both in the case of compacted fuel and voided pool water, depletion of water leads to a decrease in  $k_{eff}$ .

It would not be possible for a dropped heavy object to eject the poison material from the rack; the crushing effect of the heavy object could only act to compress the fuel and poison together.

#### 5.2.6 Seismic Incident

Seismic analyses have determined that during an SSE the pitch between two adjacent fuel assemblies could narrow locally, due to oscillations about nodal points determined by structural members locating the cells within the racks. However, at the same time, the local pitch at other locations is greater by the same amount. Thus, the net effect, although the pitch may vary locally, is that the average pitch is unaffected. In the event that the entire rack is displaced by a seismic event, the average pitch will also be unaffected.

It is concluded, therefore, that if the fuel assemblies deflect independently in random directions or move together in a single direction, the average pitch between assemblies and, consequently, the  $k_{eff}$  are unaffected.



### 5.2.7 "Worst Case" Abnormal Configuration

The "worst case" abnormal configuration considers the effect of the most adverse abnormal condition in combination with the "worst case" normal configuration. The results of the "worst case" abnormal configuration are presented in Section 7.3.3.



## 6. CRITICALITY CALCULATIONAL METHODS

### 6.1 METHOD OF ANALYSIS

For the reference configuration discussed in Section 5.1.1, the  $k_{\text{eff}}$  was determined from a three-dimensional Monte Carlo calculation using KENO IV with a 123 group cross section set. Check calculations of the reference configuration as well as the parametric studies were performed with HAMMER, lattice cell analysis code, and EXTERMINATOR, two-dimensional diffusion theory code. In both the Monte Carlo and diffusion theory methods, an infinite array of fuel assemblies loaded in spent fuel storage locations was represented by use of appropriate boundary conditions. An infinite array is used for two reasons: (1) an infinite array has a conservatively higher value of  $k_{\text{eff}}$  and (2) the problem can be suitably represented by a repeating portion of the array. Figure 6.1 shows a representation of one quarter of a storage location with reflecting boundaries on all sides. This duplicates an infinite array of storage locations.

### 6.2 REFERENCE CONFIGURATION

In the reference configuration KENO IV calculations, each fuel pin and associated cladding and water was represented as a rectangular parallelepiped with height equal to the active fuel length and the width equal to one fuel rod pitch (0.563 inch). Cladding and fuel were represented by concentric cylinders within the box with atom densities determined from the fuel parameters shown in Table 7.1. Water at 68°F filled the region outside the cladding. Guide tubes were represented in a similar fashion but with water inside the clad instead of fuel. The stainless steel sheets making up the box walls were represented as boxes with thickness of 0.0825 inch and a width equal to the fuel storage cell edge. Borated stainless steel sheets were represented by boxes 0.100 inch thick and 7 inches wide containing a homogenous concentration of boron at 1.1 w/o. Water regions were boxes of appropriate sizes needed to fill the water gaps.

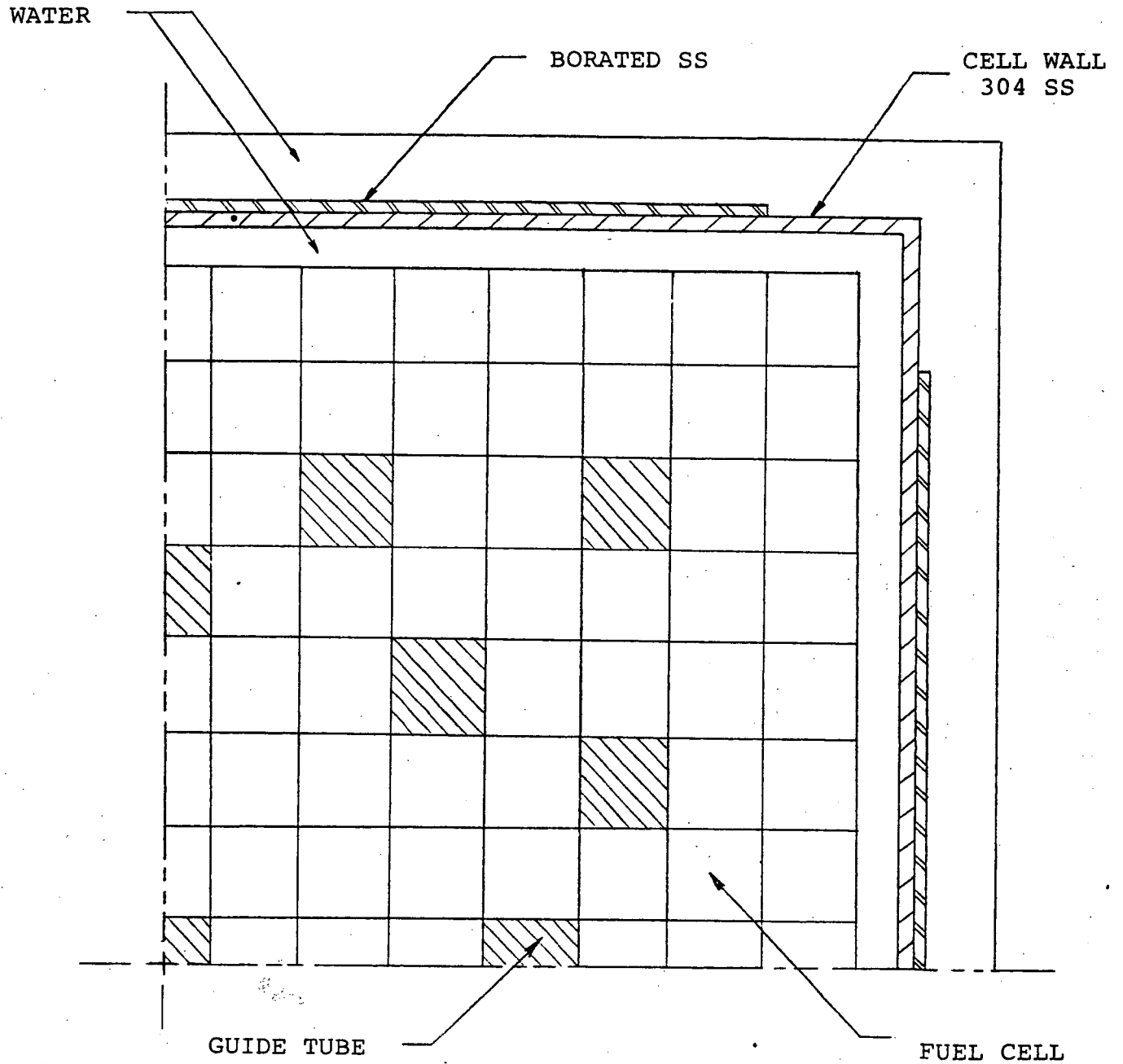


FIG. 6.1 REFERENCE CONFIGURATION



### 6.3 UNCERTAINTIES AND BENCHMARK CALCULATIONS

The uncertainties in Monte Carlo criticality calculations can be divided into two classes.

1. Uncertainty due to the statistical nature of the Monte Carlo methods.
2. Uncertainty due to bias in the calculational technique.

The first class of uncertainty can be reduced by simply increasing the number of neutrons tracked. For rack criticality calculations, the number of neutrons tracked is selected to reduce this error to less than 1%.

The second class of uncertainty is accounted for by benchmarking the calculational method against experimental results. In the benchmarking process, the calculational method is used to determine the criticality value for a critical experiment configuration. The difference between the calculated criticality value and the experimental value is identified as the calculational bias. Once determined, this bias can be applied to other calculational results obtained for similar configurations to improve the degree of calculational accuracy. If the calculated criticality value found during benchmarking is less than the experimental value, then the bias is added to other calculational results to ensure a conservative criticality value consistent with experimental results. Conversely, if the calculational criticality value is greater than the experimental value, it is appropriate to subtract the bias from the other calculational results to improve the accuracy of the criticality determination.

NES has performed benchmark calculations with KENO IV for several appropriate critical experiments reported by Babcock and Wilcox (Ref. 2), Battelle Northwest Laboratories (Ref. 3), and Allis Chalmers (Ref. 4). The results of the KENO IV calculations indicate that the calculated  $k_{\text{eff}}$  values are greater than the experimental values. Consequently, NES has concluded that KENO IV (123 groups) provides conservative results.



## 6.4 CODE DESCRIPTION

### 6.4.1 KENO IV

KENO IV is a 3-D multigroup Monte Carlo code used to determine  $k_{\text{eff}}$  (see Ref. 5).

### 6.4.2 HAMMER

HAMMER (see Ref. 6) is a multigroup integral transport theory code which is used to calculate lattice cell cross sections for diffusion theory codes. This code has been extensively benchmarked against  $D_2O$  and light water moderated lattices with good results.

### 6.4.3 EXTERMINATOR

EXTERMINATOR (see Ref. 7) is a 2-D multigroup diffusion theory code used with input from HAMMER to calculate  $k_{\text{eff}}$  values.

## 7. RESULTS OF CRITICALITY CALCULATIONS

The  $k_{\text{eff}}$  for the reference configuration was determined by means of KENO IV with 123 group cross sections. Parametric studies of enrichment, temperature, dimensional tolerances of the racks, and abnormal dislocations within racks due to seismic events, fuel handling incidents, fuel drop and heavy object drop were performed with the HAMMER/EXTERMINATOR codes.

### 7.1 REFERENCE CONFIGURATION

The  $k_{\text{eff}}$  determined by KENO IV using the 123 group cross section set was 0.933 with an uncertainty of  $\pm 0.006$  at the 95% confidence level.

### 7.2 $K_{\text{eff}}$ VALUES FOR NORMAL CONFIGURATION

#### 7.2.1 Eccentric Configuration

The  $\Delta k_{\text{eff}}$  for the eccentric configuration described in Section 5.1.2 and shown in Figure 5.1 (in which fuel assemblies are diagonally displaced towards each other) was determined to be 0.004.

#### 7.2.2 Fuel Design Variation

The enrichment of the fuel was changed from 3.5 w/o to 3.3 w/o. The results are shown in Figure 7.1 and Table 7.2.



### 7.2.3 Fuel Rack Pitch Variation

A detailed study of the effects of variation in the rack pitch was performed. The pitch was varied from 10-7/8 to 11.00 inches and the results are shown in Figure 7.2 and Table 7.2. The mechanical design of the fuel rack is such that the average pitch between boxes is maintained by structural members at 10-15/16  $\pm$  1/64 inches. The change in  $k_{\text{eff}}$  for a decrease in average pitch of 1/64 inch is +0.0013. (See Figure 7.2.)

### 7.2.4 Fuel Rack Cell Wall Thickness Variation

The value of the wall thickness used in the reference configuration calculation is nominally 0.0825 inches. A variation between 0.080 and 0.090 inches was investigated and the results are shown in Figure 7.3. The material used for the wall will have a thickness tolerance of 0.0025 inches and the  $\Delta k$  for this variation, as determined from Figure 7.3, is +0.0003.

### 7.2.5 Poison Content Variation

The boron content of the borated stainless steel sheets was reduced from the reference value of 1.1 w/o to a minimum of 1.0 w/o with a corresponding increase in  $\Delta k$  of 0.004. The results are shown in Figure 7.4 and Table 7.2.

### 7.2.6 Poison Sheet Thickness Variation

The thickness of the borated stainless steel was varied 1/16 inch to establish the sensitivity of  $k_{\text{eff}}$  to thickness variations with results shown in Figure 7.5 and Table 7.2. The  $\Delta k$  increase corresponding to 0.004 inches fabrication tolerance is 0.0013.

### 7.2.7 Cell Inside Dimension Variation

The cell inside dimension was reduced to 8-15/16 inches from the nominal value of 9 inches with a resultant change in  $k_{\text{eff}}$  of -0.006. The results are shown in Figure 7.6 and Table 7.2.



### 7.2.8 "Worst Case" Normal Configuration

Results for normal configuration can be summarized as follows:

	$k_{\text{eff}}$	$\Delta k_{\text{eff}}$
1. Reference Configuration	0.933	
2. Eccentric Positioning		0.004
3. Enrichment Variation		0.0000(Max used)
4. Minimum Cell Pitch ( $\pm 1/64$ in)		0.0013
5. Cell Wall Thickness ( $\pm 0.0025$ in)		0.0003
6. Minimum Poison Concentration ( $\pm 0.1w/o$ )		0.004
7. Poison Sheet Thickness ( $\pm 0.004$ in)		0.0013
8. Cell ID ( $\pm 1/16$ in)		0.006
9. Statistical Uncertainty in KENO		0.006

The effects of the above normal variations are combined statistically as follows:

$$\Delta k_{\text{eff}} = (0.004^2 + 0.0013^2 + 0.0003^2 + 0.004^2 + 0.0013^2 + 0.006^2 + 0.006^2)^{1/2} = 0.0104$$

The result for the "worst case" normal configuration is  $0.933 \pm 0.010$ .

### 7.3 $K_{\text{eff}}$ VALUES FOR ABNORMAL CONFIGURATIONS

#### 7.3.1 Spent Fuel Pool Temperature Variation

The  $k_{\text{eff}}$  of the rack was studied for temperatures ranging from  $68^{\circ}\text{F}$  to  $250^{\circ}\text{F}$ . Results are given in Figures 7.7 and 7.8 and Table 7.2 and show that the rack has a negative temperature coefficient with the highest  $k_{\text{eff}}$  occurring at the Indian Point 2 minimum pool water temperature of  $68^{\circ}\text{F}$ . Therefore, the  $\Delta k_{\text{eff}}$  associated with the spent fuel pool water temperature variation is zero in this analysis.



### 7.3.2 Other Abnormal Configurations

As discussed in Section 5.2, the  $\Delta k_{eff}$ 's caused by single storage cell displacement, fuel handling accident, fuel drop accident, heavy object drop and seismic incident are negligible, and no allowance on  $k_{eff}$  is made for any of these abnormal configurations.

### 7.3.3 "Worst Case" Abnormal Configuration

The "worst case" abnormal configuration combines the change in  $k_{eff}$  due to the occurrence of the most adverse abnormal condition with the  $k_{eff}$  value associated with the "worst case" normal configuration. However, since none of the abnormal conditions gives a positive  $\Delta k$ , the "worst case" abnormal condition is simply equal to the "worst case" normal condition.

	<u><math>K_{eff}</math></u>
1. Worst Case Normal Configuration (per Section 7.2.7)	0.943
2. Most Adverse Abnormal Configuration	0.000
3. Final $k_{eff}$ for "worst abnormal" configuration.	0.943

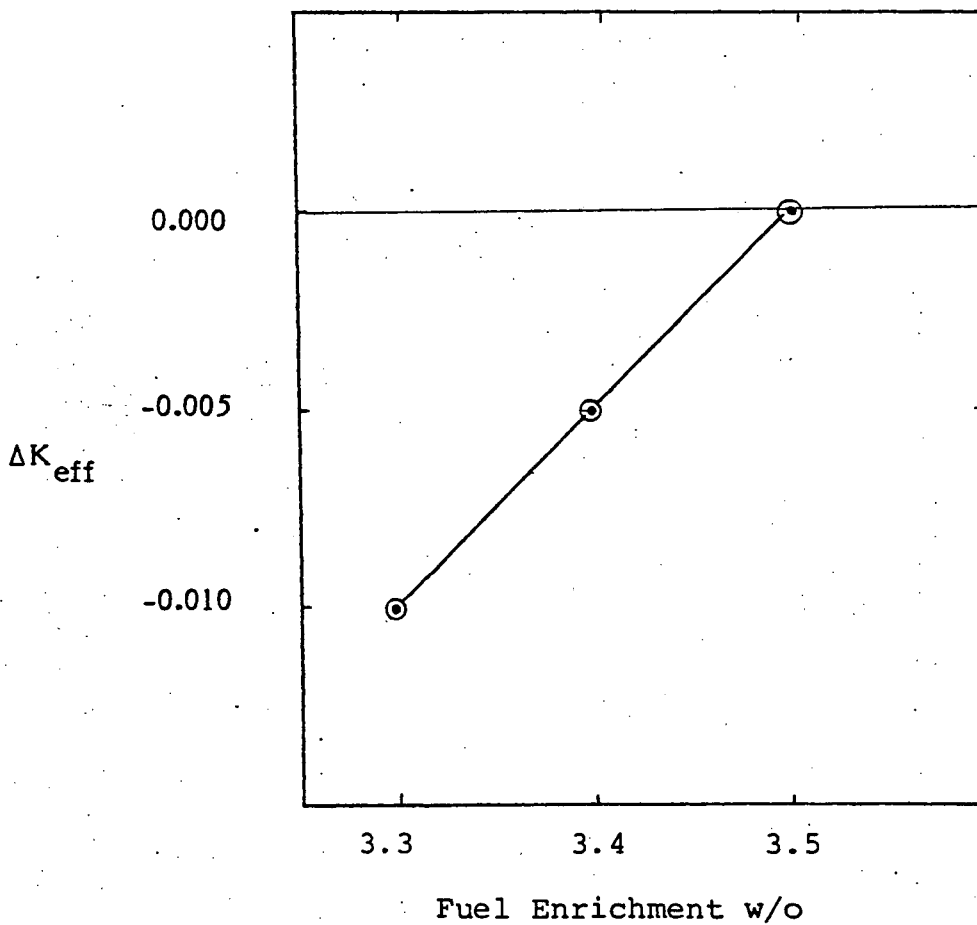


FIGURE 7.1  $\Delta K_{eff}$  vs. Fuel Enrichment

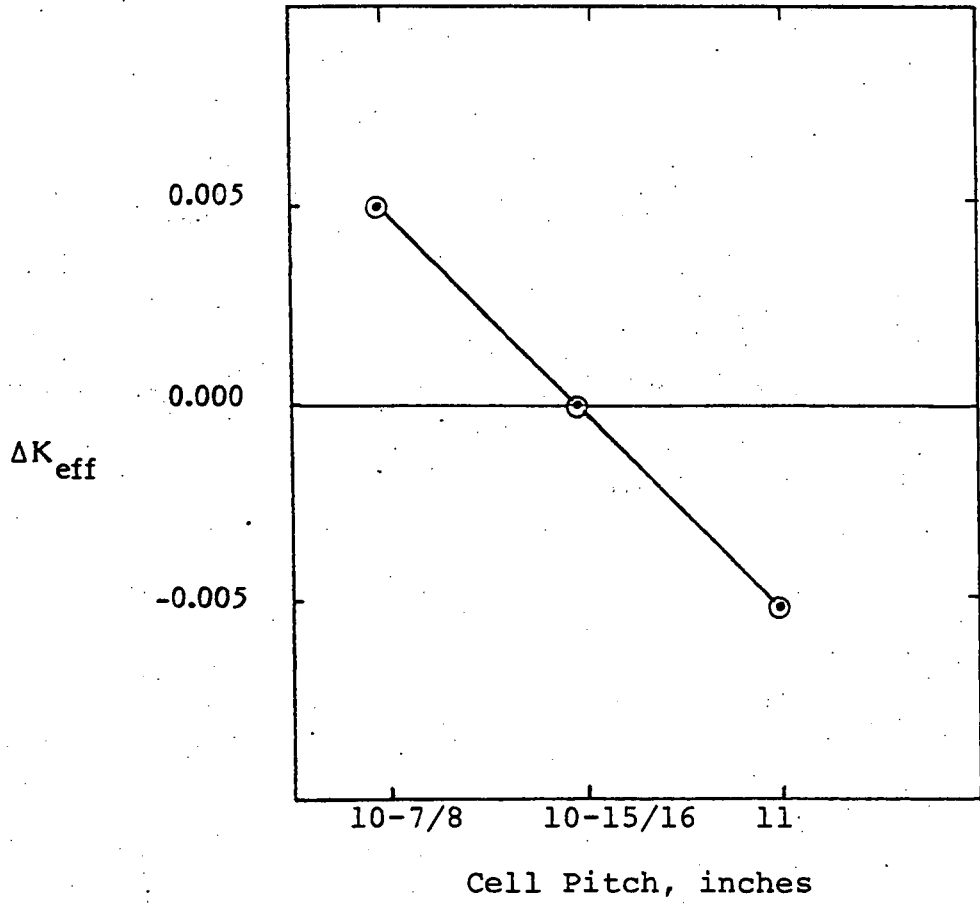


FIGURE 7.2  $\Delta K_{eff}$  vs. CELL PITCH

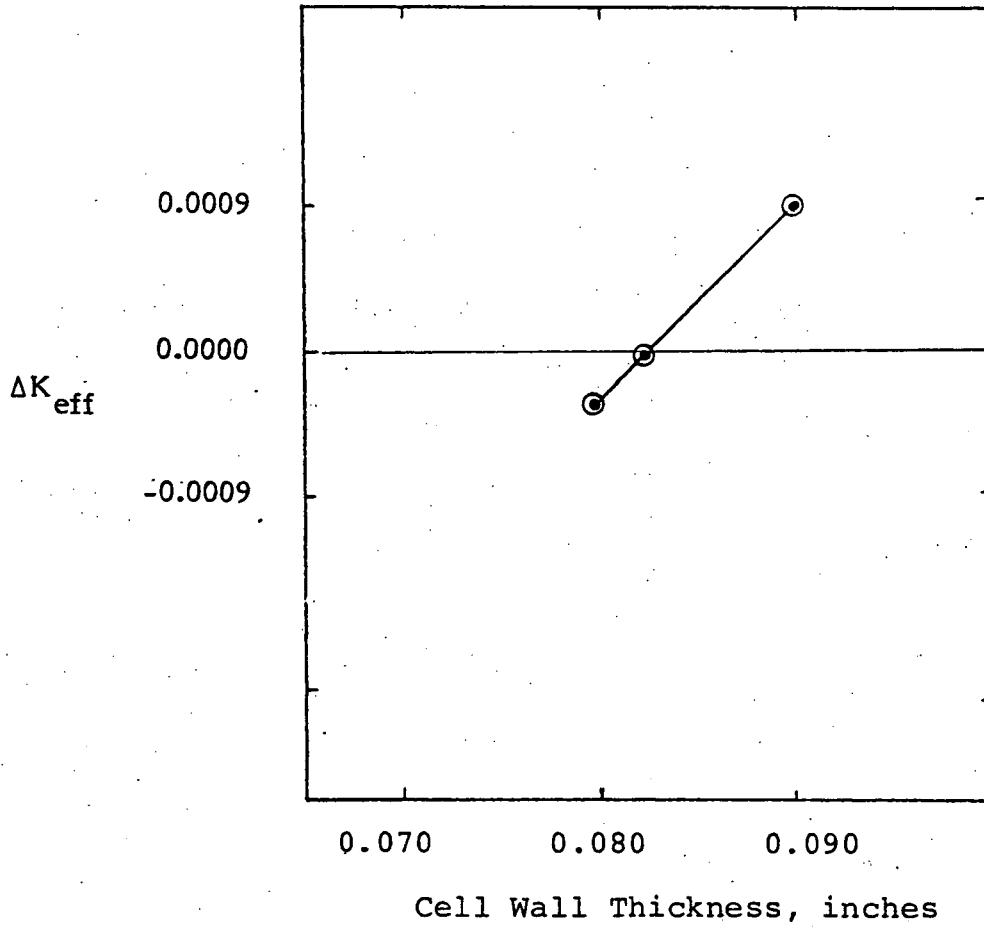


FIGURE 7.3  $\Delta K_{eff}$  vs. CELL WALL THICKNESS

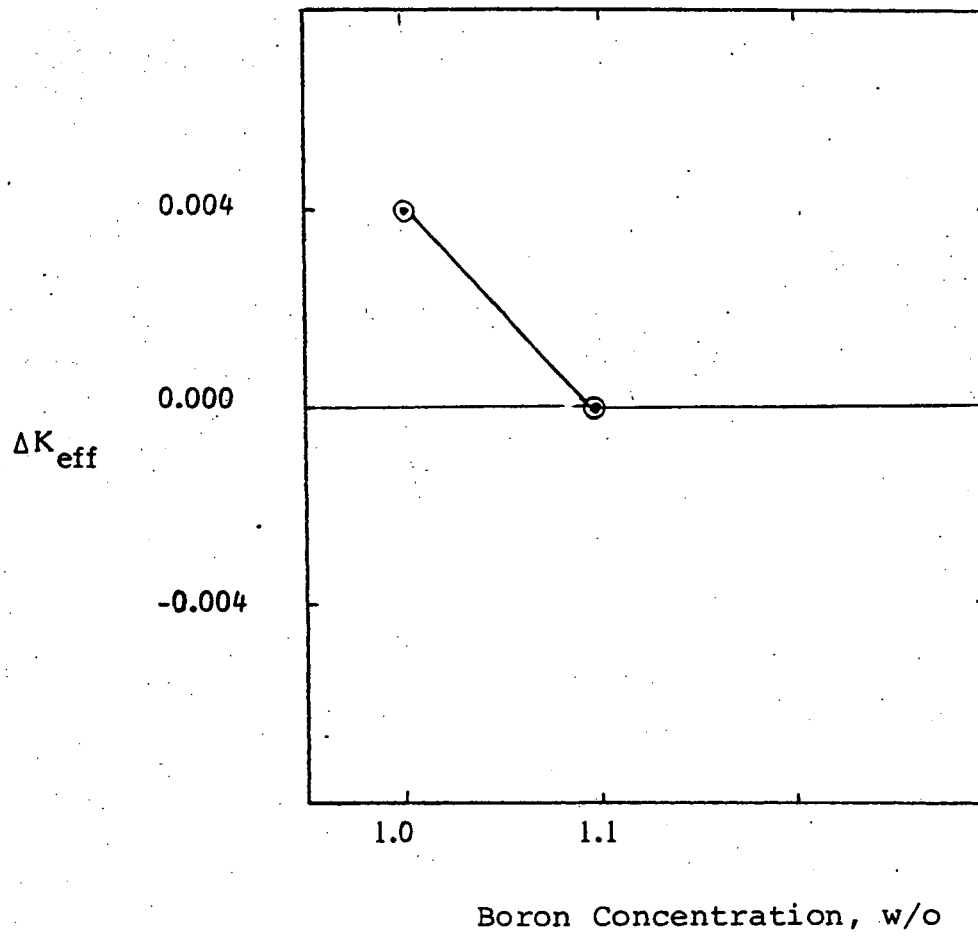


FIGURE 7.4  $\Delta K_{eff}$  vs. BORON CONCENTRATION

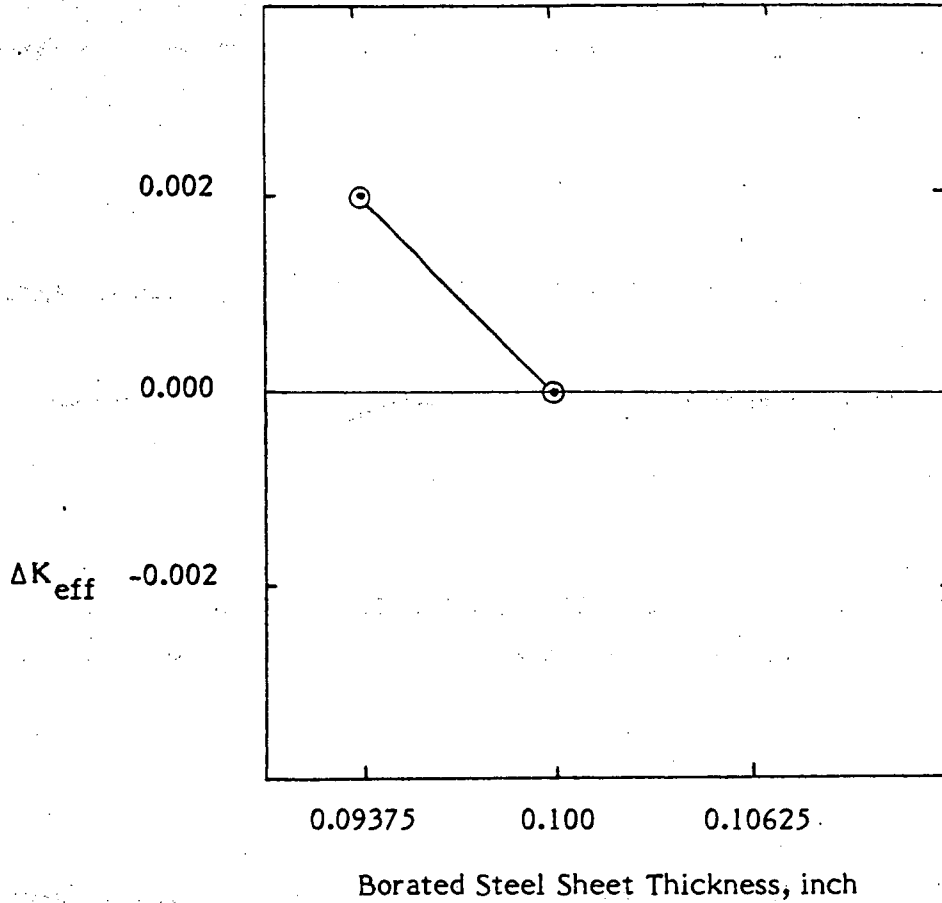


FIGURE 7.5  $\Delta K_{eff}$  vs. BORATED STEEL SHEET THICKNESS

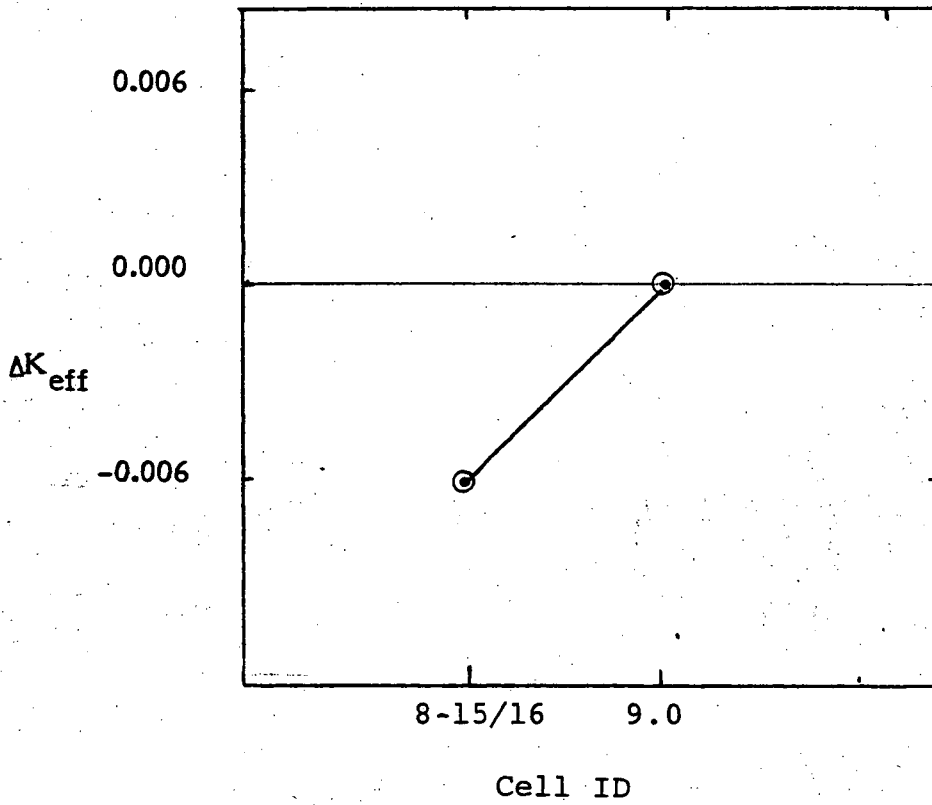


FIGURE 7.6  $\Delta K_{eff}$  vs. CELL ID

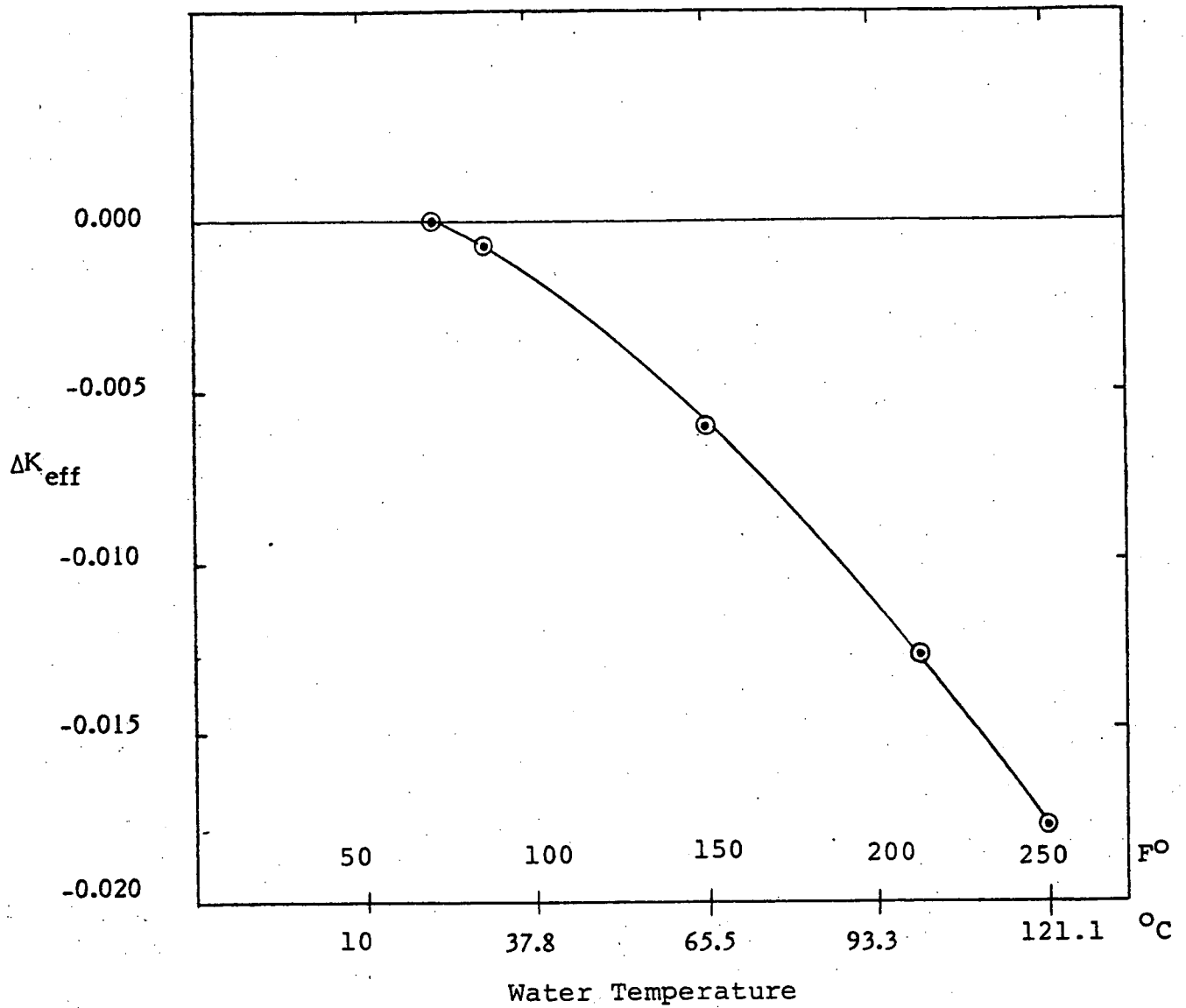


FIGURE 7.7  $\Delta K_{eff}$  vs. POOL WATER TEMPERATURE

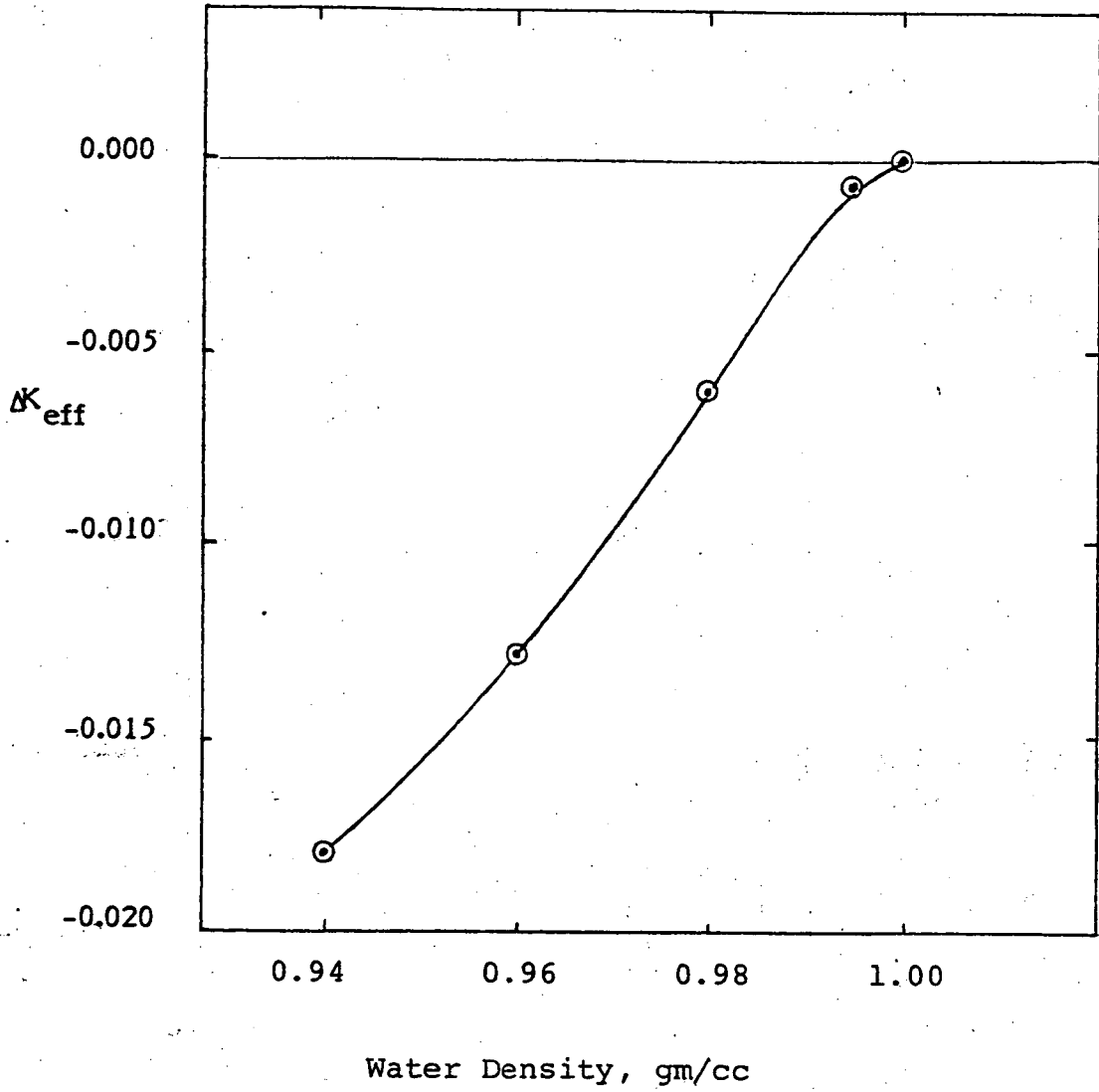


FIGURE 7.8  $\Delta K_{eff}$  vs. POOL WATER DENSITY



TABLE 7.1

## FUEL PARAMETERS

<u>Fuel Type</u>	<u>15x15 Westinghouse Fuel</u>
Fuel Enrichment	3.5 w/o
Mass of Uranium per Assembly	459 kg
Clad I.D.	0.373 in
Clad O.D.	0.422 in
Clad Thickness	0.0243 in
Clad Material	Zircaloy-4
Pitch Between Rods	0.563 in
Active Fuel Length	144.0 in
Array Dimensions	15x15
Guide Thimble Material	Zircaloy-4



	Variation	Fuel Enrich. (w/o)	Avg Pitch (in)	Cell Wall Thick. (in)	Boron Conc. (w/o)	BSS Thick. (in)	Cell ID (in)	Water Density (gm/cc)	Keff or Δ Keff
Reference Case	-	3.5	10.9375	0.0825	1.1	0.100	9.00	0.998	0.933
Eccentric Fuel	E cc.	3.5	10.9375	0.0825	1.1	0.100	9.00	0.998	0.004
Fuel Enrichment	-0.1 w/o	3.4	10.9375	0.0825	1.1	0.100	9.00	0.998	-0.005
	-0.2 w/o	3.3	10.9375	0.0825	1.1	0.100	9.00	0.998	-0.010
Average Cell Pitch	+1/16"	3.5	11.0000	0.0825	1.1	0.100	9.00	0.998	-0.005
	-1/16"	3.5	10.8750	0.0825	1.1	0.100	9.00	0.998	0.005
Cell Wall Thickness	-0.0025"	3.5	10.9375	0.080	1.1	0.100	9.00	0.998	-0.0003
	+0.0075"	3.5	10.9375	0.090	1.1	0.100	9.00	0.998	0.0009
Boron Concentration	-0.1 w/o	3.5	10.9375	0.0825	1.0	0.100	9.00	0.998	0.004
BSS Thickness	-1/16"	3.5	10.9375	0.0825	1.1	0.9375	9.00	0.998	0.002
Cell ID	-1/16"	3.5	10.9375	0.0825	1.1	0.100	8.9375	0.998	-0.006
Water Temp/Density	68°F	3.5	10.9375	0.0825	1.1	0.100	9.00	0.998	0.000
	90°F	3.5	10.9375	0.0825	1.1	0.100	9.00	0.993	-0.001
	150°F	3.5	10.9375	0.0825	1.1	0.100	9.00	0.980	-0.006
	212°F	3.5	10.9375	0.0825	1.1	0.100	9.00	0.958	-0.013
	250°F	3.5	10.9375	0.0825	1.1	0.100	9.00	0.942	-0.018

Table 7.2 - Parameters and Results of Variation Calculations



## 8. REFERENCE

1. USNRC Letter to All Reactor Licensees, from Brian K. Grimes, April 14, 1978.
2. Bromley, W.D., Olszewski, L.S. Safety Calculations and Benchmarking of Babcock & Wilcox Designed Close Spaced Fuel Storage Racks, Nuclear Technology, Vol. 41, Mid-December 1978, p. 346.
3. Bierman, S.R., Durst, B.M., Critical Separation Between Clusters of 4.29 wt% <sup>235</sup>U Enriched UO<sub>2</sub> Rods in Water with Fixed Neutron Poisons, May 1978, NUREG/GR-0073-RC.
4. NES 81A0260 "Criticality Analysis of the Atcor Vandenburg Cask" R.J. Weader, February, 1975.
5. ORNL-4938, "KENO IV - An Improved Monte Carlo Criticality Program," L.M. Petrie, N.F. Cross, November 1975.
6. DP-1064, the HAMMER System, J.E. Sutch and H.C. Honeck, January 1967.
7. ORNL-4078, EXTERMINATOR-2, T.B. Fowler et al, April 1967.

ATTACHMENT C

Radiological Analysis Report  
for the  
Indian Point Unit No. 2 Spent  
Fuel Storage Racks

Consolidated Edison Company of New York, Inc.  
Indian Point Unit No. 2  
Docket No. 50-247  
May, 1980



**RADIOLOGICAL ANALYSIS REPORT  
FOR THE  
INDIAN POINT UNIT NO. 2  
SPENT FUEL STORAGE RACKS**

**Prepared for  
Consolidated Edison Company of New York, Inc.**

**TABLE OF CONTENTS**

1. SUMMARY
  2. ASSUMPTIONS
    - 2.1 Spent Fuel Storage Pool Water Exposure Rate
    - 2.2 Spent Fuel Assembly Transfer
    - 2.3 Spent Fuel Assembly Handling Accident
    - 2.4 Cask Drop Accident
  3. RESULTS
    - 3.1 Spent Fuel Storage Pool Water Exposure Rate
    - 3.2 Spent Fuel Assembly Transfer
    - 3.3 Spent Fuel Assembly Handling Accident
    - 3.4 Cask Drop Accident
  4. REFERENCES
- Appendix A

1. SUMMARY

A radiological analysis has been performed on the spent fuel storage pool at Indian Point Unit #2 for an expanded storage capacity of 980 assemblies. This analysis included conservative estimates of exposure rates due to radionuclides in the spent fuel storage pool and spent fuel assembly movement in the pool. Accident analyses were also performed on spent fuel assembly drop and cask drop accidents in accordance with the methods outlined by Regulatory Guide 1.25 (see Appendix A).

Assumptions and methodology used in these evaluations were based partly on material in References 1 through 6.

2. ASSUMPTIONS

2.1 Spent Fuel Storage Pool Water Exposure Rate

The exposure rate due to fission and activation products in the spent fuel storage pool water has been calculated by Con Edison (Ref. 1) using the following assumptions:

1. The radionuclide concentrations in the primary coolant are based upon 0.12% failed fuel.
2. Fuel pool nuclide concentrations for all isotopes were computed considering normal cleanup prior to refueling.
3. There is a uniform mix of reactor coolant and refueling water.
4. Refueling operations begin no earlier than 90 hours after shutdown.
5. The pool water is considered as a self-attenuating slab source with a constant source distribution,  $S(x) = S$ .

2.2 Spent Fuel Assembly Transfer

The exposure rate at the surface of the spent fuel storage pool due to the transfer of one fuel assembly has been estimated by Con Edison (Ref. 6) using the following assumptions:

1. No fuel is moved until 90 hours after shutdown.
2. The fission product gamma flux for the core at 90 hours after shutdown has been calculated for a rated reactor thermal power of 3216 MWt. (Ref. 5).

3. The height of the fuel pin is 149.7 inches.
4. There is assumed to be 9-ft 4-in of water covering the fuel pins (Ref. 5)
5. The fuel element is modeled as a line source.

### 2.3 Spent Fuel Assembly Handling Accident

The following assumptions were made for the spent fuel assembly handling accident.

1. The accident occurs 90 hours after shutdown.
2. An accident (X/Q) value of  $6.6 \times 10^{-4} \text{ sec/m}^3$  has been used in the calculations (Ref. 4).
3. The methodology of Regulatory Guide 1.25 has been assumed for all calculations.
4. Doses were calculated using 3216 MWt power level. The source term for this condition was supplied in Reference 3 and is duplicated in Appendix A, Table 3.1.

### 2.4 Cask Drop Accident

1. The spent fuel transfer cask is not moved until 90 days following shutdown (Ref. 4).
2. Damage to an entire core (193 elements) is considered at a maximum power level of 3216 MWt.
3. The peaking factor is assumed to be 1.0 for this accident (Ref. 3).
4. All other assumptions for the spent fuel assembly handling accident apply for this accident analysis.

### 3. RESULTS

#### 3.1 Spent Fuel Storage Pool Water Exposure Rate

Using source terms corresponding to 0.12% failed fuel in the reactor core, an exposure rate of  $\dot{\chi} = 1.10$  mrem/hr has been calculated at the surface of the pool.

#### 3.2 Spent Fuel Assembly Transfer

The dose rate to an operator on the bridge hoist in the fuel storage building or on the manipulator crane in the containment building during fuel movement has been estimated to be less than 3.0 mrem/hr 90 hours after shutdown. This dose would be incurred only during actual movement of spent fuel.

#### 3.3 Spent Fuel Assembly Handling Accident

Using the source term and ( $\dot{\chi}/Q$ ) values provided, calculation of the absorbed doses to the total body and thyroid due to fission product releases from a fuel element at a power level of 3216 MWt, using the methodology of Regulatory Guide 1.25, yields:

$$D_{\text{total body}} = 3.11 \text{ Rem}$$

$$D_{\text{thyroid}} = 26.6 \text{ Rem}$$

These absorbed doses are a small fraction of the limits specified by 10 CFR Part 100.

#### 3.4 Cask Drop Accident

Using the assumptions outlined in Section 2.4, the absorbed doses to the total body and thyroid in a cask drop accident are:

$$D_{\text{total body}} = 12.7 \text{ Rem}$$

$$D_{\text{thyroid}} = 1.79 \text{ Rem}$$

These absorbed doses are below the limits specified by 10 CFR Part 100.

**4. REFERENCES**

1. Internal Con Edison Correspondence, dated January 9, 1980.
2. Telecopy from Con Edison to NES, October 31, 1979, Primary Coolant Concentrations of Radionuclides.
3. Internal Con Edison Correspondence, dated May 8, 1975.
4. Con Edison Spec. MP79-001, Section 6.3.1.
5. Telecon between Con Edison and NES, November 2, 1979.
6. Internal Con Edison Correspondence, dated March 10, 1980.



APPENDIX A

INDIAN POINT SPENT FUEL RACKS  
FUEL HANDLING ACCIDENT  
RADIOLOGICAL EVALUATION



INDIAN POINT 2 SPENT FUEL RACKS

*Fuel Handling Accident*

1. Assumptions

The following assumptions were made for the fuel handling accident:

- a. The accident occurs 90 hours after shutdown, which is the minimum time required by the unit Technical Specifications before fuel handling operations may begin. Credit is taken for radioactive decay from time of shutdown until the beginning of fuel handling operations.
  
- b. The new fuel rack will have a maximum height of 185". With the elevation of the fuel pool liner at 54' 7<sup>3</sup>/<sub>4</sub>" and the water level in the fuel pool at 93' 8", there will be 23' 7<sup>3</sup>/<sub>4</sub>" of water above the top of the rack.



- c. All of the gas activity in the damaged assembly is released.
1. 10% of total noble gases, other than KR-85.
  2. 30% of KR-85.
  3. 10% of total radioiodine in the rods at the time of the accident.
- d. Fission product inventories are calculated, assuming full power operation, immediately prior to shutdown, including a minimum radial peaking factor of 1.65.
- e. The iodine gas inventory is composed of 99.75% inorganic species and 0.25% organic species.
- f. Decontamination factors for the inorganic and organic species of iodine are 133 and 1 respectively giving an overall effective decontamination factor of 100. Iodines released from the fuel pool are considered to be composed of 75% inorganic and 25% organic species.
- g. There is no retention of noble gases in the fuel pool.
- h. The decontamination factor for iodine for the filters is 6.67. (Ref. 3)
- i. An accident ( $\lambda/Q$ ) value of  $6.6 \times 10^{-4}$  sec/m<sup>3</sup> has been used for this calculation. (Ref. 4)

## 2 Calculational Models

### 2.1 Thyroid Dose From The Inhalation of Radioiodines

A conservative value of the thyroid dose is given by the following equation:

$$D = \frac{F_g I F P B R (\chi/Q)}{(DF_p)(DF_f)} \quad (3.1)$$

where,

D = thyroid dose (rads)

$F_g$  = fraction of fuel rod iodine inventory in fuel rod void space (0.1)

I = core iodine inventory at time of accident (curies)

F = fraction of core damaged so as to release void space iodine

P = fuel peaking factor

B = breathing rate =  $3.47 \times 10^{-4}$  cubic meters per second (i.e., 10 cubic meters per 8 hour work day as recommended by the ICRP)

$DF_p$  = effective iodine decontamination factor for pool water

$DF_f$  = effective iodine decontamination factor for filters (if present)

$\chi/Q$  = atmospheric diffusion factor at receptor location ( $\text{sec}/\text{m}^3$ )

R = adult thyroid dose conversion factor for the iodine isotope of interest (rads per curie). Dose conversion factors for Iodine 131-135 are listed in Table I. These values were derived from "standard man" parameters recommended in ICRP Publication 2.

A slight rearrangement of Equation (3.1) to enable summation over  $i$  radioiodines yields:

$$D = \frac{(\lambda/Q)(F)(P)(B)(F_p)}{(DF_p)(DF_f)} \sum_i I_i R_i \quad (3.2)$$

## 2.2 External Whole Body Dose

The external whole body beta dose from a semi-infinite uniform  $\Delta$  cloud at the cloud center is given by the following equation:

$${}^{\beta}D = 0.23 \left( \frac{\lambda}{Q} \right) FP \sum_i \frac{F_{\beta i} I_i \bar{E}_{\beta i}}{(DF_p)_i (DF_f)_i} \quad (3.3)$$

where,

${}^{\beta}D$  = beta dose from an infinite cloud (Rads).

$\bar{E}_{\beta}$  = average beta energy per disintegration (MeV/dis).

All other terms have been previously defined. The decontamination factors ( $DF_p$  and  $DF_f$ ) are 1.0.

### 2.3 External Whole Body Gamma Dose

The external whole body gamma dose for a semi-infinite uniform cloud at the cloud center is given by the following equation:

$$\gamma D = 0.25 \left( \frac{\lambda}{Q} \right) F P \bar{E}_{\gamma} \frac{F_{g_i} I_i \bar{E}_{\gamma i}}{(DF_p)_i (DF_f)_i} \quad (3.4)$$

where,

$\gamma D$  = gamma dose from a semi-infinite cloud (Rads).

$\bar{E}_{\gamma}$  = average gamma energy per disintegration (MeV/dis).

All other terms have been previously defined. The decontamination factors for the noble gases ( $DF_p$  and  $DF_f$ ) are 1.0.

### 3. Results

If  $F$  in Equations (3.2), (3.3) and (3.4) is taken to be 0.0052 (corresponding to one failed fuel element), using the source term in Table 3.1, the thyroid and external whole body doses become respectively:

$$D = 26.6 \text{ Rads}$$

$$D_{\theta} = 1.76 \text{ Rads}$$

$$\gamma D = 1.35 \text{ Rads}$$

TABLE 3.1  
ISOTOPE RELEASES FOR FUEL HANDLING ACCIDENT AT 3216 MWT

ISOTOPE	C <sub>i</sub> /MWT	C <sub>max</sub>	F <sub>gi</sub>	λ <sub>i</sub> (hr <sup>-1</sup> )	I <sub>i</sub> (90M)	R <sub>i</sub>	E <sub>βi</sub> (MeV)	E <sub>γi</sub> (MeV)
I-131	2.51 × 10 <sup>4</sup>	8.07 × 10 <sup>7</sup>	0.1	3.58 × 10 <sup>-3</sup>	6.85 × 10 <sup>7</sup>	1.48 × 10 <sup>6</sup>	0.195	0.388
I-132	3.81 × 10 <sup>4</sup>	1.23 × 10 <sup>8</sup>	0.1	3.04 × 10 <sup>-1</sup>	1.61 × 10 <sup>4</sup>	5.35 × 10 <sup>4</sup>	0.499	2.30
I-133	5.63 × 10 <sup>4</sup>	1.81 × 10 <sup>8</sup>	0.1	3.33 × 10 <sup>-2</sup>	9.04 × 10 <sup>6</sup>	4.0 × 10 <sup>5</sup>	0.496	0.555
I-134	6.58 × 10 <sup>4</sup>	2.12 × 10 <sup>8</sup>	0.1	7.95 × 10 <sup>-1</sup>	1.79 × 10 <sup>-23</sup>	2.5 × 10 <sup>4</sup>	0.524	2.06
I-135	5.10 × 10 <sup>4</sup>	1.64 × 10 <sup>8</sup>	0.1	1.03 × 10 <sup>-1</sup>	1.55 × 10 <sup>4</sup>	1.24 × 10 <sup>5</sup>	0.330	1.77
KR-85M	1.11 × 10 <sup>4</sup>	3.57 × 10 <sup>7</sup>	0.3	1.55 × 10 <sup>-1</sup>	3.12 × 10 <sup>1</sup>	-	0.299	0.115
KR-85	3.62 × 10 <sup>2</sup>	1.16 × 10 <sup>6</sup>	0.3	7.38 × 10 <sup>-6</sup>	1.16 × 10 <sup>6</sup>	-	0.243	2.11 × 10 <sup>-3</sup>
KR-87	3.62 × 10 <sup>2</sup>	1.16 × 10 <sup>6</sup>	0.1	5.47 × 10 <sup>-1</sup>	4.83 × 10 <sup>-16</sup>	-	0.122	2.85
KR-88	3.03 × 10 <sup>4</sup>	9.74 × 10 <sup>7</sup>	0.1	2.44 × 10 <sup>-1</sup>	2.83 × 10 <sup>-2</sup>	-	0.395	1.77
XE-133M	1.44 × 10 <sup>3</sup>	4.63 × 10 <sup>6</sup>	0.1	1.32 × 10 <sup>-2</sup>	1.41 × 10 <sup>6</sup>	-	-	0.233
XE-133	5.70 × 10 <sup>4</sup>	1.83 × 10 <sup>8</sup>	0.1	5.50 × 10 <sup>-3</sup>	1.12 × 10 <sup>8</sup>	-	0.113	8.16 × 10 <sup>0</sup>
XE-135	1.55 × 10 <sup>4</sup>	4.98 × 10 <sup>7</sup>	0.1	7.62 × 10 <sup>-2</sup>	5.23 × 10 <sup>4</sup>	-	0.316	0.261

#### 4. Cask Drop Accident

##### 4.2 Assumptions

The spent fuel transfer cask is dropped on occupied spent fuel rack 90 days following shutdown. Damage to an entire core (Ref. 4) (193 elements) is considered at a maximum power level at shutdown of 3216 MWt. (See Table 3.1). The peaking factor is assumed to be one ( $P=1$ ) for the following calculations.

##### 4.2 Results

At 90 days after shutdown, the only radioisotopes <sup>of interest</sup> remaining in appreciable amounts are I-131, KR-85 and XE-133, and their activities for 193 fuel elements are: (Ref. 3)

$$I(I-131) = 3.54 \times 10^4 \text{ Ci}$$

$$I(KR-85) = 1.14 \times 10^6 \text{ Ci}$$

$$I(XE-133) = 1.27 \times 10^3 \text{ Ci}$$

Using Equations (3.2), (3.3) and (3.4), the thyroid and external beta and gamma doses are respectively:

$$D = 1.79 \text{ Rem}$$

$$D_{\beta} = 12.6 \text{ Rem}$$

$$D_{\gamma} = 0.12 \text{ Rem}$$



where  $F = P = 1.$

ATTACHMENT D

Thermal-Hydraulic Analysis Report

for the

Indian Point Unit No. 2 Spent

Fuel Storage Racks

Consolidated Edison Company of New York, Inc.  
Indian Point Unit No. 2  
Docket No. 50-247  
May, 1980



**THERMAL-HYDRAULIC ANALYSIS REPORT**  
**FOR THE**  
**INDIAN POINT UNIT NO. 2**  
**SPENT FUEL STORAGE RACKS**

**Prepared for**  
**Consolidated Edison Company of New York, Inc.**



## TABLE OF CONTENTS

1. SUMMARY
2. ASSUMPTIONS
  - 2.1 Maximum Heat Loads
  - 2.2 Heat-up Rates
  - 2.3 Verification of Assembly Cooling
3. RESULTS AND CONCLUSIONS
  - 3.1 Maximum Heat Loads
  - 3.2 Heat-up Rates
  - 3.3 Verification of Assembly Cooling

Appendix A



## 1. SUMMARY

Fuel storage racks have been designed to increase the present fuel storage capacity of the Indian Point 2 spent fuel storage pool to a total of 980 assemblies.

The maximum heat loads resulting from the expanded spent fuel storage have been calculated for both normal and abnormal fuel discharge cases (see Appendix A). Calculations indicate that the cooling capacity of the present fuel cooling system is adequate to handle the resulting normal and abnormal heat loads.

The increase of the pool water bulk temperature as a function of time has been determined assuming a failed heat removal system for normal and abnormal cases. (See Appendix B.)

The adequacy of natural circulation flow throughout the fuel racks to cool the fuel assemblies was verified (See Appendix C). Even with the bulk pool temperature at the maximum value of 150°F, sufficient circulation exists to preclude local boiling in any fuel assembly.

## 2. ASSUMPTIONS

### 2.1 MAXIMUM HEAT LOADS

The maximum heat loads, resulting from the expanded spent fuel storage capacity, have been calculated for two cases: the normal batch discharge and the abnormal full core discharge.

1. The assumed normal case consists of conservatively discharging a maximum of 90 fuel assemblies every 18 months with 90 hours of cooling time after shutdown. A plant capacity factor of 85% was assumed. The maximum heat load is scheduled to occur after the discharge of nine batches with adequate storage kept in reserve for a full core discharge.
2. The assumed abnormal case is the discharge of a full core (193 assemblies) at any time during the cycle. The maximum heat load has been determined to occur soon after the startup following the scheduled refueling outage for the discharge of the ninth batch. Cooling time to discharge is 400 hours after shutdown.

Decay heat generation is calculated according to Branch Technical Position APC SB 9-2, "Residual Decay Energy for Light Water Reactors for Long-Term Cooling", Dec. 24, 1975, including recommended uncertainty factors and actinide contributions. (For times greater than  $10^7$  seconds an uncertainty factor of 0.25 was used.) Rated reactor power is 3216 Mwt.

### 2.2 HEAT-UP RATES

Maximum pool water bulk temperature is conservatively assumed to be 150°F. The heatup rates and times to reach boiling temperature of 212°F are based on adequate mixing of the pool water.



### 2.3 VERIFICATION OF ASSEMBLY COOLING

The natural circulation flow is calculated by establishing a thermal-hydraulic balance for the worst row of assemblies (from a recent batch discharge with a 90-hour cooling period). The flow is maintained by the thermal driving head produced by the decay heat generation of each assembly. The pool is modeled as a large volume with a bulk temperature unaffected by local disturbances. The pressure losses considered in the analysis include:

1. Friction losses in the downcomer region, in the rack inlet plenum and in the fuel assembly.
2. Losses in turns.
3. Form losses in the fuel assemblies at the inlet, outlet, and grid locations.

Flow to the worst row of cells is assumed to be available from the narrowest downcomer only. Coolant from the cask handling area and rack-to-rack gaps is conservatively neglected. All fuel assemblies are assumed to have been freshly discharged (90-hour cooling time) with radial peaking factors of 1.2.

A maximum bulk pool temperature of 150°F is assumed.

## 3. RESULTS AND CONCLUSIONS

### 3.1 MAXIMUM HEAT LOADS

The maximum normal heat load anticipated would be encountered after the discharge of the ninth batch into the pool. The pool would then contain 740 assemblies. The calculated decay heat generation at that time is  $27.2 \times 10^6$  Btu/hr, assuming a 90-hour cooling period after shutdown.

The maximum abnormal heat load anticipated would occur resulting from the emergency discharge of a full core (193 assemblies) into the pool two months after the discharge of the ninth batch and one month after the subsequent startup. The pool would contain 933 assemblies. The calculated decay heat generation rate for this case is  $31.6 \times 10^6$  Btu/hr, assuming a 400-hour cooling period.

The Indian Point 2 spent fuel pool heat removal system is rated to remove  $30.8 \times 10^6$  Btu/hr from the system with a pool water temperature of 135°F. If the water temperature is allowed to increase to 150°F,  $40.7 \times 10^6$  Btu/hr can be extracted from the spent fuel water. Consequently, the cooling capacity is adequate for both the normal and abnormal discharge cases.



### 3.2 HEAT-UP RATES

In case of a complete failure of the Indian Point 2 spent fuel heat removal system, the maximum heat-up rates calculated for the maximum normal and abnormal heat loads anticipated are 13.0 and 15.1<sup>o</sup>F/hr, respectively. The total times available to perform repairs for the maximum normal and abnormal heat loads are 4.8 and 4.1 hours, respectively before makeup is required for pool boil-off. The makeup required is approximately 57 and 66 gpm of water for normal and abnormal heat loads.

### 3.3 VERIFICATION OF ASSEMBLY COOLING

The adequacy of the natural circulation flow to cool the worst row in the rack configuration was verified by establishing a thermal-hydraulic balance. The chief concern is the possibility of local boiling due to flow starvation in some cells of the rack matrix as a result of excessive pressure losses in the natural circulation loops established in the spent fuel pool.

The analysis shows that even under the most conservative assumption, the natural circulation in the pool is adequate to preclude boiling by a substantial margin, assuming a bulk pool temperature of 150<sup>o</sup>F. The maximum temperature increase in the assembly with minimum flow is 76.8<sup>o</sup>F, resulting in an outlet temperature of 226.8<sup>o</sup>F. This is below the saturation temperature of 239<sup>o</sup>F, corresponding to the static head at the top of the fuel assembly.

It should be noted that the maximum assembly outlet temperature of 226.8<sup>o</sup>F reported above is unlikely to occur in the pool, as it is the result of excessively conservative assumptions postulated to establish a calculational boundary. In the analysis, the major portion of the total pressure drop in the natural circulation loop is caused by the selection of the narrowest gap in the pool as the sole flow path to the bottom plenum from the water above the racks. The expected mode of natural circulation is for the coolant to reach the plenum via least-resistant flow paths, such as the cask area, the north wall downcomer gap of 11-9/10", the failed fuel elevator area, and between the 2-1/2" gap between racks, all of which have been neglected in the analysis.



**APPENDIX A**

**INDIAN POINT 2 SPENT FUEL POOL  
MAXIMUM HEAT LOADS**

REF.

INDIAN POINT 2 SPENT FUEL POOL  
MAXIMUM HEAT LOADS

1. STATEMENT OF PROBLEM

Calculate heat generation rates for NORMAL and ABNORMAL cases for fuel discharges scheduled.

2. ASSUMPTIONS

- 2.1 Core capacity is 193 assemblies
- 2.2 Maximum pool storage capacity is 980 assemblies.
- 2.3 Fuel discharge schedule assumed as follows \*

1  
2

DISCHARGE DATE	No. of ASS'S	Σ No of ASS'y
6-76	72	72
1-78	60	132
6-79	68	200
1-81	90	290
6-82	90	380
1-84	90	470
6-85	90	560
1-87	90	650
6-88	90	740
CORE DISCH.	193	933

\* Assuming 90 assemblies discharged every 18 months

1.



2.4 Normal cooling time is 90 hours after shutdown. ✓  
For full core discharge, cooling time is 400 hours.

1

2.5 Batch exposures calculated assuming 85% capacity factor. The following is in the pool 90 hours ✓  
after shutdown in June 1988.

1

BATCH #	DISCH DATE **	No. OF ASSEMBLY	EXPOSURE TIME *	COOLING TIME ✓
1	6-76	72	1.5 YR	12 YR
2	1-78	60	3 YR	10.5 YR
3	6-79	68	4 YR	9 YR
4	1-81	90	4 YR	7.5 YR
5	6-82	90	4 YR	6 YR
6	1-84	90	4 YR	4.5 YR
7	6-85	90	4 YR	3 YR
8	1-87	90	4 YR	1.5 YR
9	6-88	90	4 YR	90 HR

\* EXPOSURE TIMES HAVE BEEN APPROXIMATED TO NEAREST 1/2 YEAR.  
(EQUIVALENT FULL POWER OPERATING TIME).

\*\* THESE DATES HAVE BEEN SELECTED FOR CALCULATIONAL PURPOSES ONLY.

2.6 Decay Heat Generation is calculated according to APCS-9-2. The calculation includes recommended uncertainty factors and actinide contribution.

3

2.7 Plant Rated Power is 3216 Mwt ( $1.0976 \times 10^{10}$  Btu/hr) ✓

1



REF.

3. HEAT LOAD CALCULATIONS

3.1 NORMAL Case

BATCH #	No. # Ass'y	EQUIV OP TIME	COOLING TIME	P/P <sub>0</sub> * (FULL CORE)	WEIGHTED P/P <sub>0</sub>
1	72	1.5 YR	12 YR	1.22 -4	4.55 -5
2	60	3 YR	10.5 YR	1.42 -4	4.41 -5
3	68	4 YR	9 YR	1.57 -4	5.53 -5
4	90	4 YR	7.5 YR	1.63 -4	7.60 -5
5	90	4 YR	6 YR	1.70 -4	7.93 -5
6	90	4 YR	4.5 YR	1.83 -4	8.53 -5
7	90	4 YR	3 YR	2.13 -4	9.93 -5
8	90	4 YR	1.5 YR	3.26 -4	1.52 -4
9	90	4 YR	90 HR	3.94 -3	1.84 -3
	<u>740</u>				<u>2.477 -3</u>

MAXIMUM HEAT LOAD (NORMAL CASE)

$$1.0976 \times 10^{10} \times 2.477 \times 10^{-3} = 27.2 \times 10^6 \text{ BTU/HR}$$

\*  $P/P_0 = (1+K) [ P/P_0(\infty, t_s) ] - P/P_0(\infty, t_0+t_s)$   
 Uncertainty factor  $K=0.25$  used for  $t_s > 10^7$  sec



REF.

3.2 ABNORMAL CASE

(A) Full Core Discharge in AUG 1988

This case assumes Batch #9 discharged during normal outage of 6-88 (see p. 2), plant started up in 7-88, full core discharged in 8-88.

400 hours later, the following would be in the pool

BATCH #	NO. OF ASS'Y	EQUIV OP TIME	COOLING TIME	P/P <sub>0</sub> (FULL CORE)	WEIGHTED P/P <sub>0</sub> ✓
1		1.5 YR	12 YR	1.22 -4	4.55 -5
2		3 YR	10.5 YR	1.42 -4	4.41 -5
3	68	4 YR	9 YR	1.57 -4	5.53 -5
4	90	4 YR	7.5 YR	1.63 -4	7.60 -5
5	90	4 YR	6 YR	1.70 -4	7.93 -5
6	90	4 YR	4.5 YR	1.83 -4	8.53 -5
7	90	4 YR	3 YR	2.13 -4	9.93 -5
8	90	4 YR	1.5 YR	3.26 -4	1.52 -4
9	90	4 YR	65 DAYS	1.10 -3	5.12 -4
10A	64	30 DAYS	400 HR	1.02 -3	3.38 -4
10B	64	1.5 YR	400 HR	2.04 -3	6.75 -4
10C	65	3 YR	400 HR	2.14 -3	7.19 -4
<u>933</u>					<u>2.881 -3</u> ✓

MAXIMUM LOAD (ABNORMAL CASE A)

$$1.0976 \times 10^{10} \times 2.881 \times 10^{-3} = 31.6 \times 10^6 \text{ BTU/HR}$$



REF.

(B) Full Core Discharge in Jan 1990

This case assumes Batch #9 discharged during normal outage of 6-88, Plant startup up in 7-88, full core discharged 1 1/2 years later, just prior to scheduled outage of 1-90.

BATCH #	NO OF ASSEMBLY	EQUIV OP TIME	COOLING TIME	P/P <sub>0</sub> (FULL CORE)	WEIGHTED P/P <sub>0</sub>
1	72	1.5 YR	13.5 YR	1.18 -4	4.40 -5 ✓
2	60	3 YR	12 YR	1.37 -4	4.25 -5
3	68	4 YR	10.5 YR	1.51 -4	5.33 -5
4	90	4 YR	9 YR	1.57 -4	7.32 -5
5	90	4 YR	7.5 YR	1.63 -4	7.60 -5
6	90	4 YR	6 YR	1.70 -4	7.93 -5
7	90	4 YR	4.5 YR	1.83 -4	8.53 -5
8	90	4 YR	3 YR	2.13 -4	9.93 -5
9	90	4 YR	1.5 YR	3.26 -4	1.52 -4
10A	64	1.5 YR	400 HR	2.04 -3	6.75 -4
10B	64	3 YR	400 HR	2.14 -3	7.09 -4
10C	65	4 YR	400 HR	2.16 -3	7.29 -4
	<u>933</u>				<u>2.818 × 10<sup>-3</sup></u> ✓

MAXIMUM HEAT LOAD (ABNORMAL CASE B)

$$1.0976 \times 10^{10} \times 2.818 \times 10^{-3} = 30.9 \times 10^6 \text{ BTU/HR} \checkmark$$



**APPENDIX B**

**INDIAN POINT 2 SPENT FUEL POOL**

**HEAT-UP RATES**

REF.

INDIAN POINT 2 SPENT FUEL POOL  
 MINIMUM HEAT-UP TIMES

1. STATEMENT OF PROBLEM

Determine the pool temperature as a function of time assuming a heat removal system failure.

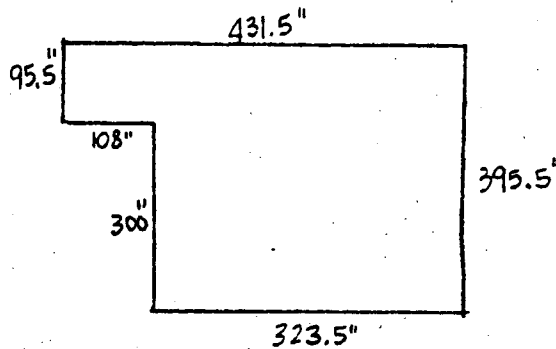
2. ASSUMPTIONS

2.1 Maximum heat loads

Normal =  $27.2 \times 10^6$  BTU/HR

Abnormal =  $31.6 \times 10^6$  BTU/HR

2.2 Pool Geometry shown below



WATER LINE =  $93'-8''$

FLOOR ELEV =  $54'-7\frac{1}{4}''$

WATER DEPTH =  $468.75''$

App A.

4

REF.

2.3  $UO_2$  weight/assembly = 1155 lb  
 Zirc weight/assembly = 275 lb  
 Empty Rack weight (avg. est'd) = 23,000 lb

5

2.4  $UO_2$  density = 643 lb/ft<sup>3</sup>  
 Zirc density = 406 lb/ft<sup>3</sup>  
 Stainless density = 492 lb/ft<sup>3</sup>  
 Water density @ 180°F = 60.6 lb/ft<sup>3</sup>  
 Water Cp = 1.0 Btu/lb-°F

2.5 Pool full to capacity : 980 locations in 12 racks.

3. HEAT-UP CALCULATIONS

$$\text{Pool Vol} = \frac{1}{1728} \left[ (95.5 \times 108) + (323.5 \times 395.5) \right] \times 468.75$$

$$= 37505 \text{ ft}^3 \checkmark$$

$$UO_2 \text{ volume} = \frac{1155 \times 980}{643} = 1760 \text{ ft}^3$$

$$\text{Zirc volume} = \frac{275 \times 980}{406} = 664 \text{ ft}^3 \checkmark$$

$$\text{Rack volume} = \frac{23,000 \times 12}{492} = 561 \text{ ft}^3$$

REF.

$$\text{Net Water Vol} = 37505 - 1760 - 664 - 561 = 34520 \text{ ft}^3$$

$$\text{Net water Wt} = 34520 \times 60.6 = 2.092 \times 10^6 \text{ lb}$$

Max Normal Heat Load Heatup Rate.

$$\frac{27.2 \times 10^6}{2.092 \times 10^6} = 13.0 \text{ } ^\circ\text{F/hr}$$

Max Abnormal Heat Load Heatup Rate

$$\frac{31.6 \times 10^6}{2.092 \times 10^6} = 15.1 \text{ } ^\circ\text{F/hr}$$

→ Times needed to take preventive action  
(from max bulk temp of 150°F to boiling 212°F)

$$\underline{\text{Normal}} = (212 - 150) / 13.0 = 4.8 \text{ hrs}$$

$$\underline{\text{Abnormal}} = (212 - 150) / 15.1 = 4.1 \text{ hrs}$$

→ Evaporation Rate at 212°F ( $h_{fg} = 970.3 \text{ Btu/lb}$ )

$$\text{Normal} = \frac{27.2 \times 10^6}{970.3} = 27,826 \text{ lb/hr} \approx 57 \text{ gpm}$$

$$\text{Abnormal} = \frac{31.6 \times 10^6}{970.3} = 32,567 \text{ lb/hr} \approx 66 \text{ gpm}$$



APPENDIX C

INDIAN POINT 2 SPENT FUEL  
VERIFICATION OF ADEQUATE COOLING



REF.

INDIAN POINT 2 SPENT FUEL POOL

VERIFICATION OF ADEQUATE COOLING

1. STATEMENT OF PROBLEM

Perform a thermal-hydraulic analysis to verify that the natural circulation in the expanded capacity rack configuration allows adequate cooling of all assemblies.

2. ASSUMPTIONS

Figure 2-1 shows the general arrangement of the Indian Point 2 storage pool. The row selected is considered the most critical area in terms of cooling for the assemblies.

2.1 The downcomer gap is 1.25" at the rack base. All other sources of cooling water (cask area, rack-to-rack spacings, other larger downcomer gaps) have been conservatively neglected.

2.2 All fuel assemblies in the 13-cell row have 4 years equivalent full power operation time, radial peaking factors of 1.2,



	REF.
and have cooled 90 hours since shutdown.	1
2.3 The pool bulk water temperature is conservatively 150°F.	
2.4 The pool water depth is 39'1". The top of the rack is 185". Saturation temperature corresponding to the static head at the top of the rack is 239°F.	
2.5 Each bundle is isolated from adjacent assemblies by the cell walls and sits in its own thermal chimney. No credit for cross flows between assemblies at the inlet plenum level is taken.	
2.6 Bundle loss coefficient $K \left( \frac{\Delta P}{\rho V^2} \right)$ is 24.1, including assembly entrance, exit and grid losses. This is based on the IP-2 core $\Delta P$ , corrected to account for fuel pin skin friction.	8
2.7 Water properties based on estimated bundle average of 170°F.	
2.8 Bundle decay heat from APCSB 9-2, $P/P_0 = 3.94 \times 10^{-3}$ ( $T_0 = 4$ years, $T = 90$ hours). Reactor rated power is 3216 Mw. Core is 193 assemblies.	3



	REF.
2.9 The can is 9" square. Pitch is 10-15/16". Inlet channel height is 10" (between floor and bottom of rack beams).	2
2.10 The assemblies are 15x15, 204 fuel rods with 0.422" $\phi$ D, 21 guide thimbles, assumed occupied, with 0.545" $\phi$ D, 9 spacers.	5
2.11 Friction Factors from Moody curves, CRANE, Flow of Fluids. Geometry factors from Idel'chik.	6 7
2.12 All rack dimensions from NES Drawings 80E3503, 80E3518 and 80E3521.	

REF.

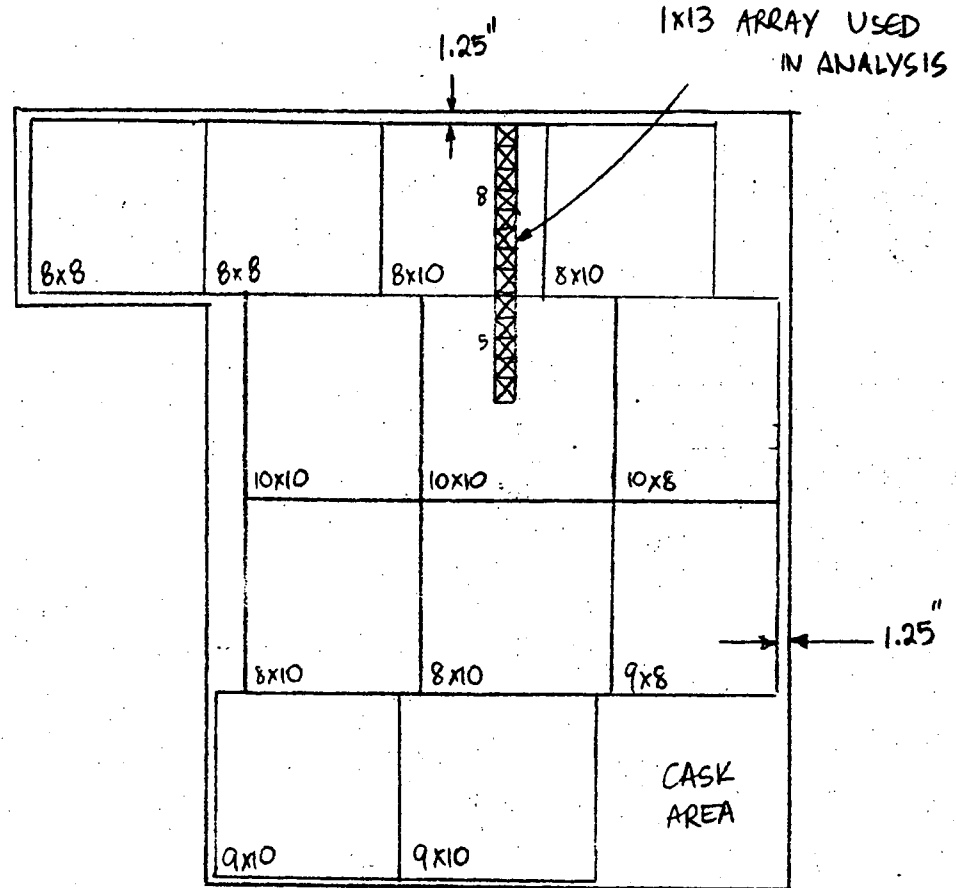


FIGURE 2-1 INDIAN POINT 2 FUEL STORAGE POOL  
AND RACK LAYOUT



REF.

3. ANALYSIS

3.1 DOWNCOMER LOSSES ( $\Delta P_{DC}$ )

3.1.1 Wall Friction ( $\Delta P_w$ )

Flow Area,  $A = 1.965 \times 10.94 = 21.50 \text{ in}^2 \checkmark$   
 $= 0.1493 \text{ ft}^2$

Wetted Perim,  $P = 2 \times 10.94 = 21.88 \text{ in} \checkmark$

Hyd Dia,  $D_e = \frac{4A}{P} = \frac{4 \times 21.50}{21.88} = 3.93 \text{ in}$   
 $= 0.328 \text{ ft}$

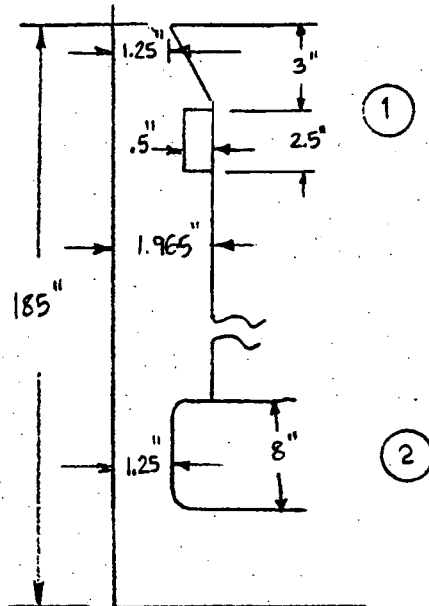
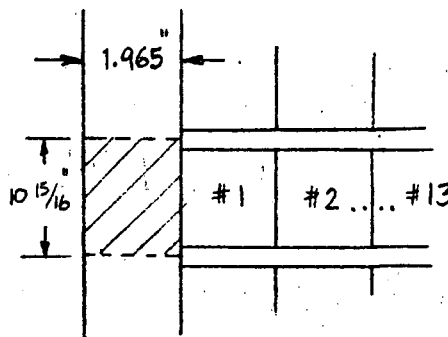
Length,  $L = 185 \text{ in} \checkmark$

Water Properties @ 170°F

density  $\rho = 60.8 \text{ lb/ft}^3 \checkmark$

visc  $\mu = 0.88 \text{ lb/hr-ft}$

Assuming identical flow  
in each assembly:

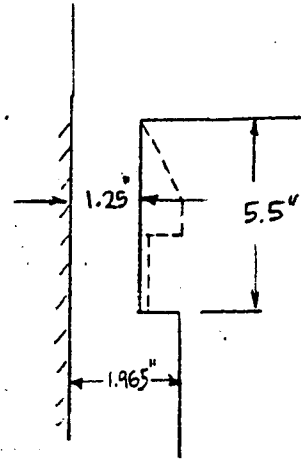


Flow/assy (lb/hr)	Total Flow(lb/hr)	Velocity (ft/sec)	Re	f	$\Delta P_w = f \frac{L}{D_e} \frac{\rho V^2}{2g}$ (psi)
2500	32500	0.99	80800	0.0185	0.0056
5000	65000	1.99 $\checkmark$	161500 $\checkmark$	0.016 $\checkmark$	0.0196
7500	97500	2.98	242300	0.015	0.0411
10,000	130,000	3.98	323000	0.014	0.0684

REF.

3.1.2 Downcomer Restrictions ( $\Delta P_r$ )

Flare opening and top bracing, Area ① modeled as indicated



From Idel'chik (REF 7), DIAGRAM 3-18

$$k = \left( \xi_0 + \lambda \frac{L}{d_h} \right) \frac{1}{f^2}$$

$$\bar{f} = \text{Area of orifice} / \text{Area of channel}$$

$$= \frac{1.25 \times 10.94}{1.965 \times 10.94} = 0.636$$

$$d_h = \frac{4 \times \text{Orifice Area}}{\text{Orifice Perimeter}} = \frac{4 \times (1.25 \times 10.94)}{2 \times 10.94} = 2.5" \checkmark$$

$$\frac{L}{d_h} = \frac{5.5}{2.5} = 2.2 \checkmark \quad \epsilon \propto \left( \frac{L}{d_h} \right) = 0.01$$

$$\begin{aligned} \xi_0 &= 0.5 + (1 - \bar{f})^2 + \epsilon (1 - \bar{f}) \\ &= 0.5 + (1 - 0.636)^2 + 0.01 (1 - 0.636) = 0.636 \checkmark \end{aligned}$$

From Idel'chik, DIAG 2-2, Conduit with smooth walls  
 for  $Re = 10^5$ ,  $\lambda = 0.018$

$$\therefore k = \left[ 0.636 + 0.018 \frac{5.5}{2.5} \right] \frac{1}{(0.636)^2} = 1.67 \checkmark$$

$$\Delta P_{r1} = K_1 \frac{\rho V^2}{2g} \quad \text{where } V \text{ is free channel (1.965").}$$

REF.

Rack Base Area ② modeled  
as indicated

From Idel'chik, DIAG 11-29

$$k = \left( \xi_0 + \lambda \frac{L}{d_h} \right) \frac{1}{f^2}$$

$$\bar{f} = 0.636 \quad \lambda = 0.18$$

$$d_h = 2.5''$$

$$L = 8''$$

$$\frac{L}{d_h} = \frac{8}{2.5} = 3.2 \quad z = 0.0$$

$$\begin{aligned} \xi_0 &= 1 + 0.5(1 - \bar{f}) + z\sqrt{1 - \bar{f}} \\ &= 1 + 0.5(1 - 0.636) = 1.182 \end{aligned}$$

$$k_2 = \left[ 1.182 + 0.018 \frac{8}{2.5} \right] \frac{1}{(0.636)^2} = 3.065$$

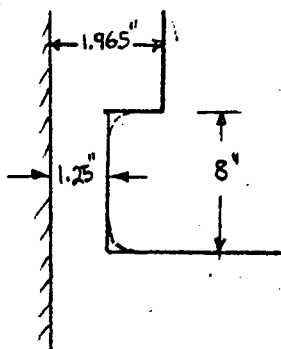
$$\Delta P_{r2} = k_2 \frac{\rho V^2}{2g}$$

(V in 1.965" channel)

TOTAL RESTRICTION  $k = k_1 + k_2$

$$\begin{aligned} &= 1.67 + 3.065 \\ &= 4.735 \end{aligned}$$

Flow/Assy (lb/hr)	Total Flow (lb/hr)	Velocity (ft/sec)	$\Delta P_r$ (psi)
2500	32500	0.99	0.031 ✓
5000	65000	1.99	0.123
7500	97500	2.98	0.276
10,000	130,000	3.98	0.492



} p6

REF.

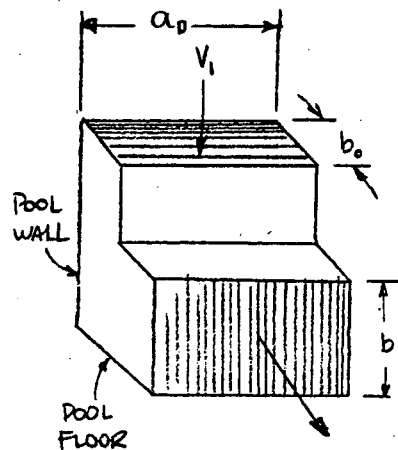
3.1.3 Downcomer Turn ( $\Delta P_t$ )

From Idel'chik, DIAGRAM 6-6

$$\frac{a_0}{b_0} \sim \infty \quad (b_0 = 1.25" \quad \checkmark \\ a_0 > 10.94" \\ b_i = 10" )$$

$$\frac{b_i}{b_0} = \frac{10}{1.25} = 8 \quad \checkmark$$

$$k = \xi_1 = 0.55 \quad \Delta P_t = k \frac{\rho V_1^2}{2g} \quad \checkmark$$



Flow/ft <sup>2</sup> (lb/hr)	Total Flow (lb/hr)	V <sub>1</sub> (ft/sec)	$\Delta P_t$	$\Delta P_{DC}$ (psi) $\Delta P_w + \Delta P_f + \Delta P_t$
2500	32,500	1.56	0.0088	0.0454 $\checkmark$
5000	65,000	3.13	0.0353	0.178
7500	97,500	4.69	0.0793	0.396
10,000	130,000	6.25	0.1409	0.701

REF.

3.2 RACK BASE LOSSES ( $\Delta P_B$ )

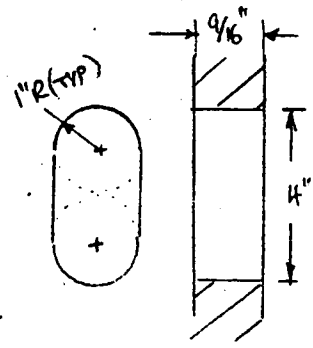
The rack base plenum losses are assumed to be negligible due to the unusual plenum height featured in the Indian Point 2 racks. The cell plates are about 18" above the pool floor, with approximately 10 inches between pool floor and bottom of rack base lattice. This provides a large volume of water that is available at all locations, especially since the whole pool floor area is open to all downcomers with no discrete channels.

Most of the cells receive coolant through 4.5-inch diameter rack base plate holes. The cells with feet are used in this analysis as they result in additional pressure drops.

3.2.1 Feet Support Holes ( $\Delta P_{sh}$ )

Two holes as indicated for each foot support configuration  
 (NES Dwg B1E3518)

|  $\Delta$



4

REF.

$$\text{Flow Area, } A = 2 \times 2 + \frac{\pi}{4} 2^2 = 7.142 \text{ in}^2 \checkmark$$

$$\text{Wetted Perm, } P = 2\pi + (2+2) = 10.283 \text{ in} \checkmark$$

$$\text{Hyd Diam, } D_e = \frac{4A}{P} = \frac{4 \times 7.142}{10.283} = 2.78 \text{ in} \checkmark$$

From IDEL'CHIK, DIAG 4-18

$$K = \xi' + \lambda \frac{L}{D_h}$$

$$\frac{L}{D_h} = \frac{0.563}{2.78} = 0.20 \quad \lambda = 0.018 \checkmark$$

$$\xi' = 2.72 \checkmark$$

$$K = 2.72 + (0.018 \times 0.20) = 2.73 \checkmark$$

Flow/Ass'y lb/hr	Flow/HOLE lb/hr	Velocity (ft/sec)	$\Delta P_{SH}$ (psi)
2500	1250	0.115	0.0002
5000	2500	0.230	0.0009
7500	3750	0.345	0.0021
10,000	5000	0.461	0.0038

### 3.2.2 Base Plate Holes ( $\Delta P_{ph}$ )

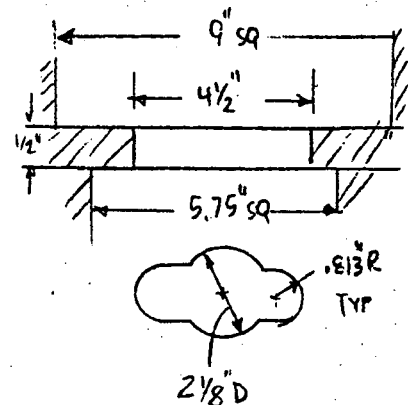
$$\text{Flow Area, } A \cong \pi (0.813)^2 + \frac{\pi}{4} (2.125)^2$$

$$+ (1.625) [4.5 - .813 - .813 - 2.125]$$

$$\cong 6.842 \text{ in}^2 \checkmark$$

$$\text{Wetted Perm, } P \cong 2\pi (0.813) + (\pi 2.125 - 2 \times 1.625)$$

$$+ 2 [4.5 - .813 - .813 - 2.125] = 10.03 \text{ in} \checkmark$$



p. 6

REF.

$$\text{Hyd Diam, } D_e = \frac{4A}{P} = \frac{4 \times 6.842}{10.03} = 2.73 \text{ in } \checkmark$$

From IDELCHIK, DIAG 4-11

$$K = \xi_0 + \lambda \frac{L}{D_h}$$

$$\lambda = 0.018 \checkmark$$

$$L = 0.5 \text{''}$$

$$D_h = 2.73 \text{''}$$

$$\xi_0 = 0.5 \left(1 - \frac{F_0}{F_1}\right) + \left(1 - \frac{F_0}{F_2}\right)^2 + z \left(1 - \frac{F_0}{F_1}\right)^{1/2} \left(1 - \frac{F_0}{F_2}\right)$$

$$F_0 = A_{\text{orifice}} = 6.84 \text{ in}^2$$

$$F_1 = (5.75)^2 = 33.06 \text{ in}^2$$

$$F_2 = 9^2 = 81 \text{ in}^2$$

$$\begin{aligned} \xi_0 &= 0.5 \left(1 - \frac{6.84}{33.06}\right) + \left(1 - \frac{6.84}{81}\right)^2 + 0.018 \left(1 - \frac{6.84}{33.06}\right)^{1/2} \left(1 - \frac{6.84}{81}\right) \\ &= .397 + .838 + .018(.890)(.916) \\ &= 1.25 \checkmark \end{aligned}$$

$$K = 1.25 + 0.018 \frac{0.5}{2.73} = 1.25 \checkmark$$

Flow/assy (lb/hr)	Vel (ft/sec)	$\Delta P_{ph}$ (psi)	$\Delta P_B = \Delta P_{sh} + \Delta P_{ph}$ (psi)
2500	0.24	0.0005	0.0007
5000	0.48	0.0019	0.0028
7500	0.72	0.0043	0.0064
10000	0.96	0.0076	0.0114

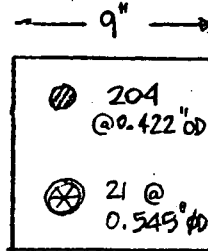
REF.

3.3 BUNDLE LOSSES ( $\Delta P_b$ )

3.3.1 Bundle Friction ( $\Delta P_{bf}$ )

$$\text{Flow Area, } A = 9^2 - 204 \frac{\pi}{4} (.422)^2 - 21 \frac{\pi}{4} (.545)^2$$

$$= 47.568 \text{ in}^2 = 0.330 \text{ ft}^2 \checkmark$$



Rad  
Length =  
150"

$$\text{Wetted Perm, } P = 4 \times 9 + 204 \pi (.422) + 21 \pi (.545) = 342.409 \text{ in} \checkmark$$

$$\text{Hyd Diam, } D_c = \frac{4 \times 47.568}{342.409} = 0.556 \text{ in} \checkmark$$

Flow/assy (lb/hr)	Vel ft/sec	Re	f*	$\Delta P_{bf}$ ✓
2500	0.035	403	0.298	0.0006
5000	0.069	806	0.149	0.0013
7500	0.104	1210	0.099	0.0019
10,000	0.138	1613	0.074	0.0025

$$* f = \frac{120}{Re}$$

9

3.3.2 Bundle Form Losses ( $\Delta P_k$ )

$$K_{\text{TOTAL}} \text{ (based on rack cell area)}$$

$$= 24.1 \left( \frac{.330}{.266} \right)^2 = 37.2 \checkmark$$

Flow/assy (lb/hr)	VEL (ft/sec)	$\Delta P_k$ (psi)	$\Delta P_b = \Delta P_{bf} + \Delta P_k$ (psi)
2500	0.035	0.0003 ✓	0.0009 ✓
5000	0.069	0.0012	0.0025
7500	0.104	0.0026	0.0045
10000	0.138	0.0046	0.0071



REF.

3.4 TOTAL PRESSURE LOSS

$$\Delta P_T = \text{Downcomer} + \text{Base} + \text{Bundle}$$

$$= \Delta P_{DC} + \Delta P_B + \Delta P_b$$

<u>Flow/Assy</u> <u>(lb/hr)</u>	<u><math>\Delta P_T</math></u> <u>(psi)</u> ✓
2500	0.047
5000	0.184
7500	0.407
10,000	0.720



REF.

5. NATURAL CIRCULATION HEAD

The driving force for the natural circulation flow is the density difference between the average hot column in the assemblies and the cooler bulk temperature in the downcomer.

The water column is assumed to be 15.5 ft (185"), conservatively neglecting any plume effects.

$$\Delta P = H (P_{\text{COLD}} - P_{\text{HOT}})$$

$$P_{\text{COLD}} (150^{\circ}\text{F}) = 61.200 \text{ lb/ft}^3$$

$$P_{\text{HOT}} (200^{\circ}\text{F}) = 60.096 \text{ lb/ft}^3$$

$$\Delta P_H = \frac{15.5 \cdot (61.2 - 60.096)}{50} \cdot \frac{1}{144} = 0.00238 \text{ psi/}^{\circ}\text{F} \checkmark$$

$$\bar{\Delta T} = \bar{T}_{\text{HOT}} - 150^{\circ}$$

Temp difference between hot column avg temp and downcomer

$$\bar{T}_{\text{HOT}} = \frac{150^{\circ} + T_{\text{OUT}}}{2}$$

$$\therefore \bar{\Delta T} = \frac{150^{\circ} + T_{\text{OUT}}}{2} - 150 = \frac{T_{\text{OUT}}}{2} - 75$$

$$\Delta P_H = 0.00238 \left[ \frac{T_{\text{OUT}}}{2} - 75 \right]$$

$\frac{\text{Flow/ASSY}}{\text{lb/hr}}$	$T_{\text{OUT}} (p. )$	$\Delta P_H$
2500	257.6	0.1280 $\checkmark$
5000	203.8	0.0640
7500	185.9	0.0427
10,000	176.9	0.0320

REF.

From FIG. 1

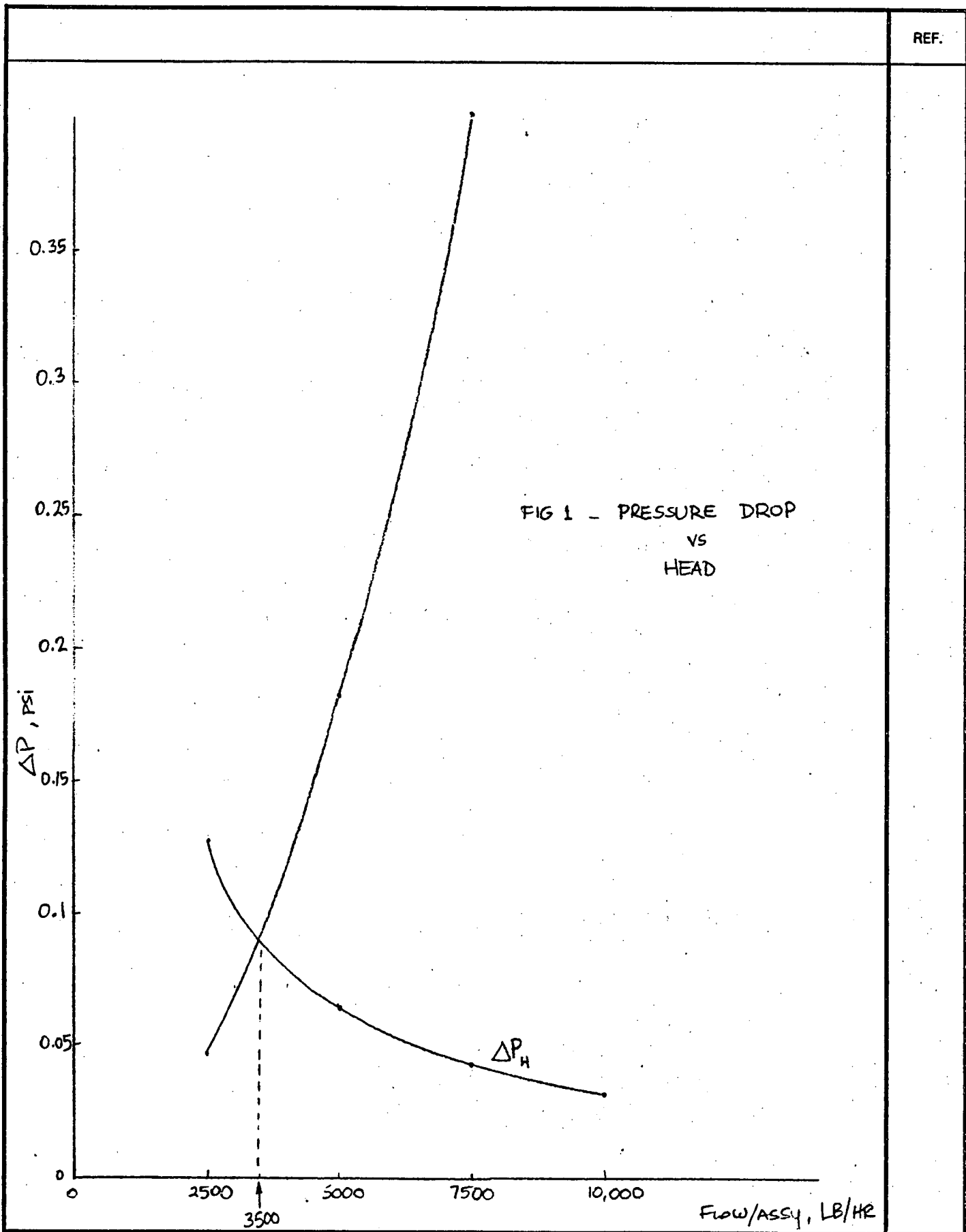
THE minimum flow per assembly = 3500 lb/hr

$$\Delta T_{\max} = \frac{268,880 \text{ Btu/hr lb}^\circ\text{F}}{3500 \times 1 \text{ lb/hr Btu}} = 76.8^\circ\text{F}$$

$$T_{\text{OUTLET, MAX}} = 150 + 76.8 = 226.8^\circ\text{F}$$

$$< T_{\text{sat}} = 239^\circ\text{F}$$

The maximum assembly outlet temperature is, therefore, substantially less than the boiling temperature of 239°F. It should be noted that even this value of 226.8°F, is unlikely to occur in the pool, since a major portion of the total pressure drop calculated is caused by the 1.25" downcomer gap, conservatively assumed to provide the only path to the plenum from the pool bulk water above the racks. The anticipated mode of natural circulation is for the coolant to reach the plenum via least-resistance flow paths, such as the cask area, the north wall downcomer gap of 11-9/16" and between the 2.5"-gap between racks.





REF.

REFERENCES FOR APPENDICES A, B, C

1. CON ED SPEC MP79-001, Section 6.5.1
2. NES QAPP B1A0606, APP A
3. Branch Technical Position 9-2, Residual Decay Energy for Light Water Reactors for Long-Term Cooling, 11-24-75.
4. NES Drawg B1E3521
5. CON ED SPEC MP79-001, TABLE 1
6. CRANE, Flow of Fluids, Tech. Paper 410, A-24.
7. Idel'chik., Handbook of Hydraulic Resistance, AEC-tr-6630.
8. Telecon between NES and Con Ed, 12-6-79
9. Rohsenow & Hartnett, Handbook of Heat Transfer, p. 7-129

ATTACHMENT E

Non-Linear Time History Seismic  
Sliding Analysis Report  
for the  
Indian Point Unit No. 2 Spent  
Fuel Storage Racks

Consolidated Edison Company of New York, Inc.  
Indian Point Unit No. 2  
Docket No. 50-247  
May, 1980



**NON-LINEAR TIME HISTORY SEISMIC SLIDING ANALYSIS REPORT  
FOR THE  
INDIAN POINT UNIT NO. 2  
SPENT FUEL STORAGE RACKS**

**Prepared for  
Consolidated Edison Company of New York, Inc.**



## TABLE OF CONTENTS

	<u>PAGE</u>
1. SUMMARY	5
2. INTRODUCTION	6
3. DESCRIPTION OF THE STORAGE RACKS	7
4. APPLICABLE SPECIFICATIONS, STANDARDS, AND CODES	10
5. ANALYSIS ASSUMPTIONS	11
6. ACCEPTANCE CRITERION	13
7. METHOD OF ANALYSIS	14
7.1 Mathematical Model	14
7.2 Mathematical Formulation of the Non-Linear Time History Seismic Analysis	15
8. RESULTS OF THE ANALYSIS	18
8.1 Fuel Storage Rack Sliding Analysis	18
8.2 Fuel Storage Rack Maximum Frictional Resistance Load	18
9. CONCLUSIONS	23
10. REFERENCES	24
APPENDIX A - ANALYTICAL MEMBER PROPERTIES	
APPENDIX B - LUMPED MASSES DISTRIBUTION	
APPENDIX C - MAXIMUM FRICTIONAL RESISTANCE LOAD	



## LIST OF FIGURES

	<u>PAGE</u>
3.1 Fuel Storage Rack Arrangement Plan	8
3.2 Indian Point 2 Borated SST Fuel Storage Rack	9
5.1 Pool Floor Absolute Acceleration Time History	12
7.1 Non-Linear Time History Seismic Analysis Lumped Mass Finite Element Non-Linear Model	17
8.1 Cumulative Sliding Time History ( $\mu = 0.2$ )	21
8.2 Frictional Resistance Load Time History ( $\mu = 1.5$ )	22

## LIST OF TABLES

8.1 Summary of Sliding Analysis Results	20
---	----



## 1. SUMMARY

The Indian Point 2 High Density Spent Fuel Storage Racks have been designed to meet the requirements for Seismic Category 1 structures. A detailed non-linear time history seismic analysis has been performed to evaluate the maximum sliding of the storage racks and to determine the maximum frictional resistance load transmitted by the storage racks to the pool floor liner plate during the Design Basis Earthquake (DBE).

The non-linear time history seismic analysis has been performed using step-by-step integration techniques. The hydrodynamic effect of the spent fuel pool water and the effect of fuel assembly impact have been included in the analyses. The analysis indicates that during a DBE seismic event: (1) the maximum sliding of an individual storage rack is approximately 0.125 inches (assuming conservatively low coefficient of friction of 0.20); (2) the maximum flexural deflection of the rack top relative to its base is approximately 0.697 inches (conservatively assuming no sliding due to high coefficient of friction); and (3) the storage rack will transmit a maximum frictional resistance load of 170,933 pounds to the pool floor liner plate (assuming a coefficient of friction sufficiently high to preclude sliding).

It has been concluded therefore, that the gaps provided between storage racks and between storage racks and pool structure are sufficient to preclude any rack-to-rack or rack-to-pool structure collisions under the DBE event.



## 2. INTRODUCTION

Nuclear Energy Services, Inc. (NES) has designed the high density spent fuel storage racks for Consolidated Edison Company (Con Ed) to be installed in the Indian Point 2 fuel pool. The racks are designed to provide storage locations for up to 980 fuel assemblies (Reference 1). The spent fuel storage racks are designed to maintain the stored fuel, having a maximum equivalent uranium enrichment of 3.5 percent of U-235 by weight in Uranium in a safe, coolable, subcritical configuration during normal and abnormal conditions.

The Indian Point 2 high density fuel storage racks are a "free-standing" design (racks are free to slide horizontally on the pool floor). The linear structural analysis of these racks is presented in NES report 81A0610 (Reference 2). Document 81A0610 presents the results of the analysis determining the maximum linear seismic structural responses (stresses and reaction loads) of the racks conservatively assuming the support feet locations to be pinned (not sliding) to the pool floor.

NES has performed a non-linear time history seismic analysis to evaluate the response of an individual fuel storage rack (maximum accumulated sliding displacement) to the Design Basis Earthquake (DBE) time history. The fuel rack is mathematically modeled as a multi-degree-of-freedom finite element structure incorporating the stiffness characteristics of the storage rack and fuel assembly/storage cell interface and the storage rack leveling pad/pool floor interface.

This report presents the results of the non-linear time history seismic analysis which was performed by NES to determine the maximum sliding displacement of the storage racks during a seismic event and to determine the maximum frictional load transmitted to the pool floor liner plate.



### 3. DESCRIPTION OF THE STORAGE RACKS

The Indian Point 2 high density fuel storage racks have been designed to provide a maximum storage capacity of 980 locations. The arrangement of the fuel storage racks in the spent fuel storage pool is shown in Figure 3.1. The fuel storage rack arrangement contains five types of storage rack arrays including:

- (1) Two racks of 8x8 array each.
- (2) Two racks of 10x10 array each.
- (3) One rack of 9x8 array.
- (4) Two racks of 9x10 array each.
- (5) Five racks of 8x10 array each.

Each rack consists of an assembly of 2x2 modules with the 9x8 and 9x10 racks incorporating 2x3 modules as well. Each 2x2 or 2x3 modular cell unit consists of four (4) or six (6) cells spaced nominally 10-15/16 inches on centers. Each storage cell is a Type 304 stainless steel box (9 inches ID). Borated stainless steel sheets are attached to the outside of the cell walls by means of welded brackets. The top opening of the storage cell is flared to facilitate insertion of the fuel assembly; the bottom member of the storage cell provides the level support surface required for the fuel assembly and contains the cooling flow orifice.

Each modular cell unit (either 2x2 or 2x3) is supported by and welded to the rack base grid structure constructed from Type 304 stainless steel wide flange and box beam members. A schematic drawing of a representative 10x10 rack structure and an individual 2x2 modular cell unit is shown in Figure 3.2. Continuous spacer beams are provided at the top of the storage cells to ensure that the required pitch is maintained between storage cells in both directions (north/south and east/west) under lateral load conditions. The spacer beams which are intermittently welded to the storage cells also maintain the vertical alignment of the cells. Support pads attached to the bottom of the rack base raise the rack above the pool floor to clear existing anchor pins on the pool floor area and to provide an adequately sized cooling water supply plenum for natural circulation. Each support pad contains a remotely adjustable jack screw to permit the rack to be leveled following wet installation. The rack support pads will rest directly on the pool floor wherever possible. In case of interference with the existing floor shims, the pads will rest on local plates designed to bridge over the shims.

The storage racks are positioned on the pool floor so that adequate clearances are provided between racks and between the racks and pool structures to avoid impacting of the sliding racks during seismic events. Adequate clearances are also provided between floor plate supports and existing floor shims to preclude impact in the case that the plates slide relative to the shims in a seismic event. The horizontal seismic loads transmitted from the rack structure to the pool floor are only those associated with friction between the rack structure and the pool liner. The vertical deadweight and seismic loads are transmitted directly to the pool floor by the support feet. The storage racks' detailed design and their layout in the spent fuel storage pool are shown in Reference 1 Drawings.

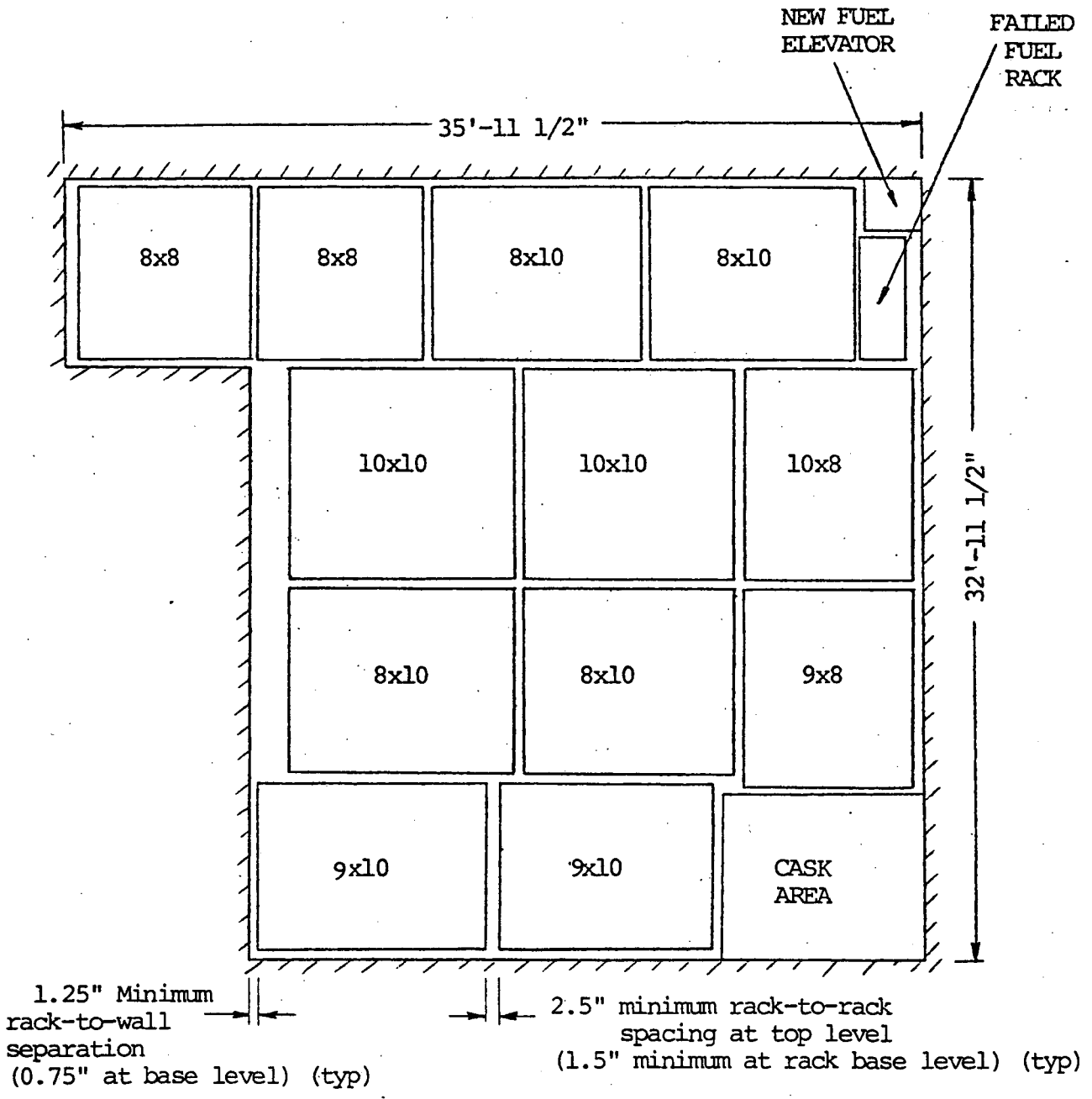


Figure 3.1 Fuel Storage Rack Arrangement Plan

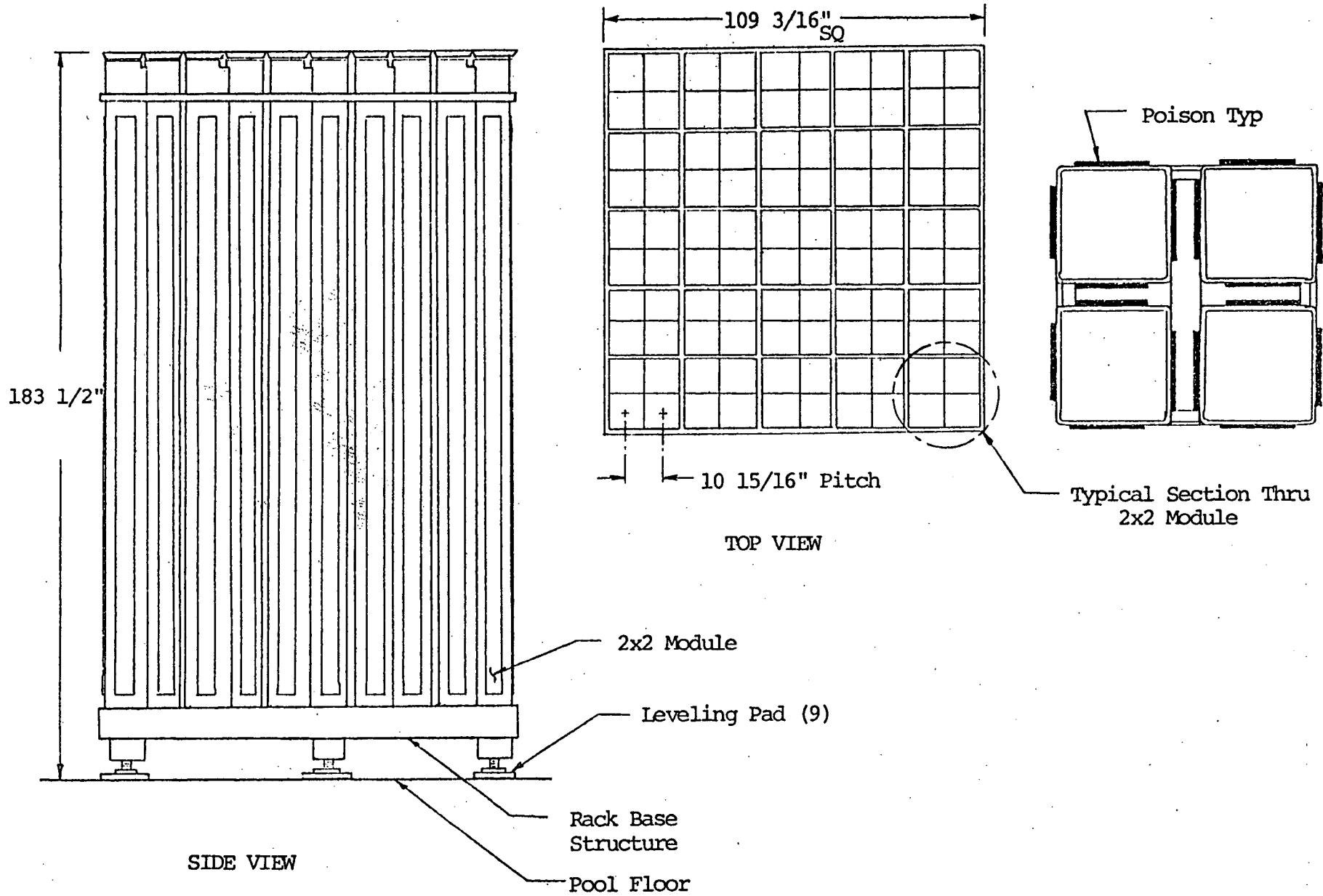


Figure 3.2 Indian Point 2  
Borated SST Fuel Storage Rack (10x10)



#### 4. APPLICABLE SPECIFICATIONS, STANDARDS, AND CODES

The following design specification, Regulatory Guides and Codes, have been used in the design/analysis of spent fuel storage racks (References 3 through 7).

1. Nuclear Energy Services, Inc. Document NES 81A0606, "Quality Assurance Program Plan for the Indian Point Generating Station Unit 2 Fuel Storage Racks," November 1979.
2. Consolidated Edison Company, "Design, Fabricate, Deliver and Installation of Spent Fuel Storage Racks," Specification No. MP79-001, Rev. 2, March 1979.
3. USNRC Regulatory Guide 1.92, "Combination of Modes and Spatial Components in Seismic Response Analysis," Rev. 1, February 1976.
4. USNRC Standard Review Plan, Section 3.8.4.
5. USNRC "Position Paper for Review and Acceptance of Spent Fuel Storage and Handling Applications," April 14, 1978 and Supplement, January 18, 1979.



## 5. ANALYSIS ASSUMPTIONS

The Indian Point Unit 2 spent fuel pool floor absolute acceleration time history shown in Figure 5.1 (Reference 8) was used to evaluate the sliding response of the storage rack structure. This 10-second duration acceleration time history represents the 1% damping spectra for the Design Basis Earthquake.

The review of available literature indicates that a wide range of static and dynamic coefficients of friction are possible for stainless steel sliding on stainless steel in a dry or wet environment. Reference 12 states that the coefficients of static and dynamic friction can range from 0.3 to 0.8 for stainless steel on stainless steel. Since the maximum sliding distance is established by the minimum coefficient of friction, a conservatively low value was selected for the analysis (0.20). In order to establish the maximum frictional load applied to the pool floor liner, it is necessary to select a coefficient of friction sufficiently high to preclude any sliding. A value of 1.5 was chosen because it represents a coefficient of friction clearly expected to eliminate any sliding.

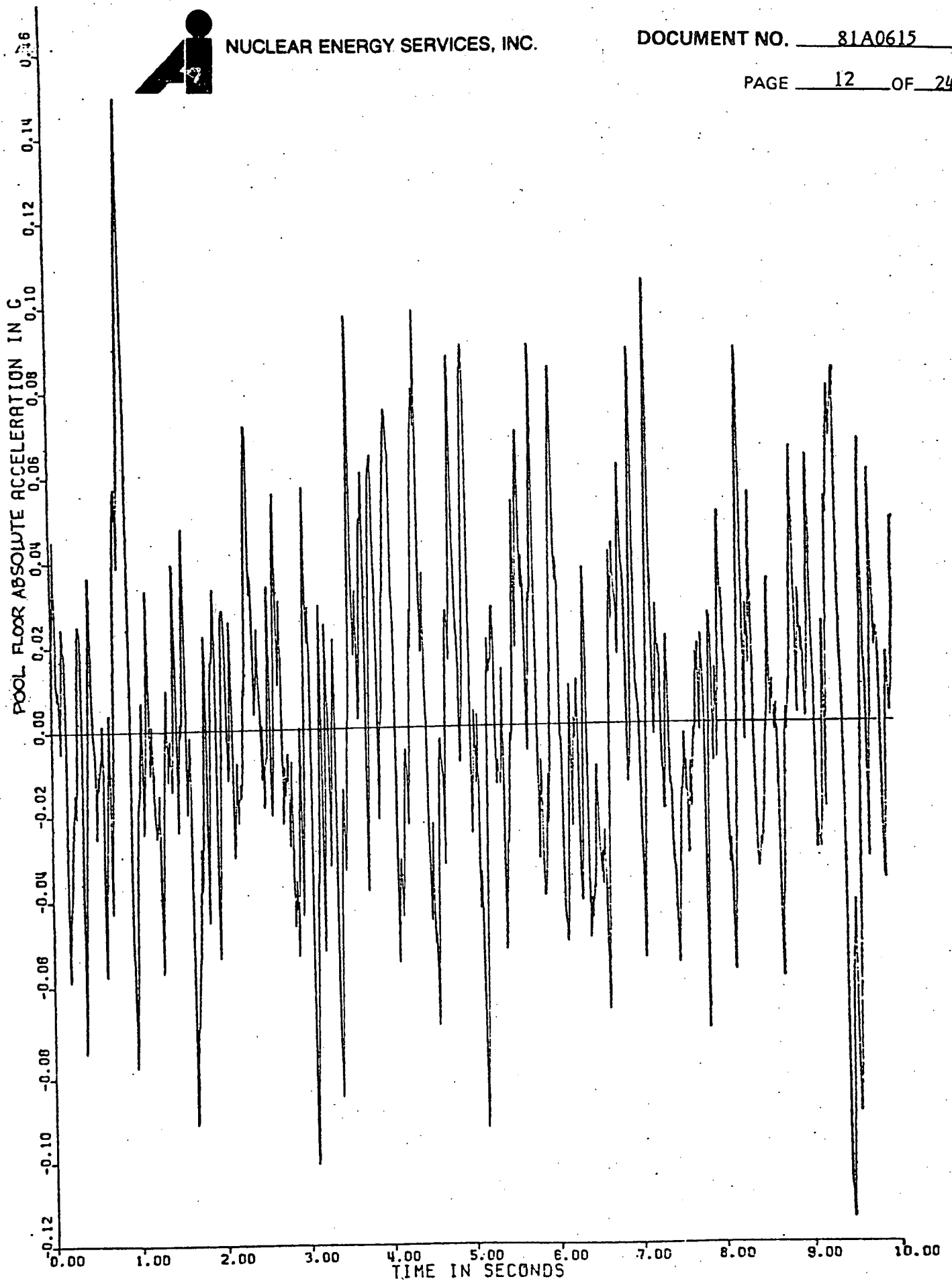


FIGURE 5.1 POOL FLOOR ABSOLUTE ACCELERATION TIME HISTORY



## 6. ACCEPTANCE CRITERIA

The acceptance criteria used in this analysis are:

- (1) The minimum separation of 1.50 inches provided at the base level between adjacent racks (0.75 inches between racks and walls) should accommodate the maximum sliding distances\* calculated. Flexural deflection and horizontal displacement distances due to tilting are not applicable at the rack base level.
- (2) The minimum separation of 2.50 inches provided at the rack flared top level\*\* between adjacent racks (1.25 inches between racks and wall) should accommodate appropriate and conservative combinations of the sliding, lifting and tilting distances calculated. The combinations include adjacent rack tops deflecting towards each other at their maximum displacement at the same time that the racks reach the maximum sliding distance; as well as maximum tilting occurring concurrently with maximum sliding. The flexural deflection and horizontal displacement due to tilting cannot both occur at their maximum values simultaneously since both mechanisms are caused by the same available external energy.

---

\* The sliding distance is the maximum displacement of the rack relative to its initial position on the floor.

\*\* The rack top separation is required to accommodate the sliding of the rack, the flexural deflection at the top of the rack, the lateral displacement of the rack top due to tilting, and appropriate combinations thereof.



## 7. METHOD OF ANALYSIS

### 7.1 MATHEMATICAL MODEL

In order to perform the non-linear time history seismic analysis of the spent fuel assembly/storage cell structure, a 10x10 storage rack and the stored fuel assemblies have been represented by a two dimensional lumped mass finite element model (Figure 7.1). The model consists basically of two coincident finite element cantilever beams; one representing the 100 storage cells and the other 100 stored fuel assemblies attached to a "floor" mass by means of a non-linear sliding element.

The fuel element cantilever beam consists of masses lumped at the nodal points interconnected by discrete beam elements. Each lumped mass represents the tributary weight of the fuel element mass. The stiffness characteristics of the beam elements are related to the effective flexural rigidity of the fuel assemblies (Appendix A).

The storage rack cantilever beam similarly consists of lumped masses interconnected by discrete elastic beam elements. Each lumped mass represents the tributary weight of the storage cells, water trapped inside the cells and the virtual water mass to account for the hydrodynamic effects. The stiffness characteristics of the storage rack beam elements are related to the dynamic characteristics (fundamental frequency of vibration) of the storage rack as determined by the Lanczos Modal Extraction method of analysis (Reference 2).

In order to account for fuel assembly impact, adjacent masses of the fuel assembly beam and the storage rack beam are laterally coupled by means of non-linear spring/gap elements. The non-linear spring/gap elements permit the adjacent masses to impact each other whenever the gap closes during a seismic event. The stiffness of the non-linear spring is taken as the stiffness value for each spacer grid. An initial gap of 0.287 inch, reflecting the lateral gap between the fuel assembly and the storage cell wall, is provided. The non-linear spring/gap elements are effective for fuel assembly impact on either side of the storage cell.

The two cantilever beams representing the storage cells and fuel assemblies are attached to the pool floor mass by means of the non-linear sliding element to best represent the rack standing freely on the pool floor. The sliding of the rack is initiated when the lateral force in the sliding element exceeds the frictional resistance force which is equal to the coefficient of friction times the vertical weight of the rack. The effective vertical weight is taken as the vertical bouyant weight of the storage rack less the uplift loads due to the vertical component of the Design Basis Earthquake.

Since the storage racks with 8x8, 9x8, 9x10 and 8x10 arrays consist of 2x2 modules (9x8 and 9x10 racks have some 2x3 modules as well), their dynamic (frequency) characteristics are essentially similar to the 10x10 storage rack. The lateral seismic inertia load and the frictional resistance load for the 8x8, 9x8, 9x10 and 8x10 storage racks would be proportional to the 10x10 storage rack. The storage rack sliding response, which depends upon the relative magnitude of the lateral seismic load and the frictional resistance load, will therefore be identical for the 10x10, 8x8x, 9x8, 9x10 and 8x10 storage racks.



## 7.2 MATHEMATICAL FORMULATION OF THE NON-LINEAR TIME HISTORY SEISMIC ANALYSIS

Considering only translational degrees of freedom and assuming viscous (velocity proportional) form of damping, the equation of motion in matrix form can be expressed as follows:

$$M (\ddot{U}_t + \ddot{U}_{gt}) + C\dot{U}_t + KU_t = 0 \quad (1)$$

Where:

$\ddot{U}_t$  = Relative acceleration time history vector

$\ddot{U}_{gt}$  = Ground acceleration time history vector

M = Mass matrix

C = Damping Matrix

K = Stiffness matrix

$\dot{U}_t$  = Velocity time history vector

$U_t$  = Relative displacement time history vector

Rearranging equation (1):

$$M\ddot{U}_t + C\dot{U}_t + KU_t = -M\ddot{U}_{gt} = F_t \quad (2)$$

The above equations of motion are solved using step-by-step numerical integration methods. The numerical integration technique used in the analysis is the Houbolt method (Reference 9). The straight-forward numerical integration of the equation of motion has the advantage that non-linear effects, such as variation in K, M or C due to closing or opening of gaps, sliding, large deflection and plasticity, can be readily included in the analysis.

In the numerical integration procedure:

$$U = f(U_t, U_{t-1}, U_{t-2}, \dots) \quad (3)$$

$$\dot{U} = g(U_t, U_{t-1}, U_{t-2}, \dots) \quad (4)$$

$$\ddot{U} = h(U_t, U_{t-1}, U_{t-2}, \dots) \quad (5)$$



For third order integration used in the analysis,  $f$  is a cubic function and the acceleration is a linear function across the time interval. Making these substitutions into Equation (2) gives:

$$(C_1 M + C_2 C + K) U_t = F_t + f(C, M, U_{t-1}, U_{t-2}, \dots) \quad (6)$$

Where  $C_1$  and  $C_2$  are functions of  $t-t_{-1}$  and  $t_{-1}-t_{-2}$ , etc.

Using an iterative procedure, Equation (6) is solved at each time point in the dynamic (seismic) transient. Since mass ( $M$ ), damping ( $C$ ) and stiffness ( $K$ ) are recalculated at each time point, they can vary with time or can be functions of the displacement.

The non-linear time history seismic analysis calculations are performed by means of step-by-step integration technique using the ANSYS computer program (Reference 10).

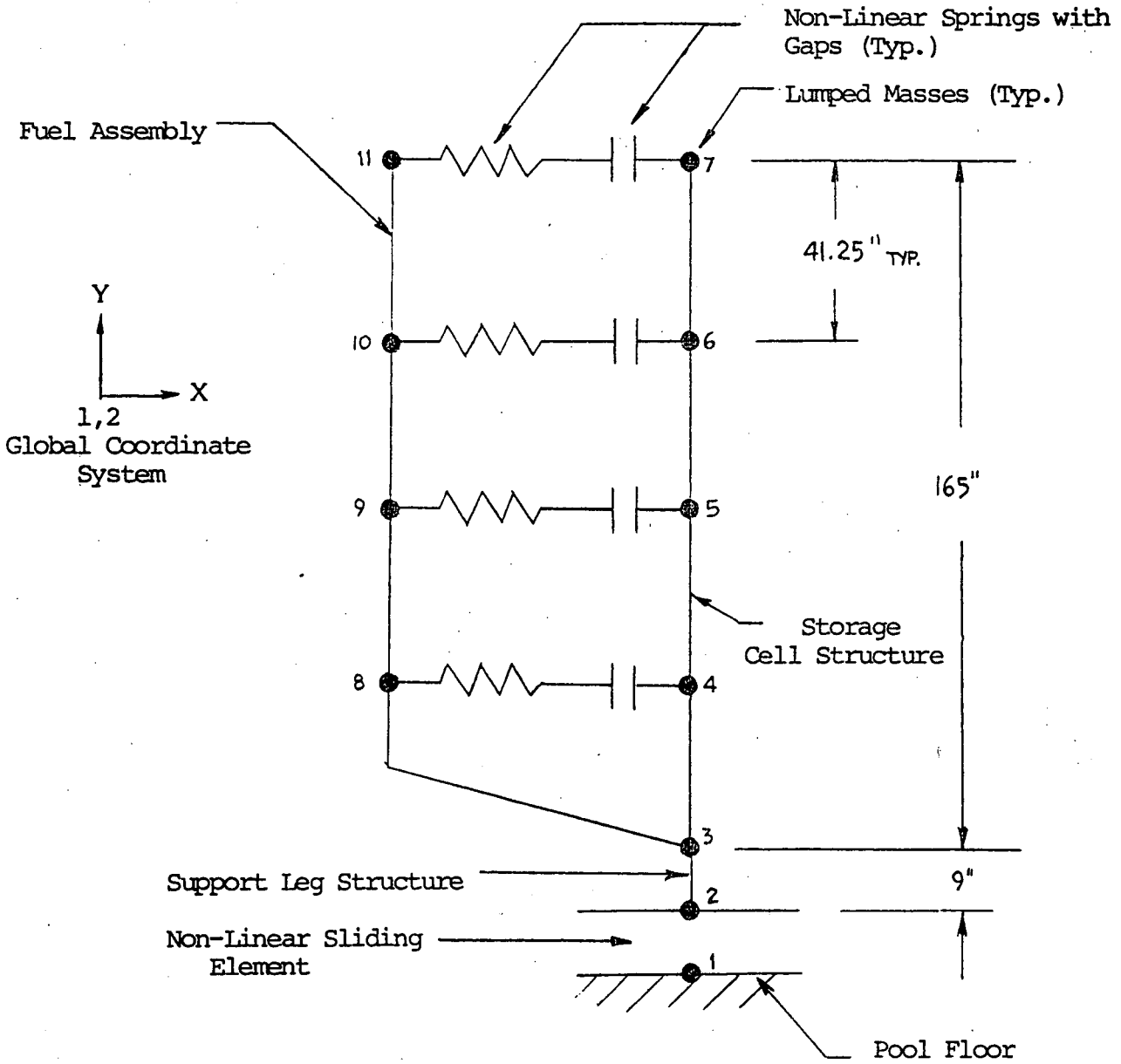


FIGURE 7.1

Non-Linear Time History Seismic Analysis Lumped Mass Finite Element Non-Linear Model



## 8. RESULTS OF THE ANALYSIS

The results of the non-linear time history seismic analysis of the Indian Point 2 free-standing high density fuel storage rack performed with the ANSYS computer code are contained in Reference 11. Appendices A through C contain the stiffness, mass properties and rack support feet reaction load calculations. The results of the analysis are summarized in Table 8.1.

### 8.1 FUEL STORAGE RACK SLIDING ANALYSIS

The maximum accumulated sliding displacement of the storage rack relative to its initial floor location has been calculated to be 0.125 inches for the coefficient of friction value of 0.20. This maximum displacement value represents the accumulated storage rack sliding response during the 10 seconds of the applied time history. A plot of this accumulated sliding displacement versus time is shown in Figure 8.1.

The maximum accumulated sliding displacement value of 0.125 inches is approximately 16.7 percent of the minimum allowable clearance of 0.75 inches available for each rack between the pool walls and their adjacent storage rack base structures, and between rack bases.

The maximum rack top deflection was calculated to be 0.697 inches for a coefficient of friction of 1.5, which precludes any sliding between the rack and the pool floor.

The maximum rack cell displacement (rack sliding plus cell top flexural deflection) is therefore 0.822 inches at the flared opening level. This value is approximately 65.8 percent of the minimum available clearance value (1.25 inches) provided for each rack.

It has therefore been concluded that the gaps provided between storage racks (2.5 inch minimum) and between pool walls and adjacent storage racks (1.25 inch minimum) are sufficient to preclude any collision of adjacent structures during a Design Basis Earthquake event. It should be noted, that the assumption used in this evaluation of two adjacent storage racks sliding towards one another during the seismic event with simultaneously opposite deflections of the rack tops is unlikely and hence very conservative.

### 8.2 FUEL STORAGE RACK MAXIMUM FRICTIONAL RESISTANCE LOAD

For the higher coefficient of friction of 1.5, the time history response of the frictional resistance load between the storage rack and the pool liner plate is shown in Figure 8.2. From Figure 8.2 it can be seen that the maximum frictional resistance load between the storage rack and the pool floor liner plate is 142,200 pounds. For this case, no sliding occurred when establishing the floor loading which verified the higher coefficient of friction.



In evaluating the effects of the horizontal orthogonal components of the earthquake, it is considered unlikely that the two peaks will occur simultaneously. Therefore, the average reaction force over a 0.05 second interval in the vicinity of the peak has been assumed as the seismic force in each orthogonal direction. The resultant effective frictional reaction force affecting the liner plate and rack support feet due to the orthogonal earthquake components is calculated to be 170,933 pounds. The results of the rack stability analysis in NES Report 81A0610 (Reference 2) indicate that during a DBE seismic event the storage racks will tilt, resulting in six of the nine rack feet effectively transmitting the lateral seismic load to the pool liner. The maximum reaction load for the individual rack feet is, therefore, 28,500 pounds. (Refer to Appendix C.)



TABLE 8.1  
SUMMARY OF SLIDING ANALYSIS RESULTS

	<u>Rack Top</u>	<u>Rack Base</u>
Maximum Rack Sliding Displacement <sup>1</sup> (in.)	0.125	0.125
Maximum Cell Tilting Horiz. Displacement <sup>2</sup> (in.)	0.662	Negl.
Maximum Cell Deflection <sup>3</sup> (in.)	0.697	Negl.
Maximum Sliding and Tilting (in.)	0.787	0.125
Maximum Sliding and Deflection (in.)	0.822	0.125
Maximum Clearances Provided	1.25 <sup>4</sup>	0.75 <sup>5</sup>
Maximum Floor Horiz. Frictional Force, One Lateral Earthquake Component (lb)	142,200	
Maximum Floor Horiz. Frictional Force, SRSS Combination of Orthogonal Earthquake Components (lb) <sup>6</sup>	170,933	
Maximum Horiz. Frictional Load per Rack Support Foot (lb) <sup>7</sup>	28,500	

NOTES:

- (1) Displacement relative to initial floor location ( $\mu = 0.2$ ).
- (2) Horizontal displacement for a 8x10 rack based on vertical lifting height reported in Section 8.5 of Reference 2.
- (3) Maximum cell flexural deflection with no sliding between rack and floor ( $\mu = 1.5$ ).
- (4) Minimum clearance provided between pool walls and adjacent rack tops (half the minimum clearance between adjacent rack tops).
- (5) Minimum clearance provided between pool walls and adjacent rack bases (half the minimum clearance between adjacent rack bases).
- (6) Average reaction force over 0.05 second interval of uni-directional earthquake response assumed for each orthogonal direction.
- (7) SRSS combination load assumed carried by six support legs.

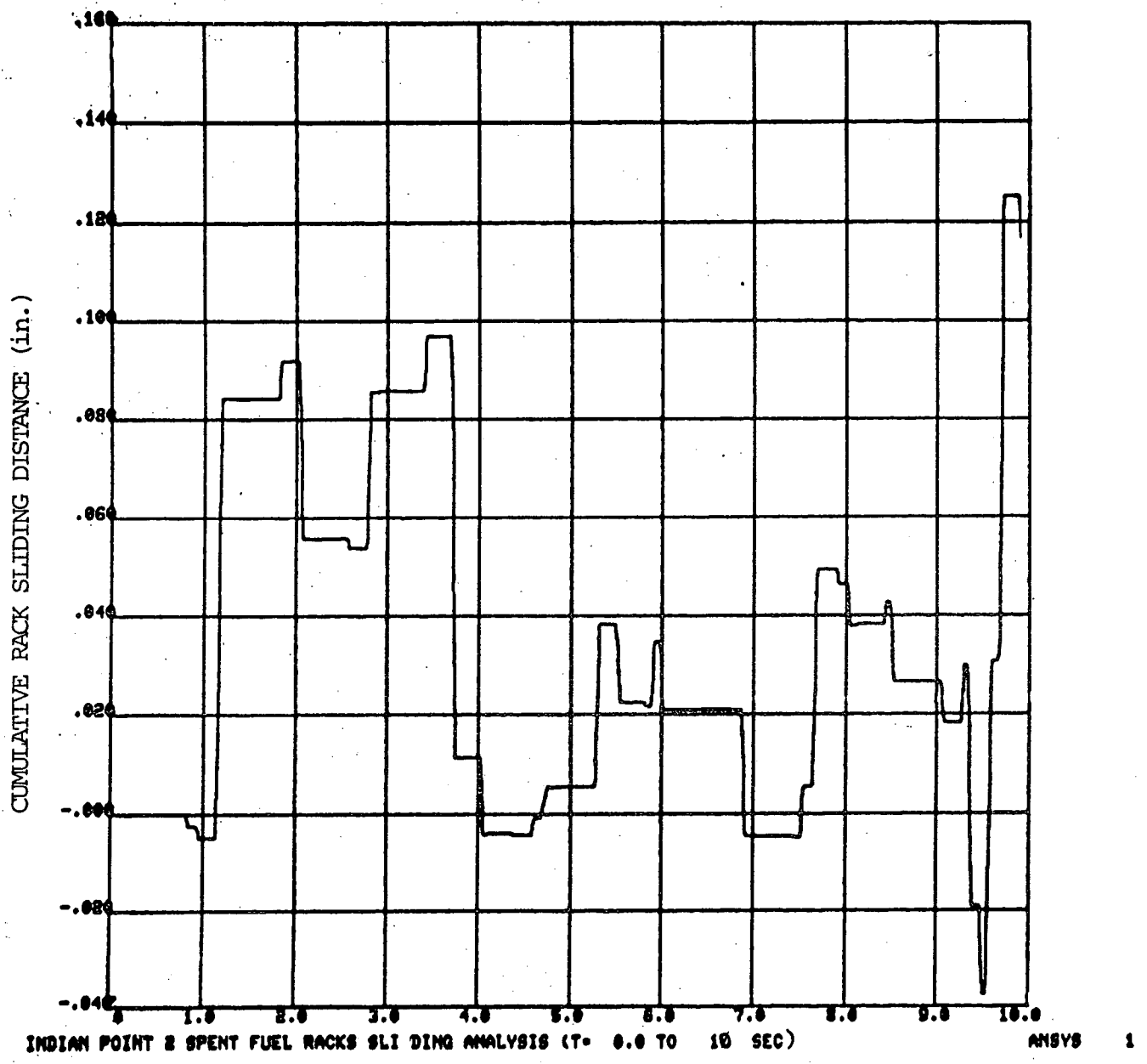


Figure 8.1 Cumulative Sliding Time History ( $\mu = 0.2$ )

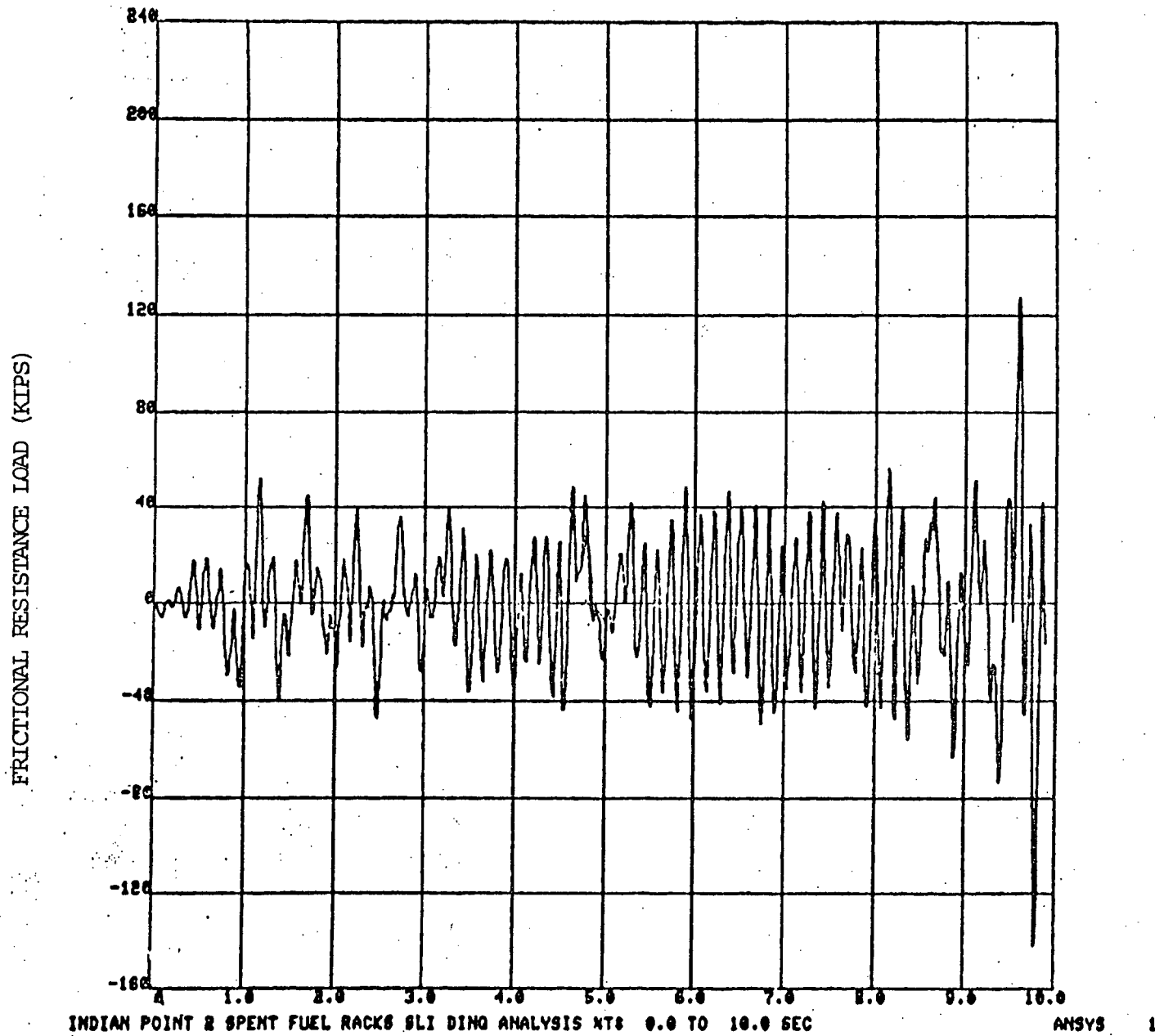


Figure 8.2 Frictional Resistance Load Time History ( $\mu=1.5$ )



## 9. CONCLUSIONS

1. The results of the non-linear time history seismic analysis indicate that the maximum sliding distance of the fuel storage rack during a Design Basis Earthquake event is within the allowable displacement values which are based on the minimum clearance to be provided between racks, between the local base plates under the rack feet and the existing pool floor shims, and between racks and pool walls.
2. During a seismic event, the fuel storage racks will not impact each other or the storage pool structures.
3. The maximum horizontal frictional resistance load transmitted by the storage rack to the pool floor liner is 170,933 pounds. The maximum frictional resistance load for the individual rack foot is 28,500 pounds.
4. The design of the Indian Point 2 free-standing high density fuel storage racks is adequate to meet the requirements for seismic Category 1 structures.



## 10. REFERENCES

1. Nuclear Energy Services, Inc. Drawings for Indian Point 2 Fuel Storage Racks (80E3503 thru 80E3526).
2. Nuclear Energy Services, Inc. Document NES 81A0610, "Structural Analysis Report for the Indian Point Generating Station Unit 2 Fuel Storage Racks," November 1979.
3. Nuclear Energy Services, Inc. Document NES 81A0606, "Quality Assurance Program Plan for the Indian Point Generating Station Unit 2 Fuel Storage Rack," November 1979.
4. Consolidated Edison, "Design, Fabricate, Deliver and Installation of Spent Fuel Storage Racks," Specification No. MP79-001, Rev. 2, March 1979.
5. USNRC Regulatory Guide 1.92, "Combination of Modes and Spatial Components in Seismic Response Analysis," Rev. 1, February 1976.
6. USNRC Standard Review Plan, Section 3.8.4.
7. USNRC "Position Paper for Review and Acceptance of Spent Fuel Storage Handling Applications," April 14, 1978 and Supplement, January 18, 1979.
8. Con Edison Letter to NES, number NF-9-025, dated August 23, 1979.
9. Houbolt, J.C., "The Recurrence Matrix Solution for the Dynamic Response for Elastic Aircraft Structures," Journal of Aeronautical Science, Volume 17, 1950.
10. Swanson Analysis Inc., "ANSYS - Engineering Analysis System," Revision 3, Update 37J, Boeing Computer Services 6600, January 1977.
11. Indian Point 2 Spent Fuel Storage Rack, ANSYS Non-Linear Time History Seismic Analysis Project 5147, Task 200, NES Computer Output Binder No. S43, November 1979.
12. USNRC Docket 50250-669 "Turkey Point Plan, Units 3 and 4". Supplemental Information, Proposed Modification of the Spent Fuel Storage Facility; Florida Power and Light Company, Miami, Florida, February 1977.



APPENDIX A - ANALYTICAL MEMBER PROPERTIES

APPENDIX A - ANALYTICAL MEMBER PROPERTIES

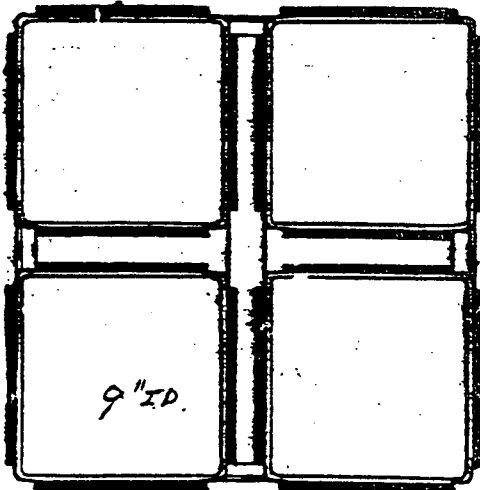
REF.

THE "SLIDING ANALYSIS MODEL" IS DEVELOPED AS AN ENTIRE 10x10 STORAGE RACK. THIS ANALYTICAL SLIDING MODEL IS COMPOSED OF 2 BEAM ELEMENTS INTERCONNECTED BY NON-LINEAR SPRING-GAP ELEMENTS.

THE ENTIRE MODEL IS ATTACHED TO THE FLOOR BY A SLIDING-GAP ELEMENT.

THE TWO BEAM ELEMENTS REPRESENT THE ACCUMULATION OF STORAGE CELLS AND FUEL ASSEMBLIES THEREFORE, THE MEMBER PROPERTIES WILL BE THE SUMMATION OF INDIVIDUAL MEMBERS.

STORAGE CELL MEMBER PROPERTIES



REF. 1

2x2 MODULE

$$AREA (2 \times 2) = 12.27 \text{ in}^2 \text{ (FROM ANALYTICAL MEMBER \# 7-LINEAR REPORT) } \times 2$$

$$AREA (10 \times 10) = 12.27 \times 25 = 306.75 \text{ in}^2$$

MOMENT OF INERTIA

$$I (2 \times 2) = 468 \text{ in}^4$$

$$I (10 \times 10) = 25 \times 468 \text{ in}^4 = 11,700.0 \text{ in}^4$$

HEIGHT - VALUE REPRESENTING THE HEIGHT OF THE STORAGE CELL FOR A 2x2 MODULE = 20.0 in

- ANALYTICAL MEMBER PROPERTIES -

REF.

SUPPORT LEG STRUCTURE -

THE 10X10 RACK IS SUPPORTED AT NINE LOCATIONS BY ADJUSTABLE JACKSCREWS. THE SUPPORT LEGS ARE MODELED AS TWO-DIMENSIONAL BEAMS WITH MEMBER PROPERTIES APPROPRIATELY REFLECTING THE LINEAR ANALYSIS RESULTS.

$$\underline{AREA} = 9 \text{ LEGS} \times 13.23 = 119.1 \text{ in}^2$$

- MOMENT OF INERTIA -

THE LINEAR DYNAMIC ANALYSIS OF A MODEL REPRESENTING A FULLY-LOADED 10X10 RACK DEPICTED THE RACK BASE FREQUENCY TO BE 3.38 CPS. THE BASE FREQUENCY REFLECTS THE FLEXIBILITY AT THE INTERSECTION OF THE BASE GRID AND SUPPORT LEGS. TO DETERMINE THE CORRECT MOMENT OF INERTIA REFLECTING THIS FLEXIBILITY, A SMALL 5 MASS MODEL WAS DYNAMICALLY ANALYZED TO ESTABLISH THE I VALUE OF THE BEAM REPRESENTING THE SUPPORT LEGS, SO THAT THE BASE FREQUENCY WAS SIMILAR TO 3.38 CPS. FROM COMPUTER RUN TALAYXH, NOV. 1979

$$\text{FOR } I = 2000.0 \text{ in}^4 \quad f = 3.74 \text{ CPS}$$

REF11

THEREFORE:  $I_{EQ.} \approx 1900.0 \text{ in}^4$

HEIGHT - ASSUME INDIVIDUAL SUPPORT LEG

$$\text{HEIGHT} = 6.875 \text{ in.}$$

ANALYTICAL MEMBER PROPERTIES

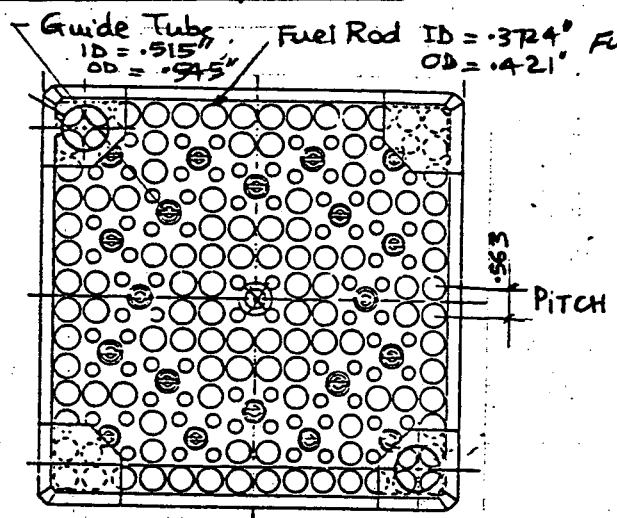
REF.

FUEL ASSEMBLY MEMBER PROPERTIES

THE ANALYTICAL INPUT DATA REQUIRES THE AREA, MOMENT OF INERTIA AND DEPTH OF FUEL ASSEMBLY REPRESENTED BY A BEAM CONFIGURATION.

FUEL ASSEMBLY AREA

(15x15 FUEL ROD ARRAY)



Fuel Rod ID = .374" OD = .421"  
 FUEL ASSEMBLY AREA =  $\frac{\pi}{4} \{ (.421)^2 - (.374)^2 \}$   
 (15 x 15 - 4 RODS x 5 GUIDE TUBES)  
 + 4 x 5  $\frac{\pi}{4} \{ (.545)^2 - (.515)^2 \}$   
 = 6.844 in<sup>2</sup> ✓

FOR A 10x10 ARRAY OF FUEL ASSEMBLIES:

$A = (10 \times 10) 6.844 = 684.4 \text{ in}^2$

- MOMENT OF INERTIA - THE MOMENT OF INERTIA FOR THE FUEL ASSEMBLIES USED IN THE ANALYSIS ARE DERIVED FROM THE FLEXURAL RIGIDITY VALUE.

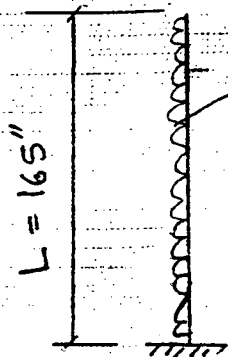
THIS FLEXURAL RIGIDITY VALUE WAS CALCULATED FROM THE LOWEST FUNDAMENTAL FREQUENCIES OF CANTILEVER MODE FOR THE INDIAN POINT #2 FUEL ASSEMBLY (1.2 to 1.7 Cycles/seconds. Com-Edison Letter NF-9-025 To Nuclear Energy Services August 23, 1979)

FOR THE SLIDING ANALYSIS USE AVERAGE FREQUENCY OF  $\frac{1.2+1.7}{2} = 1.45 \text{ cfs}$

8

MEMBER PROPERTIES

REF.



Total  $W = 1650$  lbs  
 $= 1.65$  K ✓

FUNDAMENTAL FREQUENCY  $f$  FOR CANTILEVER WITH UNIFORM LOAD  $W$  IS GIVEN BY

$$f = 3.89 \sqrt{\frac{8EI}{WL^3}}$$

$$1.45 = 3.89 \sqrt{\frac{8EI}{1.65(165)^3}}$$

$$\therefore EI = 12.873 \times 10^4 \text{ / K-in}^2 = 128.73 \times 10^6 \text{ lb-in}^2$$

THE FUEL ROD CLADDING IS COMPOSED OF ZIRCALOY-4. THE MODULUS OF ELASTICITY AT

THE MAX. BULK POOL TEMPERATURE OF  $150^\circ\text{F}$  IS  $E = 14.14 \times 10^6 (1 - 0.000936 T)$  PSI

WHERE:  $T$  IS TEMP. IN  $^\circ\text{C} = 65.56^\circ\text{C}$

$$E = 14.14 \times 10^6 (1 - 0.000936 (65.56)) = 13.27 \times 10^6 \text{ PSI}$$

$$I_{\text{EFF}} = \frac{EI}{E} = \frac{128.73 \times 10^6 \text{ lb-in}^2}{13.27 \times 10^6 \text{ #/sq}} = 9.7009 \text{ in}^4$$

$$I_{\text{EFF}} \text{ FOR } (10 \times 10 \text{ ARRAY}) = (10 \times 10) 9.7009 = 970.1 \text{ in}^4$$

HEIGHT IS ASSUMED TO BE FUEL ASSEMBLY DIMENSION

$$H = 8.426 \text{ in.}$$

p A-5

MEMBER PROPERTIES

REF.

COEFFICIENT OF THERMAL EXPANSION

$$\alpha = 5.675 \times 10^{-6} + 1.6667 \times 10^{-9} T \text{ in/in } / ^\circ\text{C}$$

$$T = 65.56^\circ\text{C}$$

$$\alpha = 5.675 \times 10^{-6} + 1.6667 \times 10^{-9} (65.56) \text{ in/in } / ^\circ\text{C}$$

$$= 5.784 \times 10^{-6} \text{ in/in } / ^\circ\text{C} \quad \text{or} \quad 3.213 \times 10^{-6} \text{ in/in } / ^\circ\text{F}$$

REFERENCE :

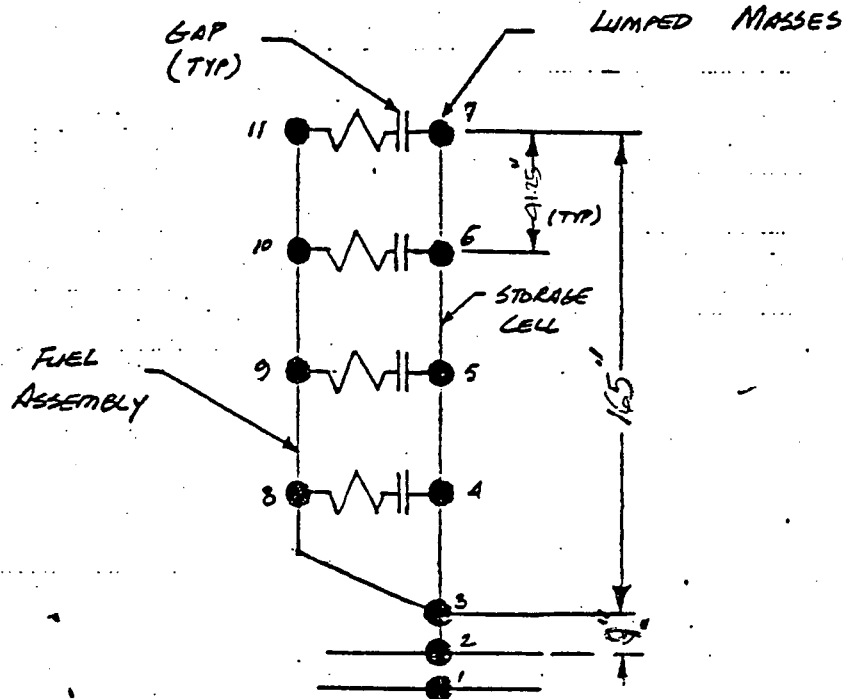
Scott, D.B. Physical and Mechanical Properties  
of Zircaloy 2 and 4, WCAP - 3269-41  
(May 1965)



APPENDIX B - LUMPED MASSES DISTRIBUTION

APPENDIX B - LUMPED MASSES DISTRIBUTION

REF.



TOTAL WEIGHT OF FUEL ASSEMBLY, STRUCTURE, STORAGE CELL, TRAPPED AND HYDRODYNAMIC WATER  
= 2500 lb/CELL

THE TOTAL IDXIO RACK MASS IS DISTRIBUTED PROPORTIONALLY TO THE 5 LUMPED MASSES.

$M_1$  = MASS REPRESENTING THE POOL STRUCTURE UNDER THE IDXIO RACK. NOTE, MASS ALLOCATION ASSIGNED TO THE NODE REPRESENTING THE POOL STRUCTURE, HAD LITTLE EFFECT ON THE RESULTS OF THE SLIDING ANALYSIS. THEREFORE, WILL BE ASSUMED 5 TIMES THE TOTAL DEAD WEIGHT.

$$M_1 = 5 \times 254000 = 1270000 \text{ lbs OR } 3286.7 \frac{\text{lb-sec}^2}{\text{in}}$$

$$M_2 = \text{MASS REPRESENTING THE RACK LEG WEIGHT (STRUCTURAL D.W.)} = 50 \text{ lbs} \times 9 \text{ LEGS} = 450 \text{ lbs} = 116 \frac{\text{lb-sec}^2}{\text{in}}$$

LUMPED MASSES

REF.

$M_3 =$  A PORTION OF THE FUEL ASSEMBLY AND STORAGE ASSIGNED AT THE STORAGE CELL BOTTOM + STORAGE RACK BASE STRUCTURE

$$M_3 = 2500 \text{ lb/CELL} (10 \times 10) \times \left( \frac{1}{8} \text{ WGT. DIST} + 4000.0 \right) = 35250 \text{ lbs}$$

OR  $91.23 \frac{\text{lb-sec}^2}{\text{IN}}$

$M_4 = M_5 = M_6 =$  MASS REPRESENTING THE 10X10 ARRAY OF STORAGE CELLS, BASE STRUCTURE, TRAPPED AND HYDRODYNAMIC WATER.

$$M_4 = M_5 = M_6 = (2500 - 1650) \times (10 \times 10) \times \left( \frac{1}{4} \text{ WGT. DIST} \right) = 21250 \text{ lbs}$$

$= 54.99 \frac{\text{lb-sec}^2}{\text{IN}}$

$$M_7 = (2500 - 1650) (10 \times 10) \left( \frac{1}{8} \text{ WGT. DIST.} \right) = 10625 \text{ lbs} = 27.50 \frac{\text{lb-sec}^2}{\text{IN}}$$

$M_8 = M_9 = M_{10} =$  MASS REPRESENTING FUEL ASSEMBLY OF 10X10 RACK ARRAY.

$$= (1650) (10 \times 10) \left( \frac{1}{4} \right) = 41250 \text{ lbs} = 106.75 \frac{\text{lb-sec}^2}{\text{IN}}$$

$$M_{11} = M_8/2 = 20625 \text{ lbs} \quad \text{OR} \quad 53.38 \frac{\text{lb-sec}^2}{\text{IN}}$$



APPENDIX C - MAXIMUM FRICTIONAL RESISTANCE LOAD

APPENDIX C

REF.

MAXIMUM FRICTIONAL RESISTANCE LOAD

The time history of the horizontal frictional resistance load for the storage rack is shown in Figure 8.2. From Figure 8.2 it can be seen that the maximum frictional resistance reaction load for a DBE seismic event is 142,200 pounds and it occurs at time 9.78 seconds. Due to phase difference, the maximum frictional resistance reaction load for the orthogonal (horizontal) component of DBE will occur at different time. Therefore, the combined frictional resistance reaction load due to the two orthogonal horizontal components of the Design Basis Earthquake (DBE) has been calculated by first taking the average of the frictional resistance reaction load over a time span of 0.05 seconds (from 9.76 seconds to 9.80 seconds) and then combining it by the square root of the sum of square (SRSS) technique. The time span of 0.05 seconds reflects the time involved in transmitting the seismic inertia and impact forces through the rack structure and the phase difference between the maximum response results of the two horizontal components of the Design Basis Earthquake event. The detail calculations for the maximum combined

REF.

Frictional resistance load are given below

<u>Time Seconds</u> (Seconds)	<u>Frictional Resistance Load</u> (pounds)
9.76	78,424
9.77	119,695
9.78	142,214
9.79	140,276
9.80	123,730
	$\Sigma = 604,339$

$$\text{Average Frictional Resistance Load} = \frac{604339}{5} = 120868 \text{ lbs.}$$

$$\text{Max. Frictional Resistance Load due to Two Orthogonal Horizontal Components of DBE} = \sqrt{(120,868)^2 + (120,868)^2} = 170933 \text{ lbs.}$$

As the overturning moment due to DBE event is greater than the stabilizing moment, the storage rack will lift up. Therefore, only 6 feet out of a total of 9 feet are effective in transmitting the lateral seismic load to the pool floor.

$$\therefore \text{Max. Frictional Load / Support Leg} = \frac{170,933}{6} = 28,489 \text{ lbs} \approx 28,500 \text{ lbs.}$$

ATTACHMENT F

Structural Analysis Report  
for the  
Indian Point Unit No. 2 Spent  
Fuel Storage Racks

Consolidated Edison Company of New York, Inc.  
Indian Point Unit No. 2  
Docket No. 50-247  
May, 1980



**STRUCTURAL ANALYSIS REPORT  
FOR THE  
INDIAN POINT UNIT NO. 2  
SPENT FUEL STORAGE RACKS**

**Prepared for  
Consolidated Edison Company of New York, Inc.**



## TABLE OF CONTENTS

1.	SUMMARY	5
2.	INTRODUCTION	6
3.	DESCRIPTION OF THE STORAGE RACK	7
4.	APPLICABLE SPECIFICATION, STANDARDS AND CODES	10
5.	LOADING CONDITIONS	11
5.1	Load Cases	11
5.2	Load Combinations	12
6.	STRUCTURAL ACCEPTANCE CRITERIA	15
7.	METHOD OF ANALYSIS	16
7.1	Rack Structural Analysis	16
7.1.1	Mathematical Models	16
7.1.2	Mathematical Formulation of the Static Analysis	17
7.1.3	Mathematical Formulation of the Dynamic Analysis	18
7.1.4	Stress Analysis	21
7.2	Water Sloshing Effects	22
7.3	Fuel Assembly Impact Loads	22
7.4	Accidental Spent Fuel Assembly Drop Analysis	22
7.5	Spent Fuel Rack Stability Analysis	22
8.	RESULTS OF ANALYSIS	31
8.1	Rack Structural/Stress Analysis	31
8.2	Spent Fuel Pool Floor Loads	31
8.3	Water Sloshing Effects	31
8.4	Accidental Spent Fuel Assembly Drop Analysis	32
8.5	Spent Fuel Rack Stability Analysis	43
9.	CONCLUSIONS	44
10.	REFERENCES	45
	APPENDIX A - Member Properties	
	APPENDIX B - Water Sloshing Effects	
	APPENDIX C - Impact Factor	
	APPENDIX D - Accidental Assembly Drop	
	APPENDIX E - Stability Analysis	
	APPENDIX F - Combined Stress Ratio	



## LIST OF TABLES

8.1	PERTINENT NATURAL FREQUENCIES OF VIBRATION AND MODAL PARTICIPATION FACTORS	33
8.2	RESULTS OF STRUCTURAL/STRESS ANALYSIS	35
8.3	MAXIMUM FLOOR LOAD SUMMARY	40
8.4	RESULTS OF ACCIDENTAL FUEL ASSEMBLY DROP	41

## LIST OF FIGURES

3.1	FUEL STORAGE RACK ARRANGEMENT PLAN	8
3.2	INDIAN POINT 2 BORATED SST FUEL STORAGE RACK	9
5.1	15% OF GRAVITY RESPONSE SPECTRA (DBE) HORIZONTAL	13
5.2	10% OF GRAVITY RESPONSE SPECTRA (DBE) VERTICAL	14
7.1.a	10x10 RACK FINITE ELEMENT MODEL DIMENSIONS AND NODE NUMBERS	23
7.1.b	10x10 RACK FINITE ELEMENT MODEL BEAM ELEMENT NUMBERS	25
7.1.c	10x10 RACK FINITE ELEMENT MODEL PLATE ELEMENT NUMBERS	26
7.2	APPLIED LOADS AND BOUNDARY CONDITIONS - LOAD CASE 1	27
7.3	APPLIED LOADS AND BOUNDARY CONDITIONS - LOAD CASE 2	28
7.4	APPLIED LOADS AND BOUNDARY CONDITIONS - LOAD CASE 3	29
7.5	LUMPED MASSES AND BOUNDARY CONDITIONS - LOAD CASES 4,5	30



## 1. SUMMARY

The Indian Point Generating Station Unit 2 (Indian Point 2) high density spent fuel storage racks have been designed to meet the requirements for Seismic Category I structures. Detailed structural and seismic analyses of the high density storage racks have been performed to verify the adequacy of the design to withstand the loadings encountered during installation, normal operation, the severe and extreme environmental conditions of the Operating Basis and Design Basis Earthquakes and the abnormal loading conditions of an accidental fuel assembly drop event.

The response of the rack structure to the specified static and dynamic loading conditions have been evaluated by means of linear elastic analysis using the finite element method. The seismic response of the rack structure has been determined using response spectrum modal superposition methods of dynamic analysis. The impact effect has been considered by applying appropriate impact factors to the stresses and reaction loads developed by the seismic analysis. Non-linear analysis and energy balance techniques have been used to evaluate structural damage resulting from an accidental fuel assembly drop. For the specified loading conditions, the maximum stresses and deflections of the rack structure have been calculated and shown to be less than the allowable values.

It has been concluded from the results of the structural and seismic analysis that the spent fuel storage racks are adequately designed to withstand the loadings associated with normal operating and abnormal conditions.

## 2. INTRODUCTION

Nuclear Energy Services, Inc. (NES) has designed the high density spent fuel storage racks for Consolidated Edison Company of New York Inc. (Con Ed) to be installed in the Indian Point 2 fuel pool. The racks are designed to provide storage locations for up to 980 fuel assemblies. The spent fuel storage racks are designed to maintain the stored fuel, having a maximum equivalent uranium enrichment of 3.5 percent of U-235 by weight in Uranium in a safe, coolable, subcritical configuration during normal and abnormal conditions.

The Indian Point 2 high density fuel storage racks are "free-standing" design (racks are free to slide horizontally on the pool floor). NES has performed the non-linear time history seismic analysis to determine the maximum sliding displacement of the storage racks during a seismic event. The results of this non-linear time history seismic analysis are provided in NES report 81A0615. Sufficient clearances will be provided between the adjacent storage racks and between the storage racks and pool walls to preclude collision during a seismic event. However, in order to determine the maximum seismic response (maximum stresses and reaction loads) of the storage racks, the storage racks are conservatively assumed to be pinned (not sliding) to the pool floor at the support feet locations.

This report presents a summary of the results of the structural analysis performed by NES to verify the design adequacy of the high density spent fuel racks to withstand loadings which could be generated during installation, normal operating and abnormal conditions, including the dynamic loadings resulting from Operating Basis Earthquake, Design Basis Earthquake and the effect of fuel assembly impact on the fuel storage cells during earthquake events. The seismic responses have been calculated using seismic response spectra of 1.0 percent equipment damping for the Operating Basis and Design Basis Earthquake (References 2 and 3). The combination of modes and spatial earthquake components in the seismic response analysis are based on NRC Regulatory Guide 1.92 (Reference 4). The impact effects have been considered by applying appropriate impact factors to the load/stresses developed by the seismic analysis.



### 3. DESCRIPTION OF THE STORAGE RACK

The Indian Point 2 high density fuel storage racks have been designed to provide a maximum storage capacity of 980 locations. The arrangement of the fuel storage racks in the spent fuel storage pool is shown in Figure 3.1. The fuel storage rack arrangement contains five types of storage rack arrays including:

- (1) Two racks of 8x8 array each.
- (2) Two racks of 10x10 array each.
- (3) One rack of 9x8 array.
- (4) Two racks of 9x10 array each.
- (5) Five racks of 8x10 array each.

Each rack consists of an assembly of 2x2 modules (the 9x8 and 9x10 racks also include 2x3 modules). Each 2x2 or 3x2 modular cell unit consists of four (4) or six (6) cells spaced nominally 10-15/16 inches on centers. Each storage cell is a Type 304 stainless steel box with 9 inch inside dimension. Borated stainless steel sheets are attached to the outside of the cell walls by means of welded brackets. The top opening of the storage cell is flared to facilitate insertion of the fuel assembly; the bottom member of the storage cell provides the level support surface required for the fuel assembly and contains the cooling flow orifice.

Each modular cell unit (either 2x2 or 2x3) is supported by and welded to the rack base grid structure constructed from Type 304 stainless steel wide flange and box beam members. A schematic drawing of a representative 10x10 rack structure and an individual 2x2 modular cell unit is shown in Figure 3.2. Continuous spacer beams are provided at the top of the storage cells to ensure that the required pitch is maintained between storage cells in both directions (north/south and east/west) under lateral load conditions. The spacer beams which are supported on the storage cells also maintain the vertical alignment of the cells. Support pads attached to the bottom of the rack base raise the rack above the pool floor to the height required to clear existing anchor pins on the pool floor area and to provide an adequately sized cooling water supply plenum for natural circulation. Each support pad contains a remotely adjustable jack screw to permit the rack to be leveled following wet installation. The rack support pads will rest directly on the pool floor wherever possible. In case of interference with the existing floor shims, the pads will rest on local plates designed to bridge over the shims.

The storage racks are positioned on the pool floor so that adequate clearances are provided between racks and between the racks and pool structures to avoid impacting of the sliding racks during seismic events. The horizontal seismic loads transmitted from the rack structure to the pool floor are only those associated with friction between the rack structure and the pool liner. The vertical deadweight and seismic loads are transmitted directly to the pool floor by the support feet. The storage racks' detailed design and their layout in the spent fuel storage pool are shown in Reference 1 Drawings.

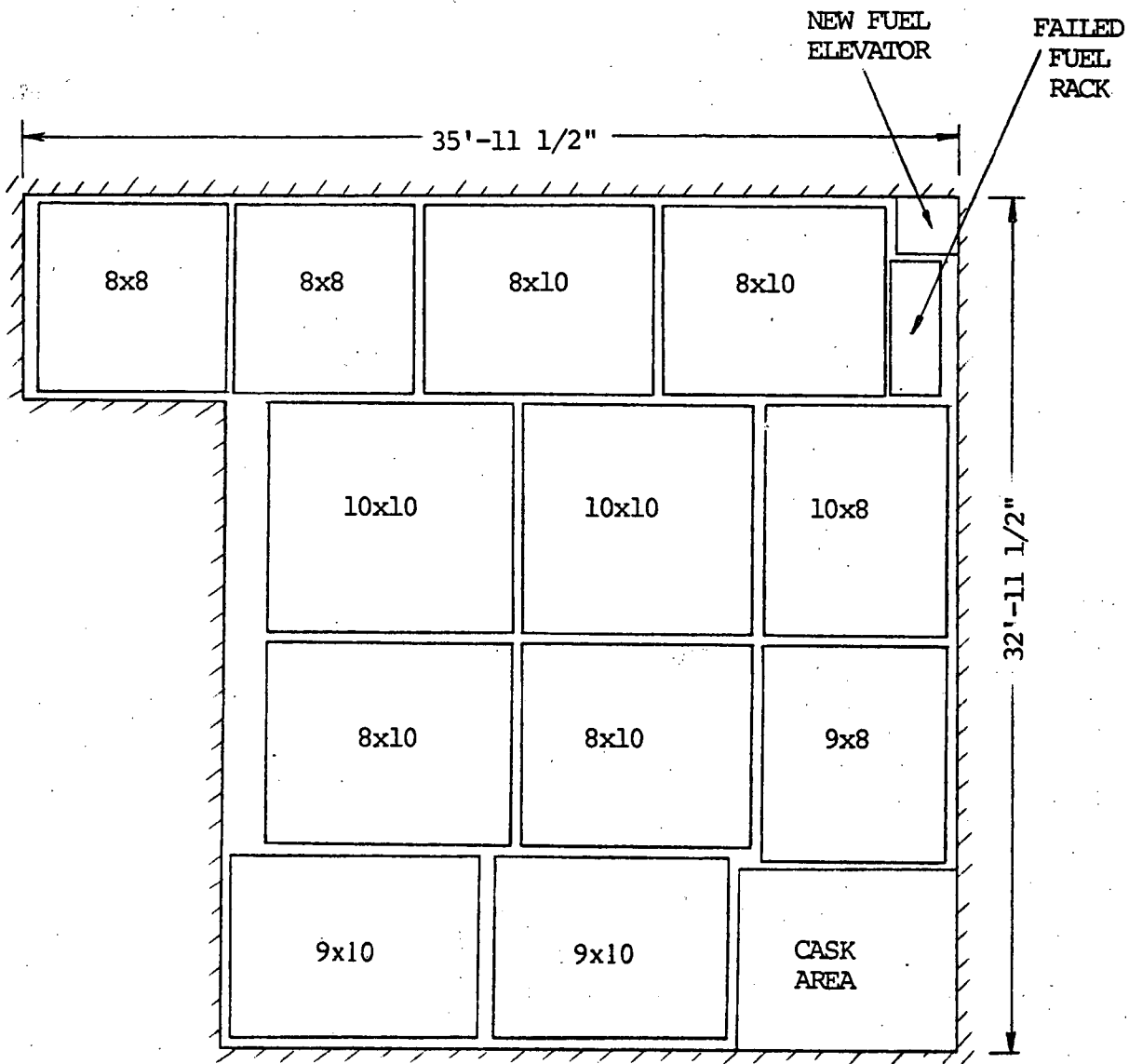


Figure 3.1 Fuel Storage Rack Arrangement Plan

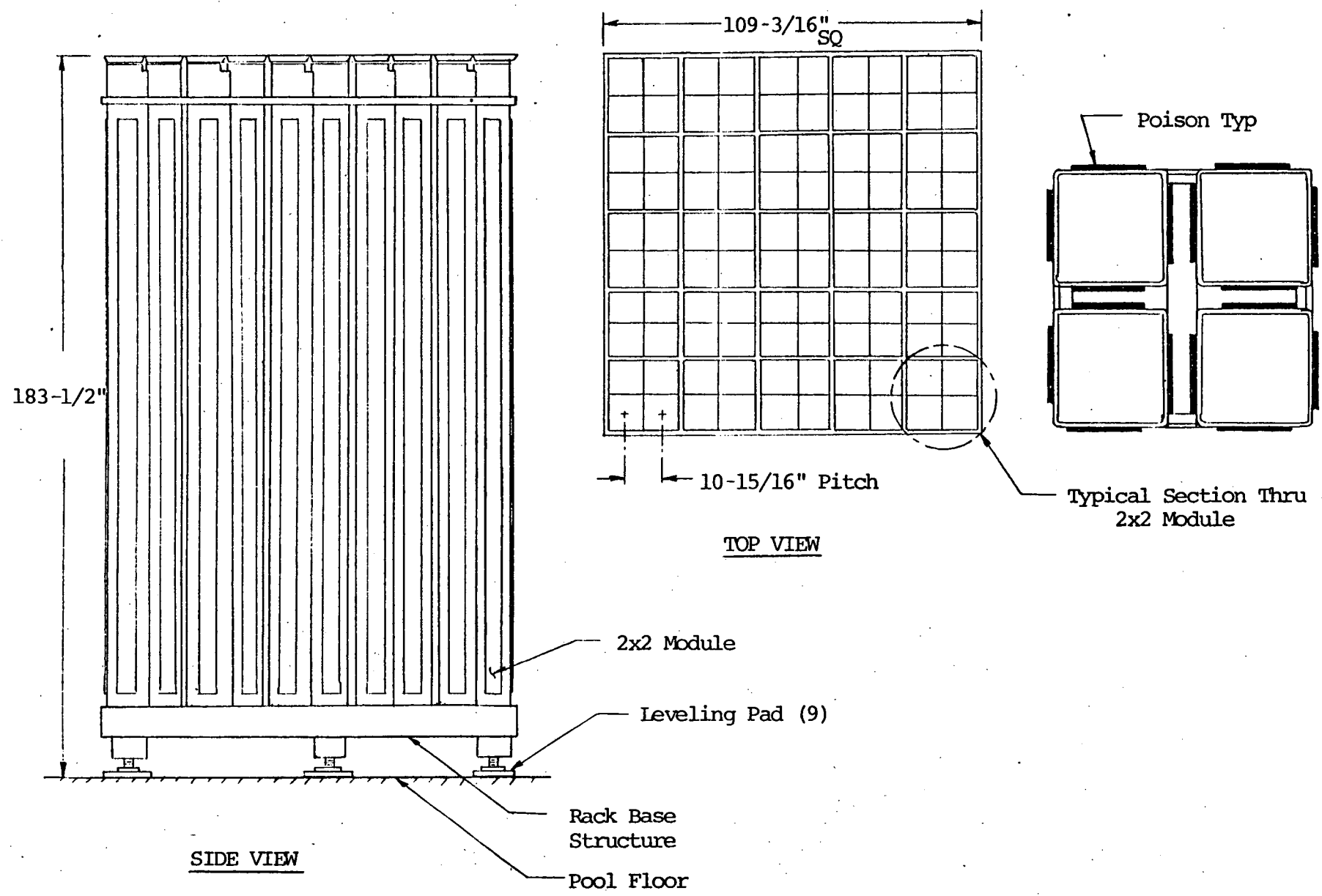


Figure 3.2 Indian Point 2  
Borated SST Fuel Storage Rack (10x10)



#### 4. APPLICABLE SPECIFICATION, STANDARDS AND CODES

The following design specification, Regulatory Guides and Codes, have been used in the design/analysis of spent fuel storage racks (References 2 through 7 and 14).

1. Nuclear Energy Services, Inc. Document NES 81A0606, "Quality Assurance Program Plan for the Indian Point Generating Station Unit 2 Fuel Storage Racks," November 1979.
2. Consolidated Edison Company, "Design, Fabricate, Deliver and Installation of Spent Fuel Storage Racks," Specification No. MP79-001, Rev. 2, March 1979.
3. USNRC Regulatory Guide 1.92, "Combination of Modes and Spatial Components in Seismic Response Analysis," Rev. 1, February 1976.
4. USNRC Standard Review Plan, Section 3.8.4.
5. USNRC "Position Paper for Review and Acceptance of Spent Fuel Storage and Handling Applications," April 14, 1978 and Supplement, January 18, 1979.
6. AISC Manual of Steel Construction, Seventh Edition, 1970.
7. 1977 Annual Book of ASTM Standards, Parts 3 and 5.



## 5. LOADING CONDITIONS

The following load cases and load combinations have been considered in the analysis in accordance with the requirements of USNRC Standard Review Plan, Section 3.8.4 (Reference 5) and the USNRC Position Paper (Reference 6).

### 5.1 LOAD CASES

#### Load Case 1 - Deadweight of Rack, D + L (Normal Load)

Under normal operating conditions, the rack is subjected to the deadweight loading of the rack structure itself plus the loads resulting from the storage cells and the full complement of fuel assemblies stored in the cells.

#### Load Case 2 - Deadweight Of Rack Plus 1g Vertical Installation Load, D + I.L. (Normal Load)

During installation the rack is subjected to the loading resulting from its own structural weight, weight of empty storage cells, plus a 1g vertical load resulting from a suddenly applied crane load.

#### Load Case 3 - Deadweight of Rack Plus Uplifting Load, (D + U.L.) (Abnormal Load)

The possibility of the fuel handling bridge fuel hoist grapple getting hooked on a fuel storage cell was considered. The axial upward force considered for this load case was 3,000 pounds, applied at two critical locations as indicated in Figure 7.4.

#### Load Case 4 - Operating Basis Earthquake, E (Severe Environmental Load)

The rack, fuel assemblies, and virtual water mass are subjected to the three-dimensional simultaneous loading of the horizontal and vertical components of the seismic response acceleration spectra specified for the Operating Basis Earthquake (2/3 DBE) in the Indian Point 2 Fuel Storage Rack Specifications (Reference 3) and presented in Figure 5.1 and 5.2. The seismic analysis is performed for the fully loaded rack since this loading condition results in higher stresses and higher reaction loads. The effects of fuel assembly impact during a seismic event are taken into account.

#### Load Case 5 - Design Basis Earthquake, E' (Extreme Environmental Load)

Same as Load Case 4 except that the seismic response acceleration spectra corresponding to the Design Basis Earthquake was used in the analysis (Figure 5.1 and 5.2).

#### Load Case 6 - Assembly Drop Impact Load, D.L. (Abnormal Load)

The possibility of dropping a spent fuel assembly on the rack from the highest possible elevation during spent fuel handling was considered. A 1650 pound weight (spent fuel assembly) was postulated to drop on the rack from a height of 48 inches above the top of the rack. Three cases were considered: (1) a direct drop on the top of a 2x2 module; (2) a subsequent tipping of the assembly onto the surrounding storage cans; (3) a straight drop through the storage cell and impact onto the rack base grid structure.

Thermal Loading, T (Normal Load)

The stresses and reaction loads due to thermal loadings are insignificant since clearances are provided to allow unrestrained growth of the racks for the maximum pool temperature of 150°F.

**5.2 LOAD COMBINATIONS**

A. For service load conditions, the following load combinations are considered:

- (1)  $D + L$
- (2)  $D + L + T$
- (3)  $D + LL$
- (4)  $D + L + E$
- (5)  $D + L + E + T$

B. For factored load conditions, the following load combinations are considered:

- (6)  $D + L + T + E'$
- (7)  $D + T + U.L.$
- (8)  $D + L + T + D.L.$

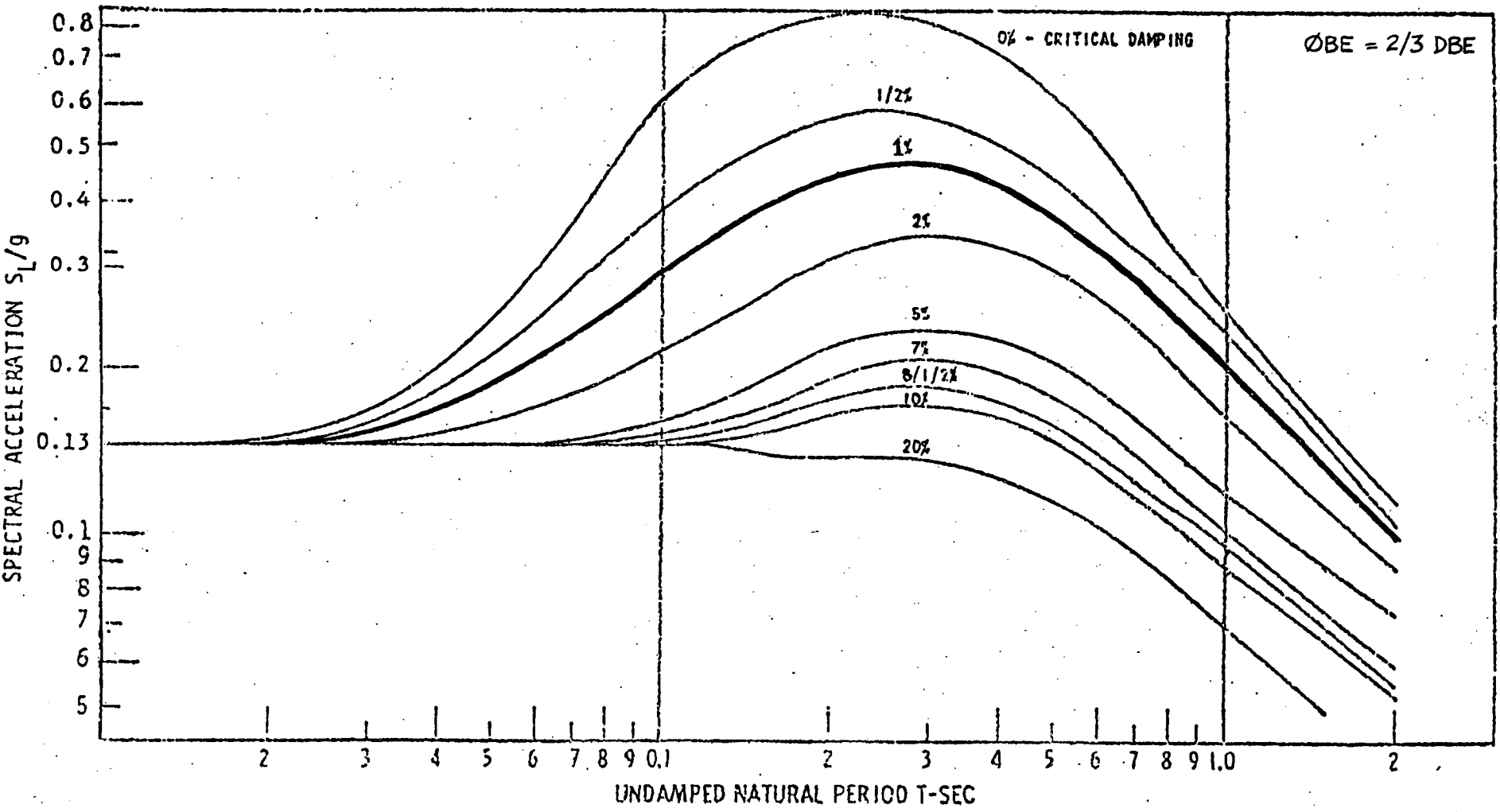
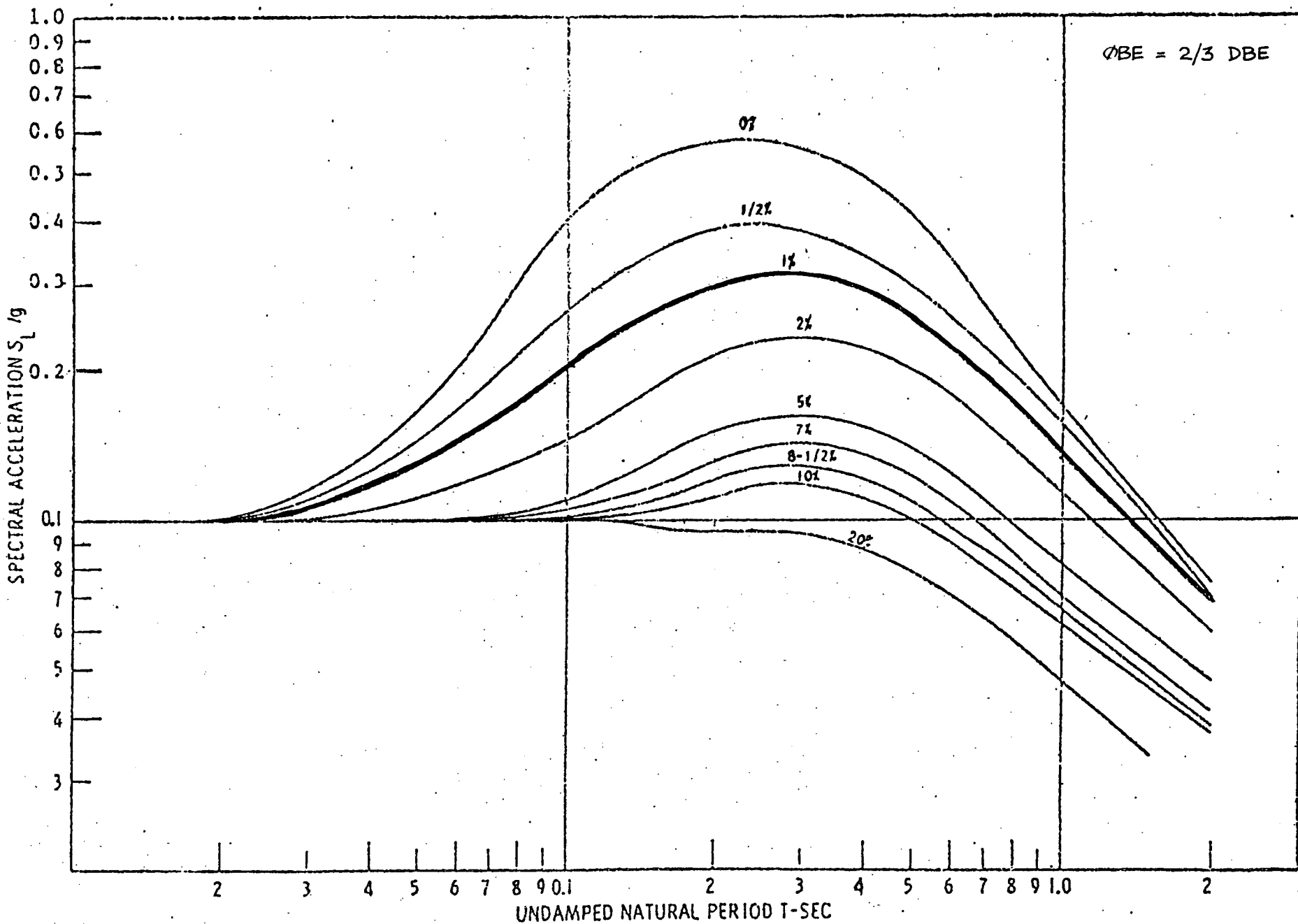


FIGURE 5-1 15% OF GRAVITY RESPONSE SPECTRA (DBE). HORIZONTAL



$\phi_{BE} = 2/3$  DBE

FIGURE 5-2. 10% OF GRAVITY RESPONSE SPECTRA (DBE) VERTICAL



## 6. STRUCTURAL ACCEPTANCE CRITERIA

The following allowable stress limits constitute the structural acceptance criteria used for each of the loading combinations presented in Section 5.2.

<u>Load Combinations</u>	<u>Limit*</u>
1, 3, 4	S
2, 5	1.5S
6, 7	1.6S or $F_y$ (whichever is less)
8	**

Where S is the required section strength based on the elastic design methods and the allowable stresses defined in Part 1 of the AISC "Specification for the Design, Fabrication and Erection of Structural Steel for Buildings," February 12, 1969. The yield stress value ( $F_y$ ) for Type 304 stainless steel is taken as 30.0 ksi from the American Society for Testing and Material, specification ASTM A240.

---

\* The acceptance criteria are based on the applicable sections of the NRC Position Paper on Fuel Storage Racks, SRP 3.8.4, and AISC Specification for the Design, Fabrication and Erection of Structural Steel for Building, The Uniform Building Code.

\*\* The acceptance criteria for Load Combination 8, the accidental spent fuel assembly drop on the rack, is that the resulting impact will not adversely affect the overall structural integrity of the rack, the leak-tightness integrity of the fuel pool floor and liner plate and that the deformation of the impacted storage cells will not adversely affect the value of  $K_{eff}$  or ability to cool adjacent fuel elements.



given in References 8 and 9. The horizontal and vertical weights are distributed such that the resulting lumped mass multi-degree-of-freedom model best represents the dynamic characteristics of the fuel storage rack. The seismic analysis are performed for the fully loaded racks since this loading condition results in higher stresses and reaction loads. The boundary conditions and lumped mass locations for the horizontal and vertical seismic analyses are shown in Figure 7.5.

### 7.1.2 Mathematical Formulation of the Static Analysis

The static analysis of the finite element model has been performed using the direct stiffness methods of structural analysis. If the force displacement relationship of each of the discrete structural elements is known (the element stiffness matrix) then force-displacement relationship for the entire structure can be assembled using standard matrix methods as shown below.

For each element:

$$k u = f \quad (1)$$

Where:

- k = Element stiffness matrix
- u = Element nodal displacement vector
- f = Element nodal force vector

For the idealized system the equation of equilibrium may be written, in matrix form as follows:

$$K U = F \quad (2)$$

Where:

- K = Assembled stiffness matrix for the system  
=  $\sum k$
- U = Nodal displacement vector for the system
- F = External nodal point force vector

If sufficient boundary conditions are specified on U to guarantee a unique solution, Equation (2) can be solved for the nodal point displacements at each node in the structure, knowing the system stiffness matrix and external force matrix. From the displacement response of the system, the internal forces and stresses in each structural element can be calculated.



## 7. METHOD OF ANALYSIS

### 7.1 RACK STRUCTURAL ANALYSIS

#### 7.1.1 Mathematical Models

A 10x10 rack has been analyzed in detail. This rack conservatively represents the controlling structural case since it has the longer beam span and will be loaded by greater seismic loads than the smaller racks. The dynamic (frequency) characteristic of the rack is essentially controlled by the dynamic characteristics of its component 2x2 or 3x2 modular cell units. Although the fundamental frequency of the 3x2 modular cell unit is higher than that of the 2x2 modular cell units, the design seismic spectra is such that the lateral seismic G loading for the 2x2 and 2x3 modular cell units will be essentially similar.

In order to perform static, dynamic and stress analyses of the fuel storage rack structure, the rack has been mathematically modeled as a finite element structure consisting of discrete three-dimensional elastic beam and plate elements interconnected at a finite number of nodal points. Stiffness characteristics of the structural members are related to the plate thickness, cross sectional area, effective shear area and moment of the inertia of the element section.

Appropriate support connections are provided at the support feet for both static and dynamic analysis. The feet locations have been selected to represent a conservative support configuration that will result in maximum stresses in the rack base structure. Six degrees of freedom (three translations and three rotations) are permitted at each nodal point. The three-dimensional finite-element model of the fuel storage rack with node and element numbers is shown in Figures 7.1.a through 7.1.c.

For the static deadweight and live load analysis, the distributed masses of the structural elements, storage cells and fuel elements are lumped at the 2x2 module system nodal points. Similarly, for Load Case 2, rack installation and removal analysis, the distributed masses of the structural elements and the cells are lumped at the 2x2 module system nodal points. The effect of suddenly applied crane load is considered by applying a 1g vertical load in addition to the deadweight loading. For Load Case 3, a net vertical uplift load of 3,000 pounds is applied at the worst location of the storage rack. Applicable loading and boundary conditions for the static load cases are shown in Figure 7.2 through 7.4.

For the horizontal and vertical seismic analyses, a mathematical model was developed to represent the 10x10 rack. This model consists of twenty-five (25) lumped mass cantilever beams (representing twenty-five 2x2 modules) rigidly attached to the rack base structure and attached to each other at the top by spacer bars. Each lumped mass cantilever beam has three masses and has the same dynamic (frequency) characteristics as a 2x2 module. This model is used in calculating the maximum stresses in the rack base structure and the reaction loads and stresses in the rack support feet. The distributed masses corresponding to the fuel assembly storage cells, poison elements and contained plus hydrodynamic mass are lumped at appropriate nodal points. The hydrodynamic mass calculations are based on recommendations



### 7.1.3 Mathematical Formulation of the Dynamic Analysis

#### A. Eigenvalue Analysis

The eigenvalues (natural frequencies) and the eigenvectors (mode shapes) for each of the natural modes of vibration are calculated by solving the following frequency equation:

$$(K - \omega_n^2 M) \{\phi_n\} = \{0\} \quad (3)$$

Where:

- $\omega_n$  = Natural angular frequency for the  $n^{\text{th}}$  mode
- $M$  = System mass matrix
- $\phi_n$  = Mode shape vector for the  $n^{\text{th}}$  mode
- $0$  = Null vector

The eigenvalue/eigenvector extraction is performed using the Lanczos Modal Extraction Methods.

#### B. Dynamic (Seismic) Load Analysis

Considering only translational degrees of freedom and assuming viscous (velocity proportional) form of damping, the equation of motion in matrix form can be expressed as follows:

$$M (\ddot{U}_t + \ddot{U}_{gt}) + C \dot{U}_t + K U_t = 0 \quad (4)$$

Where:

- $\ddot{U}_t$  = Relative acceleration time history vector
- $\ddot{U}_{gt}$  = Ground acceleration time history vector
- $C$  = Damping matrix
- $\dot{U}_t$  = Velocity time history vector
- $U_t$  = Relative displacement time history vector



Rearranging equation (4):

$$M\ddot{U}_t + C\dot{U}_t + KU_t = -M\ddot{U}_{gt} = P_{eff} \quad (5)$$

To uncouple equation (5), assume:

$$U = \phi Y_t$$

Where:

$$\phi = \text{Characteristic free vibration mode shapes matrix}$$

$$Y_t = \text{Generalized coordinate displacement time history vector}$$

Applying the above coordinate transformation and multiplying equation (5) by the transpose of  $\phi$  and using orthogonality conditions, the following uncoupled equations of motion are obtained:

$$\ddot{Y}_{nt} + 2\omega_n \lambda_n \dot{Y}_{nt} + \omega_n^2 Y_{nt} = -M_n^{*-1} R_n \ddot{U}_{gt} \quad (6)$$

Where:

$$Y_{nt} = \text{Generalized displacement coordinate time history for } n^{\text{th}} \text{ mode.}$$

$$\lambda_n = \text{Damping ratio for the } n^{\text{th}} \text{ mode expressed as percent of critical damping.}$$

$$M_n^* = \text{Generalized mass for the } n^{\text{th}} \text{ mode}$$

$$= \phi_n^T M \phi_n = \sum M_i \phi_{in}^2$$

The mode shape  $\phi_n$  is normalized such that  $M_n^* = 1$

$$R_n = \text{Participation factor for the } n^{\text{th}} \text{ mode.}$$

$$= \phi_n^T M I = M_i \phi_{in}$$

$$I = \text{Column vector whose elements are generally unity}$$

The solution for the differential equation (6) is given by the Duhamel Integral:

$$\ddot{Y}_{nt} = \frac{R_n}{M_n^* \omega_n} \int_0^t \ddot{U}_{gt} e^{-\lambda_n \omega_n (t-\tau)} \sin \omega_n (t-\tau) d\tau$$



Using the response spectrum method of analysis, the maximum values of the generalized response for each mode is given by:

$$\ddot{Y}_{n \max} = \frac{R_n S_{an}}{M_n^*}$$

Where:

$\ddot{Y}_{n \max}$  = Maximum generalized coordinate acceleration response for the  $n^{\text{th}}$  mode.

$S_{an}$  = Maximum spectral acceleration value for the  $n^{\text{th}}$  mode (from the applicable response spectrum curve, considering a  $\pm 10\%$  variation in the calculation natural frequency for the  $n^{\text{th}}$  mode).

From the maximum generalized coordinate response the maximum acceleration ( $\ddot{U}_{n \max}$ ) and maximum inertia forces ( $F_{n \max}$ ) at each mass point are given by:

$$\ddot{U}_{n \max} = \ddot{Y}_{n \max} \phi_{in}$$

$$F_{n \max} = M_n \ddot{U}_{n \max}$$

The inertia forces ( $F_{n \max}$ ) for each of the system natural modes are applied as external static forces, and system response (displacements, member internal forces and stresses) are calculated using the procedure described in Section 7.1.2. Total system response is then obtained by combining the individual modal response values in accordance with Regulatory Guide 1.92 (Reference 4); lower modes having large contribution to the response are considered and higher modes with negligible participation are neglected.

The combined seismic response of the three spatial components of the earthquake has been obtained by taking the square root of the sum of the squares of the corresponding maximum response values due to the three components calculated independently (Regulatory Guide 1.92, Reference 4).



### 7.1.4 Stress Analysis

From the internal forces at the ends of each structural member, the stresses are calculated using the following equations:

$$f_a = \frac{F_{x1}}{A}$$

$$f_{bx2} = \frac{M_{x2}}{I_2} \times C_3$$

$$f_{bx3} = \frac{M_{x3}}{I_3} \times C_2$$

$$f_{max} = f_a + f_{bx2} + f_{bx3}$$

$$f_{min} = f_a - f_{bx2} - f_{bx3}$$

Where:

$f_a$  = Axial stress

$f_{bx2}$  = Bending stress due to moment about member x2 axis

$f_{bx3}$  = Bending stress due to moment about member x3 axis

$f_{max}$  = Maximum tensile stress due to axial load plus bi-axial bending moments

$f_{min}$  = Maximum compression stress due to axial load plus bi-axial bending moments

$F_{x1}$  = Member axial force in member x1 direction

$M_{x1}, M_{x2}, M_{x3}$  = Moment about member x1, x2, x3 axes respectively

$A$  = Member cross sectional area

$I_2, I_3$  = Moment of inertia about member x2 and x3 axes respectively

$C_2, C_3$  = Edge distance of the structural section from neutral axes in x2 and x3 direction of member coordinate system.

The structure analysis and stress analysis calculations are performed using the STARDYNE computer program (Reference 10).



## 7.2 WATER SLOSHING EFFECTS

The sloshing effects of water on the fuel racks have been evaluated using the analytical methods given in USAEC's TID7024 "Nuclear Reactors and Earthquakes," Reference 11.

## 7.3 FUEL ASSEMBLY IMPACT LOADS

Clearances are provided between fuel assemblies and the storage cells to avoid interferences during fuel storage and removal operations. The storage cell/fuel assembly clearance or gap results in the impacting of the fuel assembly and storage cell during a seismic event. The Indian Point 2 fuel storage racks have been analyzed using the linear response spectrum modal superposition methods of dynamic analysis. In these seismic analyses, the effect of impacting masses has been conservatively accounted for by imposing the following assumptions:

1. All storage cells contain the fuel assembly.
2. All fuel assemblies simultaneously impact the storage cells.
3. The effect of fuel assembly impact is a two-fold increase in the seismic inertia loadings produced by the impacting fuel assemblies mass\*.
4. The impact and seismic inertia loads of the impacting masses are added to the seismic inertia loads of the non-impacting masses. The calculations for the effective impact factors are presented in Appendix C.

## 7.4 ACCIDENTAL SPENT FUEL ASSEMBLY DROP ANALYSIS

Linear and non-linear analysis techniques using energy balance methods as indicated in Appendix D are used to evaluate the structural damage resulting from a spent fuel assembly drop onto the rack.

## 7.5 SPENT FUEL RACK STABILITY ANALYSIS

The stability of the free-standing fuel storage rack has been evaluated using energy balance methods as indicated in Appendix E.

---

\* The use of an impact factor of 2.0 is conservative as verified by comparing the base shear and overturning moment response results of the linear response spectrum modal superposition analysis (this report) and the non-linear time history analysis (NES 81A0615, Ref. 13).

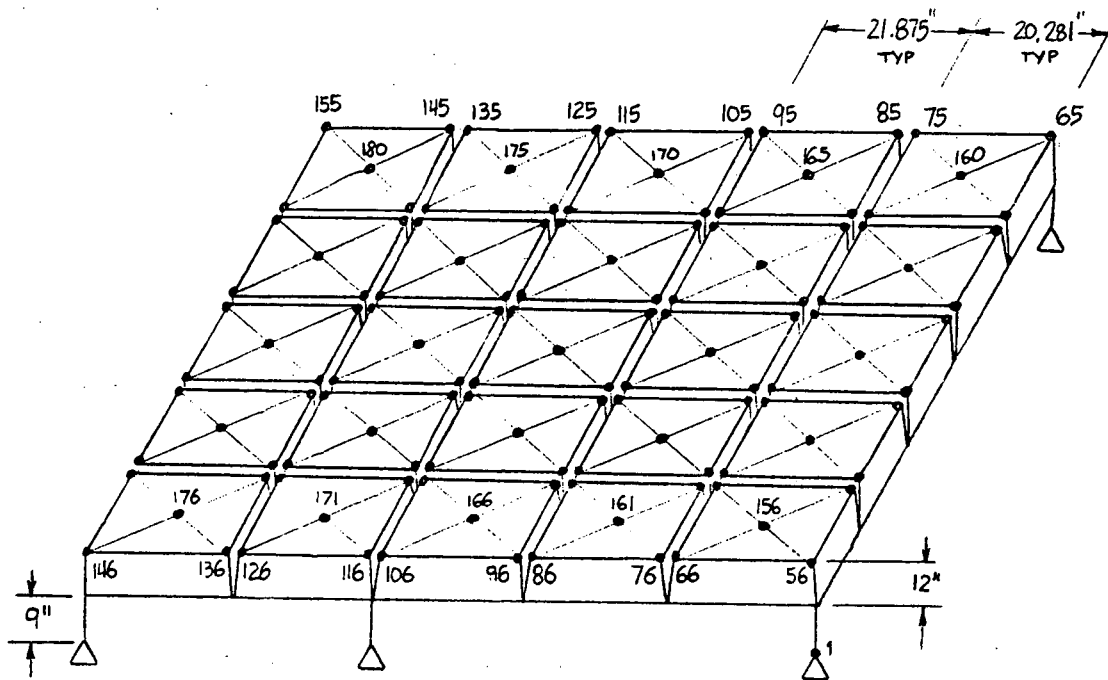
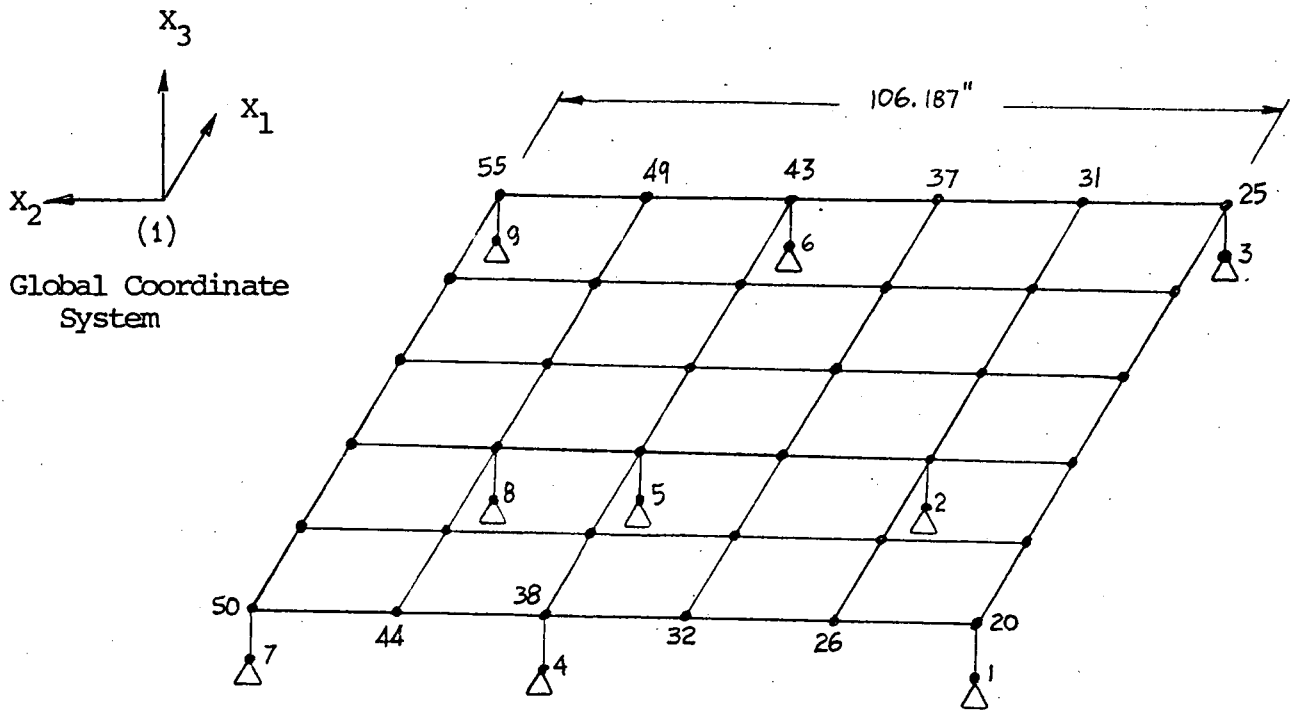


FIGURE 7.1.a  
10 x 10 RACK FINITE ELEMENT MODEL  
DIMENSIONS AND NODE NUMBERS

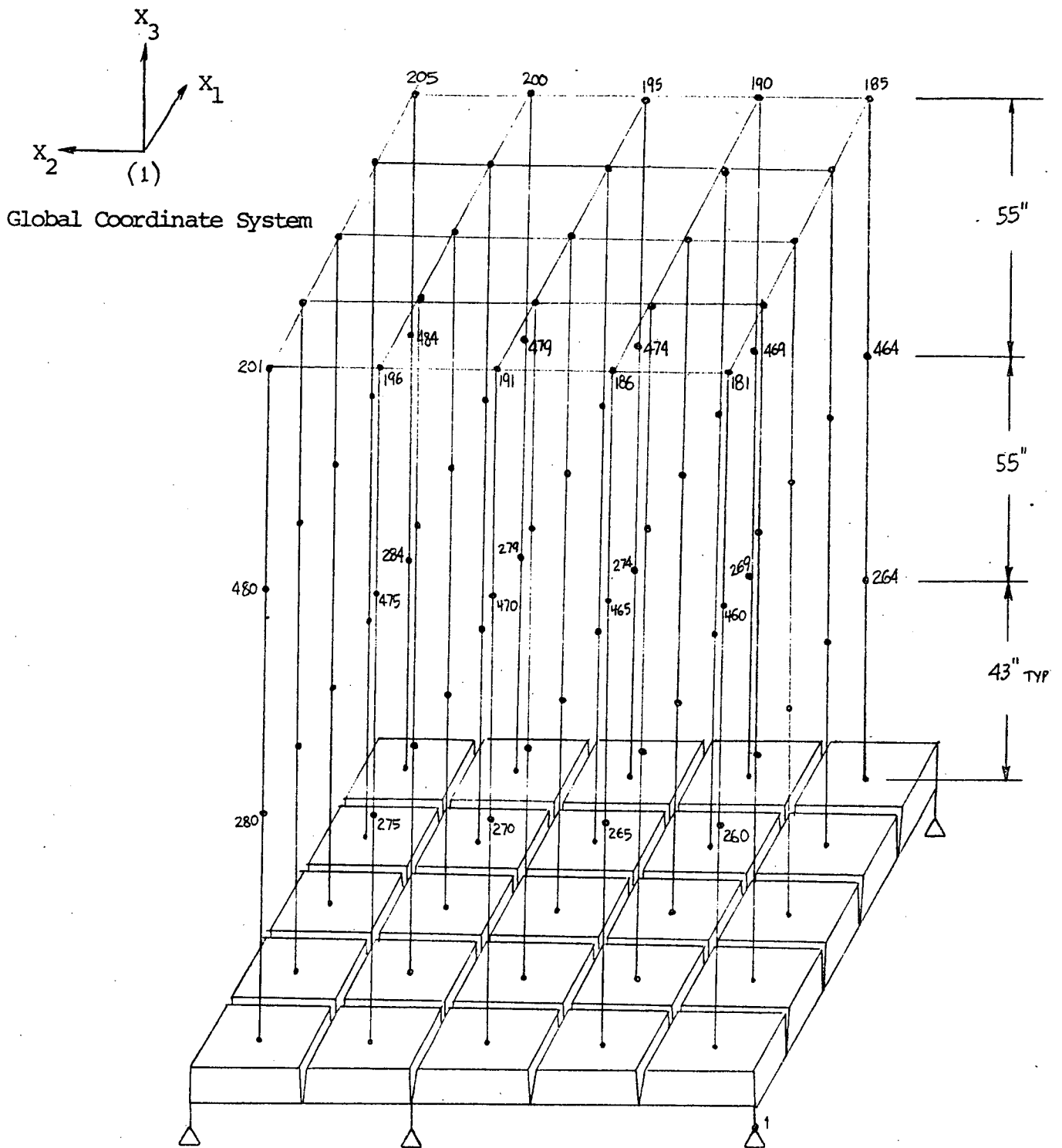


FIGURE 7.1.a  
10 x 10 RACK FINITE ELEMENT MODEL  
DIMENSIONS AND NODE NUMBERS - (Cont'd)

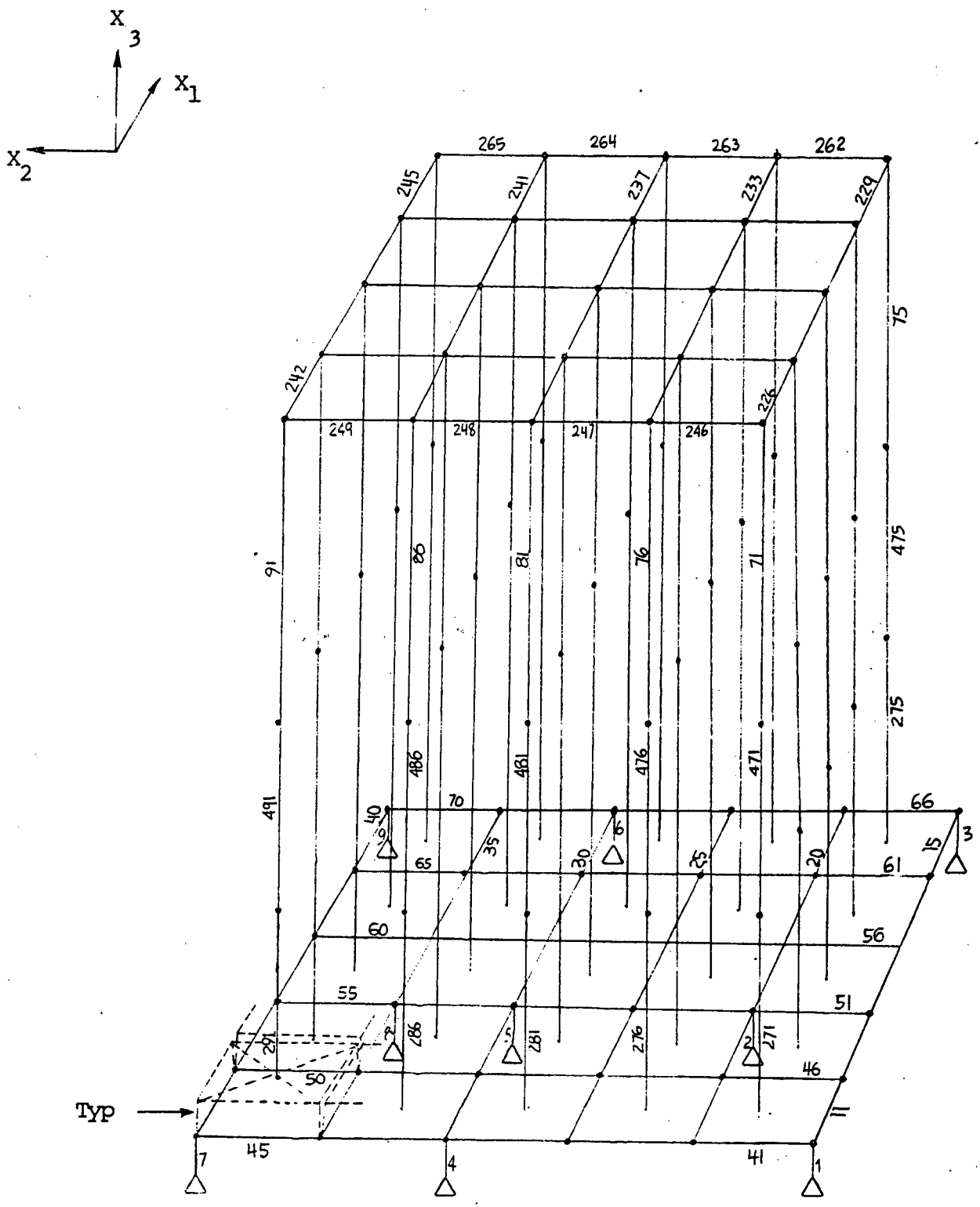
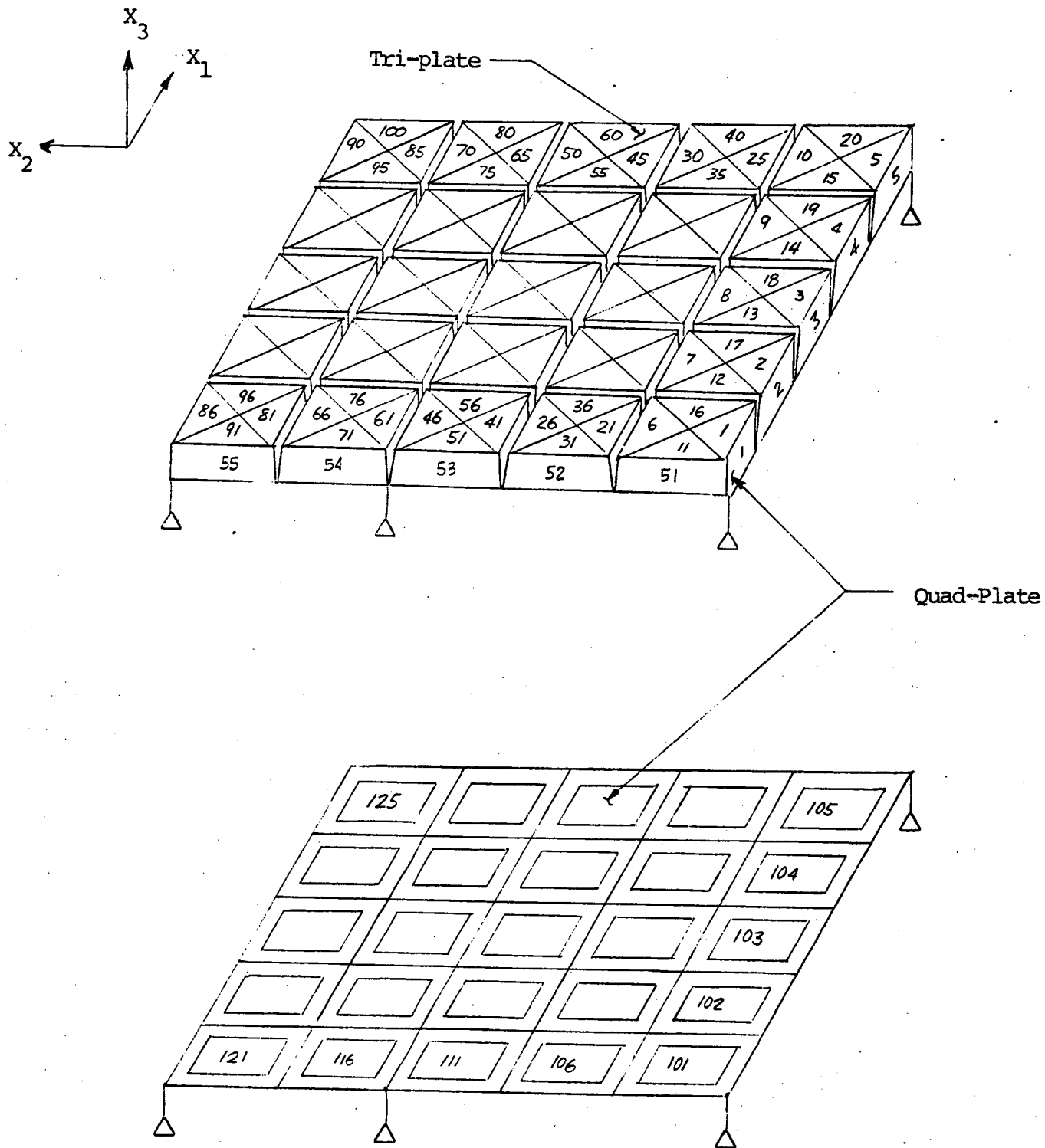


FIGURE 7.1.b  
10 x 10 RACK FINITE ELEMENT MODEL  
BEAM ELEMENT NUMBERS

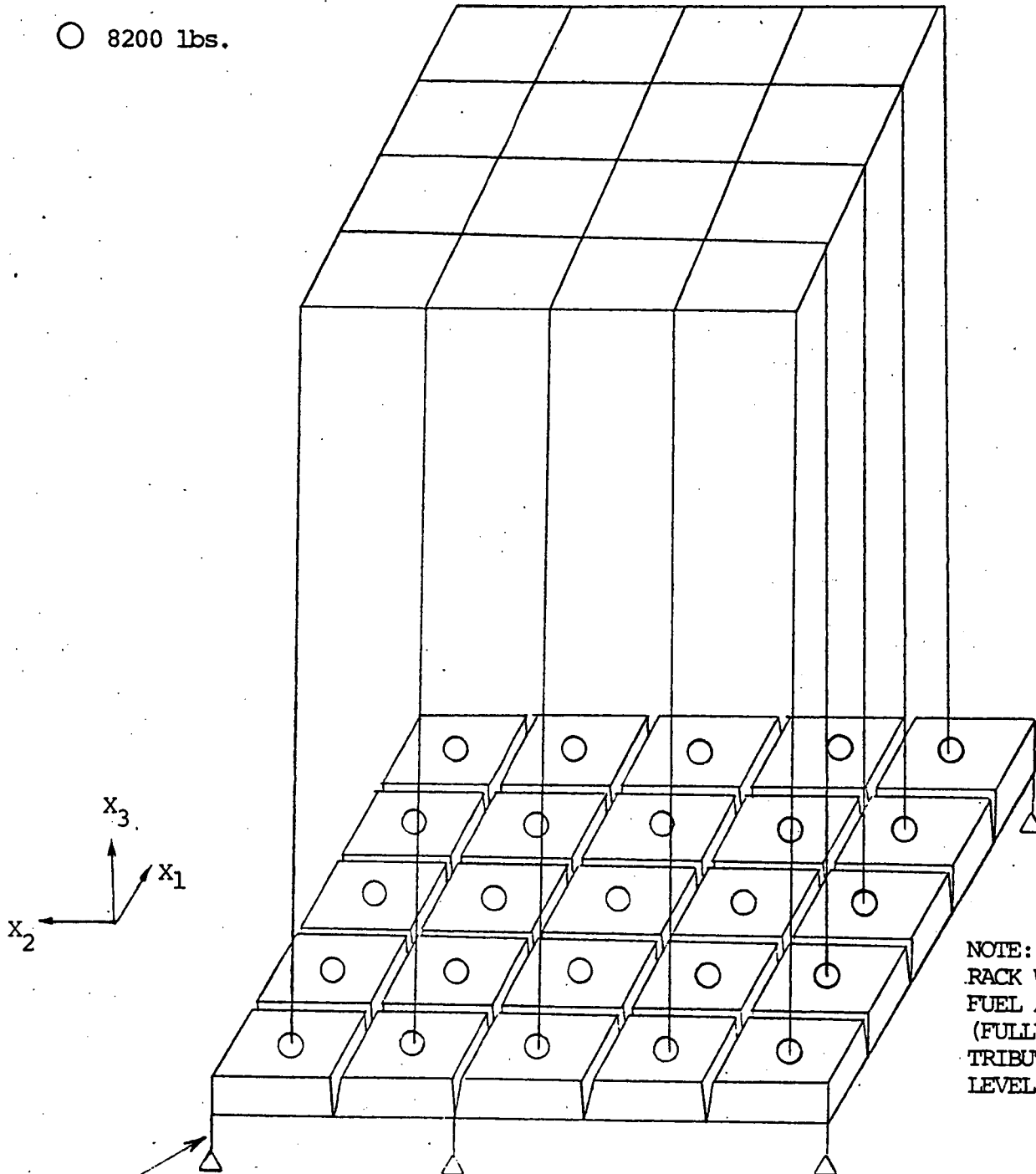


7.1.c  
10 x 10 RACK FINITE ELEMENT MODEL  
PLATE ELEMENT NUMBERS



Vertical Masses  
and Loads

○ 8200 lbs.



NOTE: LOADS INCLUDE  
RACK WEIGHT PLUS 100  
FUEL ASSEMBLIES  
(FULLY LOADED) DIS-  
TRIBUTED AT GRID  
LEVEL.

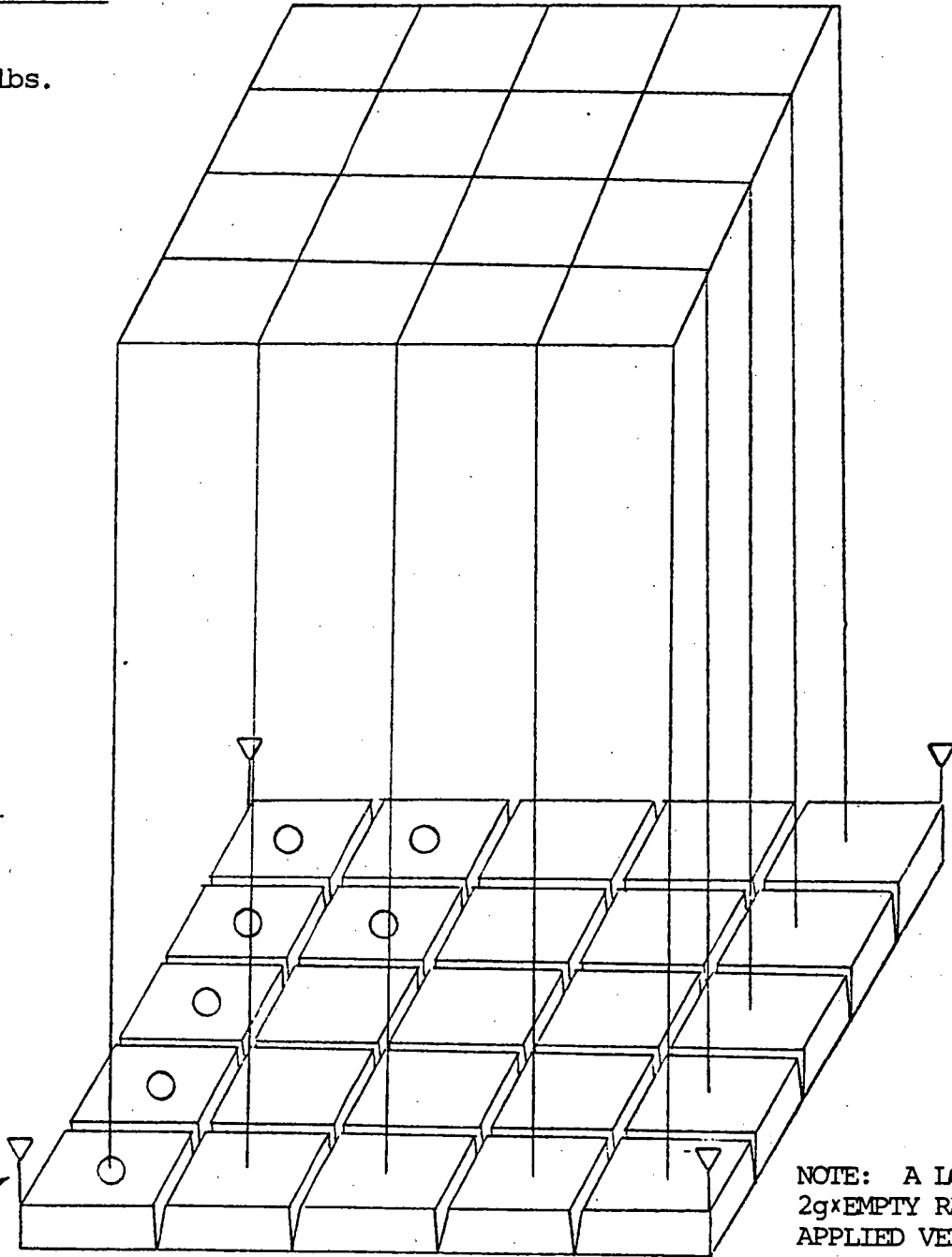
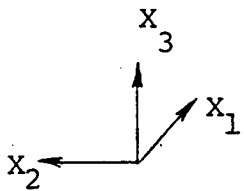
Vertical and  
Horizontal Support (Typ.)

FIGURE 7.2  
APPLIED LOADS AND BOUNDARY CONDITIONS - LOAD CASE 1  
DEAD WEIGHT OF FULLY LOADED RACK (10 x 10), D + L



Vertical Masses  
and Load

○ 3200 lbs.



Typical  
Installation  
Lifting Location

NOTE: A LOAD EQUAL TO  
 $2g \times$  EMPTY RACK MASS IS  
APPLIED VERTICALLY  
DOWNWARD TO SIMULATE AN  
INSTALLATION IMPACT LOAD.

FIGURE 7.3  
APPLIED LOADS AND BOUNDARY CONDITIONS - LOAD CASE 2  
EMPTY RACK WEIGHT PLUS INSTALLATION LOAD ANALYSIS - D + I.L.

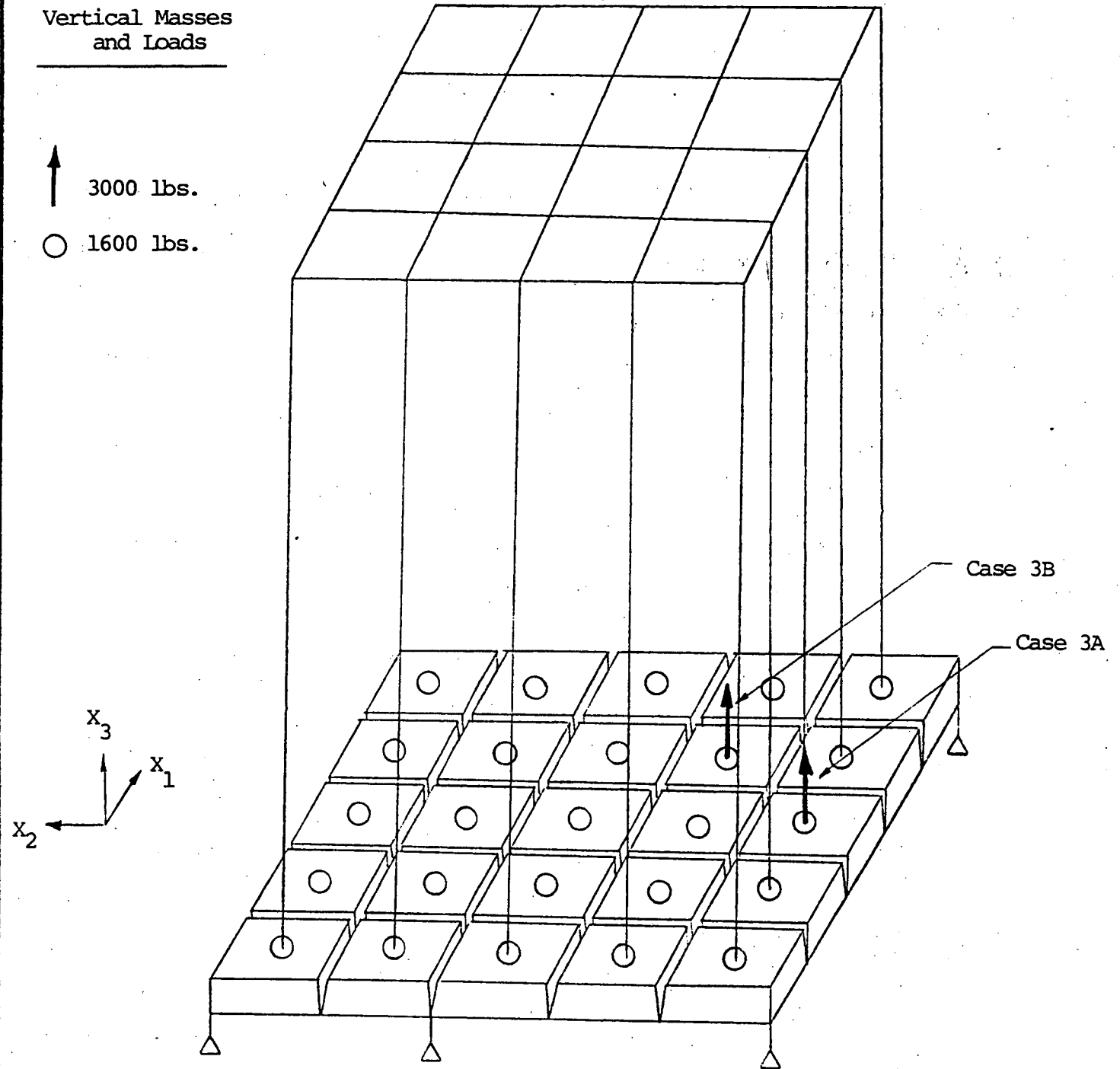
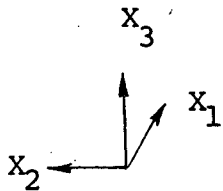


FIGURE 7.4  
APPLIED LOADS AND BOUNDARY CONDITIONS - LOAD CASE 3  
ACCIDENTAL UPLIFT LOAD ON 10 x 10 RACK - D + U.L.



Horizontal and Vertical Masses

- 1699 lbs.
- ⊗ 5096 lbs.
- ◐ 3397 lbs.
- ◑ 8200 lbs.



Dynamic Degrees of Freedom (Typ)

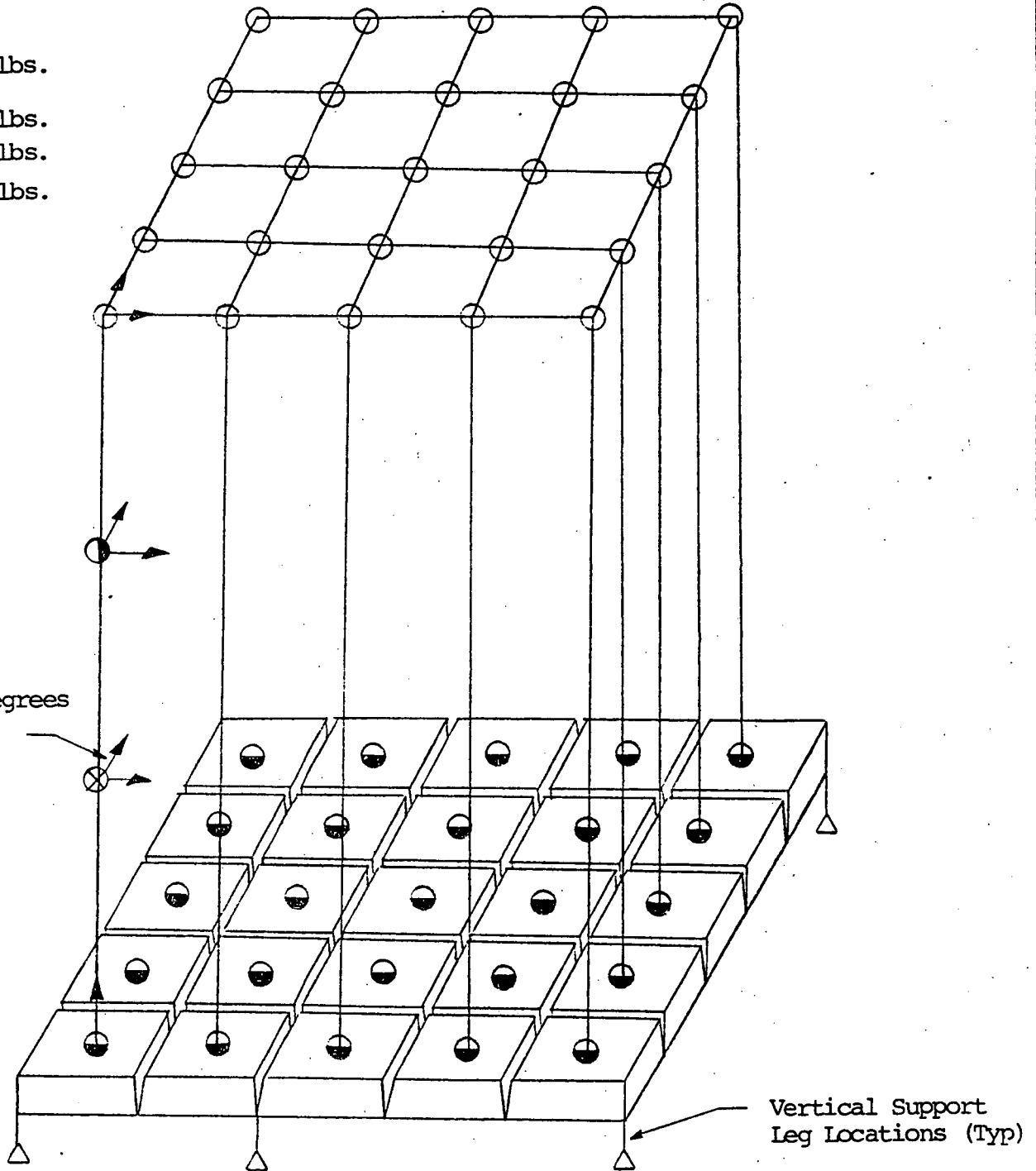


FIGURE 7.5  
LUMPED MASSES AND BOUNDARY CONDITIONS - LOAD CASES 4 & 5  
SEISMIC ANALYSIS OF FULLY LOADED 10 x 10 RACK - E AND E'



## 8. RESULTS OF ANALYSIS

The results of static and seismic structural/stress analysis of the Indian Point 2 high density fuel storage racks performed with the STARDYNE computer code are contained in Reference 12.

Appendices A through E contain the beam property table used in the rack analysis, the water sloshing analysis, the effective impact factor calculation, the accidental fuel drop analysis and spent fuel rack stability analysis.

### 8.1 RACK STRUCTURAL/STRESS ANALYSIS

The natural frequencies of vibration of the representative 10x10 fuel storage rack are given in Table 8.1 along with their corresponding modal participation factors. The first mode frequency of 3.39 cycles per second represents the first mode frequency of the storage rack structure including the flexibility characteristics of the rack base structure and support feet.

The results of the rack structural/stress analysis, which included rack and fuel assembly impact, are summarized in Table 8.2. Table 8.2 presents the maximum stresses and deflections in each type of rack structural member for the various load combinations developed in accordance with the NRC Standard Review Plan, Section 3.8.4 and compares them with the allowable values as specified in the acceptance criteria of Section 6. From these tables it can be seen that the maximum stresses in various structural members of the rack are nominal and within the allowable limits.

### 8.2 SPENT FUEL POOL FLOOR LOADS

The maximum reaction loads transmitted to the pool floor resulting from the dead weight, live loads, thermal effects and seismic loadings are presented in Table 8.3. These maximum reaction loads are calculated considering the storage rack to be fully loaded with spent fuel assemblies and include the impact effects of the fuel assemblies.

### 8.3 WATER SLOSHING EFFECTS

The effects of water sloshing in the fuel storage pool for a Design Basis Earthquake has been evaluated using the analytical method described in Reference No. 11.

Detailed calculations to evaluate the effects of sloshing water on the storage racks indicate that the sloshing water mass will exert small convective forces on the storage racks. The maximum convective forces on the storage racks resulting from the North/South and East/West Design Basis Earthquake are calculated to be 0.31 kips and 0.75 kips respectively. These convective forces are significantly smaller than the impulsive water forces (27.25 kips) resulting from the effects of constrained water mass on the storage racks. The effects of the impulsive water forces have been considered in the seismic analysis by adding the hydrodynamic and trapped water mass to the real weight of the rack structure and fuel elements. It has, therefore, been concluded that the sloshing water mass will have insignificant effects on the fuel storage racks.



#### 8.4 ACCIDENTAL SPENT FUEL ASSEMBLY DROP ANALYSIS

The results of the spent fuel assembly drop analysis using energy balance methods (Appendix D) are summarized in Table 8.4. From Table 8.4, it can be seen that for a straight drop of a fuel assembly on top of the storage cell, the maximum stress in the storage cell is slightly greater than the dynamic yield stress for stainless steel, thus indicating that the storage cell and its flare will undergo local permanent deformation but the overall storage rack structure will not yield. It can also be seen that the maximum stresses in the rack base structure are within the allowable values. The maximum punching shear stress in the liner plate is less than the allowable shear stress value, thus indicating no damage to the liner plate. The external kinetic energy of the dropped fuel will be absorbed in the local deformation of the storage cell flare at the top of the storage cell. However, the liner plate will not be perforated, insuring the leak-tight integrity of the fuel pool liner plate will be maintained.

For the case of the inclined drop of the fuel assembly on top of the storage rack, the maximum external kinetic energy (25.08 in-k) per storage cell is less than the kinetic energy for the straight drop of a fuel assembly on top of the storage cell (79.20 in-k). Therefore, the damage to the storage rack and the liner plate from the inclined drop of a fuel assembly on the top of a storage rack will be less severe than that of the straight drop event.

The free fall of a fuel assembly through the storage cell from a height of 48 inches above the top of a storage rack and its impact on top of the cell base plate and rack base structure was analyzed using empirical missile equations (the Ballistic Research Laboratory).

The results indicate that the maximum thickness of steel plate that could be perforated by such a missile is slightly greater than the thickness of the cell base plate. Therefore, during a fuel assembly drop accident of this type, the fuel assembly lower end fitting feet will perforate the cell base plate, however the lower end fitting support plate will prevent further penetration of the fuel assembly and subsequent impact to the pool floor liner plate. The kinetic energy developed during the free fall will be absorbed by both the bending and shearing of the cell base plate.

Since for this fuel assembly drop case, the external energy is absorbed in the flexural deformation of the flexible cell base plate and rack base structure, the reaction load transmitted to the rack base structure, rack feet and pool floor is less than that for fuel assembly drop on top of the storage cell. Therefore, the damage to the pool floor will be less severe for the fuel assembly drop through the storage cell than that for the fuel assembly drop on top of the storage rack.

It should be noted that the fuel assembly drop analyses have been performed by conservatively assuming that: (1) the fuel assembly drops from a height of 48 inches above the top of the storage cell, and (2) no energy will be absorbed by the fuel assembly itself. During fuel handling operations, the fuel assembly will actually be lifted less than 48 inches above the top of the storage cells. The energy absorbed in the deformation of the flexible fuel assembly should result in less damage to the storage rack and the pool liner plate than that predicted by the conservative analysis.

It has, therefore, been concluded that neither the straight nor inclined drop of the fuel assembly on top of the storage cell, or the straight drop of the fuel assembly through the storage cell and impact on top of the rack base structure will damage the storage rack and the pool liner plate sufficiently to adversely affect the value of  $k_{eff}$  or the leak-tight integrity of the pool.



TABLE 8.1

PERTINENT NATURAL FREQUENCIES OF VIBRATION AND MODAL  
PARTICIPATION FACTORS (10 x 10 RACK FULLY LOADED)MODAL PARTICIPATION FACTORS

<u>MODE NUMBER</u>	<u>FREQUENCY (CPS)</u>	<u>X1 DIRECTION</u>	<u>X2 DIRECTION</u>	<u>X3 DIRECTION</u>
1	3.390	-0.059	1.977	0.0
2	3.572	2.073	0.078	-0.007
3	3.637	0.325	0.218	-0.002
4	3.705	1.515	-0.064	0.0
5	3.744	-0.023	-0.739	0.0
6	3.752	-0.089	0.023	0.0
7	3.768	0.161	0.025	0.0
8	3.771	0.276	-0.040	0.0
9	3.771	0.006	0.407	0.0
10	3.772	0.211	0.012	0.0
11	20.023	0.017	-0.725	-0.004
12	20.485	-0.783	-0.010	0.038
13	21.491	-0.172	-0.071	-0.023
14	22.697	-0.077	0.057	-0.141
15	23.107	-0.003	-0.175	0.026
16	23.218	-0.042	-0.002	-0.097
17	23.352	-0.015	-0.001	-0.060
18	23.367	-0.014	0.001	-0.073
19	23.436	0.014	-0.005	0.060



TABLE 8.1 (cont'd)

<u>MODE NUMBER</u>	<u>FREQUENCY (CPS)</u>	<u>MODAL PARTICIPATION FACTORS</u>		
		<u>X1 DIRECTION</u>	<u>X2 DIRECTION</u>	<u>X3 DIRECTION</u>
20	23.439	-0.003	-0.028	0.003
21	24.117	0.044	-0.015	0.979
22	26.259	-0.008	0.014	0.069
23	27.629	-0.042	0.226	0.226
24	28.343	0.088	0.042	-0.646
25	28.423	-0.044	-0.007	-0.105
26	29.568	-0.002	0.001	-0.080
27	29.649	-0.004	0.018	0.160
28	29.725	-0.008	-0.016	0.115

TABLE 8.2 RESULTS OF STRUCTURAL/STRESS ANALYSIS  
FULLY LOADED 10x10 RACK



NUCLEAR ENERGY SERVICES, INC.

DOCUMENT NO. 81A0610

PAGE 35 OF 46

LOAD COMBINATION	STRUCTURAL ELEMENT DESCRIPTION	ELEM NO.	MAXIMUM BEAM STRESSES (KSI)				COMBINED* STRESS RATIO
			AXIAL		BENDING		
			CALCULATED $f_a$	ALLOWABLE $F_a$	CALCULATED $f_{b2}/f_{b3}$	ALLOWABLE $F_{b2}/F_{b3}$	
1. D + L	Support Leg	2	3.55	20.0	2.40/2.70	20.0/20.0	0.433
2. D + L + T  Dead Weight of Rack, Storage Cells and Fuel Assemblies (Negligible Thermal Load)	Interior Support Beams	28	0.27	20.0	5.83/0.18	20.0/20.0	0.314
	Exterior Support Beams	68	0.36	20.0	5.36/0.12	20.0/20.0	0.292
	Interior Spacer Beams	241	0.31	20.0	---	---	0.016
	Exterior Spacer Beams	244	0.27	20.0	---	---	0.014
	Storage Cell	290	Negligible	—	0.10/1.06	18.0/18.0	0.064

\*Must be  $\leq 1.0$  for component acceptability per AISC.

TABLE 8.2 RESULTS OF STRUCTURAL/STRESS ANALYSIS  
FULLY LOADED 10x10 RACK (Cont'd)

LOAD COMBINATION	STRUCTURAL ELEMENT DESCRIPTION	ELEM NO.	MAXIMUM BEAM STRESSES (KSI)				COMBINED* STRESS RATIO
			AXIAL		BENDING		
			CALCULATED $f_a$	ALLOWABLE $F_a$	CALCULATED $f_{b2}/f_{b3}$	ALLOWABLE $F_{b2}/F_{b3}$	
3. D + I.L.	Support Leg	9	1.60	20.0	4.10/4.10	20.0/20.0	0.490
Dead Weight of Rack Including Storage Cells Plus 1 G. Vertical Installation Load	Interior Support Beams	54	0.12	20.0	0.26/2.54	20.0/20.0	0.146
	Exterior Support Beams	45	0.53	20.0	0.71/5.83	20.0/20.0	0.354
	Interior Spacer Beams	232	0.29	20.0	---	---	0.015
	Exterior Spacer Beams	247	0.50	20.0	---	---	0.025
	Storage Cell	295	Negligible	---	1.45/1.43	18.0/18.0	0.160

\*Must be  $\leq 1.0$  for component acceptability per AISC.



TABLE 8.2 RESULTS OF STRUCTURAL/STRESS ANALYSIS  
FULLY LOADED 10x10 RACK (Cont'd)



NUCLEAR ENERGY SERVICES, INC.

DOCUMENT NO. 81A0610

PAGE 37 OF 46

LOAD COMBINATION	STRUCTURAL ELEMENT DESCRIPTION	ELEM NO.	MAXIMUM BEAM STRESSES (KSI)				COMBINED* STRESS RATIO
			AXIAL		BENDING		
			CALCULATED $f_a$	ALLOWABLE $F_a$	CALCULATED $f_{b2}/f_{b3}$	ALLOWABLE $F_{b2}/F_{b3}$	
4. D + L + E	Support Leg	3	8.45	20.0	5.38/5.42	20.0/20.0	0.700 <sup>**</sup>
5. D + L + T + E	Interior Support Beams	30	0.76	20.0	10.78/0.59	20.0/20.0	0.607
Dead Weight of Rack, Storage Cells, Fuel Assembly Plus the OBE Seismic Event (Negligible Thermal Load Included)	Exterior Support Beams	43	1.45	20.0	15.46/0.45	20.0/20.0	0.868
	Interior Spacer Beams	257	0.82	20.0	---	---	0.041
	Exterior Spacer Beams	244	1.10	20.0	---	---	0.055
	Storage Cell	278	Negligible	---	7.97/14.85	18.0/18.0	0.936 <sup>**</sup>

\*Must be  $\leq 1.0$  for component acceptability per AISC.

\*\* See App F

TABLE 8.2 RESULTS OF STRUCTURAL/STRESS ANALYSIS  
FULLY LOADED 10x10 RACK (Cont'd)



LOAD COMBINATION	STRUCTURAL ELEMENT DESCRIPTION	ELEM NO.	MAXIMUM BEAM STRESSES (KSI)				COMBINED* STRESS RATIO
			AXIAL		BENDING		
			CALCULATED fa	ALLOWABLE Fa	CALCULATED fb <sub>2</sub> /fb <sub>3</sub>	ALLOWABLE Fb <sub>2</sub> /Fb <sub>3</sub>	
6. D + L + T + E'	Support Leg	3	10.90	30.0	9.35/11.24	30.0/30.0	0.760**
Dead Weight of Rack, Storage Cells, Fuel Assemblies, Plus DBE Seismic Event (Negligible Thermal Load Included)	Interior Support Beams	55	1.10	30.0	19.49/0.98	30.0/30.0	0.719
	Exterior Support Beams	15	2.10	30.0	21.00/0.64	30.0/30.0	0.798
	Interior Spacer Beams	257	1.17	30.0	---	---	0.039
	Exterior Spacer Beams	228	1.52	30.0	---	---	0.051
	Storage Cell	278	Negligible	--	18.94/13.74	28.8/28.8	0.812**

\*Must be  $\leq 1.0$  for component acceptability per AISC.

\*\* See App F

TABLE 8.2 RESULTS OF STRUCTURAL/STRESS ANALYSIS  
FULLY LOADED 10x10 RACK (Cont'd)

LOAD COMBINATION	STRUCTURAL ELEMENT DESCRIPTION	ELEM NO.	MAXIMUM BEAM STRESSES (KSI)				COMBINED* STRESS RATIO
			AXIAL		BENDING		
			CALCULATED $f_a$	ALLOWABLE $F_a$	CALCULATED $f_{b2}/f_{b3}$	ALLOWABLE $F_{b2}/F_{b3}$	
7. D + T + U.L.	Support Leg	6	0.60	30.0	0.43/0.50	30.0/30.0	0.051
Dead Weight of Rack Plus 3000 lb. Uplift Load	Interior Support Beams	28	Negligible	--	1.12	30.0	0.037
	Exterior Support Beams	68	Negligible	--	1.01	30.0	0.034
	Interior Spacer Beams	--	Negligible	--	--	--	--
	Exterior Spacer Beams	--	Negligible	--	--	--	--
	Storage Cell	288	Negligible	--	1.20/0.08	28.8/28.8	0.044

\*Must be  $\leq 1.0$  for component acceptability per AISC.





TABLE 8.3

## MAXIMUM FLOOR LOAD SUMMARY

	MAX HORIZONTAL REACTION LOAD (K) *		MAX VERTICAL REACTION LOAD (K)		
	OBE	DBE	D + L	D + L + OBE	D + L + DBE
INDIVIDUAL SUPPORT PAD	33.18	47.12	45.16	106.67	137.98
10x10 RACK ARRAY	173.90	263.85	204.77	228.11	239.99

\* The maximum horizontal reaction loads are conservatively generated assuming no sliding between the support pads and the pool floor.



TABLE 8.4

## RESULTS OF AN ACCIDENTAL SPENT FUEL ASSEMBLY DROP (LOAD CASE 6)

<u>Straight Drop on Top of Storage Cell</u>	<u>Calculated Value</u>	<u>Allowable Value</u>
Weight of Fuel Assembly (kip)	1.650	—
Maximum Drop Height (in)	48.0	—
Kinetic Energy of Drop to be Absorbed (in-k)	79.2	—
Maximum Strain in Storage Cell (in/in)	0.00445	0.485 <sup>1</sup>
Maximum Cell Axial Deformation (in)	0.735	—
Maximum Stress in Cell (ksi)	39.58	36.00 <sup>2</sup> (103.00) <sup>4</sup>
Maximum Transmitted Reaction Load (kips)	129.27	—
Maximum Stress in Rack Base Structure (ksi)	35.58	36.00 <sup>2</sup>
Maximum Support Leg Load (kips)	135.65	—
Maximum Local Bearing Stress on Concrete Floor (ksi)	2.70	3.57
Maximum Punching Shear Stress in the Liner Plate (ksi)	21.60	23.04 <sup>3</sup>
<u>Inclined Drop on Top of Storage Cell</u>		
Maximum External Kinetic Energy per Storage Cell (in-k)	25.08	79.2
Maximum External Kinetic Energy (in - k)	131.12	—



TABLE 8.4 (Cont'd)

## RESULTS OF ACCIDENTAL SPENT FUEL ASSEMBLY DROP (LOAD CASE 6)

<u>Straight Drop Through the Storage Cell</u>	<u>Calculated Value</u>	<u>Allowable Value</u>
Maximum Drop Height (in.)	213.25	—
Maximum Free Fall Impact Velocity (ft/sec)	33.81	—
Maximum External Kinetic Energy (in. k)	351.86	—
Maximum Unsupported Plate Thickness That May be Perforated by Missile Free Fall Velocity, (in.)	0.6113	—
BRL Formula	0.454	0.50
Maximum Transmitted Reaction Load (kips)	57.65	—

1. Ultimate strain for stainless steel.
2. The allowable stress value represents dynamic yield stress for stainless steel.
3. Allowable shear stress value  $36.0 \times 1.6 \times 0.4 = 23.04$  ksi.
4. Ultimate stress for stainless steel.



### 8.5 SPENT FUEL RACK STABILITY ANALYSIS

The results of the 10x10 spent fuel storage rack stability analysis using energy balance methods (Appendix E) indicate the following:

1. The storage rack will remain stable during Operating Basis Earthquake (OBE) and Design Basis Earthquake (DBE) events. During OBE event, the storage rack will not lift up. During DBE event, one edge of the rack will lift up no more than 0.3182 inches.
2. For DBE event, the maximum impact load that will be generated during recontact with the pool floor has been calculated to be 511 kips. The maximum impact load will act as an impulse load on the pool floor. It should be noted that all the racks will not recontact the pool floor simultaneously.
3. A maximum reaction load of 106.6 kips will be developed in any single foot of the rack. The reaction load of 106.6 kips is smaller than the maximum reaction load of 137.98 kips resulting from dead plus live plus DBE seismic loadings.
4. The maximum stresses generated in the rack base structure is in the order of 35.4 ksi, which is less than the allowable stress value of 36.0 ksi\*.

The spent fuel storage rack stability analysis has been performed by conservatively assuming that no energy will be absorbed in the local deformation of the rack base structure, pool floor liner plate and concrete under the rack feet.

It has, therefore, been concluded that the storage rack will maintain its structural integrity during liftup and recontact to the pool floor.

---

\* Dynamic Yield Strength



## 9. CONCLUSIONS

1. The results of the seismic and structural analysis indicate that the stresses in the rack structure resulting from the loadings associated with the normal and abnormal conditions are within allowable stress limits for Seismic Category I structures.
2. Sloshing of pool water in a seismic event will have insignificant effects on the fuel storage racks.
3. The analysis of the accidental fuel assembly drop condition indicates acceptable local structural damage to the storage cells with no buckling or collapse, and no puncturing of the stainless steel liner. Therefore, no significant changes in the value of  $k_{eff}$  will occur and the leak-tightness of the fuel pool will be maintained.
4. It is concluded that the designs of the Indian Point 2 high density fuel storage racks are adequate to withstand the loadings of normal and abnormal conditions.



## 10. REFERENCES

1. Nuclear Energy Services, Inc. Drawings for Indian Point Generating Station Unit 2 Fuel Storage Racks, (80E3503 through 80E3526).
2. Nuclear Energy Services, Inc. "Quality Assurance Program Plan for Indian Point Generating Station Unit 2 Fuel Storage Racks," Document NES 81A0606, November 1979.
3. Consolidated Edison Company "Design, Fabricate, Deliver and Installation, Spent Fuel Storage Racks," Specification No. MP 79-001, Rev. 2, March 1979.
4. USNRC Regulatory Guide 1.92: "Combination of Modes and Spatial Components in Seismic Response Analysis," Rev. 1, February 1976.
5. USNRC Standard Review Plan, Section 3.8.4.
6. USNRC: "Position Paper for Review and Acceptance of Spent Fuel Storage and Handling Applications," April 14, 1978 and Supplement January 18, 1979.
7. American Institute of Steel Construction: "Manual of Steel Construction," Seventh Edition, 1970.
8. Dong, R. G. "Effective Mass and Damping of Submerged Structures," Lawrence Livermore Laboratory, UCRL-52342, April 1978.
9. Fritz, R. J. "The Effects of Liquids on the Dynamic Motions of Immersed Solids," Journal of Engineering for Industry, Trans. ASME, February 1972.
10. MRI/STARDYNE 3 - Static and Dynamic Structural Analysis Systems for Scope 3.4 Operating System User's Information Manual, Revision A, Control Data Corporation, August 1976.
11. "Nuclear Reactors and Earthquakes" prepared by Lockheed Aircraft Corporation and Holmes and Narver, Inc., TID 7024; Atomic Energy Commission, Washington D.C.
12. Indian Point 2 Fuel Storage Racks, STARDYNE Structural Analysis Project 5147, Task 200, NES Computer Output Binder No. S-43, November 1979.
13. Nuclear Energy Services, Inc., "Non-linear Time History Seismic Sliding Analysis Report for Indian Point Generating Station Unit 2," Document NES 81A0615, Nov. 1979.
14. American Society for Testing and Material, 1977 Annual Book of ASTM Standards, Parts 3 and 5.



**APPENDICES**



**APPENDIX A**  
**MEMBER PROPERTIES**

APPENDIX A MEMBER PROPERTIES

REF.

INDIAN POINT No 2 SPENT FUEL RACK MEMBER PROPERTIES						
MEMBER DESCRIPTION	AREA (IN <sup>2</sup> )	I <sub>2</sub> (IN <sup>4</sup> )	I <sub>3</sub> (IN <sup>4</sup> )	K (IN <sup>4</sup> )	r <sub>2</sub> (IN)	r <sub>3</sub> (IN)
RACK BASE BEAM PERIPHERAL BOX BEAM	9.19	79.24	12.243	29.31	2.99	1.15
RACK BASE BEAM TYPICAL INTERIOR BEAM	7.344	61.022	6.694	0.257	2.88	0.955
RACK BASE BEAM REINFORCED INTERIOR	9.344	96.915	9.361	0.257	3.22	1.00
RACK BASE LEG (EFFECTIVE)	13.23	38.38	38.38	8.49	1.70	1.70
STORAGE CELL 2x2 MODULE	12.27	468.0	468.0	935.9	6.18	6.18



**APPENDIX B**  
**WATER SLOSHING EFFECTS**

**APPENDIX B**

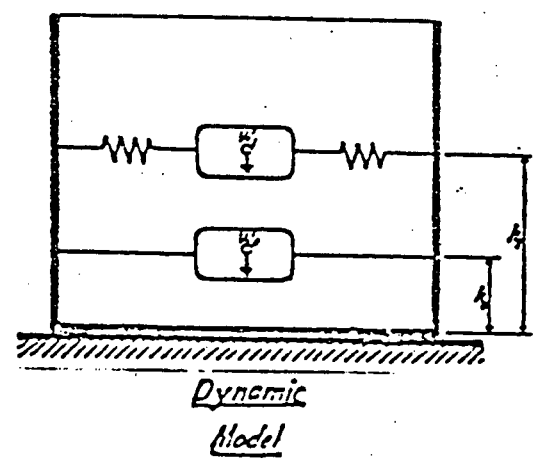
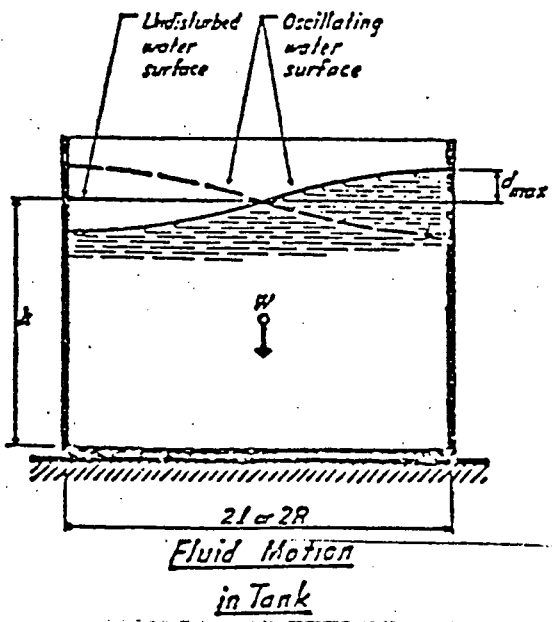
REF.

WATER SLOSHING EFFECTS ON THE SPENT FUEL STORAGE RACKS

THE WATER SLOSHING EFFECTS ON THE FUEL RACKS HAVE BEEN EVALUATED USING ANALYTICAL METHODS DESCRIBED IN THE FOLLOWING REFERENCE:

"NUCLEAR REACTORS AND EARTHQUAKES" PREPARED BY LOCKHEED AIRCRAFT CORPORATION AND HOLMES & NARVER, INC., WASHINGTON D.C., TID-7024: ATOMIC ENERGY COMMISSION. (REF B-1)

B-1



Dynamic Model for Fluid Tank Supported on the Ground

DURING A SEISMIC EVENT, HORIZONTAL ACCELERATION OF THE SPENT FUEL POOL GENERATES HORIZONTAL HYDRODYNAMIC PRESSURES. A CERTAIN PORTION OF THE WATER IN THE POOL ACTS AS A SOLID.

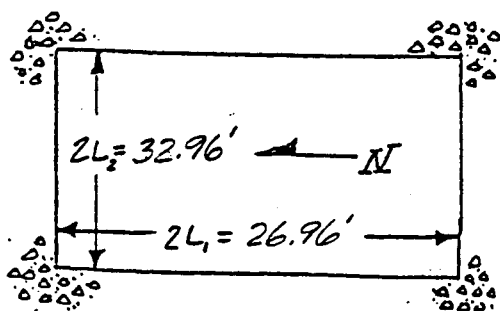
**APPENDIX B (CONT)**

REF.

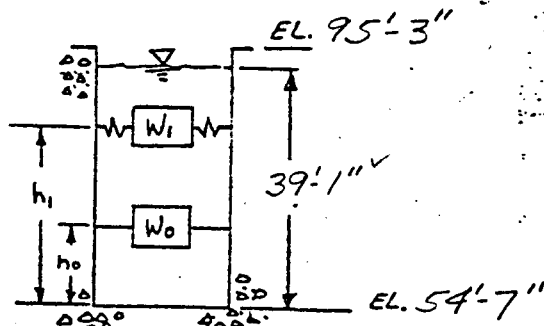
MASS IN RIGID CONTACT WITH THE POOL WALLS, PRODUCING IMPULSIVE HYDRODYNAMIC PRESSURES DIRECTLY PROPORTIONAL TO THE MAXIMUM ACCELERATION OF THE STORAGE POOL. THE HORIZONTAL ACCELERATION ALSO INDUCES OSCILLATIONS OF THE UPPER LAYER OF WATER CONTRIBUTING ADDITIONAL DYNAMIC (CONVECTIVE) PRESSURES. THE WATER MASS RESPONDS AS IF IT WERE A SOLID OSCILLATING MASS FLEXIBLY CONNECTED TO THE POOL WALLS. ASSUMING THE POOL STRUCTURE TO BE A RIGID BODY, THE MAXIMUM DISPLACEMENT OF THIS OSCILLATING MASS EQUALS THE MAX. SLOSHING HEIGHT OF THE POOL WATER. THE SEPARATION OF THE HYDRODYNAMIC PRESSURES INTO IMPULSIVE AND CONVECTIVE PRESSURES LEADS TO A DYNAMIC MODEL REPRESENTED BY A RIGID AND SPRUNG MASS SHOWN ON Pg. B1.

USING FORMULAS GIVEN IN REFERENCE B-1 WITH THE VARIOUS PARAMETERS OF THE INDIAN POINT POOL, THE EFFECTS OF WATER SLOSHING ON THE FUEL RACKS ARE CALCULATED.

B-1



PLAN



ELEVATION

REF. U.E. # C DWj.  
No. 9321F-1392-6

B-2



## APPENDIX B (CON'T)

REF.

THE MAX. SLOSHING EFFECTS (FORCES ON RACKS AND MAX. WATER DISPLACEMENT) OCCUR WHEN THE POOL IS SUBJECTED TO LATERAL ACCELERATIONS RESULTING FROM A DESIGN BASIS EARTHQUAKE. THEREFORE THE WATER SLOSHING EFFECTS ARE ANALYZED FOR A DBE EVENT ONLY.

### FOR A N-S DBE EVENT

THE INDIAN POINT POOL IS CONSIDERED TO BE A SLENDER POOL IN THE N-S DIRECTION ( $h/l = 39.08/13.46 = 2.89 > 1.5$ ). THEREFORE, THE ENTIRE MASS BELOW THIS LEVEL TENDS TO RESPOND AS A RIGID BODY (CONSTRAINED WATER) WITH RESPECT TO THE IMPULSIVE PRESSURES.

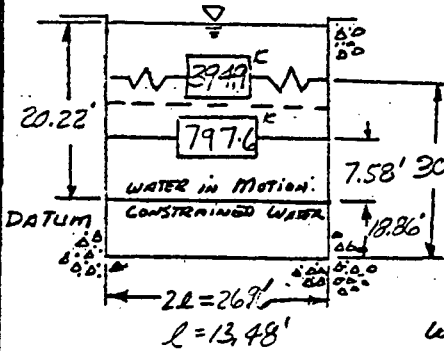
THE IMPULSIVE FORCES ARE CALCULATED WITH RESPECT TO THE FICTITIOUS BOTTOM AT DATUM ( $1.5 l = (1.5)(13.46) = 20.22'$ ) AND COMBINED WITH THE ACTUAL WEIGHT IN THE CONSTRAINED REGION TO DETERMINE THE OVERALL IMPULSIVE FORCE AND ITS CENTER OF GRAVITY ( $H_0$ ). THE CONVECTIVE FORCES DUE TO THE OSCILLATING WATER ARE CALCULATED AS A FUNCTION OF FULL WATER DEPTH AND APPLIED AT ITS CALCULATED CENTER OF GRAVITY ( $H_1$ ) TO DETERMINE THE SLOSHING WATER EFFECTS.

NOTE: SINCE THE FICTITIOUS DATUM (20.22) IS  $(39.08 - 20.22) = 18.86'$  ABOVE POOL FLOOR, THE RACKS WILL BE SUBJECTED TO SOME IMPULSIVE PRESSURES.

APPENDIX B (CONT)

REF.

FOR N-S DIRECTION



WEIGHT OF WATER IN MOTION =  $\frac{62.4}{1000} \times 20.22 \times 33 \times 27' = 1124.2^k$

WEIGHT OF CONSTRAINED WATER =  $\frac{62.4}{1000} \times 18.86 \times 33 \times 27' = 1048.6^k$

FROM REF. IMPULSIVE FORCE (P<sub>0</sub>)

$\frac{W_0}{W} = \frac{\text{Tanh} \left( \sqrt{3} \frac{L}{h_f} \right)}{\sqrt{3} \frac{L}{h_f}}$

WHERE:  $W = 1124.2^k$   
 $\frac{L}{h_f} = \frac{13.48}{20.22} = 2/3$

$W_0 = \frac{\text{Tanh} \left( \sqrt{3} \times 2/3 \right)}{\sqrt{3} \times 2/3} \times 1124.2^k = 797.6^k$

CENTER OF GRAVITY  $h_0$  (ABOVE DATUM) =  $\frac{3}{8} h_f = (.375)(20.22) = 7.58'$

THE POOL STRUCTURE IS ASSUMED RIGID. FROM THE "DBE HORIZONTAL ACCELERATION RESPONSE SPECTRA" FOR A MINIMUM PERIOD T, THE G VALUE IS 0.15.

IMPULSIVE FORCE =  $0.15 (797.6 + 1048.6) = 276.9^k \checkmark$

CENTER OF GRAVITY OF TOTAL IMPULSIVE FORCE

$= h_0' = \frac{(797.6^k \times 26.44') + (1048.6^k \times 18.86'/2)}{(797.6^k + 1048.6^k)} = 16.78'$   
ABOVE POOL FLOOR

CONVECTIVE FORCE (P<sub>L</sub>)

WEIGHT OF WATER IN POOL =  $\frac{62.4}{1000} \times 39.08 \times 33 \times 27' = 2172.8^k$

$\frac{W_L}{W} = 0.527 \frac{L}{h} \text{Tanh} \left( 1.58 \frac{h}{L} \right)$  WHERE:  $W_L = \text{CONVECTIVE WEIGHT}$   
 $W = 2172.8^k \checkmark$

$W_L = 0.527 (0.3449) \text{Tanh} \left( 1.58 \times \frac{39.08}{13.48} \right) \times 2172.8^k = 394.9^k$   
 $\frac{L}{h} = \frac{13.48}{39.08} = 0.3449$

NATURAL FREQUENCY OF OSCILLATING WATER  $\omega^2 = \frac{1.58 g}{L} \text{Tanh} \left( 1.58 \frac{h}{L} \right)$



APPENDIX B (CONT)

REF.

$$\omega^2 = \frac{1.58 (32.2)}{13.48'} \tanh \left( 1.58 \times \frac{39.08}{13.48} \right) = 3.773 \checkmark \text{ OR } \omega = 1.943 \checkmark$$

$$T = \frac{2\pi}{\omega} = \frac{2\pi}{1.943} = 3.235 \text{ SEC} ; f = \frac{1}{T} = \frac{1}{3.235} = 0.309 \checkmark \text{ CP}$$

FROM THE " DBE HORIZONTAL ACCELERATION RESPONSE SPECTRA " (REF B-3) FOR  $f = 0.309 \checkmark \text{ CP}$

MAX.  $G = 0.1$  (1.0% DAMPING AT  $T > 2.0 \text{ SEC}$ )

$$\text{MAX. SPECTRAL DISPLACEMENT} = \frac{0.10 \times 32.2 \times 12}{3.773} = 10.24 \checkmark \text{ IN.}$$

THE MAX. SPECTRAL DISPLACEMENT IS 10.24 INCHES FOR A DBE EVENT.

$$\theta_h \text{ (ANGULAR AMPLITUDE OF THE OSCILLATING FLUID SURFACE)} = 1.58 \frac{A_f}{L} \tanh \left( 1.58 \frac{h}{L} \right)$$

WHERE:  $A_f = 10.24 \text{ INCHES OR } 0.853 \text{ FT.}$

$$L = 13.48' \quad \& \quad \frac{h}{L} = \frac{39.08}{13.48} = 2.899$$

$$\theta_h = 1.58 \frac{0.853}{13.48} \tanh \left( 1.58 \times 2.899 \right) = 0.10 \checkmark$$

CONVECTIVE FORCE  $P_1 = W_1 \theta_h \sin \omega t$

$$P_1 = (394.9 \text{ K}) (0.10) (\sin \omega t = 1) = 39.5 \text{ K}$$

CENTER OF GRAVITY OF CONVECTIVE FORCE  $h_1$ :

$$\frac{h_1}{h} = 1 - \frac{\cosh \left( 1.58 \times \frac{h}{L} \right) - 1}{1.58 \frac{h}{L} \sinh \left( 1.58 \frac{h}{L} \right)}$$

$$\text{OR } h_1 = \left\{ 1 - \frac{\cosh (1.58 \times 2.899) - 1}{1.58 \times 2.899 \sinh (1.58 \times 2.899)} \right\} \times 39.08' = 37.72'$$

B-3

APPENDIX B WATER SLOSHING EFFECTS

REF.

THE EFFECTS OF THE IMPULSIVE WATER FORCES ON THE SPENT FUEL STORAGE ARE CONSIDERED BY APPLYING AN ADDITIONAL HYDRODYNAMIC AND TRAPPED WATER MASS TO THE STRUCTURAL DEAD WEIGHT AND LIVE LOADS.

THE CENTER OF GRAVITY OF THE CONVECTIVE WATER PRESSURE ACTS AT A LOCATION 30.72' FEET ABOVE THE POOL FLOOR AND (30.72' - 15.27') = 15.45' FEET ABOVE THE UPPER SURFACE OF THE FUEL STORAGE RACKS. THE CONVECTIVE WATER PRESSURE ON THE STORAGE RACKS IS:

$$P_w = \rho \frac{l^2}{3} \sqrt{\frac{5}{2}} \frac{\cosh \sqrt{\frac{5}{2}} \frac{y}{l}}{\sinh \sqrt{\frac{5}{2}} \frac{h}{l}} \omega^2 \theta_h \sin \omega t$$

THE MAX WATER PRESSURE IS:

$$P_w(\text{max}) = \rho \frac{l^2}{3} \sqrt{\frac{5}{2}} \frac{\cosh \sqrt{\frac{5}{2}} \frac{y}{l}}{\sinh \sqrt{\frac{5}{2}} \frac{h}{l}} \omega^2 \theta_h$$

WHERE:  $l = 13.48 \text{ FE}$   $\theta_h (\text{DBE}) = 0.10$   
 $h = 39.08 \text{ FE}$   $\omega^2 = 3.773 \text{ (Pg. B-5)}$   
 $\rho = \frac{62.4}{32.2} = 1.938 \frac{\text{#-SEC}^2}{\text{FE}^3}$

THE CONVECTIVE FORCE PER FEET OF RACK:

$$P_2 = \int_{h_1}^{h_2} P_w dy = \int_{h_1}^{h_2} \left[ \frac{62.4}{32.2} \times \frac{(13.48)^2}{3} \sqrt{\frac{5}{2}} \times \frac{\cosh \sqrt{\frac{5}{2}} \frac{y}{l}}{\sinh \sqrt{\frac{5}{2}} \frac{39.08}{13.48}} \right] (3.773) (0.10) dy$$



APPENDIX B WATER SLOSHING EFFECTS

REF.

$$P_R = \frac{1,431}{1000} \int_{h_1}^{h_2} \cosh \frac{\sqrt{5}}{2} y \, dy$$

$h_1 = 0.23'$  = STORAGE RACK LOWER SURFACE ABOVE POOL FLOOR (FT)  
 $h_2 = 15.27'$  = STORAGE RACK UPPER SURFACE ABOVE POOL FLOOR (FT)

$$P_R = \frac{1,431}{1000} \times 13.98 \left[ \sinh \sqrt{\frac{5}{2}} \frac{y}{13.98} \right]_{0.83}^{15.27} = 0.034 \text{ kip/ft}$$

TOTAL CONVECTIVE FORCE ON A RACK =  $0.034 \times \frac{1.09}{12} = 0.31 \text{ kip}$

CONCLUSIONS:

THE RESULTS OF THE DETAILED CALCULATIONS OF THE WATER SLOSHING EFFECTS ON THE SPENT FUEL RACKS DUE TO AN N/S DBE EVENT INDICATE THAT THE CENTER OF GRAVITY OF THE CONVECTIVE WATER PRESSURE IS AT AN ELEVATION 15.45 FEET ABOVE THE TOP SURFACE OF THE FUEL STORAGE RACKS. THE CONVECTIVE WATER FORCE ON A STORAGE RACK (0.31 kips) IS INSIGNIFICANT WITH RESPECT TO THE IMPULSIVE WATER FORCES.

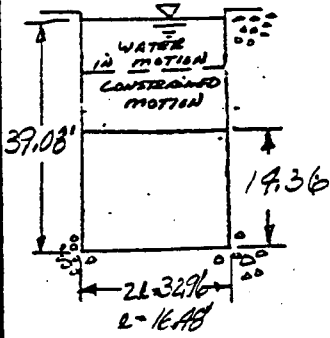
THE IMPULSIVE FORCES ARE ACCOUNTED FOR BY APPLYING AN ADDITIONAL HYDRODYNAMIC AND TRAPPED WATER MASS TO THE STRUCTURAL WEIGHT. THEREFORE, ANY SLOSHING WATER WILL HAVE INSIGNIFICANT EFFECTS ON THE SPENT FUEL RACKS.

APPENDIX B

REF.

E-W DBE EVENT:

$2L = 32.96'$  ✓  $L = 16.48'$  ✓



SINCE THE DEPTH OF THE FLUID (39.08') EXCEEDS  $\frac{3}{4}$  OF THE POOL LENGTH, THE ENTIRE MASS BELOW THE DEPTH 1.5L BELOW WATER SURFACE TENDS TO RESPOND AS A RIGID BODY.

FICTITIOUS DATUM  $h_f = 1.5L = 1.5(16.48) = 24.72'$  ✓  
OR  $(39.08' - 24.72') = 14.36'$  ✓ ABOVE POOL FLOOR.

WEIGHT OF WATER IN MOTION =  $\frac{62.4}{1000} \times 27' \times 33' \times 24.72' = 1374.4$  ✓ K

WEIGHT OF CONSTRAINED WATER =  $\frac{62.4}{1000} \times 27' \times 33' \times 14.36' = 798.4$  ✓ K

IMPULSIVE FORCES (P<sub>0</sub>)

$\frac{W_0}{W} = \frac{\tanh(\sqrt{3} \frac{L}{h_f})}{\sqrt{3} \frac{L}{h_f}}$  WHERE:  $W = 1374.4$  ✓ K  
 $\frac{L}{h_f} = \frac{16.48}{24.72} = \frac{2}{3}$

$W_0 = \frac{\tanh(\sqrt{3} \times \frac{2}{3})}{\sqrt{3} \times \frac{2}{3}} \times 1374.4$  ✓ K = 975.2

CENTER OF GRAVITY OF IMPULSIVE FORCE (MOTION) =  $\frac{3}{8} h_f$ .

$h_0 = \frac{3}{8} (24.72) = 9.27'$  ✓ ABOVE DATUM

THE IMPULSIVE FORCE IS CALCULATED BY ASSUMING THE POOL STRUCTURE IS RIGID. THE LATERAL ACCELERATION VALUE IS OBTAINED FROM THE "DBE HORIZONTAL ACCELERATION RESPONSE SPECTRA" FOR A MINIMUM PERIOD T (0.15G) AND APPLIED TO THE CONSTRAINED WEIGHTS.

IMPULSIVE FORCE =  $0.15 (975.2$  ✓ K  $+ 798.4$  ✓ K) = 266.0K ✓



# APPENDIX B

REF.

CENTER OF GRAVITY OF TOTAL IMPULSIVE FORCE  $h_0'$ :

$$h_0' = \frac{(798.4^k \times \frac{14.36'}{2}) + 975.2^k (9.27 + 14.36)}{798.4^k + 975.2^k} = 16.22'$$

ABOVE POOL FLOOR

CONVECTIVE FORCE -  $P_i$

WEIGHT IN POOL = 2172.8<sup>k</sup> (Pg. B-4)

$$\frac{w_1}{w} = 0.527 \frac{L}{h} \tanh\left(1.58 \frac{h}{L}\right) \quad \text{WHERE: } \frac{h}{L} = \frac{39.08}{16.48} = 2.37$$

$$w_1 = (0.527)(0.422) \tanh(1.58 \times 2.37)(2172.8^k) \quad \frac{L}{h} = \frac{16.48}{39.08} = 0.422$$

$$= 482.7^k \quad w = 2172.8^k$$

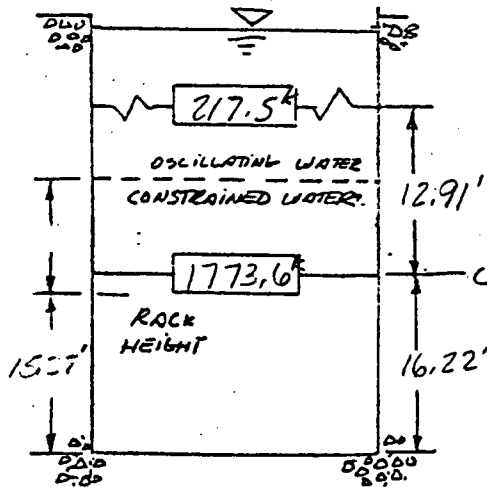
NATURAL FREQ. OF OSCILLATING WATER =  $\omega^2 = \frac{1.58g}{L} \tanh\left(1.58 \frac{h}{L}\right)$

$$\omega^2 = \frac{(1.58)(32.2)}{16.48} \tanh(1.58 \times 2.37) = 3.08 \quad \omega = 1.756$$

$$T(\text{PERIOD}) = \frac{2\pi}{\omega} = \frac{2\pi}{1.756} = 3.578 \quad ; \quad f = \frac{1}{T} = 0.279 \text{ cps}$$

FROM DBE SPECTRA FOR  $f = 0.279 \text{ cps}$  -  $G = 0.10$

FOR A DBE EVENT THE MAX. SPECTRAL DISPLACEMENT IS  $\frac{0.10 \times 32.2 \times 12}{3.08} = 12.55 \text{ IN.}$  W/ 1.0% DAMPING



$\theta_n$  (ANGULAR AMPLITUDE OF OSCILLATING FLUID)

$$= 1.58 \frac{Af}{L} \tanh\left(1.58 \frac{h}{L}\right)$$

$$= (1.58) \left(\frac{12.55/12}{16.48}\right) \tanh(1.58 \times 2.37)$$

$$= 0.10$$

CONVECTIVE FORCE

$$P_i = w_1 \theta_n \sin \omega t ; \sin \omega t = 1.0$$

$$P_i = (482.7^k)(0.10) = 48.3^k$$

ELEVATION



APPENDIX B WATER SLOSHING EFFECTS

REF.

CENTER OF GRAVITY OF  $P_1$  ( $h_1$ ):

$$\frac{h_1}{h} = 1 - \frac{\cosh(1.58 \frac{h}{L}) - 1}{1.58 \frac{h}{L} \sinh(1.58 \frac{h}{L})} \quad \text{WHERE: } h = 39.08' \\ L = 16.48'$$

$$h_1 = \left[ 1 - \frac{\cosh(1.58 \times \frac{39.08}{16.48}) - 1}{1.58 (\frac{39.08}{16.48}) \sinh(1.58 \frac{39.08}{16.48})} \right] 39.08' = 29.13' \quad \checkmark \\ \text{ABOVE POOL FLOOR.}$$

THEREFORE, THE CENTER OF GRAVITY OF THE CONVECTIVE WATER FORCE IS 29.13' FEET ABOVE THE POOL FLOOR OR  $(29.13' - 15.27') = 13.86$  FEET ABOVE THE UPPER SURFACE OF THE SPENT FUEL RACKS. THE MAX. CONVECTIVE WATER PRESSURE ON THE RACKS IS EVALUATED (REF. 14) TO

BE EQUAL TO:  $P_w = \rho \frac{L^2}{3} \sqrt{\frac{5}{2}} \frac{\cosh \sqrt{\frac{5}{2}} \frac{y}{L}}{\sinh \sqrt{\frac{5}{2}} \frac{h}{L}} w^2 \Theta_n$

WHERE:  $\rho = \text{MASS DENSITY} = \frac{62.4}{32.2} = 1.938 \text{ } \checkmark \text{ } \text{-SEC}^2/\text{FT}^3$   
 $L = 16.48'$   
 $h = 39.08'$   
 $\Theta_n = 0.10 \checkmark$   
 $w^2 = 3.08 \checkmark \text{ (Pg B9)}$

THE CONVECTIVE FORCE PER FOOT-WIDTH OF RACK:

$$P_R = \int_{h_1}^{h_2} P_w dy = \int_{h_1}^{h_2} \left[ 1.938 \frac{(16.48)^2}{3} \sqrt{\frac{5}{2}} (3.08)(0.10) \frac{\cosh \sqrt{\frac{5}{2}} \frac{y}{16.48}}{\sinh \sqrt{\frac{5}{2}} \frac{39.08}{16.48}} \right] dy$$

$$P_R = 4.024 \int_{h_1}^{h_2} \cosh \sqrt{\frac{5}{2}} \frac{y}{16.48} dy$$

$$P_R = 4.024 \frac{16.48}{\sqrt{5}} \left[ \sinh \sqrt{\frac{5}{2}} \frac{y}{16.48} \right]_{-0.83}^{15.27} = 0.083 \text{ K/FT-WIDTH}$$

TOTAL CONVECTIVE FORCE ON A RACK =  $0.083 \text{ K} \times \frac{109}{12} = 0.752$

APPENDIX B WATER SLOSHING EFFECTS

REF.

CONCLUSIONS:

THE RESULTS OF THE DETAILED CALCILATIONS OF THE WNTER SLOSHING EFFECTS ON THE SPENT FUEL RACKS DUE TO POOL ACCELERATION BY A E/W DBE EVENT INDICATE THAT THE CENTER OF GRAVITY OF THE CONVECTIVE WATER FORCES IS 13.86 FEET ABOVE THE RACKS RESULTING IN AN INSIGNIFILANT FORBE OF 0.752 KIPS BEING APPLIED TO AN INDIVIDUAL RACK STRUCTURE. THE IMPULSIVE WATER FORCES ARE ACCOUNTED FOR BY APPLYING ADDITIONAL HYDRODYNAMIC AND TRAPPED WATER MASS TO THE STRUCTURAL WEIGHT. THEREFORE, ANY WATER SLOSHING WILL HAVE INSIGNIFICANT EFFECTS ON THE SPENT FUEL RACK STRUCTURE.

MAXIMUM IMPULSIVE WATER FORCE :

FOR N-S & E-W DBE EVENT TOTAL HORIZONTAL REACTION LOAD FOR A 10X10 RACK = 263.85 K (TABLE 8.3 OF NES REPORT 81A0610 Rev.0)

TOTAL WEIGHT OF FUEL ASSEMBLY, STORAGE CELL, POISON, TRAPPED AND HYDRODYNAMIC WATER MASS / CELL =  $\frac{10}{4} = 2.5K$

WEIGHT OF TRAPPED & HYDRODYNAMIC WATER MASS / CELL =  $\frac{2.0015}{4} = 0.5004K$

EFFECTIVE IMPACT FACTOR = 1.66

EFFECTIVE HORIZONTAL LOAD REDUCTION FACTOR FOR N-S OR E-W DBE EVENT =  $\sqrt{(1.66)^2 + 1} = 1.938$

MAX. IMPULSIVE WATER FORCE FOR N-S OR E-W DBE EVENT = HORIZONTAL REACTION LOAD DUE TO TRAPPE & HYDRODYNAMIC WATER MASS =  $\frac{263.85 \times 0.5004}{1.938 \times 2.50} = 27.25K$

I.P.2  
Design  
Note  
Book

Att.C



APPENDIX B REFERENCES

REF.

REFERENCES

- B-1 "Nuclear Reactors and Earthquakes" prepared by Lockheed Aircraft Corporation and Holmes and Narver, Inc., TID 7024; Atomic Energy Commission, Washington D.C.
- B-2 UNITED ENGINEERS & CONSTRUCTORS INC DRAWING NUMBER 7321-F-1392-6, "FUEL STORAGE BUILDING SPENT FUEL RACKS SHEET No 3"
- B-3 SPECIFICATION NO. MP79-001, CONSOLIDATED EDISON COMPANY OF NEW YORK, INC. "DESIGN, FABRICATE, DELIVER, AND INSTALLATION SPENT FUEL STORAGE RACKS".



**APPENDIX C**  
**IMPACT FACTOR**



APPENDIX-C

REF.

IMPACT FACTOR TO ACCOUNT FOR THE IMPACT  
BETWEEN FUEL ASSEMBLY AND STORAGE  
CELL

GAPS IN THE ORDER OF 0.287 INCHES ARE PROVIDED BETWEEN THE FUEL ASSEMBLY AND STORAGE CELL TO FACILITATE INSERTION AND REMOVAL OF THE FUEL ASSEMBLIES. DURING A SEISMIC EVENT, THESE GAPS ALLOW THE FUEL ASSEMBLY TO RATTLE. TO ACCOUNT FOR THE IMPACT EFFECTS OF THE FUEL ASSEMBLY RATTLING IN THE STRUCTURAL / SEISMIC ANALYSIS, THE MAXIMUM STRESSES AND REACTION LOADS DUE TO AN EARTHQUAKE ARE INCREASED BY A DYNAMIC INCREASE IMPACT FACTOR (EFFECTIVE IMPACT FACTORS). THE EFFECTIVE IMPACT FACTORS ARE CALCULATED BY APPLYING AN IMPACT FACTOR OF TWO TO THE SEISMIC INERTIA LOADS OF THE IMPACTING MASSES

APPENDIX C (CON'T)

REF.

WEIGHT OF FUEL ASSEMBLY = 1.65<sup>✓</sup>k

TOTAL WEIGHT OF FUEL ASSEMBLY, STORAGE  
CELL AND TRAPPED WATER PLUS HYDRODYNAMIC  
WATER MASS = 2.50<sup>✓</sup>k

$$\text{Impact Factor} = \frac{2(1.65) + (2.5 - 1.65)}{2.5} = 1.66^{\checkmark}$$

VERIFICATION OF THE USE OF AN IMPACT FACTOR  
OF 2.0 :

FOR A 10x16 RACK - DESIGN BASIS EARTHQUAKE EVENT;  
MAX. BASE SHEAR FROM THE LINEAR SEISMIC  
ANALYSIS (TABLE 8.3 OF THIS REPORT) = 263.85 K

MAX. HORIZONTAL FRICTIONAL FORCE (BASE SHEAR)  
FROM NON-LINEAR TIME HISTORY SEISMIC ANALYSIS  
(TABLE 8.1 OF NES REPORT 81A0615, REF. 13)  
= 170.93 K

THE NON-LINEAR TIME HISTORY ANALYSIS MODEL  
INCLUDED GAP ELEMENTS (IMPACT EFFECTS) BETWEEN  
THE FUEL ASSEMBLY AND STORAGE CELL, THE LINEAR  
SEISMIC ANALYSIS INCLUDED AN IMPACT FACTOR OF 2.0.  
THE BASE SHEAR VALUE (263.85K) FOR THE LINEAR  
SEISMIC ANALYSIS IS GREATER THAN THAT FOR THE  
NON-LINEAR TIME HISTORY SEISMIC ANALYSIS, THERE-  
FORE THE USE OF AN IMPACT FACTOR OF 2.0 IS  
CONSERVATIVE.

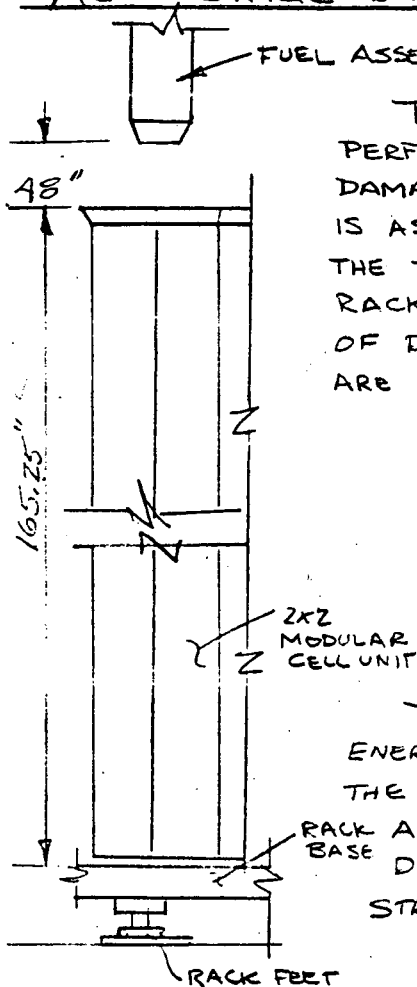


**APPENDIX D**  
**ACCIDENTAL ASSEMBLY DROP**

APPENDIX - D

REF.

ACCIDENTAL SPENT FUEL ASSEMBLY DROP ANALYSIS



THE FUEL ASSEMBLY DROP ANALYSIS HAS BEEN PERFORMED TO DETERMINE THE RESULTING STRUCTURAL DAMAGE TO THE STORAGE RACKS. THE FUEL ASSEMBLY IS ASSUMED TO FALL FROM A HEIGHT OF 48.0" ABOVE THE TOP OF THIS STORAGE RACK AND IMPACT THE RACK AT A LOCATION WHERE THE CRITICAL AMOUNT OF DAMAGE WILL RESULT. THREE FUEL DROP CASES ARE CONSIDERED.

1. STRAIGHT DROP ON TOP OF RACK
2. SUBSEQUENT TIPPING ANALYSIS
3. DROP THROUGH STORAGE CELL AND IMPACT AT STORAGE CELL BASE PLATE LOCATION

THIS ANALYSIS CONSERVATIVELY NEGLECTS THE ENERGY LOSSES IN THE LOCAL DEFORMATION OF THE SPENT FUEL ASSEMBLY WHICH RESULTS IN A MORE CONSERVATIVE ANALYSIS OF THE DAMAGE DONE TO THE STORAGE CELLS, AND RACK BASE STRUCTURE.

ELEVATION

APPENDIX - D CON'T

REF.

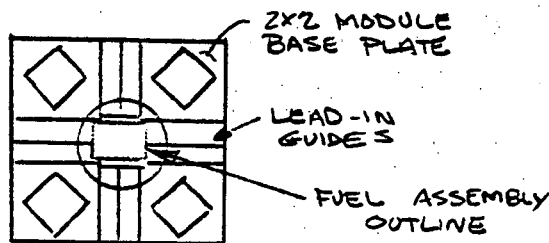
CASE #1 STRAIGHT DROP ON TOP OF RACK

ASSUMING UNIFORM STORAGE CELL COMPRESSION THE EXTERNAL KINETIC ENERGY DEVELOPED IN THE FALL = (FALL HEIGHT) X (WEIGHT OF FUEL ASSEMBLY).  
 NEGLECTING ANY BUOYANT OR DRAG FORCES ON THE FALLING ASSEMBLY -

DROP HEIGHT = 48 INCHES ✓  
 FUEL ASSEMBLY WEIGHT = 1650 LBS ✓

EXTERNAL KINETIC ENERGY =  $\frac{48 \times 1650}{1000} = 79.2 \text{ K-IN} \checkmark$

THE MAXIMUM REACTION LOADS ARE GENERATED WHEN THE FUEL ASSEMBLY IMPACTS A 2X2 MODULE AT THE INTERSECTION OF THE 4 CELLS (STIFFEST REGION OF TYPICAL 2X2). THE FUEL ASSEMBLY IS ASSUMED TO IMPACT AN AREA EQUIVALENT TO THAT OF A STORAGE CELL, TRANSMITTING AND ABSORBING THE KINETIC ENERGY GENERATED DURING THE FALL. DURING IMPACT, THE LEAD-IN GUIDES WILL COLLAPSE ABSORBING SOME PERCENTAGE OF THE EXTERNAL KINETIC ENERGY. THE STORAGE CELLS ARE EXTREMELY RIGID BECAUSE OF THEIR CONFIGURATION AND THEREFORE IS CONSERVATIVELY ASSUMED TO TRANSMIT THE REACTION LOADS INTO THE YIELDING 2X2 MODULE BASE PLATE.



2X2 CELL MODULE  
PLAN



## APPENDIX D (CON'T)

REF.

CONSERVATIVELY NEGLECT THE ENERGY LOSSES DUE TO THE LOCAL DEFORMATION OF THE FLARE AT THE TOP OF THE CELL. THE LOCAL DEFORMATION WILL REDUCE THE DAMAGE TO THE CELL; THEREFORE THERE WILL BE LESS DAMAGE TO THE STORED FUEL, AND WILL ALSO REDUCE THE DAMAGE TO THE LINER PLATE AND REINFORCED CONCRETE FLOOR UNDER THE STORAGE CELL.

### CALCULATE THE LOAD FROM IMPACT ON THE MODULE.

ASSUME AXIAL COMPRESSION OVER ONE STORAGE MODULE AREA. FIND THE FORCE BY SETTING THE INTERNAL ENERGY ABSORBED EQUAL TO THE EXTERNAL ENERGY OF THE FALLING FUEL ASSEMBLY.

$$\text{EXTERNAL KINETIC ENERGY OF FUEL ASSEMBLY} = 79.2 \text{ K-IN} \checkmark$$

INTERNAL STRAIN ENERGY OF STORAGE CELL (AT 20% STRESS INCREASE) REF. "FINAL STRUCTURAL DESIGN OF A FUEL STORAGE WELL CRASH PAD FOR THE LACBWR NUCLEAR POWER PLANT" Pg. A-18

D.1

$$E_x = \frac{116.9}{1.2} E_x^{1.20} A \cdot L \cdot N \checkmark$$

WHERE  $E_x$  = STRAIN IN STORAGE CELL  
 $A$  = CROSS-SECTIONAL AREA OF CELL MODULE = 3.26609 IN<sup>2</sup>  $\checkmark$   
 $L$  = LENGTH OF CELL MODULE = 165.25  $\checkmark$   
 $N$  = NUMBER OF CELLS = 1.0  $\checkmark$

$$E_x = E_x$$

$$E_x = \left[ \frac{1.2 E_x}{116.9 A \cdot L \cdot N} \right]^{1/1.20} = \left[ \frac{1.2 \times 79.2}{116.9 \times 3.26609 \times 165.25 \times 1.0} \right]^{1/1.20} = 0.00445 \text{ in/in.} \checkmark$$

CALCULATE % ULTIMATE STRAIN

$$\% E_u = \frac{E_x}{E_u} \times 100 = \frac{0.00445}{0.485} = 0.918\% \checkmark$$

D.1

MAX DEFORMATION OF THE CELL =  $\delta_x$

$$\delta_x = E_x L = 0.00445 \times 165.25 = 0.735 \checkmark$$

MAX STRESS IN THE CELL

$$\sigma_x = 116.9 E_x^{0.2} = 116.9 (0.00445)^{0.2} = 39.58 \text{ KSI} \checkmark$$

D.1  
Pg  
A-31

## APPENDIX D (CON'T)

REF.

USING DYNAMIC YIELD STRESS FOR STAINLESS STEEL = 1.20%  
OF YIELD = 1.2(30) = 36.0 KSI ✓ FOR 304 SS.  $F_y = 30 \text{ ksi}$

MAXIMUM TRANSMITTED REACTION LOAD

$$R_x = \sigma_x A = 39.58 \times 3.26604 = 129.27 \text{ K} \checkmark$$

### CELL BASE PLATE ANALYSIS

THE STORAGE CELL LOADS WILL BE TRANSFERRED INTO THE BASE STRUCTURE THROUGH THE BASE PLATES. THE BASE PLATE WOULD YIELD IF SUCH A LOAD WERE PLACED DIRECTLY ON IT. SINCE THE INDIVIDUAL CELL IS ONLY A PART OF A BUNDLE OF FOUR, ANY FORCE WILL BE DISTRIBUTED THROUGHOUT A MINIMUM OF FOUR CELLS. NEGLECTING ANY ENERGY LOSS DUE TO THE PLATE DEFORMATION, THE IMPACT LOAD WILL BE DISTRIBUTED INTO THE BASE GRID. FROM LOAD CASE 6A AND 6B OF COMPUTER PRINTOUT "JOB007T" THE FOLLOWING STRESSES ARE TAKEN:

$$\text{MAXIMUM PLATE STRESS} = 35.58 \text{ KSI}$$

$$\text{MAXIMUM BEAM BENDING STRESS} = 22.92 \text{ KSI}$$

THIS LOAD CASE WAS A 189 K LOAD PLACED AT THE WORST LOCATION IN ORDER TO FIND MAXIMUM STRESSES. TO FIND THE MAXIMUM STRESSES PROPORTIONAL TO THESE STRESSES.

$$\text{MAX. PLATE STRESS} = \frac{129.27}{189} \times 35.58 = 24.36 \text{ KSI}$$

$$\text{MAX. BEAM BENDING STRESS} = \frac{129.27}{189} \times 22.92 = 15.68 \text{ KSI}$$

THE MAXIMUM LOAD ON A LEG WILL BE TAKEN AS 70% OF THE 129.27 PLUS THE MAXIMUM DEAD + LIVE LOAD CASE LEG FROM COMPUTER PRINTOUT "JOB 007T" LOAD CASE #1 EQUALS 45.16 K AT NODE 2.

$$\text{MAX LEG LOAD} = 0.70 \times 129.27 + 45.16 = 135.65 \text{ K}$$

APPENDIX D (CONT)

REF.

CASE # 2 FUEL ASSEMBLY DROP AND SUBSEQUENT TIPPING

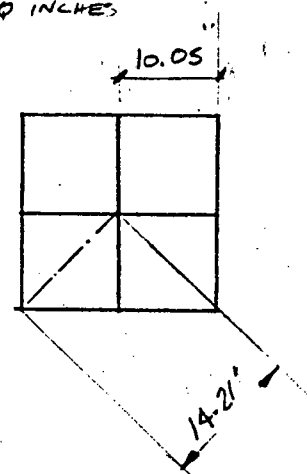
AFTER A FUEL ASSEMBLY IMPACTS THE RACK, IT WILL TIP OVER AND FALL ONTO SEVERAL ADJACENT CELLS. CONSERVATIVELY ASSUME THAT THE FUEL ASSEMBLY WILL FALL DIAGONALLY IMPACTING THE MINIMUM NUMBER OF CELLS.

LENGTH OF FUEL ASSEMBLY = 160 INCHES  
 NUMBER OF CELLS ON DIAGONAL

$$N = \frac{160}{14.21} = 11.26 > 10$$

ASSUME 10 CELLS MAX. ARE IMPACTED THEREFORE  $\frac{1}{10}$  OF FUEL ASSEMBLY IMPACTS THE 10<sup>TH</sup> CELL

$$KE = \frac{165}{10} \left[ 160 \cdot \frac{160}{10 \times 2} \right] = 2508 \text{ KIN}$$



SINCE THE KINETIC ENERGY PER CELL (25.08 KIN) IS LESS THAN THE KINETIC ENERGY GENERATED IN THE STRAIGHT DROP (79.2 K-IN). THE STRUCTURAL DAMAGE WILL BE LESS SEVERE THAN THE FUEL ASSEMBLY DROP SEE CASE # 1.

APPENDIX D (CONT)

REF.

CASE # 3 STRAIGHT DROP THROUGH A STORAGE CELL  
AND IMPACT A STORAGE CELL BASE PLATE

THE FUEL ASSEMBLY IS ASSUMED TO FALL FROM A HEIGHT 4 FEET ABOVE THE STORAGE RACK, ENTER INTO A SINGLE STORAGE LOCATION AND CONTINUE DOWN THROUGH THE STORAGE CELL IMPACTING THE STORAGE CELL BASE PLATE. THE ANALYSIS CONSERVATIVELY NEGLECTS ANY DRAG OR BUOYANT FORCES ACTING ON THE ASSEMBLY.

MAXIMUM KINETIC ENERGY AT IMPACT =  $1.65(48 + 165.25)$   
 =  $351.86 \text{ K-IN}$

MAXIMUM IMPACT VELOCITY =  $\sqrt{2gh}$

=  $\sqrt{2 \times 32.17 \times \frac{48 + 165.25}{12}} = 33.81 \text{ FT/SEC}$

THE FUEL ASSEMBLY IS ASSUMED TO ACT AS A MISSILE STRIKING THE STAINLESS STEEL BASE PLATE. THE THICKNESS OF PLATE THAT A MISSILE, REPRESENTED BY THE FUEL ASSEMBLY, CAN JUST PERFORATE IS CALCULATED USING THE BALLISTIC RESEARCH LABORATORY (BRL) EQUATION GIVEN IN REFERENCE D.2

$T = \left( \frac{M V_s^2}{2 \cdot 672 D} \right)^{2/3}$

WHERE:  $M = \text{MASS OF THE MISSILE} = \frac{1650}{32.17} = 51.29 \frac{\text{LB} \cdot \text{SEC}^2}{\text{FT}}$

$T = \text{THICKNESS JUST PERFORATED (IN)}$

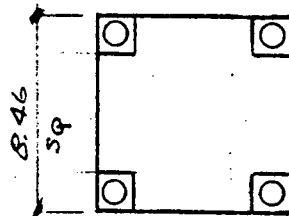
$V_s = \text{STRIKING VELOCITY (33.81 FT/SEC)}$

$D = \text{DIAMETER OF MISSILE}$

CHANGING AREA INTO EQUIVALENT DIAMETER CIRCLE

$A = 4 \times \left[ 1.5^2 - \pi \frac{0.875^2}{4} \right] = 6.59 \text{ IN}^2$

$D = \sqrt{\frac{4A}{\pi}} = 2.90 \text{ IN}$



APPENDIX D (CONT)

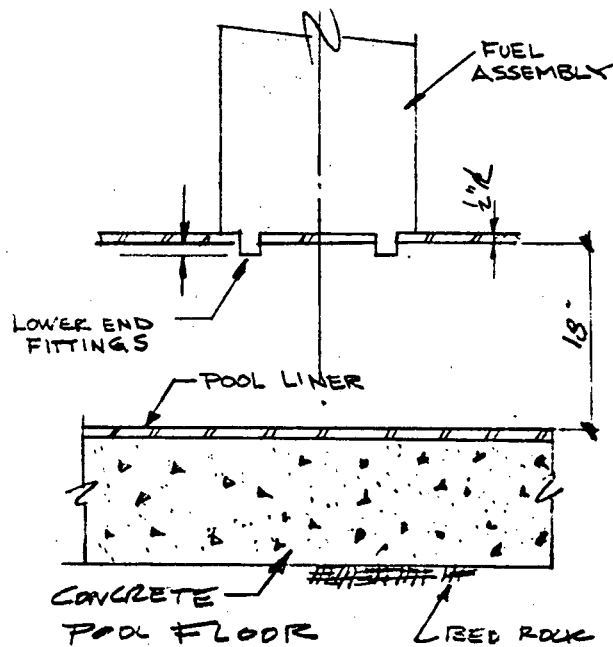
REF.

$$\text{THICKNESS} = T = \frac{[51.29 \times 33.81^2]}{2}^{2/3} = 0.489 \text{ IN}$$

672 x 290

RECOMMENDED THICKNESS TO PREVENT PENETRATION = 1.25 T = 1.25 x 0.489 = 0.6113 IN

CONCLUSION THE FUEL ASSEMBLY WILL PENETRATE THE 1/2" STORAGE CELL BASE PLATE. ABSORBING A CONSIDERABLE AMOUNT OF THE DROP ENERGY. THE FUEL CELL WILL STOP TO PENETRATE AT THE RETENTION GRID. SINCE THE BASE PLATE IS LOCATED ABOUT 18 INCHES ABOVE THE POOL LINER AND THE END FITTINGS ONLY PROTRUDE 1 1/2" BELOW THE RETENTION GRID, THE POOL LINER WILL NOT BE DAMAGED. SEE SKETCH BELOW.



## APPENDIX D (CONT)

REF.

THE MAXIMUM REACTION LOAD GENERATED BY THE FUEL ASSEMBLY IMPACT WILL BE ESTIMATED BY CALCULATING THE COLLAPSE LOAD FOR A SQUARE PLATE FIXED AT ALL FOUR EDGES. SINCE THE ACTUAL BASE IS WELDED TO THE BASE BEAM SOME STIFFNESS WILL BE DEVELOPED THRU FLANGE BENDING. BOTH THICKNESS WILL BE USED IN THE CALCULATION, THUS INCREASING THE LEG REACTION.

THE COLLAPSE LOAD MECHANISM FOR A SQUARE PLATE USING AN ANALYTICAL APPROACH IS GIVEN ON PAGE 21 OF REF. #D.3

$$\text{THE COLLAPSE LOAD } P_c = 6.28(M+m) \quad \checkmark$$

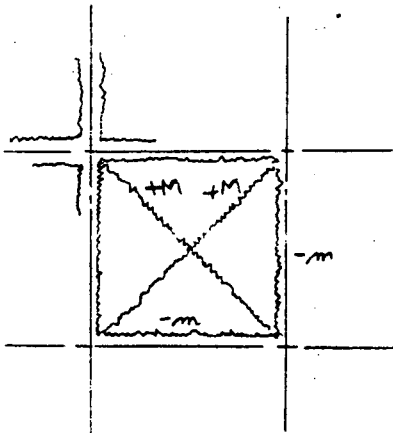
WHERE  $M$  = THE POSITIVE MOMENT CARRYING CAPACITY OF THE PLATE PER UNIT LENGTH

$$M = \frac{1 \times t^2}{6} \sigma_y =$$

$$t = 0.375 + 0.5 = 0.875 \quad \checkmark$$

$m$  = THE NEGATIVE MOMENT CARRYING CAPACITY OF THE PLATE PER UNIT LENGTH.

$$m = \frac{1 \times 0.875^2}{6} \times 1.2 \times 30 = 4.59 \frac{\text{K-IN}}{\text{IN}}$$



THE YIELD STRESS WILL BE INCREASED BY 20% TO ACCOUNT FOR THE DYNAMIC YIELD  $1.2 \times 30 = 36 \text{ KSC}$

THEREFORE, THE MAXIMUM LOAD THAT CAN BE GENERATED DURING THE FUEL ASSEMBLY DROP EVENT IS :

$$\text{Collapse Load } - P = 6.28(M+m)$$

$$P = 6.28(4.59 + 4.59) = 57.65 \text{ K} \quad \checkmark$$

$$\text{MAX TRANSMITTED REACTION} = 57.65 \text{ K} \quad \checkmark$$

APPENDIX-D (CONT)

REF.

THE REACTION LOAD OF 57.65<sup>k</sup> GENERATED DURING THE FUEL ASSEMBLY DROP THROUGH THE CELL AND IMPACT ONTO THE BASE PLATE IS LOWER THAN THAT FOR CASE #1 (PAGE D-3). IT CAN BE CONCLUDED THAT THE EFFECTS ON THE RACK BASE, SUB-BASE MEMBERS, AND RACK SUPPORT LEGS WILL BE LESS SEVERE FOR THE FUEL ASSEMBLY DROP CASE #3 THAN CASE #1 EVEN THOUGH LOCAL DEFORMATION OF THE BASE PLATE WILL BE GREATER.

APPENDIX D (CONT)

REF.

USING MAXIMUM LOAD FROM CASE #1

CALCULATE MAX. STRESS ON POOL LINER AND CONCRETE FLOOR

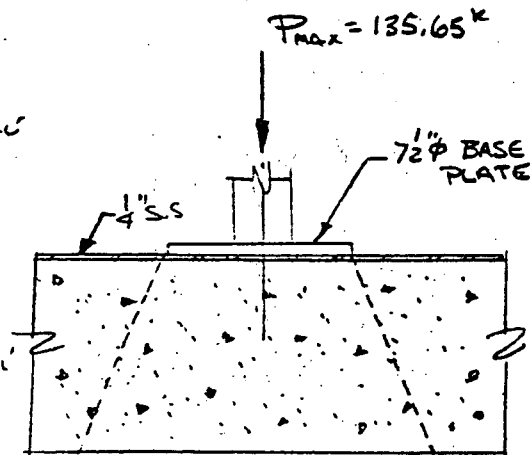
CHECK BEARING STRESS ON CONCRETE

$$A_p = \frac{\pi D^2}{4} = \frac{\pi (7\frac{1}{2} + \frac{1}{2})^2}{4} = 50.27 \text{ IN}^2$$

$$\text{BEARING STRESS} = \frac{P}{A} = \frac{135.65}{50.27} = 2.70 \text{ KSI}$$

ALLOWABLE BEARING STRESS =  $2 \times .85 \phi f'_c$   
ACI 318-77 SEC 10.16

$$2 \times .85 \times 7 \times 3.0 = 3.57 \text{ KSI} > 2.70 \text{ KSI}$$



CHECK PUNCHING SHEAR OF POOL LINER

$$\text{SHEAR AREA} = \pi D t = \pi (7.5) \times (\frac{1}{4}) = 5.89 \text{ IN}^2$$

$$\text{SHEAR STRESS } f_v = \frac{P}{A} = \frac{135.65}{5.89} = 23.03 \text{ KSI}$$

$$\text{ALLOWABLE STRESS} = 1.2 \times 30 \text{ KSI} = 36 \text{ KSI} \text{ DYNAMIC YIELD STRESS}$$

CONCLUSIONS

1. ACCIDENTAL DROP OF THE FUEL ASSEMBLY ON THE FUEL STORAGE CELL WILL CAUSE THE FOLLOWING.

A. THERE WILL BE LOCAL DEFORMATION AT THE TOP OF THE STORAGE CELLS THROUGH LOCAL BUCKLING AND CRUSHING. BUT THE INTEGRITY OF THE RACK BASE SYSTEM WILL NOT BE DAMAGED.

B. THE LINER PLATE WILL NOT BE PERFORATED, THEREFORE THE LEAK TIGHT INTEGRITY OF THE POOL FLOOR WILL BE MAINTAINED.

APPENDIX D (CONT)

REF.

REFERENCES:

D.1 NUCLEAR ENERGY SERVICES INC.; "FINAL STRUCTURAL DESIGN OF A FUEL STORAGE WELL CRASH PAD FOR LACBWR NUCLEAR POWER PLANT, DOCUMENT NES 81A0426. REV. 1, MARCH 31, 1976.

D.2 LINDERMAN R.B., ROTZ, J.V. AND YE H G, C.K.; "DESIGN OF STRUCTURES FOR MISSILE IMPACT," BECHTEL POWER CORPORATION, BC-TOP-9A-REV. 2, SEPT 1974.

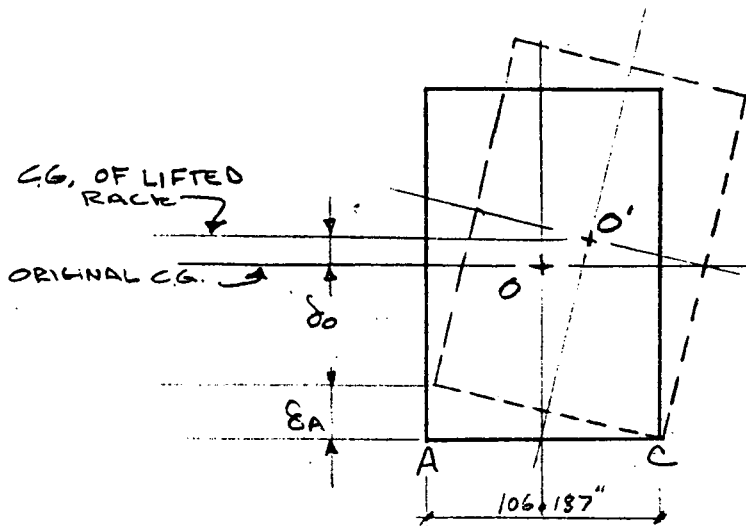
D.3 WOOD, R. H. - "PLASTIC AND ELASTIC DESIGN OF SLABS AND PLATES," THE RONALD PRESS COMPANY, N.Y. N.Y.



**APPENDIX E**  
**STABILITY ANALYSIS**

APPENDIX E STABILITY ANALYSIS

REF.



DURING A SEISMIC EVENT, HORIZONTAL SEISMIC INERTIA AND IMPACT LOADS WILL TEND TO TIP THE STORAGE RACK ABOUT POINT C (RACK FEET). THE DEAD WEIGHT OF THE STORAGE RACK WILL RESIST THE TIPPING OF THE RACK. IF THE OVERTURNING MOMENT DUE TO HORIZONTAL SEISMIC INERTIA LOADS IS GREATER THAN THE STABILIZING MOMENT DUE TO THE DEAD WEIGHT OF THE STORAGE RACK; THE ORIGINAL CENTER OF GRAVITY (O) OF THE STORAGE RACK WILL BE LIFTED UP BY AN AMOUNT  $\delta_0$ . THE MAXIMUM UPLIFT OF THE CENTER OF GRAVITY AND END "A" OF THE RACK CAN BE ESTIMATED BY EQUATING THE EXTERNAL KINETIC ENERGY OF THE STORAGE RACK TO THE POTENTIAL ENERGY REQUIRED TO RAISE THE CENTER OF GRAVITY OF THE RACK TO O'.

FROM COMPUTER PROGRAM OUTPUT "NYSAVAW" WHICH GIVES THE RESULTS OF THE SLIDING ANALYSIS WITH A HIGH COEFFICIENT OF FRICTION  $\mu=1.5$  THE FOLLOWING CAN BE FOUND.

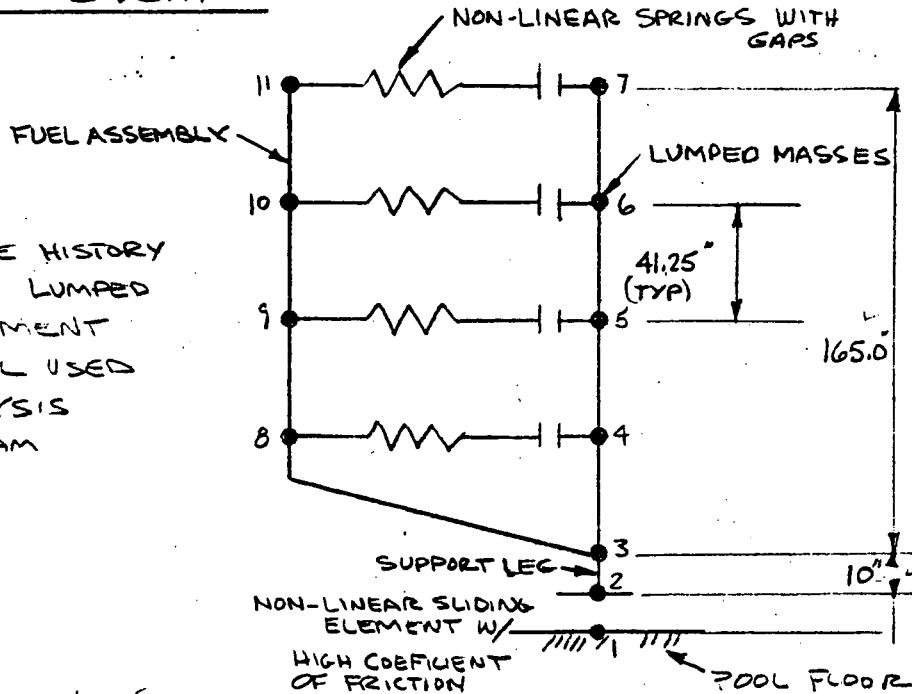
1. THE MAXIMUM OVERTURNING MOMENT OCCURS @  
 TIME 9.79 SECONDS ON THE TIME HISTORY  
 $M_2 = 15,014.9 \text{ IN-K}$
2. THE VELOCITY OF THE 11 NODES BY TAKING THE  
 REL. DISPLACEMENT / TIME STEP
3. THE MASSES OF THE 11 NODES

**APPENDIX E STABILITY ANALYSIS**

REF.

FOR THE DBE EVENT

NON-LINEAR TIME HISTORY  
SEISMIC ANALYSIS LUMPED  
MASS FINITE ELEMENT  
NON-LINEAR MODEL USED  
IN SLIDING ANALYSIS  
COMPUTER PROGRAM  
"NYSAAVAV"



MASSES ( $\frac{lb \cdot sec^2}{IN}$ )	* (RELATIVE) MAX. VELOCITIES	KINETIC ENERGY = $\frac{1}{2}mv^2$
$m_1 = 0$	-	-
$m_2 = 0$	-	-
$m_3 = 91.23$	0.18	1.48
$m_4 = 54.94$	1.14	35.70
$m_5 = 54.94$	3.09	262.29
$m_6 = 54.94$	5.18	737.09
$m_7 = 27.50$	7.14	754.99
$m_8 = 106.75$	1.23	80.75
$m_9 = 106.75$	6.56	2296.92
$m_{10} = 106.75$	14.69	11518.12
$m_{11} = 53.38$	23.83	15220.09
		<u>15220.09</u>

KE = 30,967.43 <sup>10-#</sup>

THE MAXIMUM KINETIC ENERGY IS FOUND TO OCCUR AT TIME 9.89 SECONDS.

\* RELATIVE VELOCITIES WERE CALCULATED FROM RELATIVE DISPLACEMENTS ON MISL. CALC. SHEETS FOLLOWING REGULAR SHEETS. ALL DISPLACEMENTS WERE TAKEN FROM COMPUTER PRINTOUT "NYSAAVAV"

Design  
Note-  
Book

## APPENDIX E STABILITY ANALYSIS

REF.

TOTAL VERTICAL WEIGHT FROM DYNRE 4 COMPUTER PRINTOUT "TALAYPK" & "TALAYBT"

TOTAL WEIGHT = 204.77 ✓

\* AVERAGE VERTICAL ACCELERATION =  $0.0726g$  ✓  
(SEE MISC. CALC.)

∴ MAX. STABILIZING MOMENT =  $ma \frac{d}{2}$

$$M_s = \frac{204.77}{2g} (1 - 0.0726) \frac{g}{g} \times 106.185 \text{ IN-K}$$

$$M_s = 10,082.46 \text{ IN-K} ✓$$

SINCE THE STABILIZING MOMENT (10,082.46<sup>IN-K</sup>) IS LESS THAN THE OVERTURNING MOMENT (15,014.9<sup>IN-K</sup>), THE STORAGE RACK WILL LIFT UP DURING A DBE. EVENT. THE MAXIMUM AMOUNT OF LIFT UP CAN BE ESTIMATED BY EQUATING THE KINETIC ENERGY TO POTENTIAL ENERGY REQUIRED TO LIFT UP THE C.G. OF THE RACK.

$$\text{POTENTIAL ENERGY} \cdot P.E = 204.77 (1 - \frac{0.0726}{\sqrt{2}}) g_0 = 194.26 g_0$$

THE VERTICAL ACCELERATION OF 0.0726G WAS REDUCED BY A FACTOR OF  $\frac{1}{\sqrt{2}}$  TO ACCOUNT FOR SRSS (SQUARE ROOT OF THE SUM OF SQUARES) COMBINATION OF THE THREE SPATIAL COMPONENT OF THE EARTHQUAKE.

SETTING P.E. = K.E.

$$194.26 g_0 = 30.907 \text{ IN-K} ✓$$

$$g_0 = 0.1591 \text{ IN} ✓$$

$$\text{MAX. LIFT UP} = g_a = 2g_0 = 2 \times 0.1591 = 0.3182 \text{ IN} ✓$$

THE EDGE OF THE RACK WILL LIFT UP 0.3182 INCHES AND THEN DROP BACK, SINCE THE C.G. OF THE TILTED RACK WILL REMAIN WITHIN AC. THE RACK STRUCTURE WILL NOT OVERTURN.

\* AVERAGE VERTICAL ACCELERATION WAS CALCULATED ON MISC. CALC. SHEETS. FOLLOWING REGULAR CALC. THE VERTICAL ACCELERATION FOR ALL THE BASE NODES WAS TAKEN FROM THE COMPUTER OUTPUT "TALAYPK" AND DIVIDED BY THE NUMBER OF NODES. (SEE MISC. CALC.)

Design  
Note-  
Book

APPENDIX E STABILITY ANALYSIS

REF.

ANALYSIS FOR IMPACT LOADS AND STRESSES IN THE RACK  
STRUCTURE RESULTING FROM RECONTACT OF THE POOL FLOOR

DURING RECONTACT, THE EXTERNAL ENERGY WILL BE ABSORBED IN THE DEFORMATIONS OF VARIOUS RESISTING ELEMENTS ESSENTIALLY ACTING IN SERIES THRU THE PROCESS OF LOCAL, AXIAL, FLEXURAL AND SHEAR DEFORMATIONS. THE RESISTING ELEMENTS CONSIST OF THE STORAGE CELL BASE PLATE, RACK BASE BEAMS, RACK FEET, POOL FLOOR LINER PLATE AND CONCRETE UNDER THE IMPACTED LINER PLATE. THE LOAD DEFORMATION CHARACTERISTICS OF THE SERIES COMBINATION OF RESISTING ELEMENTS CAN BE EVALUATED BY DETERMINING THE LOAD DEFORMATION CHARACTERISTICS OF THE INDIVIDUAL ELEMENTS. ELEMENTS WITH LOW LOAD CARRYING CAPACITIES WILL BE DEFORMED FIRST AND WILL ABSORB A GREATER PART OF THE EXTERNAL ENERGY, THE REMAINDER OF THE EXTERNAL ENERGY WILL BE ABSORBED IN THE DEFORMATION OF OTHER STIFFER ELEMENTS. CONSERVATIVELY NEGLECTING THE ENERGY ABSORBED IN THE LOCAL DEFORMATION OF THE LINER PLATE AND CONCRETE UNDER THE RACK FEET, ANALYSIS INDICATES THAT THE CELL BASE PLATES BEING THE WEAKEST ELEMENTS WILL ABSORB THE LARGEST PORTION OF THE EXTERNAL ENERGY. THE REMAINDER OF THE ENERGY WILL BE ABSORBED BY THE RACK BASE STRUCTURE.

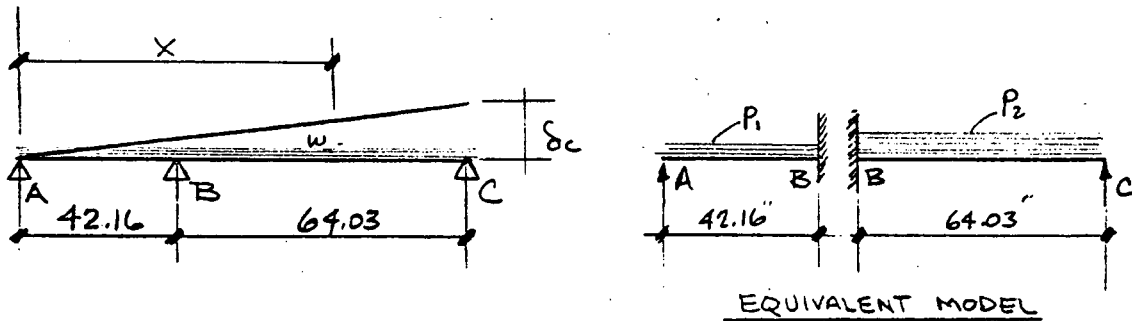
DURING RECONTACT THE CELL BASE PLATE UNDER EACH 2x2 MODULE WILL DEFORM AS A SQUARE PLATE FIXED AT ITS FOUR EDGES. THE RACK BASE SQUARE WILL RESPOND AS A CONTINUOUS BEAM SUPPORTED BY THE RACK FEET DUE TO DIFFERENCES IN THE TWO SPANS OF THE CONTINUOUS BEAM, TWO CASES AS SHOWN BELOW HAVE BEEN EVALUATED.



APPENDIX E STABILITY ANALYSIS

REF.

CASE I RACK LIFTING UP AT END C



ENERGY ASSOCIATED WITH LIFTING THE WEIGHT IN THE TWO SPANS AB AND BC ARE DIFFERENT, THEREFORE DURING RE-CONTACT THE EQUIVALENT VERTICAL LOADS DEVELOPED IN THESE SPANS WILL BE DIFFERENT. LARGER VERTICAL LOAD AND MOMENT WILL BE GENERATED IN SPAN BC THAN SPAN AB. THE TWO SPANS THEREFORE CAN BE ANALYZED AS TWO SEPARATE BEAMS FIXED AT THE MID SUPPORT POINT (B).

EXTERNAL ENERGY ASSOCIATED WITH SPAN AB AND BC CAN BE CALCULATED AS FOLLOWS.

$$\delta_x = \frac{\delta_c}{(42.16 + 64.03)} (x)$$

THE ENERGY ASSOCIATED WITH LIFTING A WEIGHT OF  $w dx$  THROUGH A HEIGHT  $\delta_x$  IS GIVEN BY

$$e_x = w dx \delta_x = \frac{w \delta_c}{106.19} x dx$$

∴ TOTAL ENERGY OF LIFTING

$$\begin{aligned} P. E. &= \int_0^L e_x = \int_0^L \frac{w \delta_c}{106.19} x dx \\ &= \frac{w \delta_c}{106.19} \left[ \frac{x^2}{2} \right]_0^L \\ &= \frac{w \delta_c L^2}{106.19 \times 2} = \frac{w \delta_c 106.19}{2} \end{aligned}$$

## APPENDIX E STABILITY ANALYSIS

REF.

WHERE  $W$  = UNIFORMLY DISTRIBUTED VERTICAL WEIGHT OF THE RACK =  $\frac{204.77 \times (1 - \frac{0.0726}{\sqrt{2}})}{106.19}$  ✓

UNIFORM WEIGHT -  $W = 1.829$  W/IN ✓

EQUATING EXTERNAL KINETIC ENERGY TO POTENTIAL ENERGY

$$KE = 30.907 \text{ IN} \cdot \text{K} = P.E = W \delta_c \frac{106.19}{2} = \frac{1.829 \times 106.19 \delta_c}{2}$$

$$\delta_c = 0.3183 \text{ IN} \quad \text{O.K.} \quad \checkmark$$

THE ENERGY ASSOCIATED WITH BEAM SPAN  $\overline{AB}$

$$E_1 = \left[ \frac{W \delta_c}{106.19} \times \frac{1}{2} x^2 \right]_0^{42.16} \quad \checkmark$$

$$E_1 = \frac{1.829 \times 0.3183}{106.19} \times \frac{1}{2} \times (42.16)^2$$

ENERGY  $E_1 = 4.87 \text{ IN} \cdot \text{K}$  ✓

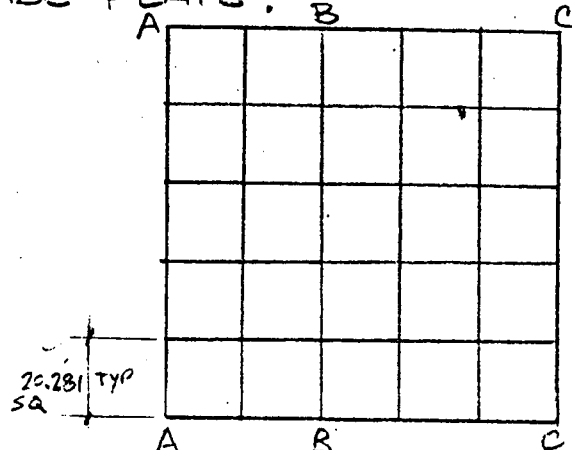
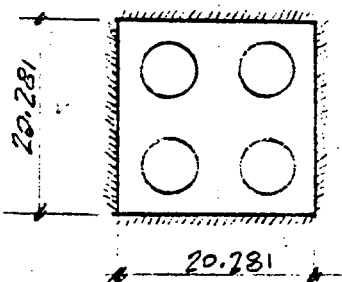
THE ENERGY ASSOCIATED WITH BEAM SPAN  $\overline{BC}$

$$E_2 = \left[ \frac{W \delta_c}{106.19} \times \frac{x^2}{2} \right]_{42.16}^{106.19}$$

$$= \frac{1.829 \times 0.3183}{106.19 \times 2} (106.19^2 - 42.16^2)$$

ENERGY  $E_2 = 26.04 \text{ IN} \cdot \text{K}$  ✓

LOAD DEFORMATION CHARACTERISTICS OF THE CELL BASE PLATE:



**APPENDIX E STABILITY ANALYSIS**

REF.

A 10X10 STORAGE RACK CONSISTS OF 25 CELL BASE PLATES (ONE UNDER EACH 2X2 MODULE). THE CELL BASE PLATE IS  $\approx 20.3$  IN X  $20.3$  IN X  $\frac{1}{2}$ " THICK WITH 4- $5\frac{1}{2}$ " DIAMETER HOLES. THE EFFECTIVE THICKNESS OF THE CELL BASE PLATE IS CALCULATED BELOW:

$$VOLUME = \frac{1}{2} [ 20.281^2 - 4 \pi \frac{(5.5)^2}{4} ] = 158.19 \text{ IN}^3$$

$$t_{eff} = \frac{158.19}{20.281^2} = 0.3845 \text{ IN THICK}$$

CONSIDERING FIXED END BOUNDARY CONDITION, THE MAXIMUM DEFLECTION AND STRESSES IN THE PLATE FOR A UNIFORMLY DISTRIBUTED LOAD IS GIVEN IN TABLE X "FORMULAS FOR STRESS AND STRAIN" BY R.J. ROARK, 4TH EDITION, MCGRAW HILL BOOK Co. (P225) (REF E-1)

E-1

MAX. DEFLECTION  $y = \frac{0.0138 W a^4}{E t_e^3}$  ✓

MAX. STRESS @ CENTER OF EACH EDGE =

$$S_a = \frac{0.308 W a^2}{t_e^2}$$
 ✓

MAX STRESS @ CENTER =

$$S_o = \frac{6 w (m+1) a^2}{47 m t_e^2}$$
 ✓

WHERE  $W$  = UNIFORMLY DISTRIBUTED LOAD  $\text{K/sg.in}$

$$m = \frac{1}{\nu} = \frac{1}{0.3} = 3.333$$
 ✓

$$a = 20.281$$
 ✓

$$t_e = \text{EFFECTIVE THICKNESS} = 0.3845 \text{ IN}$$

$$t = \text{THICKNESS OF PLATE AT ENDS} = 0.50 \text{ IN}$$

$$E = 28,000 \text{ KSI}$$
 ✓

SINCE THE DEFLECTION WILL VARY FROM 0.0 AT THE ENDS OF THE PLATE TO MAXIMUM IN THE CENTER, ASSUME THAT THE INTERNAL STRAIN ENERGY IS EQUAL TO THE TOTAL LOAD  $W a^2$  UNDERGOING AN AVERAGE DEFLECTION OF  $\frac{Y}{2}$

## APPENDIX E STABILITY ANALYSIS

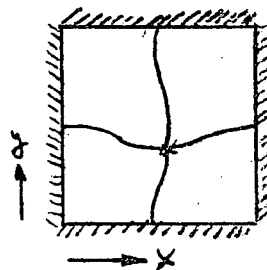
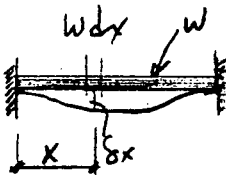
REF.

THE INTERNAL STRAIN ENERGY IN THE PLATE =  $W a^2 \times \frac{Y}{2}$

$$E_{PL} = \frac{W a^2 (0.0138) W a^4}{2 E (t_e)^3}$$

$$E_{PL} = \frac{0.0069 W^2 a^6}{E (t_e)^3}$$

THIS EQUATION COULD BE FURTHER VERIFIED USING THE FOLLOWING PROCEDURE



FOR A FIXED END BEAM DEFLECTION  $\delta_x$  AT DISTANCE  $x$  IS GIVEN BY

$$\delta_x = \frac{W x^2}{24 E I} (a-x)^2$$

A SQUARE PLATE FIXED AT ALL EDGES IS TWICE AS STIFF AS A FIXED END BEAM.

$$\therefore \delta_{xPL} = \frac{\delta_x}{2} = \frac{W x^2 (a-x)^2}{2 \times 24 E I}$$

$$\text{WHERE } I = \frac{1 \times t_e^3}{12}$$

$$\therefore \delta_{xPL} = \frac{W x^2 (a-x)^2}{4 E t_e^3}$$

$$\therefore \text{INTERNAL STRAIN ENERGY } e_x = W dx \delta_{xPL}$$

$$= \frac{W dx W x^2 (a-x)^2}{4 E t_e^3}$$

E-2  
Pg 2-203



## APPENDIX E STABILITY ANALYSIS

REF.

$$\therefore \text{TOTAL STRAIN ENERGY} = E_{pl} \int_0^a \int_0^a \frac{w dx w x^2 (a-x)^2 dy}{4E t_e^3}$$

$$E_{pl} = \frac{w^2}{4E t_e^3} \int_0^a \int_0^a (a^2 + x^2 - 2ax) x^2 dx dy$$

$$E_{pl} = \frac{w^2}{4E t_e^3} \int_0^a \left[ \frac{a^2 x^3}{3} + \frac{x^5}{5} - \frac{2ax^4}{4} \right]_0^a dy$$

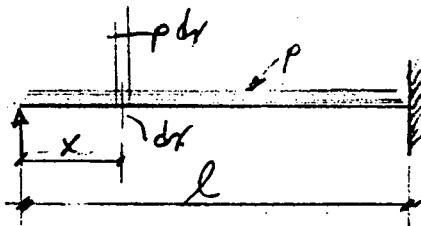
$$E_{pl} = \frac{w^2}{4E t_e^3} \int_0^a \frac{a^5}{30} dy$$

$$E_{pl} = \frac{w^2 a^5}{120 E t_e^3} (a) = \frac{w^2 a^6}{120 E t_e^3}$$

$$E_{pl} = \frac{0.00833 w^2 a^6}{E t_e^3} \checkmark \approx \frac{0.0069 w^2 a^6}{E t_e^3}$$

THE DEFORMATION CHARACTERISTICS OF RACK BASE STRUCTURE :

THE RACK BASE STRUCTURE CAN BE TAKEN AS TWO SEPARATE BEAMS, SUPPORTED AT ONE END AND FIXED AT THE OTHER END.



$$\text{DEFLECTION } \Delta x = \frac{p x}{48EI} (l^3 - 3lx^2 + 2x^3)$$

$$\text{ENERGY } \Delta x = p dx \Delta x = \frac{p p x}{48EI} (l^3 - 3lx^2 + 2x^3) dx$$

E-2  
Pg 2-201

APPENDIX E STABILITY ANALYSIS

REF.

$$\begin{aligned} \therefore E_{beam} &= \int_0^L e_x \\ &= \int_0^L \frac{p^2}{48EI_b} (lx^3 - 3lx^3 + 2x^4) dx \\ &= \frac{p^2}{48EI_b} \left[ lx^3 \frac{x^2}{2} - \frac{3lx^4}{4} + \frac{2x^5}{5} \right]_0^L \\ &= \frac{p^2}{48EI_b} \left[ \frac{3l^5}{20} \right] = \frac{p^2 l^5}{320EI_b} \checkmark \end{aligned}$$

WHERE  $E_{BEAM}$  = STRAIN ENERGY IN BEAMS

$l$  = BEAM SPAN

$I_b$  = MOMENT OF INERTIA OF THE BEAMS

(2 BOX BEAMS AND 4 WIDE FLANGE BEAMS)

$$I_b = 2 \times 79.29 + 4 \times 61.022 = 402.568 \text{ in}^4$$

$$I_b = 402.568 \text{ in}^4 \checkmark$$

$p$  = TRIBUTORY LOADS ON THE BEAMS

$$p_{AB} = 5 W_{AB} a \text{ (K/IN)} \checkmark$$

$$p_{BC} = 5 W_{BC} a \text{ (K/IN)} \checkmark$$

FOR SPAN AB

$$\text{EXTERNAL ENERGY} = E_1 = 4.87 \text{ in-k} \text{ (FROM PAGE E-6)}$$

$$l = 42.16 \text{ inches}$$

TOTAL NO. OF EFFECTIVE CELL BASE PLATES = 10

INTERNAL STRAIN ENERGY IN 10 CELL BASE PLATES =  $10 E_{pl}$

$$E_{pl} = \frac{10 \times 0.00833 W^2 a^6}{E l^3}$$

$$= \frac{0.0833 W^2 (20.731)^6}{28000 \times (0.3945)^3}$$

$$E_{pl} = 3641.95 W_{AB}^2 \text{ in-k} \checkmark$$

DESIGN  
NOTEBOOK

## APPENDIX E STABILITY ANALYSIS

REF.

### INTERNAL STRAIN ENERGY IN THE RACK BASE BEAMS

$$\begin{aligned}
 E_{i_b} &= \frac{p^2 L^5}{320 EI_b} \\
 &= \frac{(5W_{AB})^2 \times (42.16)^5}{320 \times 28000 \times 402.568} \\
 &= \frac{(5W_{AB} \times 20.281)^2 \times (42.16)^5}{320 \times 28000 \times 402.568} = 379.73 W_{AB}^2 \text{ in-in}
 \end{aligned}$$

EQUATING EXTERNAL ENERGY TO INTERNAL STRAIN ENERGY

$$E_1 = 4.87 W_{AB}^2 = 3641.95 W_{AB}^2 + 379.73 W_{AB}^2$$

PRESSURE LOAD =  $W_{AB} = 0.0348 \text{ } \frac{\text{L}}{\text{IN}^2}$

TOTAL LOAD GENERATED IN SPAN  $\overline{AB} = 10(20.281)^2 \times 0.0348$

TOTAL LOAD  $P_{AB} = 143.14 \text{ K}$

MAX STRESS IN THE BASE PLATE AT THE CENTER OF EACH EDGE

SEE PAGE E-15  $\rightarrow$

$$S_0 = \frac{0.308 W_{AB} L^2}{t^2} = \frac{0.308 (0.0348) (20.281)^2}{0.5^2}$$

MAX STRESS AT CENTER  $S_0 = \frac{0.0348}{0.0679} \times 32.27 = 16.07 \text{ KSI} < 1.2 \times 30 = 36 \text{ KSI}$

MAX BENDING MOMENT IN BEAM AB  $\checkmark = 36 \text{ KSI}$

$$\begin{aligned}
 &= \frac{pL^2}{8} = \frac{5 W_{AB} (42.16)^2}{8} \\
 &= \frac{5 \times 0.0348 \times 20.281 (42.16)^2}{8}
 \end{aligned}$$

$M_b = 784.06 \text{ in-in}$

### SECTION MODULUS OF BASE BEAMS

$$\begin{aligned}
 S_b &= 2 \times \frac{79.29}{4.69} + 4 \times \frac{61.022}{4.521} \\
 S_b &= 87.73 \text{ in}^3
 \end{aligned}$$

MAX BENDING STRESS =  $\frac{M}{S} = \frac{784.06}{87.73} = 8.93 \text{ KSI OK}$

DESIGN NOTEBOOK

**APPENDIX E STABILITY ANALYSIS**

REF.

FOR SPAN BC

EXTERNAL ENERGY  $E_2 = 26.04 W^2$  (FROM PAGE 6)  
 $l = 64.03$

TOTAL NO OF EFFECTIVE CELL BASE = 15

INTERNAL STRAIN ENERGY IN 15 CELL BASE =  $15 E_{pl}$

$$15 E_{pl} = \frac{15 (0.00833) W^2 (l)^6}{E \times l^3}$$

$$E_{pl} = \frac{15 \times 0.00833 W^2 (20.281)^6}{28000 \times (0.3845)^3}$$

$$E_{1pl} = 5443.25 W^2 \text{ IN}\cdot\text{IN}$$

INTERNAL STRAIN ENERGY IN THE RACK BASE BEAMS

$$E_{1b} = \frac{p^2 l^5}{320 E I b} = \frac{(5W 20.281)^2 (64.03)^5}{320 \times 28000 \times 402.568}$$

$$E_{1b} = 3068.24 W^2$$

EQUATING EXTERNAL ENERGY TO INTERNAL ENERGY

$$E_2 = 26.04 = 5443.25 W^2 + 3068.24 W^2$$

PRESSURE LOAD  $W_{BC} = 0.0553 \text{ K/IN}^2$

TOTAL LOAD GENERATED IN SPAN BC =  $0.0553 \times 15 (20.281)^2$

TOTAL LOAD  $P_{BC} = 341.19 \text{ K}$

MAX. STRESS IN THE BASE PLATE AT CENTER OF EACH EDGE =

$$S_a = \frac{0.308 (0.0553) (20.281)^2}{.5^2} \quad F_y = 30 \text{ KSI}$$

$$S_a = 28.02 \text{ KSI} < 1.2 \times 30 = 36 \text{ KSI}$$

OK

THE DYNAMIC YIELD STRESS IS 20% GREATER THAN THE STATIC YIELD.

APPENDIX E STABILITY ANALYSIS

REF.

$$\text{MAX STRESS @ CENTER OF PLATE} = \frac{6W(m+1)a^2}{47m(t_e)^2}$$

$$S_o = \frac{6 \times 0.0553 \left(\frac{1}{0.3} + 1\right) 20.281^2}{47 \left(\frac{1}{0.3}\right) (0.3895)^2}$$

$$S_o = 25.53 \text{ KSL} < 1.2 \times 30 = 36 \text{ KSL}$$

OK

MAX BENDING MOMENT IN BEAM BC

$$M_b = \frac{Pl^2}{8} = \frac{5 \times 0.0553 \times 20.281 (64.03)^2}{8}$$

$$M_b = 2873.83 \text{ in-k} \checkmark$$

$$\text{MAX BENDING STRESS IN BASE BEAMS} = \frac{2873.83}{87.78} = 32.74 \text{ KSL} < 1.2 \times 30 = 36 \text{ KSL} \checkmark$$

TOTAL LOAD GENERATED DURING RE-CONTACT OF THE STORAGE RACK TO POOL FLOOR

$$P_{AB} + P_{BC} = P_{TOTAL}$$

$$P_{TOTAL} = 143.14 + 341.19 = 484.33 \text{ K} \checkmark$$

MAX REACTION LOAD FOR ANY ONE LEG

$$= \frac{5}{8} \times \frac{484.33}{3} = 100.90 \text{ K}$$

$$\text{MAX LEG LOAD} = 100.90 \text{ K} \checkmark$$

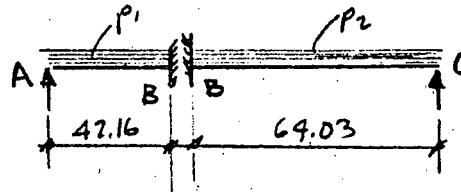
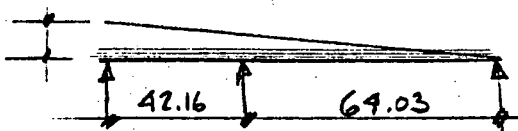
\* 1.2 IS DYNAMIC YIELD FACTOR

# APPENDIX E STABILITY ANALYSIS

REF.

## CASE 2. RACK LIFTUP AT END A

$$\delta_A = 0.3182$$



EQUIVALENT MODEL

ENERGY ASSOCIATED WITH SPAN  $\bar{AB}$

$$E_1 = \frac{1.829 \times 0.3182 (106.19^2 - 64.03^2)}{106.19 \times 2}$$

$$\text{ENERGY } E_1 = 19.67 \text{ in-in}^2$$

ENERGY ASSOCIATED WITH SPAN  $\bar{BC}$

$$E_2 = \frac{1.829 \times 0.3182 (64.03^2)}{106.19 \times 2}$$

$$\text{ENERGY } E_2 = 11.23 \text{ in-in}^2$$

FOR SPAN AB

$$\text{EXTERNAL ENERGY } E_1 = 19.67 \text{ in-in}^2$$

$$l = 42.16 \text{ in}$$

TOTAL NO OF EFFECTIVE CELL BASE PLATES = 10.

INTERNAL STRAIN ENERGY IN BASE PLATES =

$$E_{\text{apl}} = \frac{10 \times 0.00833 W^2 a^6}{E t_c^3}$$

$$E_{\text{apl}} = \frac{10 \times 0.00833 W^2 (20.281)^6}{28000 (0.3845)^3}$$

$$E_{\text{apl}} = 3641.95 W^2 \text{ in-in}^2$$



## APPENDIX E STABILITY ANALYSIS

REF.

THE INTERNAL STRAIN ENERGY IN THE RACK  
BASE BEAMS

$$E_{i,b} = 379.72 W^2 \text{ in}^k \quad (\text{FROM PAGE 11})$$

EQUATING EXTERNAL AND INTERNAL ENERGY

$$19.67 = 3641.95 W^2 + 379.72 W^2$$

$$\boxed{\text{PRESSURE LOAD } W_{AB} = 0.0699 \frac{\text{K}}{\text{IN}^2}}$$

$$\therefore \text{LOAD GENERATED IN SPAN } \overline{AB} = 10(20.281)^2 \times 0.0699$$

$$\boxed{P_{AB} = 287.51 \text{ K}}$$

MAX. STRESS IN THE BASE PLATE AT CENTER OF  
EACH EDGE =

$$S_a = \frac{0.0699}{0.0348} \times 17.63 = 35.41 \text{ KSI}$$

$$< 1.2 \times 30 = 36 \text{ KSI}$$

MAX. STRESS IN THE BASE PLATE AT CENTER

$$S_o = \frac{6 \times 0.0699 \left(\frac{1}{0.3} + 1\right) (20.281)^2}{47 \left(\frac{1}{.3}\right) (0.3845)^2}$$

$$S_o = 32.27 \text{ KSI}$$

$$\text{MAX STRESS IN BASE BEAMS } \overline{AB} = \frac{0.0699 \times 8.93}{0.0348} = 17.94 \text{ KSI}$$

$$< 1.2 \times 30 = 36 \text{ KSI}$$

FOR SPAN BC

$$\text{EXTERNAL ENERGY } E_2 = 11.23 \text{ in}^k$$

$$l = 64.03 \text{ in}$$

No. BASE PLATES EFFECTIVE = 15

INTERNAL STRAIN ENERGY IN BASE PLATES

$$\frac{15}{10} 3641.95 W^2 = 5462.93 W^2$$



## APPENDIX E STABILITY ANALYSIS

REF.

INTERNAL STRAIN ENERGY IN RACK BASE BEAMS

$$E_{i0} = \frac{r^2 L^5}{320 EI_b} \frac{(5W)^2 L^5}{320 EI_b} = \frac{5^2 W^2 (20.28)^2 (64.03)^5}{320 \times 28000 \times 402.568}$$

$$E_{i0} = 3068.23 W^2 \checkmark$$

EQUATING EXTERNAL AND INTERNAL ENERGY

$$E_2 = 11.23 = 5462.93 W^2 + 3068.23 W^2$$

$$\boxed{\text{PRESSURE LOAD } W = 0.0363 \text{ } \frac{\text{K}}{\text{IN}^2} \checkmark}$$

LOAD GENERATED IN SPAN  $\overline{BC} = 15 (20.28)^2 \times 0.0363$

$$\boxed{P_{BC} = 223.96 \text{ K} \checkmark}$$

MAX. STRESS IN THE BASE PLATE AT CENTER OF EACH EDGE =

$$S_a = \frac{0.0363}{0.0553} \times 28.02 = 18.39 \text{ KSI} < 1.2 \times 30 = 36 \text{ KSI} \checkmark$$

O.K.

MAX. STRESS AT THE CENTER OF THE PLATE

$$S_0 = \frac{0.0363}{0.0553} \times 25.53 = 16.76 \text{ KSI} < 1.2 \times 30 = 36 \text{ KSI} \checkmark$$

O.K.

MAX. STRESS IN THE BASE BEAMS =

$$f_b = \frac{0.0363}{0.0553} \times 32.74 = 21.49 \text{ KSI} < 1.2 \times 30 = 36 \text{ KSI} \checkmark$$

TOTAL LOAD GENERATED DURING RECONTACT OF THE STORAGE RACK TO THE POOL FLOOR FOR CASE 2

$$P = P_{AB} + P_{BC}$$

$$P_{\text{TOTAL}} = 287.51 + 223.96$$

$$P_{\text{TOTAL}} = 511.47 \text{ K} \checkmark$$

MAX REACTION LOAD FOR ANY ONE LEG

$$= \frac{5}{8} \frac{511.47}{3} = 106.56 \text{ K} \checkmark$$

$$\boxed{\text{MAX. LEG LOAD} = 106.56 \text{ K}}$$

APPENDIX E STABILITY ANALYSIS

REF.

FOR THE OBE EVENT

THE MAXIMUM OVERTURNING MOMENT WILL BE  
 $\frac{2}{3}$  OF THE OVERTURNING MOMENT FOR THE DBE  
CASE.

SEE PAGE

$$M_o = \frac{2}{3} 15,019.9 = 10,009.93 \text{ IN-K}$$

WHICH IS LESS THAN THE STABILIZING MOMENT

$$M_s = 10,082.46 \text{ IN-K}$$

∴ NO TIPPING WILL OCCUR UNDER THE  
OBE EVENT.

**APPENDIX E STABILITY ANALYSIS**

REF.

SUMMARY STABILITY ANALYSIS

MAXIMUM OVERTURNING MOMENT = 15,014.90 <sup>IN-K</sup> ✓  
 MAXIMUM KINETIC ENERGY = 30,907.43 <sup>IN-K</sup> ✓  
 MAXIMUM STABILIZING MOMENT = 10,082.46 <sup>IN-K</sup> ✓  
 MAXIMUM LIFT UP = 0.3183 INCHES ✓

CASE 1

CASE 2

FOR SPAN AB

ENERGY SPAN AB ( $E_1$ ) = 4.87 <sup>IN-K</sup> ✓      19.67 <sup>IN-K</sup> ✓  
 PRESSURE LOAD AB ( $W_{AB}$ ) = 0.0348 <sup>K/IN<sup>2</sup></sup> ✓      0.0699 <sup>K/IN<sup>2</sup></sup> ✓  
 LOAD GENERATED AB ( $P_{AB}$ ) = 143.14 K ✓      287.51 K ✓  
 MAX. STRESS BASE PLATE  
 (CENTER OF EDGES) ( $S_a$ ) = 17.63 KSL ✓      35.41 KSL ✓  
 MAX. STRESS BASE PLATE  
 (CENTER) ( $S_o$ ) = 16.07 KSL ✓      32.27 KSL ✓  
 MAX. BEAM BENDING STRESS = 8.73 KSL ✓      17.94 KSL ✓

FOR SPAN BC

ENERGY SPAN BC ( $E_2$ ) = 26.09 <sup>IN-K</sup> ✓      11.23 <sup>IN-K</sup> ✓  
 PRESSURE LOAD BC ( $W_{BC}$ ) = 0.0553 <sup>K/IN<sup>2</sup></sup> ✓      0.0363 <sup>K/IN<sup>2</sup></sup> ✓  
 LOAD GENERATED BC ( $P_{BC}$ ) = 341.19 K ✓      223.96 K ✓  
 MAX. STRESS BASE PLATE  
 (CENTER OF EDGES) ( $S_a$ ) = 28.02 KSL ✓      18.39 KSL ✓  
 MAX. STRESS BASE PLATE  
 (CENTER) ( $S_o$ ) = 25.53 KSL ✓      16.76 KSL ✓  
 MAX. BEAM BENDING STRESS = 32.74 KSL ✓      21.49 KSL ✓  
 MAX. REACTION LOAD/ONE LEG = 100.90 K ✓      106.56 K ✓



APPENDIX E REFERENCE LISTS

REF.

REFERENCES

- E-1 ROARK, R.J.: " FORMULAS FOR STRESS AND STRAIN ",  
FOURTH EDITION, MCGRAW - HILL , 1965.
  
- E-2 AMERICAN INSTITUTE OF STEEL CONSTRUCTION: " STEEL  
CONSTRUCTION MANUAL ", NEW YORK, SEVENTH EDITION,  
1970.



**APPENDIX F**  
**COMBINED STRESS RATIO**

APPENDIX F - COMBINED STRESS RATIO

REF.

The combined stress ratio for the storage rack support leg and the storage cell module has been calculated based on the requirements of USNRC Regulatory Guide 1.92: "Combination of Modes and Spatial Components in Seismic Response Analysis," Rev. 1, February 1976 and American Institute of Steel Construction (AISC): "Manual of Steel Construction," Seventh Edition. USNRC Regulatory Guide 1.92 states that the representative maximum values of the structural responses to each of the three components of earthquake motion should be combined by taking the square root of the sum of the squares (SRSS) of the maximum representative values of the co-directional responses caused by each of the three components of earthquake motion. Section 1.6 of AISC specification requires that members subjected to axial compression and bending must meet the following combined stress ratio criteria

$$\text{for } \frac{f_a}{F_a} \leq 0.15 \quad \checkmark$$

$$\frac{f_a}{F_a} + \frac{f_{bx}}{F_{bx}} + \frac{f_{by}}{F_{by}} \leq 1.0 \quad \checkmark \quad (1)$$

where  $f_a$  = Computed Axial Stress



APPENDIX F

REF.

$f_{bx}, f_{by}$  = COMPUTED COMPRESSIVE BENDING STRESS

$F_a$  = ALLOWABLE AXIAL STRESS

$F_{bx} = F_{by}$  = ALLOWABLE COMPRESSIVE BENDING STRESS

IN ACCORDANCE WITH USNRC REGULATORY GUIDE 1.92, THE STRESS RATIOS DUE TO INDIVIDUAL COMPONENTS OF EARTHQUAKE ARE CALCULATED AND COMBINED USING SRSS METHODS AS INDICATED BELOW:

$$\frac{f_{a DL}}{F_a} + \left[ \left( \frac{f_{ax}}{F_{ax}} + \frac{f_{bx}}{F_{bx}} \right)^2 + \left( \frac{f_{ay}}{F_{ay}} + \frac{f_{by}}{F_{by}} \right)^2 + \left( \frac{f_{az}}{F_{az}} + \frac{f_{bz}}{F_{bz}} \right)^2 \right]^{1/2} \leq 1.0 \quad (2)$$

WHERE

$f_{a DL}$  = AXIAL STRESS DUE TO DEAD PLUS LIVE LOAD

$f_{ax}$  &  $f_{bx}$  = AXIAL AND BENDING STRESSES DUE TO EARTHQUAKE IN HORIZONTAL X DIRECTION (GLOBAL X1 DIRECTION OF PAGE 30)

$f_{ay}$  &  $f_{by}$  = AXIAL AND BENDING STRESSES DUE TO EARTHQUAKE IN HORIZONTAL Y DIRECTION (GLOBAL X2 DIRECTION OF PAGE 30)

$f_{az}$  &  $f_{bz}$  = AXIAL AND BENDING STRESSES DUE TO EARTHQUAKE IN VERTICAL Z DIRECTION (GLOBAL X3 DIRECTION OF PAGE 30)

STRESS RATIOS FOR THE STORAGE RACK SUPPORT FEET AND THE STORAGE CELL MODULE ARE CALCULATED USING EQUATION No. 2.

Revised  
By JP  
Checked By  
DH.  
3-26-80